THE STUDY OF HEALTH HAZARDS DUE TO RADON IN THE ENVIRONS OF THE CENTRAL KASHMIR VALLEY, J&K, INDIA

Thesis Submitted for the Award of the Degree of

DOCTOR OF PHILOSOPHY

in

Physics

By

Tanveer Ahmad Pandith

Registration Number: 12108744

Supervised By

Dr. Jeeban Prasad Gewali (21059)
School of Chemical Engineering &
Physical Sciences (Assistant Professor)
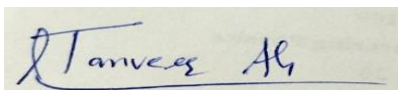Lovely Professional University

Co-Supervised by

Dr. Syed Shakeel Ahmad Simnani
Department of Physics
(Associate Professor)
University of Kashmir

LOVELY PROFESSIONAL UNIVERSITY, PUNJAB
2025

DECLARATION

I, hereby declared that the presented work in the thesis entitled **"The Study of Health Hazards Due To Radon in the Environs of the Central Kashmir Valley, J&k, India"** in fulfilment of degree of **Doctor of Philosophy (Ph.D.)** is outcome of research work carried out by me under the supervision of **Dr. Jeeban Prasad Gewali**, working as **Assistant Professor,** in the Department of Physics, School of Chemical Engineering and Physical Science of Lovely Professional University, Punjab and under the Co-supervision of **Dr. Syed Shakeel Ahmad Simnani** working as **Associate Professor** in Department of Physics, University of Kashmir, India. In keeping with general practice of reporting scientific observations, due acknowledgements have been made whenever work described here has been based on findings of other investigator. This work has not been submitted in part or full to any other University or Institute for the award of any degree.

(Signature of Scholar)

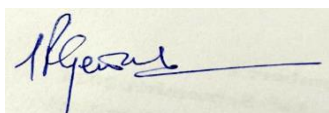Name of the scholar: **Tanveer Ahmad Pandith**

Registration No.: **12108744**

Department/school: **Department of Physics, School of Chemical Engineering and Physical Science**

Lovely Professional University, Punjab, India

CERTIFICATE

This is to certify that the work reported in the Ph.D. thesis entitled "**The Study of Health Hazards Due To Radon in the Environs of the Central Kashmir Valley, J&k, India**" submitted in fulfillment of the requirement for the award of degree of **Doctor of Philosophy (Ph.D.)** in the Physics, School of Chemical Engineering and Physical Science Lovely Professional University is a research work carried out by **Tanveer Ahmad Pandith**, (Registration No.) **12108744**, is bonafide record of his/her original work carried out under my supervision and that no part of thesis has been submitted for any other degree, diploma or equivalent course.
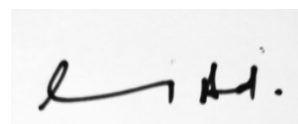
(Signature of Supervisor)

Name of supervisor

Dr. Jeeban Prasad Gewali (21059)

School of Chemical Engineering &

Physical Science (Assistant Professor)

Lovely Professional University

(Signature of Co-Supervisor)

Name of Co-Supervisor

Dr. Syed Shakeel Ahmad Simnani

Department of Physics

(Associate Professor)

University of Kashmir

Abstract

Radio nuclides and naturally occurring radioactive materials (NORM) are inherent components of the Earth's crust, present in soil, groundwater, rocks, and aquifers. While naturally occurring, excessive concentrations of these radio nuclides pose significant radiological and chemo-toxic risks to human health. This study provides a comprehensive evaluation of natural radioactivity across various districts of Jammu and Kashmir, India, focusing on groundwater contamination, radon distribution, and potential health hazards. The research aims to bridge the existing knowledge gap by exploring the geogenic influences on radionuclide distribution and their implications for public safety. This study presents a detailed evaluation of radionuclide distribution and its associated health risks across Baramulla, Pattan, Ladakh, and Budgam districts. The findings provide critical insights into the geogenic influences on natural radioactivity and emphasize the importance of continuous environmental monitoring to safeguard public health. In regions like Baramulla and Pattan, where radon concentrations in groundwater are significant, targeted mitigation strategies are essential. Meanwhile, Ladakh's groundwater remains largely safe, with minimal uranium contamination, and Budgam's soil radioactivity poses no immediate threats. The research contributes valuable baseline data for future radiological risk assessments, policy development, and environmental safety measures in the region.

Investigations in Baramulla District, North Kashmir, revealed elevated radon concentrations in groundwater, with values ranging from 19 ± 0.7 to 93 ± 1.5 Bq L^{-1}, averaging 41.3 ± 1.0 Bq L^{-1}. Notably, over 51% of the samples exceeded the USEPA and UNSCEAR safety limits, though all remained below the WHO threshold of 100 Bq L^{-1}. A significant novel aspect of this study is the identification of a potential association between increased radon levels and underlying tectonic perturbations, marking the first such prediction for the region. Radon distribution patterns suggest that geological faults may play a crucial role in radon mobilization, making the region a potential site for future tectonic studies and fault investigations. A comprehensive dose assessment revealed that

newborns are the most vulnerable to radon exposure via inhalation and ingestion. Despite radon concentrations surpassing WHO recommendations, dose values remained within the permissible limits set by UNSCEAR and ICRP, with an estimated excess cancer risk ranging from 0.52 to 3 cases per thousand individuals. The findings underscore the need for continuous monitoring of radon levels, particularly in areas with active geological structures, to mitigate potential health risks. The study confirms that indoor radon and thoron levels in central Kashmir are within international safety limits, indicating minimal radiological hazard. However, elevated thoron equilibrium factors and increased winter concentrations highlight the need for improved ventilation to mitigate localized exposure risks.

In Pattan, North Kashmir, groundwater-dependent communities were assessed for radioactive contamination in drinking water. The study recorded an average radon concentration of 37.65 Bq/L, with values ranging from 19.88 to 74.37 Bq/L. While these levels exceeded USEPA limits, they remained within WHO and ICRP safety thresholds. The research examined 31 water samples from various sources, including hand pumps, springs, and wells, revealing weak correlations between radon levels and environmental factors such as gamma radiation, pH, and temperature. This suggests that geological characteristics, particularly aquifer depth and lithological composition, are primary determinants of radon distribution. Health risk assessments indicated that children and infants are more susceptible to radon exposure due to higher water consumption rates relative to body weight. The study emphasized the importance of implementing mitigation strategies, such as aeration and adsorption techniques, to reduce radon levels in drinking water. Additionally, public awareness campaigns and periodic monitoring programs were recommended to ensure safe water consumption in radon-prone regions.

The study extended to Ladakh in the Upper Himalayas, where uranium concentrations in groundwater were analyzed across 73 samples using LED Fluorimetry. The results indicated an average uranium concentration of 2.57 ppb, with only one sample exceeding the USEPA limit of 30 ppb, while all remained below the Atomic Energy Regulatory

Board (AERB) threshold of 60 ppb. Risk assessments confirmed that ingestion doses, hazard quotients (HQ), and lifetime average daily doses (LADD) were well within permissible safety limits, suggesting minimal radiological or chemo-toxic risks. The study found that uranium concentrations were slightly elevated in hand pump sources due to deeper groundwater extraction and geological influences. Although localized variations were linked to lithological factors, overall groundwater quality in Ladakh met drinking water standards. These findings highlight the necessity for continuous groundwater monitoring, particularly in regions with complex geological formations, to ensure long-term drinking water safety.

Natural radioactivity assessments in Budgam District involved NaI detector-based gamma spectrometry to analyze soil samples. The results confirmed that the dose contributions from these soil samples were well below internationally established reference limits, ensuring the region's safety for residential construction and habitation. This suggests that natural radioactivity levels in Budgam pose no significant health risks to the local population.

PREFACE

CHAPTER 1 INTRODUCTION

This chapter provides a comprehensive overview of radioactivity, its origins, and its impact on both the environment and human health. It discusses the early discoveries by scientists like Becquerel and the Curies, highlighting the initial lack of awareness regarding radiation hazards. The harmful effects of prolonged radiation exposure, particularly among early miners exposed to radon gas, are explored. The nature and classification of ionizing radiation, including alpha, beta, gamma, and neutron emissions, are explained, along with their biological and environmental effects. The chapter also examines the role of radioactivity in geological studies, particularly in radiometric dating and mineral exploration. Finally, key radiation measurement units and dosimetric quantities are introduced, emphasizing their importance in assessing exposure levels and ensuring safety in various settings.

CHAPTER 2 REVIEW OF LITERATURE

This chapter provides a detailed review of the literature on natural radioactivity analysis, with a particular focus on radon, thoron, uranium, radium, thorium, and potassium. It examines the potential sources of indoor radon, emphasizing soil as the primary contributor and explaining its various entry routes into dwellings. The role of uranium as the main precursor of radon is discussed, along with its behavior in groundwater substrates. Additionally, factors such as exhalation rate, porosity, and moisture content, which influence radon transport, are thoroughly analyzed. The chapter also explores the use of radon as a geochemical tracer and its correlation with geological faults, as documented in various case-control studies and the present research. Lastly, a comprehensive overview of existing literature on radon distribution in water, soil, and indoor environments is presented.

CHAPTER 3 INSTRUMENTATION TECHNIQUES AND METHODS

This chapter explores the various methods and techniques employed in the evaluation of natural radioactivity, utilizing both active and passive measurement approaches. A key instrument, the Smart Radon Monitor, has been used to assess radon concentrations in water as well as radon and thoron exhalation rates. Indoor dosimeters have been deployed to analyze radon and thoron progeny, with their potential health implications examined through track counting analysis using a spark counter. Additionally, NaI gamma spectrometry has been applied to evaluate natural radioactivity levels in the soils of the Budgam region within the study area. Furthermore, LED Fluorimetry has been utilized to determine uranium concentrations in underground water sources in the Leh-Ladakh region of the Upper Himalayas. These techniques provide valuable insights into the distribution and impact of natural radioactivity in different environmental settings.

CHAPTER 4 TECTONIC ACTIVITY AND DOSE ASSESSMENT VIA GROUND WATER MONITORING OF RADON IN BARAMULLA, KASHMIR, INDIA

This chapter evaluates radon levels in groundwater sources across the Baramulla district of Jammu and Kashmir using a scintillation-based Smart RnDuo detector. The study reveals significant variations in radon concentrations, ranging from 19 ± 0.7 to 93 ± 1.5 Bq L^{-1}, with an arithmetic mean of 41.3 ± 1.0 Bq L^{-1}. Notably, 51% of the samples exceeded USEPA and UNSCEAR limits, while all remained below WHO's 100 Bq L^{-1} threshold. The study also assesses the annual inhalation and ingestion doses across different age groups, showing that newborns receive the highest exposure. While doses surpass WHO recommendations, they remain below UNSCEAR and ICRP safety limits. The estimated cancer risk ranges from 0.52 to 3 excess cases per thousand people, staying within UNSCEAR's permitted value. Additionally, physiochemical parameters, aquifer characteristics, and geological factors influencing radon distribution are analyzed. These findings provide critical insights for future epidemiological studies and fault investigations in the region.

CHAPTER 5 RADON QUANTIFICATION AND AGE-BASED DOSE ASSESSMENT IN DRINKING WATER OF PATTAN, KASHMIR

This chapter quantifies radon levels in water sources of the Pattan region, North Kashmir, and evaluates associated health risks through inhalation and ingestion across age groups. The study finds an average radon concentration of 37.65 Bq/L, ranging from 19.88 to 74.37 Bq/L, exceeding USEPA limits but remaining within WHO and ICRP safety thresholds. Analysis of 31 water samples from hand pumps, springs, and wells reveals weak correlations between radon levels and gamma radiation, pH, and temperature, suggesting the influence of geological factors. The study highlights increased susceptibility of children and infants to radon exposure, emphasizing the need for regular monitoring, water treatment, and public awareness in radon-prone areas. Mitigation strategies, including aeration and adsorption techniques, are recommended to reduce radon levels in water. The findings contribute to baseline radon data and stress the importance of continued monitoring for public health protection.

CHAPTER 6 URANIUM ANALYSIS IN GROUNDWATER OF KARGIL AND LADAKH, INDIA

This chapter discusses uranium concentrations in 73 groundwater samples from Ladakh, Northwest Himalayas, using an LED Fluorimetry. The results showed an average uranium concentration of 2.57 ppb, with only one sample exceeding the USEPA limit of 30 ppb, while all remained below the AERB threshold of 60 ppb. Radiological and chemical risk assessments confirmed safe levels, with ingestion doses, Hazard Quotients (HQ), and Lifetime Average Daily Doses (LADD) well within permissible limits. Higher uranium levels were observed in hand pump sources due to deeper extraction and lithological influences. While localized variations were linked to geological factors, overall water quality adhered to drinking standards. The study emphasizes the importance of regular monitoring and further geochemical investigations to ensure long-term groundwater safety in the Upper Himalayan region.

CHAPTER 7 SEASONAL VARIATION IN INDOOR RADON / THORON PROGENY LEVELS AND ASSOCIATED DOSE IN BARAMULLA, J &K

The chapter discusses the annual indoor concentrations of radon (^{222}Rn) and thoron (^{220}Rn) across 50 dwellings, finding averages of **79.73 Bq/m³** and **67.35 Bq/m³**, respectively both within WHO limits. Radon showed more uniform distribution, while thoron varied locally due to its shorter half-life. Equilibrium factors for radon were consistent and within global norms, while thoron factors were higher than recommended, indicating potential localized emissions. Seasonal analysis revealed higher concentrations and doses in winter due to poor ventilation. The annual inhalation doses from both gases were within UNSCEAR and ICRP safety limits. Most dwellings had higher radon-related doses, and overall dose distributions showed moderate exposure levels with few extremes.

CHAPTER 8 ASSESSMENT OF EXHALATION RATE AND NATURAL RADIOACTIVITY IN (BUDGAM), CENTRAL KASHMIR

This study assesses radon and thoron exhalation from soils in central Kashmir, revealing that radon levels are well within UNSCEAR safety limits, while thoron levels slightly exceed the reference threshold likely due to local mineralogical variations. Radiological indices, including radium equivalent activity, annual effective dose, and hazard indices, all fall below international safety standards, confirming minimal health risks. Moderate correlations among Ra, Th, and K suggest a shared geochemical origin, while weak associations between these radio nuclides and radiological parameters highlight the role of environmental factors like soil properties. Overall, the region's soils are deemed radiologically safe for habitation and agriculture, though further multivariate analysis is recommended for a more nuanced understanding of the underlying factors influencing radioactivity distribution.

CHAPTER 9 FUTURE SCOPE OF THE WORK

This chapter discusses the findings of the present work and research gap for exploring the current study to more advancement.

CONTENTS

List of Figures

List of Tables

SYMBOLS AND ABBREVIATIONS

- **NORM:** Naturally Occurring Radioactive Materials
- **^{220}Rn:** Thoron
- **^{222}Rn:** Radon
- **α :** Denotes Alpha Particles
- **β:** Denotes Beta particles
- **γ:** Denotes Gamma Rays
- **NCRP:** National Council on Radiation Protection and Measurements
- **LET:** Linear Energy Transfer
- **BEIR:** Biological Effects of Ionizing Radiation
- **UNSCEAR:** United Nations Scientific Committee on the Effects of Atomic Radiation
- **R:** Roentgen
- **RAD:** Radiation absorbed dose
- **Gy:** Gray
- **Sv:** Sievert
- **RBE:** Relative Biological Effectiveness
- **HT:** Dose Equivalent
- **Wt:** Weighting factor
- **CEDE**: Committed Effective Dose Equivalent
- **WL:** Working Level
- **WLM:** Working Level Month
- **ICRP:** International Commission on Radiological Protection
- **IAEA**: International Atomic Energy Agency
- **OECD**: Organization for Economic Cooperation and Development
- **NEA**: Nuclear Energy Agency
- **WHO**: World Health Organization
- **AERB**: Atomic Energy Regulatory Board

- **BIS:** Bearaeu of Indian Standards
- **WQI:** Water Quality Index
- **BSS:** Basic Safety Standards
- **ALARA:** As Low as Reasonably Achievable
- **ALI:** Annual Limit on Intake
- **USEPA:** United States Environmental Protection Agency
- **COPD:** Chronic Obstructive Pulmonary Disease
- **Bq/L:** Becquerel per litre
- **Φ:** Emanation Coefficient
- **mSv:** Milli Sievert
- **µSv:** Micro Sievert
- **nSv :** Nano Sievert
- **DER** : Dose Equivalent Range
- **K:** Partition Coefficient between air and water
- **DRPS:** Direct Radon Progeny Sensor
- **DTPS:** Direct Thoron Progeny Sensor
- **Q_r:** Calibration Factors for Radon
- **Q_t :** Calibration Factors for Thoron
- **SSNTD:** Solid State Nuclear Track Detector
- **F:** Equilibrium Factor
- **H_z^Q:** Hazard Quotient
- **ELCR:** Excess Lifetime Cancer Risk
- **TDS:** Total Dissolved Salts
- **E_c:** Electrical Conductivity
- **N:** Number of Samples

CHAPTER 1

INTRODUCTION

1.1 Early Contributions to Radioactivity

Naturally occurring radioactive Materials (NORM) have been present since beginning of the environment in both living and inanimate objects in varying amounts. Despite its abundance, the concept of radioactivity was only discovered in the late 19th century, which is relatively late in the history of human science (Kathren, 1998). A key factor in this discovery was Henri Becquerel's revolutionary study on uranium compounds. After Röntgen, Becquerel first time studied phosphorescent characteristics of uranium-containing minerals to determine if luminescence was an essential requirement for X-ray emission. When he put uranium samples and photographic plates in a dark drawer, considering that exposure to sunlight would be required for any noticeable effects, he made his breakthrough. Unexpectedly, the plates remained foggy even when there was no sunlight present, confirming that uranium released radiation on its own. This was the first radioactivity observation (Allisy, 1996).

Becquerel's study developed on previous findings, which included the 1789 identification of uranium by Martin Heinrich Klaproth, followed by investigations of Carl Wilhelm Scheele and Bucholz, who observed that uranium could undergo chemical reactions initiated by light. C.J. Burnett's 1857 work identified uranium's particular interactions with radiation and showed how uranium salts could be used in photographic printing. Moreover, before the radiological properties of uranium were fully understood, its uses in electrical discharge tubes and glassmaking were identified. (Magill & Magill, 2003).Between 1883 and 1896, Becquerel, a third-generation scientist, published an extensive amount of work on phosphorescence and infrared radiation, which ultimately

lead to his discovery of radioactivity. His meticulous studies on the phosphorescence decay and absorption spectra of uranium formed the foundation for the development of nuclear science and paved the way for Marie and Pierre Curie's subsequent discoveries. By highlighting the significance of naturally occurring radioactive materials, these early contributions laid the foundation for future research in radiation physics and its applications (Donald Blaufox, 1996).

1.2 Discovery of Radioactive Elements, Radium Applications, and Early Awareness of Radiation Hazards

Decades before Henri Becquerel discovered radioactivity in 1896, the presence of thorium in monazite was first identified in 1839. However, in 1898, Marie Curie in France and Gerhard Schmidt in Germany independently examined its radioactive qualities. Initially known as "Becquerel rays," Marie Curie and her husband Pierre studied this phenomenon further and developed sophisticated methods to measure radiation. Based on their outcomes, some uranium ores emitted radiation at concentrations higher than those of uranium (DASH et al., 2021). The discovery of Ra and Po, in 1898 as a result of this observation made a significant contribution to the study of radioactivity (Friedrich & Remane, 2011). Marie Curie's theory that pitchblende contained anonymous radioactive substances was confirmed in 1899 when André-Louis Debierne identified actinium, extending the ongoing discovery of other radioactive elements (Debierne, A. 1899). When the Curies were able to isolate about 100 mg of radium chloride by 1902, Marie Curie calculated its atomic weight to be 225 (later changed to 226.0254), placing it in the alkaline-earth metals category. Due to her groundbreaking work, she became the first woman to receive a doctorate from the Sorbonne in 1902. The Curies and Becquerel got the 1903 Nobel Prize in Physics in honor of their innovative research (Flakus, 1982).

Figure 1.1: Picture showing Curie working in her lab (Mohammad Bagher, 2014).

Due to its continuous radiation emissions, radium immediately caught a lot of attention. Its luminous characteristics made it important for a variety of uses and even made an appearance in works of literature. Radium was rapidly examined for potential medical uses in addition to its cultural significance. Early uses in the treatment of skin tuberculosis (lupus vulgaris) resulted from Pierre Curie and other researchers' examination of its therapeutic potential. Radium-based glass applicators for throat cancer were first developed by John MacLeod at Charing Cross Hospital in 1904, and Benjamin Barringer designed radium-filled needles for the treatment of prostate cancer in 1917. Modern brachytherapy, earlier known as "Curie therapy" in Europe, was made possible by these discoveries (George, 2005; Luo et al., 2021).

While radium showed its promising applications in medicine, it was quickly utilized for commercial gain. Despite radium extraction from mining tailings being expensive and time-consuming, customer demand was driven by the metal's alleged health benefits. This gave rise to the promotion of many unregulated consumer products that contained radium as health-promoting products, such as toothpaste, skincare creams, hair tonics, and chocolates. The most famous misuse of radium-based luminescent paints was in the

watch making industry, where they were applied to instrument and clock dials. When workers, mainly young women, licked the tips of their paintbrushes, they unknowingly consumed radium, which resulted in severe radiation poisoning and, frequently, death (Marieskind, 1976). Reports of skin burns and eye irritation due to X-ray exposure were noticed in early 90's. After keeping a radium sample in his pocket, Henri Becquerel experienced radiation burns himself, demonstrating the harmful effects of radiation through repeated exposure (Caufield, 1990). In addition, Pierre Curie self-experimented, which resulted in radio necrosis and serious skin damage. As a result of her prolonged exposure, Marie Curie developed severe burns, chronic exhaustion, and eventually a blood cancer. With over 300 casualties linked to excessive radiation exposure, many early radio chemists and radiation workers went through similar outcomes (Baatout, 2023).

Before the 1945 nuclear bombings of Hiroshima and Nagasaki, which exposed the harmful effects of atomic energy, the public was not well aware of the hazards posed by radiation (Lindell, 2020).

Figure 1.2: Picture Showing X-Ray Print of Roentgen's wife's hand (D raganil et al., 1993).

This was a historic event that resulted in stricter safety rules and guidelines for handling radioactive materials. The development of radioactivity throughout history, from its discovery to its many uses and an understanding of its dangers, suggests both the need for responsible nuclear practices and advances in science (Epperly et al., 2017; Kardamakis et al., 2023).

1.3 Rutherford's Contributions to Radioactive Emanations and Alpha Particles

Through his scientific investigations in radioactivity, Rutherford discovered thorium transmutation in 1900, identifying thorium X (^{224}Ra) and thorium emanation (^{220}Rn). He observed a radioactive gas while studying the ionization effects of thorium; this gas came to be known as "thorium emanation," though initially its chemical composition was unknown. The mystery took an interesting direction when similar emanations from actinium and radium were discovered. Rutherford, working with Frederick Soddy at McGill University, demonstrated experimentally that these emissions were inert gases, which are now known as radon. The idea of "half-life" as the fundamental property of radioactive materials was also introduced by their observation that these gases gradually lost their activity ("Lord Rutherford, 1871–1937," 1938).

The scope of Rutherford's work went beyond emanations. He and Hans Geiger attained a major achievement in measuring radioactive decay in Manchester when they made precise measurements of alpha particle emissions per gram of radium. In 1899, he carried out experiments that showed uranium rays were affected by magnetic fields and could be classified as either beta or alpha radiation. He later used alpha particles to study the atomic structure and proved that they were helium nuclei. The foundation for the nuclear model of the atom was established by the results of his research (Kragh, 2012).The contribution by Hess, Plank, Einstein and Villard Collectively, revolutionized our knowledge of atomic and subatomic processes and strengthened Rutherford's position as

an important figure in the study of radioactivity (Gill, 1900; Rutherford, 1900; National Committee on Radiation Protection & Measurements, 1987; Magill, 2003).

1.4 Discovery, Characteristics of Radon and Thoron, and Early Hypothesis on Radon's Link to Lung Cancer

Friedrich Dorn made the initial discovery of the radioactive gas that is now known as radon in 1900, but Ernest Rutherford had previously identified thoron (^{220}Rn) in 1899. In order to determine that thoron and radon were identical members of the noble gas family, Rutherford gave Frederick Soddy the task of studying the chemical characteristics of thoron (Marshall & Marshall, 2003). Despite being inert and unable to form chemical compounds, they were radioactive and produced decay progenies that stuck to surfaces when radium and thorium were present (Valentin & Clement, n.d.).The Radium emanation called radon (Rn) being inert has the electronic configuration [Xe core] $4f^{14}$ $5d^{10}$ $6s^2$ $6p^6$. With an energy of 5.48MeV, the most frequently discussed isotope, ^{222}Rn and others include (^{219}Rn) and (^{220}Rn), with half life in seconds decay quickly. Despite not being chemically reactive, these gases hold significance for studying environmental radiation and radioactive decay chains (Riudavets et al., 2022).In the beginning, miners from Schneeberg and Joachimsthal, where an elevated frequency of a deadly lung disease called "mountain sickness" had been noted for centuries, were suspected of being exposed to radon, which causes lung cancer. Lung cancer was found to be the cause of 42% of miner deaths in 1913 by Arnstein (Vinson et al., 2009).

Radon was first suggested by Margarete Uhlig as a potential cause in 1921. Based on Rajewsky's radioactivity measurements, Lorenz's 1944 investigations revealed that although radon was a major contributing factor, there were other factors at play as well. It was retrospectively linked to radon exposure in the 1920s and is now known as radiation-induced lung cancer (Doll, 1995; IAEA & WHO, 1967).

1.5 Types of Radioactive Nuclides

Radioactive nuclides, or radio nuclides, are unstable isotopes that emit ionizing radiation as they decay and are broadly categorized into four types based on their origin: primordial, cosmogenic, natural decay series, and anthropogenic (Draganić et al., 2020).

Primordial Radio Nuclides like potassium-40 (^{40}K) have existed since Earth's formation and contribute significantly to background radiation due to their long half-lives and widespread natural occurrence (Thorne et al., 2003).

Cosmogenic Radio Nuclides, such as carbon-14 (^{14}C) and tritium (^{3}H), are generated when cosmic rays interact with atmospheric or terrestrial matter; ^{14}C is particularly important for radiocarbon dating despite its minor dose contribution (De Angelis, 2014; Airey et al., 2012).

Natural Decay Series Radio Nuclides, primarily from uranium-238, thorium-232, and actinium-235 chains, dominate natural radiation exposure especially through radon gas (^{222}Rn), a major indoor health hazard linked to lung cancer (Cowart & Burnett, 1994; Mohan & Chopra, 2022).

Anthropogenic Radio Nuclides, including cesium-137 (^{137}Cs), strontium-90 (^{90}Sr), and man-made ^{14}C and ^{3}H, originate from nuclear testing, energy production, and medical uses, and can persist environmentally, entering the food chain and raising health concerns (von Blanckenburg & Willenbring, 2014). While natural sources remain the predominant contributors, growing anthropogenic inputs necessitate robust monitoring and radiation protection measures (Johnson, 1973).

1.6 Units of Radioactivity and Radiation Measurement

Radiation measurement involves a range of specialized units, each designed to capture different aspects of radioactive exposure and its biological implications. Units such as the Rad, Sievert, and Roentgen provide details regarding the type of radiation and its dosimetric effects.

Exposure, measured in **Roentgen (R)** or **coulombs per kilogram (C/kg)**, quantifies the ionization produced in air by x-rays or gamma rays, serving primarily to assess radiation intensity in atmospheric contexts (Jennings, 2007). **Absorbed dose**, expressed in **rad** or the SI unit **gray (Gy)**, represents the amount of radiation energy deposited per unit mass of any material, including biological tissues, where 1 Gy equals 100 rad or 1 joule per kilogram, an essential metric for evaluating potential tissue damage across radiation types (Wambersie et al., 2005).

To address the differing biological effects of various radiation types, the **dose equivalent** is introduced, measured in **sievert (Sv)**, and calculated as the absorbed dose multiplied by a radiation weighting factor (Q), thus reflecting the relative biological effectiveness (RBE) of the radiation (Nair & Nambi, 1997). Further refining this concept, the **effective dose equivalent (EDE)** incorporates **tissue weighting factors (WT)** to account for variable sensitivity among body organs, offering a more comprehensive risk assessment when radiation is distributed unevenly across tissues (Jennings, 2007).

Long-term internal exposure, especially via ingestion or inhalation of radioactive substances, is captured by the **committed effective dose equivalent (CEDE)**, which estimates cumulative dose over a standard lifetime period, typically 50 to 60 years. For **radon-specific exposure**, especially in occupational settings, the **working level (WL)** and **working level month (WLM)** are used; 1 WL represents the alpha energy (1.3×10^5 MeV) released from radon decay products in one liter of air, and WLM quantifies exposure over time. Together, these units form an integrated framework critical to monitoring, assessing, and managing radiological risks in both environmental and occupational contexts (Roy et al., 2024).

1.7 Radiation: Nature, Types, and Effects

Radiation refers to the propagation of energy through space or matter in the form of electromagnetic waves or subatomic particles. Based on its interaction with matter,

particularly its ability to ionize atoms, radiation is broadly categorized into ionizing and non-ionizing types (Alsop, 1999).

1.7.1 Ionizing and Non-Ionizing Radiation

Ionizing radiation includes alpha (α) particles, beta (β) particles, gamma (γ) rays, X-rays, and neutron radiation. Alpha particles, despite their high energy, are weakly penetrating and can be stopped by paper or skin. Beta particles penetrate further but are blocked by materials like plastic or aluminum, while gamma rays and X-rays are deeply penetrating and require dense shielding such as lead or concrete (Nilsson et al., 2015). The primary biological target of ionizing radiation is DNA, which, upon exposure, can suffer strand breaks, base damage, and chromosomal aberrations that may culminate in mutations, cancer, or hereditary effects if improperly repaired (Sankaranarayanan & Wassom, 2008).

Non-ionizing radiation which includes radiofrequency waves, infrared, visible light, and low-energy ultraviolet (UV) rays lacks the energy to ionize atoms. While generally less harmful, prolonged exposure to high-frequency UV radiation can still result in DNA damage, oxidative stress, and increased risk of skin cancers (Hatra, 2018).

1.7.2 Sources of Ionizing Radiation

Human radiation exposure originates from both natural (81%) and man-made (19%) sources (Eisenbud, 1984; NCRP, 1987). Figure 1.3 below shows the detailed overview of radiation exposure. Radon gas, a decay product of uranium, is the dominant natural contributor (~55%), especially in enclosed spaces with poor ventilation. Cosmic rays (~8%) add to exposure, increasing with altitude, while terrestrial sources (~8%) stem from radio nuclides like uranium-238, thorium-232, and potassium-40 in the earth's crust. Internal exposure (~10%) occurs through ingestion or inhalation of isotopes like ^{40}K and ^{14}C. Among anthropogenic sources, medical applications such as X-rays and CT scans contribute the most (~15%), with smaller amounts from consumer products (3%) and

occupational exposure (1%), especially in fields like healthcare, aviation, and nuclear industries (Zakariya & Khan, 2014).
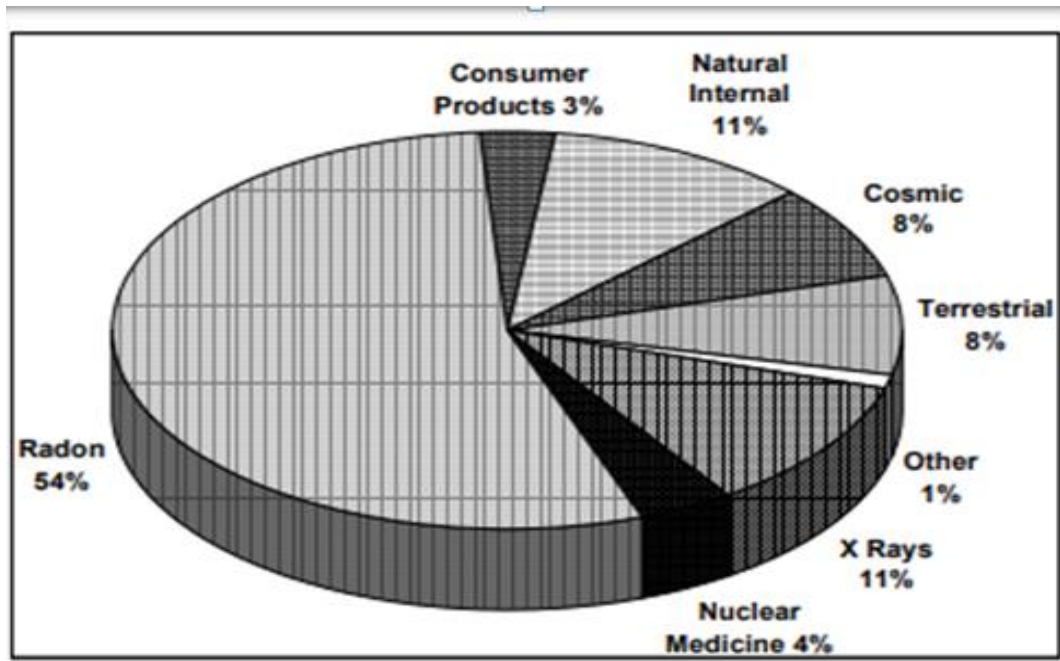
Figure 1.3: Detailed overview of Radiation Exposures (NCRP, 1987).

1.7.3 Radiation Exposure and Dose-Dependent Effects

The biological outcome of radiation exposure depends on several parameters, including the type of radiation, its energy, dose, tissue sensitivity, and duration of exposure. Based on dose-response relationships, the effects are broadly categorized as deterministic or stochastic.

1.7.3.1 Deterministic Effects These occur above a certain threshold dose and increase in severity with dose. These include Acute Radiation Syndrome (ARS), observed at doses exceeding 1 Gray (Gy), characterized by hematopoietic suppression, gastrointestinal failure, and neurovascular complications (BEIR, 1990; UNSCEAR, 1986, 1993; Mavragani et al., 2017). Chronic deterministic outcomes may include cataracts, tissue fibrosis, and impaired organ function due to cumulative cellular damage.

1.7.3.2 Stochastic Effects, by contrast, have no dose threshold and occur randomly, though the likelihood increases with dose. Examples include radiation-induced cancers such as leukemia, thyroid, lung, and breast cancers, often linked to radon inhalation or medical radiation (BEIR & UNSCEAR, 1988). Stochastic effects may also involve heritable genetic mutations transmitted to offspring, even if the exposed individual remains unaffected (Burgio et al., 2018).

1.7.4 Mechanisms of Tissue Damage and the Role of LET

Radiation induces biological damage via direct and indirect mechanisms. Direct interactions involve ionization of critical bio molecules such as DNA, while indirect effects occur through radiolysis of water, generating reactive oxygen species (ROS) like hydroxyl radicals that attack cellular structures (Cohen et al., 1979; Dainiak, 2002).

A crucial factor influencing the extent of damage is the Linear Energy Transfer (LET) the amount of energy deposited per unit track length of radiation. High-LET radiation (e.g., alpha particles, neutrons) delivers concentrated energy over short distances, resulting in complex DNA damage and reduced repair efficiency. Conversely, low-LET radiation (e.g., gamma rays, beta particles) causes more diffuse damage, often via ROS-mediated pathways (Feinendegen et al., 2004). The mode of exposure also shapes biological outcomes. Internalized radio nuclides (e.g., inhaled radon or ingested cesium) may localize in organs and continuously irradiate tissues, whereas external sources (e.g., cosmic rays, X-rays) interact based on their penetration depth and exposure duration (Miousse et al., 2017).

1.8 Environmental distribution of Radiation and Natural Radioactivity

Geology and human activities both influence how radiation spreads through the air, water, and soil. Air quality is affected by radon buildup indoors, especially in basements. Large regions can become contaminated by radioactive fallout from nuclear

testing or industrial accidents. The safety of drinking water can also be impacted by the presence of dissolved radio nuclides like radon and uranium in water sources.

Unstable atomic nuclei naturally release energy in an attempt to change into more stable isotopes by means of a process known as radioactive decay. This change is accomplished by a series of decays, generating a decay chain in which a parent radionuclide goes through multiple radioactive transitions before producing a stable daughter product. Environmental radioactivity, which is crucial to understanding radiation exposure and its impacts on ecosystems and human health, is largely influenced by the radio nuclide decay. The natural radioactive decay of uranium-238, uranium-235, and thorium-232 forms radiation exposure levels in different ecosystems and makes a significant contribution to environmental radioactivity. Alpha, beta, and gamma radiation are among the radioactive emissions produced by their decay chains that affect soil, water, and air (Eisenbud & Paschoa, 1989).Chemical and physical factors affect how these decay chains behave, and because of their mobility and health risks, radon gas is one of the most harmful environmental hazards. Understanding decay characteristics, radionuclide mobility in the environment and their long-term impacts is essential for assessing radiation risks and implementing protective measures when necessary (Supartinah, 1989).

1.8.1 Decay Chain Significance and Type of Radiation Emitted During Decay Processes

A vital aspect of radioactive decay is decay chains, which are a stepwise transformation in which a radioactive parent isotope produces a number of unstable daughter isotopes before becoming stable. Every isotope in the chain undergoes either beta or alpha decay during this anticipated process, sometimes releasing gamma radiation in the process. (^{238}U), (^{235}U), and (^{232}Th), all long-lived isotopes found naturally under earth, are the foundations of the three main natural decay chains. These decay series have an impact on the composition of soil, water, and the atmosphere and are essential for preserving natural background radiation levels.

Before stabilizing as Lead-206 (Pb-206), the Uranium-238 decay chain goes through 13 steps, resulting in intermediate radioactive isotopes like Radon-222 (Rn-222) and Radium-226 (Ra-226). These isotopes all emit ionizing radiation, which affects the amount of radiation in the environment. The Actinium Series, a substitute for the Uranium-235 decay chain, has a shorter sequence and eventually produces Lead-207 (Pb-207). Even though it only makes up 0.72% of natural uranium, uranium-235 is still a contributor to environmental radioactivity despite being far less common than uranium-238. The decay chain of Thorium-232 is mainly defined by a sequence of alpha decays, such as those of Radon-220 (Rn-220) and Polonium-216 (Po-216), and ends with the stable isotope Lead-208 (Pb-208) (Craft et al., 2004).

Environmental radioactivity is shaped by the various forms of radiation that radio nuclides emit as they move through their decay chains. Heavy, positively charged particles that ionize atoms strongly but have a low penetration power make up alpha radiation (α), which is dangerous mainly when inhaled or consumed. High-speed electrons or positrons, which can travel farther and more efficiently through biological tissues than alpha particles, participate in beta radiation (β). When alpha or beta decays, high-energy electromagnetic radiation known as gamma radiation (γ) is released, which raises the risk of exposure and deep penetration (Nazaroff, 1992). Together, these emissions contribute to environmental radiation levels and establish the possible risks of radionuclide contamination (Dunn, 1981; Dyck, 1979; Linsalata, 1989).
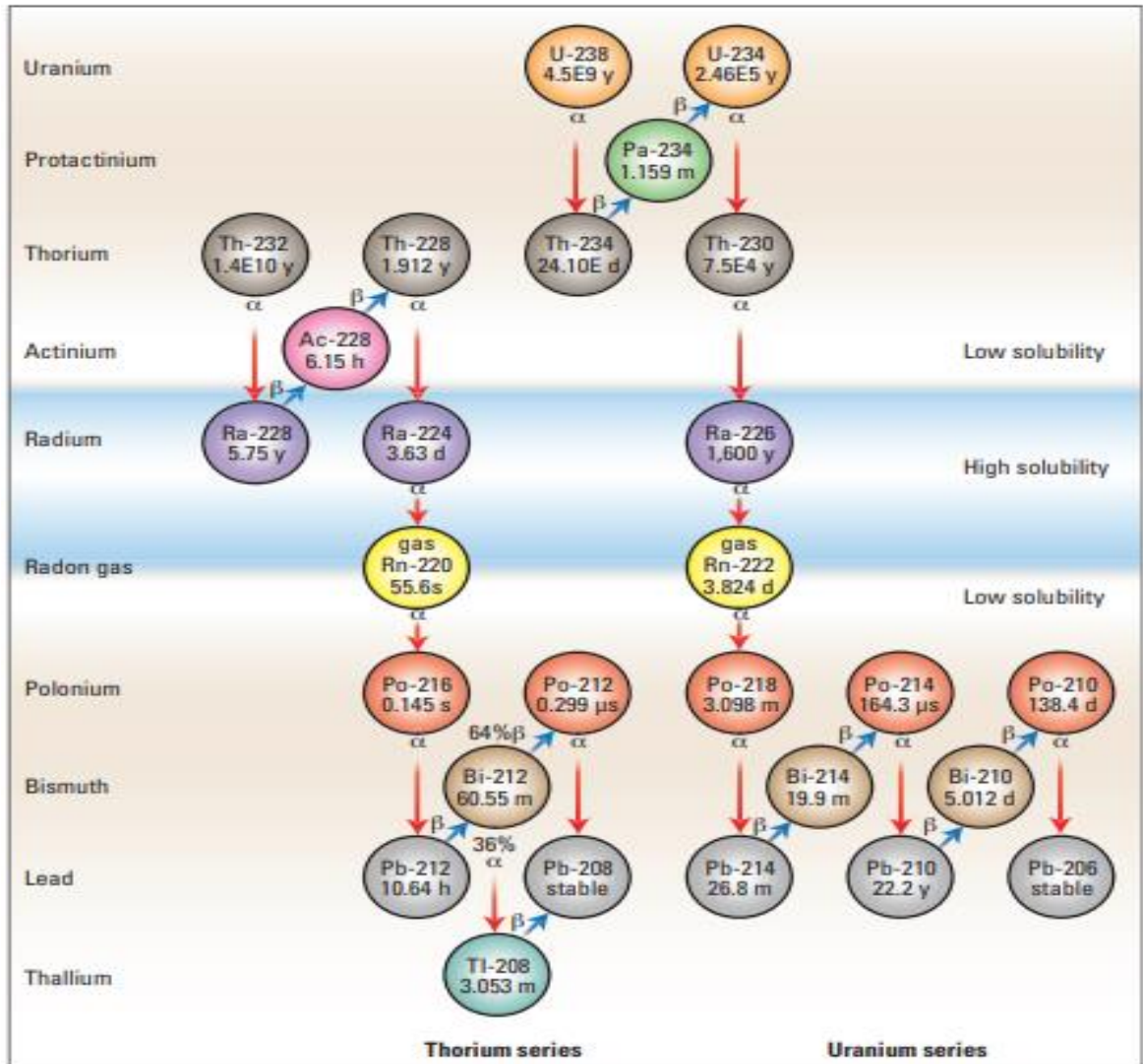
Figure 1.4: Natural Uranium and Thorium decay chain and various intermediate daughter products with α and β emitters (Nelson et al., 2015).

1.8.2 Properties and Behavior of Decay Chains

The decay chains of uranium and thorium display predictable trends that are controlled by secular equilibrium, in which, over extended periods of time, the activity of each parent-daughter isotope becomes equal. However, physical and chemical processes have the ability to disrupt equilibrium. For example, uranium can move through

groundwater systems because it is more soluble in oxygen-rich water, while thorium is usually insoluble and immobile in soil. Localized variations in radiation levels result from this difference in chemical behavior, which additionally impacts the environmental distribution of radio nuclides (Olley et al., 1996).Of special concern among the decay products is radon gas (Rn-222 and Rn-220), which can move through soil and build up in enclosed spaces, posing serious health risks. When radon is inhaled, it breaks down into radioactive daughter progenies like polonium-218 (Po-218) and polonium-214 (Po-214), which can effect lung tissue and increase the risk of lung cancer. Under certain environmental circumstances, especially in regions with high water salinity, other isotopes, like radium-226 (Ra-226), can become mobile and contaminate groundwater (Sadat-Noori et al., 2015).

1.8.3 Environmental Impact of Natural Radioactivity Decay

Several environmental processes are influenced by the ongoing decay of natural radio nuclides. Background radiation is produced by uranium and thorium-containing soil and rock formations, and these elements are carried into water bodies by weathering and erosion. Through foundation cracks, radon gas can enter buildings and greatly increase indoor radiation exposure. Lead and polonium isotopes can also adhere to dust particles and enter food and water supplies, posing a risk of inhalation. Radionuclide distributions can also be changed by disruptions in secular equilibrium. Similar to this, uranium can be separated from its decay chain by natural processes like groundwater flow, which can lead to an imbalance where some radioactive daughters accumulate up in the environment (IAEA, 1990; Chauvel, 2021; Lavarnway, 2006).

1.9 Role of Various International Organizations in Radiation Regulation and Safety Guidelines

It has become evident over time that human tissues can sustain severe damage from exposure to high levels of ionizing radiation. This knowledge has generated

concerns about potential hazards of radiation exposure, which has led to the creation of regulatory organizations tasked with controlling and reducing those risks. The main objective of these various international and national organizations is to work together to regulate the use of ionizing radiation and ensure safety. These organizations play a key role in developing safety standards, monitoring radiation levels, and managing waste in protecting people and the environment from the radiation hazards (Boudia, 2007).

The ICRP previously used to be a separate organization of radiation protection specialists with its main focus to provide fundamental recommendations and proposals for radiation protection. Later, it was renamed the (ICRP). The United Nations established the (UNSCEAR) in 1955. This international agency was tasked with gathering, assessing, and distributing data on levels of natural and artificial ionizing radiation in the environment, and examining its effects on both ecosystems and human health.

An important role for the (IAEA) is to control sources of ionizing radiation. The IAEA works closely with UNSCEAR and other agencies like (OECD/NEA), (WHO), and the International Labor Organization (ILO). Together, these groups focus on ionizing radiation safety research and implementation, especially in nuclear facilities. In order to ensure that humans are protected from radiation hazards, IAEA additionally developed the International Basic Safety Standards (BSS). All nuclear power and atomic energy-related operations and facilities, both new and old, must adhere to these safety regulations in order to minimize hazards to the environment and public health. Uncontrolled sources, such as cosmic radiation at the Earth's surface and 40K in the human body, are exempt from these rules.

In an effort to protect the environment and human health from radiation exposure, many radiation protection organizations have been set up in India. The installation of nuclear power plants and the utilization of atomic energy are also supervised by these organizations. In this context, two significant organizations are the (DAE) and (BARC). The development of radiation monitoring technologies, environmental monitoring, and

radiological impact assessments are their main areas of interest. Projects involving BARC and DAE include radon exhalation rates from soil, uranium levels in water, and seasonal variations in indoor radon and thoron. They measure the levels of terrestrial radio nuclides in soil in various parts of India, including 226Ra, 232Th, and 40K.

Radiation exposure from nuclear facilities in India needs to remain within acceptable limits, according to (AERB). With public health and safety in mind, the board makes sure that radioactive waste generated by nuclear facilities is managed safely and supervises radiation protection programs.

In order to reduce exposure and to avoid the health effects linked with radiation exposure, radiation regulation is important. ALARA (As Low as Reasonably Achievable) regulations, for instance, guarantees the limited exposure from radiation while still attaining the desired outcomes. Essential components of radiation safety consist of external dose which describes radiation, such as gamma or X-rays, that originates outside the body. The term "internal dose" describes the radiation that is taken up by the body from radio nuclides, usually through ingestion, breathing or by absorption (Hendee & Marc Edwards, 1986).

1.10 Study Area

The Union Territories of Jammu & Kashmir and Ladakh, located in the northwestern Indian Himalayas, form a geologically and topographically diverse region characterized by vast elevation gradients and complex mountain systems, including the Siwaliks, Pir Panjal, Greater Himalaya, Zanskar, and Karakoram ranges. This varied terrain contributes to distinct climatic zones ranging from subtropical lowlands in Jammu to the temperate Kashmir Valley and the cold desert of Ladakh, which in turn shape land use, vegetation, and settlement patterns. Ladakh, though sparsely populated, covers over half the total area and is dominated by glaciated high-altitude landscapes. The geological history of the region spans from ancient Archean rocks to recent alluvium, reflecting key phases of Himalayan evolution. Hydrologically, the area relies on glacial and snowmelt-fed rivers

such as the Indus, Jhelum, and Chenab, which are vital to the broader Indus Basin's water and energy systems. With over 3,650 wetlands and water bodies, the region plays a crucial ecological role and supports rich biodiversity within the Himalayan hotspot. However, its fragile geology, steep slopes, and climatic extremes heighten susceptibility to natural hazards like earthquakes, landslides, and floods, challenges that demand integrated environmental management amid mounting anthropogenic pressures and climate change (Romshoo et al., 2020).
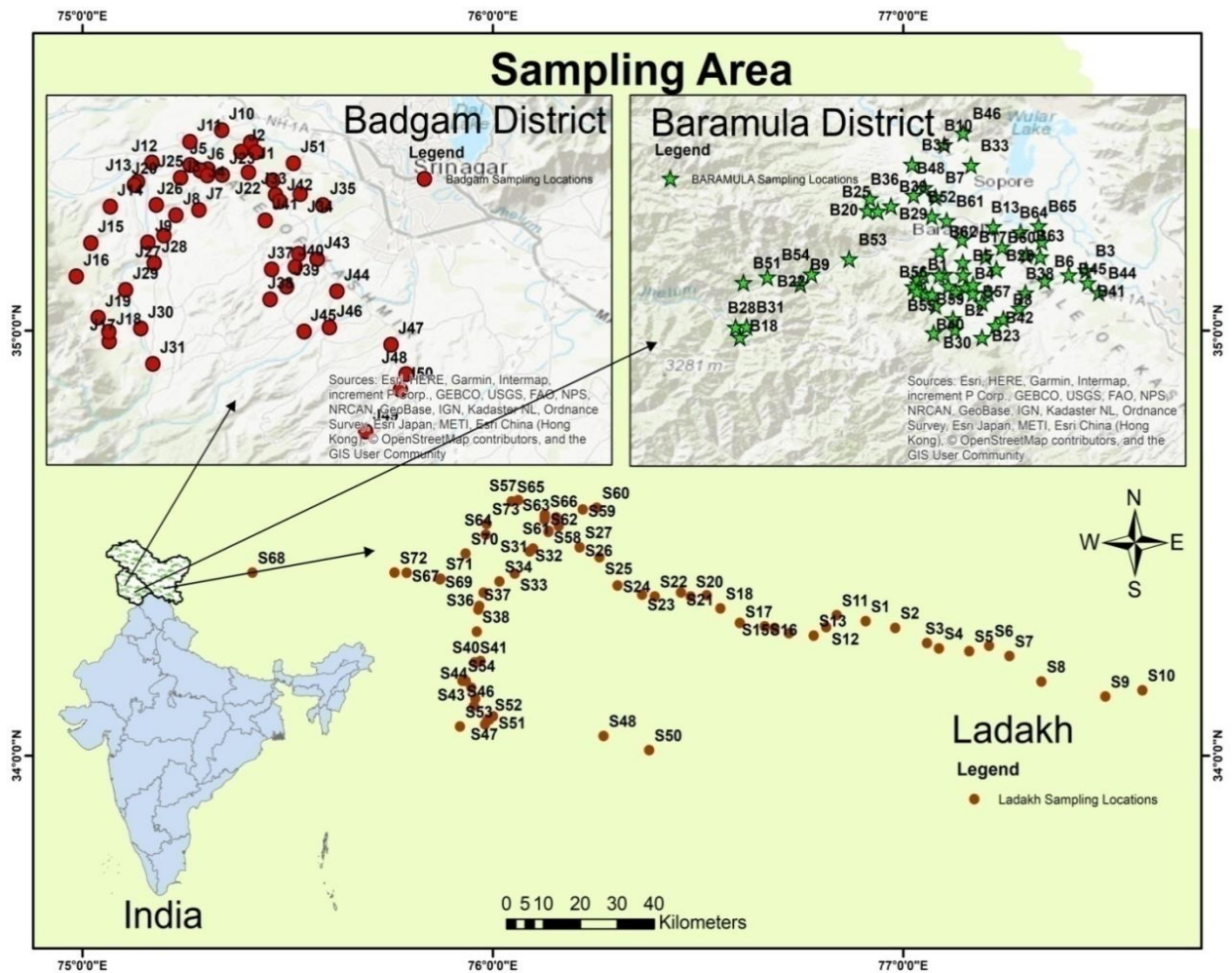
Figure 1.5: Study area sampling map

1.10.1 Rationale and Origin of Problem

Amid the expanding worldwide discussion on environmental risks, ionizing radiation's underlying risk has been a topic of considerable public and scientific concern. While nuclear accidents and man-made contaminants are frequently the subject of attention, naturally occurring radio nuclides that are lodged in the Earth's crust are a more prevalent and covert source of radiation exposure. This includes radon and thoron gases, which are known to be byproducts of the decay of uranium and thorium and pose a serious health risk, especially in indoor environments and groundwater systems. This issue is particularly significant in geologically sensitive areas since complex geomorphology, tectonic activity, and uranium-rich lithologies all contribute to elevated levels of natural radioactivity. Examples of this are the Jammu & Kashmir and Ladakh Union Territories in the Indian Himalayan arc. Even though these areas are recognized for their dramatic landscapes and strategic significance, geological indicators, including active faults, seismicity, and uranium-bearing rock formations, are significantly linked to elevated radon and thoron emissions.

Despite these factors, little scientific research has been done in the field of radioactive exposure and the potential risks to public health that are associated with it. On the other hand, many investigations have focused on neighboring Indian Himalayan states like Punjab, Himachal Pradesh, and Uttarakhand, exposing a crucial knowledge gap regarding the Himalayan frontier of J&K and Ladakh. The current study was brought about by this underrepresentation in radiological risk investigations. The study focuses on the districts of Baramulla, Budgam, and Leh-Ladakh in particular because of their varied geological complexity, climatic variability, and altitudinal profiles. Due to the local population's reliance on groundwater and conventional building methods that could encourage radon buildup indoors, these locations present a rare chance to evaluate natural radiation exposure in both residential settings and drinking water sources.

This study adopts an interdisciplinary approach rather than merely assessing radioactivity, looking at the ways that geological characteristics, environmental variables, and human activity interact to affect exposure risk. The assessment of radiological health takes note of a wider range of factors, including soil permeability, construction materials, and inadequate ventilation. The study also highlights the possible contribution of uranium-rich aquifers in high-altitude regions like Leh and Kargil to radon ingestion through water, a pathway that is frequently disregarded in standard monitoring procedures.

1.10.2 Study Highlights and Significance

- This study reflects an important advance in the knowledge of natural radiological exposure in the Himalayan regions of Jammu & Kashmir and Ladakh. It is the first regionally integrated study to quantify and understand the environmental distribution of radon and thoron radioactive gases, which are known to be carcinogenic around the world.

- The study's strength is its geospatial and geotectonic depth, which concisely links important geological parameters like fault zones and uranium-rich formations to rising radionuclide activity.

- By focusing on both ingestion and inhalation pathways, the study successfully connects environmental factors with public health hazards, especially the increased risk of lung cancer due to prolonged exposure. This draws attention to these susceptible groups and raises a public health issue that is still underrepresented in the literature.

- The present research goes beyond hazard identification by using an interdisciplinary approach involving environmental toxicology, health risk analysis, and geoscience to produce a knowledge base that could lead to useful, community-level solutions.

- This work provides the foundation for long-term monitoring, localized risk mapping, and sound evidence-based decision-making in environmental safety via establishing a regional radiological baseline.

References

- Airey, P., Hinton, T., & Twining, J. (2012). *The Scientific Basis* (pp. 1–57). https://doi.org/10.1016/B978-0-08-045016-2.00001-1

- Alsop, S. (1999). Understanding understanding: A model for the public learning of radioactivity. *Public Understanding of Science*, *8*(4), 267–284. https://doi.org/10.1088/0963-6625/8/4/301

- Allisy, A. (1996). Henri Becquerel: The Discovery of Radioactivity. *Radiation Protection Dosimetry*, *68*(1), 3–10. https://doi.org/10.1093/oxfordjournals.rpd.a031848

- Baatout, S. (Ed.). (2023). *Radiobiology Textbook*. Springer International Publishing. https://doi.org/10.1007/978-3-031-18810-7

- Beir,V.(1990). Health effects of exposure to low levels of ionizing radiation. *Biological effects of ionizing radiations.*, 22-45.

- Boudia, S. (2007). *Global Regulation : Controlling and Accepting Radioactivity Risks*. *23*(4), 389–406. https://doi.org/10.1080/07341510701527443

- Burgio, E., Piscitelli, P., & Migliore, L. (2018). Ionizing Radiation and Human Health: Reviewing Models of Exposure and Mechanisms of Cellular Damage. An Epigenetic Perspective. *International Journal of Environmental Research and Public Health*, *15*(9), 1971. https://doi.org/10.3390/ijerph15091971

- Chauvel, C. (2021). Long-Lived Radionuclides. In *Encyclopedia of Geology* (pp. 125–133). Elsevier. https://doi.org/10.1016/B978-0-08-102908-4.00177-6

- Caufield, C. (1990). *Multiple exposures: Chronicles of the radiation age*. University of Chicago Press.

- Committee on the Biological Effects of Ionizing Radiations, & U.S. Nuclear Regulatory Commission. (1988). *Health risks of radon and other internally deposited alpha-emitters: BEIR IV (Vol. 4)*. National Academies Press.

- Cohen, B. S., Eisenbud, M., Wrenn, M. E., & Harley, N. H. (1979). Distribution of Polonium-210 in the Human Lung. *Radiation Research*, *79*(1), 162.

https://doi.org/10.2307/3575029

- Cowart, J. B., & Burnett, W. C. (1994). The Distribution of Uranium and Thorium Decay-Series Radionuclides in the Environment—A Review. *Journal of Environmental Quality*, *23*(4), 651–662. https://doi.org/10.2134/jeq1994.00472425002300040005x

- Craft, E. S., Abu-Qare, A. W., Flaherty, M. M., Garofolo, M. C., Rincavage, H. L., & Abou-Donia, M. B. (2004). DEPLETED AND NATURAL URANIUM: CHEMISTRY AND TOXICOLOGICAL EFFECTS. *Journal of Toxicology and Environmental Health, Part B*, *7*(4), 297–317. https://doi.org/10.1080/10937400490452714

- Dainiak, N. (2002). Hematologic consequences of exposure to ionizing radiation. *Experimental Hematology*, *30*(6), 513–528. https://doi.org/10.1016/S0301-472X(02)00802-0

- DASH, S., HIAL, P., SENAPATI, S., & DALAİ, B. (2021). A Survey on Various Methods of Extraction and Recovery of Thorium. *Journal of the Turkish Chemical Society Section A: Chemistry*, *8*(4), 1197–1210. https://doi.org/10.18596/jotcsa.955211

- Debierne, A. (1899). Sur une nouvelle matière radio-active. *Comptes rendus, 129*(16), 593–595

- De Angelis, A. (2014b). Atmospheric ionization and cosmic rays: Studies and measurements before 1912. *Astroparticle Physics*, *53*(C), 19–26. https://doi.org/10.1016/j.astropartphys.2013.05.010

- Dunn, C. E. (1981). The biogeochemical expression of deeply buried uranium mineralization in Saskatchewan, Canada. *Journal of Geochemical Exploration*, *15*(1–3), 437–452. https://doi.org/10.1016/0375-6742(81)90078-9

- De Angelis, A. (2014a). Atmospheric ionization and cosmic rays: Studies and measurements before 1912. *Astroparticle Physics*, *53*(C), 19–26. https://doi.org/10.1016/j.astropartphys.2013.05.010

- Donald Blaufox, M. (1996). Becquerel and the discovery of radioactivity: Early

concepts. *Seminars in Nuclear Medicine*, *26*(3), 145–154. https://doi.org/10.1016/S0001-2998(96)80019-5

- Draganić, I. G., Draganić, Z. D., & Adloff, J.-P. (2020). *Radiation and Radioactivity on Earth and Beyond*. CRC Press. https://doi.org/10.1201/9781003069089

- Dyck, W. (1979). *Application of hydro geochemistry to the search for uranium.*

- Eisenbud, M. (1984). Sources of Ionizing Radiation Exposure. *Environment: Science and Policy for Sustainable Development*, *26*(10), 6–33. https://doi.org/10.1080/00139157.1984.9931267

- Epperly, M. W., Sacher, J. R., Krainz, T., Zhang, X., Wipf, P., Liang, M., Fisher, R., Li, S., Wang, H., & Greenberger, J. S. (2017). Effectiveness of analogs of the GS-Nitroxide, JP4-039, as total body irradiation mitigators. *In Vivo*, *31*(1), 39–44. https://doi.org/10.21873/invivo.11022

- Feinendegen, L. E., Pollycove, M., & Sondhaus, C. A. (2004). Responses to Low Doses of Ionizing Radiation in Biological Systems. *Nonlinearity in Biology, Toxicology, Medicine*, *2*(3). https://doi.org/10.1080/15401420490507431

- Flakus, F. N. (1982). Radiation detection Detecting and measuring ionizing radiation-a short history. *IAEA Bulletin*, *23*(4), 31–36.

- George, A. C. (2005). Historical development of the Natural Radiation Environment Symposia. *Radioactivity in the Environment*, *7*(C), 3–11. https://doi.org/10.1016/S1569-4860(04)07001-9

- Gill, M. (1900). *MAGAZINE*. *49*(296).

- Hatra, G. (2018). Radioactive pollution: An overview. *The Holistic Approach to Environment, 2018*, *8*, 48–65. https://hrcak.srce.hr/202085

- Hendee, W. R., & Marc Edwards, F. (1986). ALARA and an integrated approach to radiation protection. *Seminars in Nuclear Medicine*, *16*(2), 142–150. https://doi.org/10.1016/S0001-2998(86)80027-7

- International Atomic Energy Agency & World Health Organization. (1967). *Risk evaluation for protection of the public in radiation accidents (No. 21)*. IAEA.

- International Atomic Energy Agency. (1990). *The environmental behaviour of radium (Vol. 1, No. 310).* International Atomic Energy Agency.

- International Commission on Radiological Protection. (1977). *Recommendations of the International Commission on Radiological Protection (ICRP Publication 26).*

- International Commission on Radiological Protection. (1990). *Recommendations of the International Commission on Radiological Protection (ICRP Publication 60).*

- International Commission on Radiological Protection. (2008). *Recommendations of the International Commission on Radiological Protection (ICRP Publication 103).*

- Jennings, W. A. (2007). Evolution over the past century of quantities and units in radiation dosimetry. *Journal of Radiological Protection*, *27*(1), 5–16. https://doi.org/10.1088/0952-4746/27/1/R01

- Kathren, R. L. (1998). NORM sources and their origins. *Applied Radiation and Isotopes*, *49*(3), 149–168. https://doi.org/10.1016/S0969-8043(97)00237-6

- Kardamakis, D., Baatout, S., Bourguignon, M., Foray, N., & Socol, Y. (2023). History of Radiation Biology. In *Radiobiology Textbook* (pp. 1–24). Springer International Publishing. https://doi.org/10.1007/978-3-031-18810-7_1Kolodny, Y., & Kaplan, I. . (1970). Uranium isotopes in sea-floor phosphorites. *Geochimica et Cosmochimica Acta*, *34*(1), 3–24. https://doi.org/10.1016/0016-7037(70)90148-1

- Kragh, H. (2012). *Rutherford, Radioactivity, and the Atomic Nucleus*. 1–30. http://arxiv.org/abs/1202.0954

- Linsalata, P. (1989). Exposure to long-lived members of the uranium and thorium decay chains. *International Journal of Radiation Applications and Instrumentation. Part C. Radiation Physics and Chemistry*, *34*(2), 241–250. https://doi.org/10.1016/1359-0197(89)90232-4

- Lavarnway, K. (2006). *Radon-a Dangerous Link in the Decay Series of Uranium.*

1–66.

- Lord Rutherford, 1871 - 1937. (1938). *Obituary Notices of Fellows of the Royal Society*, *2*(6), 394–423. https://doi.org/10.1098/rsbm.1938.0025

- Lindell, B. (2020). Pandora's Box. In *The Ocean Reader.* https://doi.org/10.1215/9781478007456-068

- Luo, G., Sun, L., Li, H., Chen, J., He, P., Zhao, L., Tang, W., & Qiu, H. (2021). The potent radioprotective agents: Novel nitronyl nitroxide radical spin-labeled resveratrol derivatives. *Fitoterapia*, *155*, 105053. https://doi.org/10.1016/j.fitote.2021.105053

- Magill, J. (2003). *Nuclides.net: An integrated environment for computations on radio nuclides and their radiation (with 79 tables and a CD-ROM).* Springer Science & Business Media.

- Magill, J., & Magill, J. (2003). Background on Radioactivity. Nuclides. net: An Integrated Environment for Computations on Radio nuclides and their Radiation, 25-66.

- Marshall, J. L., & Marshall, V. R. (2003). Ernest Rutherford, the "true discoverer" of radon. *Bulletin for the History of Chemistry*, *28*(2), 76–83.

- Marieskind, H. I. (1976). Environmental carcinogens. *Women and Health*, *1*(2), 2. https://doi.org/10.1093/jaoac/64.2.348

- Mavragani, I., Nikitaki, Z., Souli, M., Aziz, A., Nowsheen, S., Aziz, K., Rogakou, E., & Georgakilas, A. (2017). Complex DNA Damage: A Route to Radiation-Induced Genomic Instability and Carcinogenesis. *Cancers*, *9*(7), 91. https://doi.org/10.3390/cancers9070091

- Mohan, S., & Chopra, V. (2022). Biological effects of radiation. In *Radiation Dosimetry Phosphors* (pp. 485–508). Elsevier. https://doi.org/10.1016/B978-0-323-85471-9.00006-3

- Miousse, I. R., Kutanzi, K. R., & Koturbash, I. (2017). Effects of ionizing radiation on DNA methylation: from experimental biology to clinical

applications. *International Journal of Radiation Biology*, *93*(5), 457–469. https://doi.org/10.1080/09553002.2017.1287454

- Nair, P. V. N., & Nambi, K. S. V. (1997). *Progress report of Environmental Assessment Division: 1995-1997*. India.

- National Committee on Radiation Protection & Measurements (US). (1987). *NCRP Report*. National Council on Radiation Protection and Measurements.

- Nelson, A. W., Eitrheim, E. S., Knight, A. W., May, D., Mehrhoff, M. A., Shannon, R., Litman, R., Burnett, W. C., Forbes, T. Z., & Schultz, M. K. (2015). Understanding the radioactive ingrowth and decay of naturally occurring radioactive materials in the environment: An analysis of produced fluids from the marcellus shale. *Environmental Health Perspectives*, *123*(7), 689–696. https://doi.org/10.1289/ehp.1408855

- Nilsson, J., Bauden, M. P., Nilsson, J. M., Strand, S.-E., & Elgqvist, J. (2015). Cancer Cell Radiobiological Studies Using In-House-Developed α-Particle Irradiator. *Cancer Biotherapy and Radiopharmaceuticals*, *30*(9), 386–394. https://doi.org/10.1089/cbr.2015.1895

- Olley, J. M., Murray, A., & Roberts, R. G. (1996). The effects of disequilibria in the uranium and thorium decay chains on burial dose rates in fluvial sediments. *Quaternary Science Reviews*, *15*(7), 751–760. https://doi.org/10.1016/0277-3791(96)00026-1

- Radvanyi, P., & Villain, J. (2017a). The discovery of radioactivity. *Comptes Rendus. Physique*, *18*(9–10), 544–550. https://doi.org/10.1016/j.crhy.2017.10.008Rutherford, E. (1900). *321 By. LXXXI.*

- Riudavets, M., Garcia de Herreros, M., Besse, B., & Mezquita, L. (2022). Radon and Lung Cancer: Current Trends and Future Perspectives. *Cancers*, *14*(13), 3142. https://doi.org/10.3390/cancers14133142

- Roy, R., Halder, S., & Singh, P. K. (2024). Internal Dose Evaluation, Quality Assurance and Uncertainty Analysis. In *Handbook on Radiation Environment, Volume 2* (pp. 507–539). Springer Nature Singapore. https://doi.org/10.1007/978-

981-97-2799-5_18

- Romshoo, S.A., Rashid, I., Altaf, S., Dar, G.H., 2020. Jammu and Kashmir State: An Overview. pp. 129–166. https://doi.org/10.1007/978-981-32-9174-4_6
- Sadat-Noori, M., Santos, I. R., Sanders, C. J., Sanders, L. M., & Maher, D. T. (2015). Groundwater discharge into an estuary using spatially distributed radon time series and radium isotopes. *Journal of Hydrology*, *528*, 703–719. https://doi.org/10.1016/j.jhydrol.2015.06.056
- Sankaranarayanan, K., & Wassom, J. S. (2008). Reflections on the impact of advances in the assessment of genetic risks of exposure to ionizing radiation on international radiation protection recommendations between the mid-1950s and the present. *Mutation Research/Reviews in Mutation Research*, *658*(1–2), 1–27. https://doi.org/10.1016/j.mrrev.2007.10.004
- Supartinah. (1989). *NBER Working Paper Series*, *58*(58), 99–104. https://www.unhcr.org/publications/manuals/4d9352319/unhcr-protection-training-manual-european-border-entry-officials-2-legal.html?query=excom 1989
- Thorne, M., Limited, A., & Mount, K. (2003). Background radiation: natural and man-made Background radiation: natural and man-made M C Thorne. *J. Radiol. Prot*, *23*, 29–42. http://iopscience.iop.org/0952-4746/23/1/302
- UNSCEAR. 1986. United Nations Scientific Committee on the Effects of Atomic Radiation. Sources and effects of ionizing radiation. New York, NY
- UNSCEAR. 1993. United Nations Scientific Committee on the Effects of Atomic Radiation. Sources and effects of ionizing radiation. New York, NY.
- Valentin, J., & Clement, C. H. (n.d.). *Bo Lindell ' s History of Radiation , Radioactivity , and Radiological Protection*. 1–4.
- Vinson, D. S., Vengosh, A., Hirschfeld, D., & Dwyer, G. S. (2009). Relationships between radium and radon occurrence and hydrochemistry in fresh groundwater from fractured crystalline rocks, North Carolina (USA). *Chemical Geology*, *260*(3–4), 159–171. https://doi.org/10.1016/j.chemgeo.2008.10.022
- Von Blanckenburg, F., & Willenbring, J. K. (2014). Cosmogenic Nuclides: Dates and Rates of Earth-Surface Change. *Elements*, *10*(5), 341–346.

https://doi.org/10.2113/gselements.10.5.341

- Wambersie, A., Zoetelief, J., Menzel, H. G., & Paretzke, H. (2005). The ICRU (International Commission on Radiation Units and Measurements): its contribution to dosimetry in diagnostic and interventional radiology. *Radiation Protection Dosimetry*, *117*(1–3), 7–12. https://doi.org/10.1093/rpd/nci701

- Zakariya, N. I., & Kahn, P. M. (2014). Review Article Benefits and Biological Effects of Ionizing Radiation. *Scholars Academic Journal of Biosciences (SAJB)*, *2*(9), 583–591. www.saspublisher.com

CHAPTER 2

REVIEW OF LITERATURE

2.1 Uranium

Uranium is considered to be the ancestor of radon gas, which is generated when uranium undergoes various decay processes in a radioactive disintegration process. Therefore, uranium becomes an important point of discussion in the present thesis and is significantly summarized from various literature surveys. Uranium, a naturally occurring radioactive heavy metal, is toxic and found abundantly in the environment. According to Waseem et al. (2015), uranium a lithophlic element that is as prevalent as silver, gold, and light rare earth elements with three its three primary uranium ore minerals davidite, pitchblende, and uraninite.

The Colorado Plateau, Western Central Plateau and other geologically diverse regions of the United States have been reported where naturally occurring uranium exists in groundwater at high concentrations (Orloff et al., 2004). In contrast, uranium levels in groundwater are typically low in the eastern United States. However, isolated areas, especially in South Carolina, have been found to have higher uranium concentrations.

Brindha and Elango (2013) evaluated uranium levels found in groundwater in the Nalgonda district of Andhra Pradesh and reported that nearly 2% of the groundwater in the area is considered unfit for human consumption, based on the 60 ppb guideline provided by the (AERB, India). Similarly, Virk et al. (2016) conducted an analysis using LED flourimetry to assess uranium concentrations in groundwater across 33 locations of North Punjab and observed its average concentration of 16.93μg/L, lying within the (AERB) safe limit of 60μg/L.

Wu et al. (2014) highlight applications of uranium (U) in nuclear energy production and ammunition as among its most common uses. Its chemical toxicity,

specifically when consumed through food and drinking water, is considered to be more serious than the radiological risk. The assessment of health risks related to uranium occurance in water is a major issue in a highly populated nation like India (D. N., B. Panda, C. S., et al., 2021). The growing population and rising demands for water, especially in the southern regions, intensify this urgency. Exposure to uranium-contaminated water can be detrimental to health in both chemical and radiological ways. Ramesh et al. (2021) described uranium as a nephro-toxic chemical that may result in kidney damage, reduction in bone density, and other adverse effects.

Over the past 18 years, uranium exposure guidelines have evolved from being based on radiological risks to considering chemical toxicity. Studies indicate that there may be subclinical renal effects, but major health effects are uncommon at concentrations above 100μg/L. In 2011, the drinking water limit was increased from 2 to 30μg/L to align with the MCL set by the USEPA. However, concerns remain about whether the current recommendation adequately accounts for the toxicological and epidemiological potential risks associated with uranium (Corlin et al., 2016).

Geological makeup of a region and human influences such as mining activities, coal ash waste from thermal plants and phosphate fertilizer use in agriculture primarily influence the underground uranium concentrations. Rocks and minerals that contain uranium weather and release it into the soil and water. Due to its potential to exist in several oxidation states, mainly tetravalent and hexavalent, it is more prevalent in granitic formations. U(VI) compounds are more mobile than U(IV) compounds due to their high solubility in water, more atomic radius (0.97 Å), and high reactivity. Under oxidizing conditions, groundwater in fractures contains dissolved oxygen, which facilitates uranium transformation into its more soluble hexavalent form (Balaram et al., 2022).

Igneous rocks, particularly granites rich in silica, concentrate uranium during geological processes like partial melting and fractional crystallization, whereas basaltic and ultramafic rocks have lower uranium levels. Through geochemical enrichment, uranium

is more prevalent in phosphorite (0.01%–1% U) and forms primary and secondary uranium ores (0.1%–5% U). Weathering and rock interactions contribute to uranium concentrations in groundwater, and uranium is abundant in seawater as well (World Health Organization, 2001).

Hard rocks, especially granites, report the highest uranium concentrations in groundwater (Adithya et al., 2019). Hydrodynamic conditions, groundwater flow direction, and redox processes in transition zones significantly affect the formation of economically viable uranium deposits (Chen et al., 2021). According to Rose & Wright (1980), over 90% of sedimentary rock-hosted uranium deposits result from crucial geochemical processes. Global climate change could increase groundwater exposure to toxic elements. Reduced aquifer flushing could result in higher uranium concentrations in water sources, and less humid arid regions that rely more on groundwater (Mitchell et al., 2011).

Various uranium remediation techniques have been proposed, including biological, chemical, and physical methods (Li & Zhang, 2012). Physical methods like membrane separation, coagulation, and reverse osmosis are effective but expensive. High-efficiency chemical co-precipitation methods include FeS_2, MnO_2, zero-valent iron, and photochemical phosphates. Among biological methods, bioremediation offers a promising solution for uranium removal from water.

2.2 General Overview of Radon in the Environment: Sources, Health Risks, and Advanced Measurement Techniques

2.2.1 Introduction

Radon ($222Rn$) a radioactive gas primarily generated from its precursor U, which is naturally present in various geological substrates rocks, soil, and water. The amount of radon released depends largely on geological factors and uranium concentration in the surrounding materials (Nunes, 2023). Higher radon concentrations are commonly found

in regions rich in uranium deposits, such as granite, metamorphic rocks, and shale (Dobrzyńska et al., 2023).

Radon emissions from geogenic sources, including radio nuclides in rocks and soils, are important in analyzing the (GRP) an essential indicator of radon hazards (Benà et al., 2024). Soil composition, permeability, and interstitial pore spaces significantly influence radon movement and accumulation. Radon gas can migrate through cracks and fractures, allowing it to reach distant locations before decaying (Khan et al., 2023). It can accumulate indoors due to infiltration from soil gas, particularly in confined spaces like homes and mines (Muhammad et al., 2023).The movement of radon is governed by variables such as soil porosity, permeability, and diffusion coefficient. Water has a lower diffusion coefficient than air, which reduces radon mobility through soil (Stoulos, 2024). Moreover, the temperature differential between indoor and outdoor spaces significantly affects radon accumulation in buildings. Poor ventilation can elevate indoor radon, stressing the necessity of continuous monitoring and mitigation strategies (Baltrocchi et al., 2024).

2.2.2 Radon Levels in Variable Environmental Conditions and Health Risks Associated with its Exposure

Radon exposure, primarily through inhalation and contaminated groundwater, poses significant health risks. Studies indicate that radon exposure may contribute to approximately 2% of cancer deaths in Europe and 1%–7% of lung cancer deaths in the US, particularly in regions where groundwater use is prevalent (Giammanco et al., 2023). Although some studies suggest an association between radon in drinking water and stomach and intestinal cancers, conclusive evidence remains lacking. Similarly, research has not definitively established a connection between high radon exposure and thyroid cancer in volcanic regions.

Next to smoking, ^{222}Rn along with its progenies pose a serious effect to human health (T.K. Abed et al.). These decay products, initially positively charged, interact with

atmospheric trace gases, forming radioactive aerosols that contribute significantly to radiation exposure (Vaupotič, 2024). Regulatory agencies recommend maintaining radon levels below 100Bq/L in drinking water to minimize public health risks.

Radon concentrations vary globally due to differences in geological formations, soil composition, and aquifer interactions. Radon emissions from radium-rich soils and natural gas used in homes can elevate indoor radon levels (Bulut & Şahin, 2024). Exposure from indoor radon accounts for approximately more than 20000 lung cancer cases per annum in the United States. The primary cause is alpha radiation, which induces severe genetic damage, including chromosomal alterations and mutations. Alpha particles primarily damage DNA through double-strand breaks, which may be misrepaired, leading to genomic instability. Initially thought to affect only the nucleus, research suggests alpha irradiation can also impact extra nuclear structures, influencing overall DNA integrity. Continued in vivo research is crucial for refining micro dosimetric models and improving radon-related cancer risk assessments (Radford & Hunt, 1964; Samet et al., 1987; Blöcher, 1988; Puskin & Nelson, 1989; Evans, 1992; Little, 1993; Prise, 1994; WHO, 2007).

	European pooling study[a]		North American pooling study[b]	
	% risk increase (95% CI)			% risk increase (95% CI)
Sex				
	Men	11 (4,21)	Men	3 (-4, 24)
	Women	3 (-4,14)	Women	19 (2, 46)
	p for heterogeneity	*0.19*		
Age at disease occurrence (years)				
	<55	<0 (<0, 20)	<60	2 (<0, 35)
	55-64	14 (3, 31)	60-64	80 (13, 257)
	65+	7 (1, 16)	65-69	2 (-5, 28)
			70-74	33 (1, 102)
			75+	-2 (-10, 30)
	p for trend	*0.98*		
Smoking status				
	Current cigarette smoker	7 (-1, 22)	Never smoked	
	Ex-smoker	8 (0, 21)	cigarettes	10 (-9, 42)
	Lifelong non-smoker	11 (0, 28)	Current or ex-cigarette	
	Other	8 (-3, 56)	smoker	10 (-2, 33)
	p for heterogeneity	*0.92*		
Overall				
	Based on measured radon	8 (3, 16)	Based on measured radon	11 (0, 28)

Table 2.1: Research from Europe and North America shows a higher risk of lung cancer linked to each 100 Bq/m³ rise in radon levels (Darby et al., 2005; Krewski et al., 2006).

Groundwater from uranium-rich aquifers can also have high radon concentrations due to prolonged interaction with surrounding rocks (Yousefian et al., 2024). Awareness of radon-prone areas is essential for effective risk assessment, regulatory compliance, and mitigation strategies (Malakootian & Nejhad Soltani, 2017). Surface water generally contains negligible amounts of radon; however, groundwater, particularly in granitic regions, can exhibit significantly high concentrations (Rani et al., 2023). Geological formations also influence uranium and radium distribution, impacting soil particle composition, gamma dose rates, and associated health risks (Singh et al., 2024).

2.2.3 Advanced Radon Measurement Techniques

Accurate radon measurement is critical for health and environmental risk assessments. The twin cup dosimeter, designed with a pinhole mechanism, enables accurate measurement of ^{222}Rn and ^{220}Th concentrations in controlled settings (Singh & Kant, 2023). The RnDuo developed by BARC facilitates the assessment of radon, thoron exhalation rates, allowing for comprehensive indoor air quality assessments (Rani et al., 2023).

Additionally, the RAD-7 detector provides real-time monitoring and advanced detection capabilities, supporting regulatory compliance and public health initiatives (Kaur et al., 2024). These modern techniques enhance research efforts and improve the management of radon risks in water and indoor environments.

2.2.4 Environmental and Geological Influences

Local geology plays a critical role in radon risk assessment. High radon levels are common in uranium- or radium-rich regions. However, even low-risk areas can have elevated indoor radon concentrations due to building design as described in figure below .Radon risk assessments rely on geological surveys, soil permeability data, surface radiation maps, and direct radon measurements (Ummah, 2019).
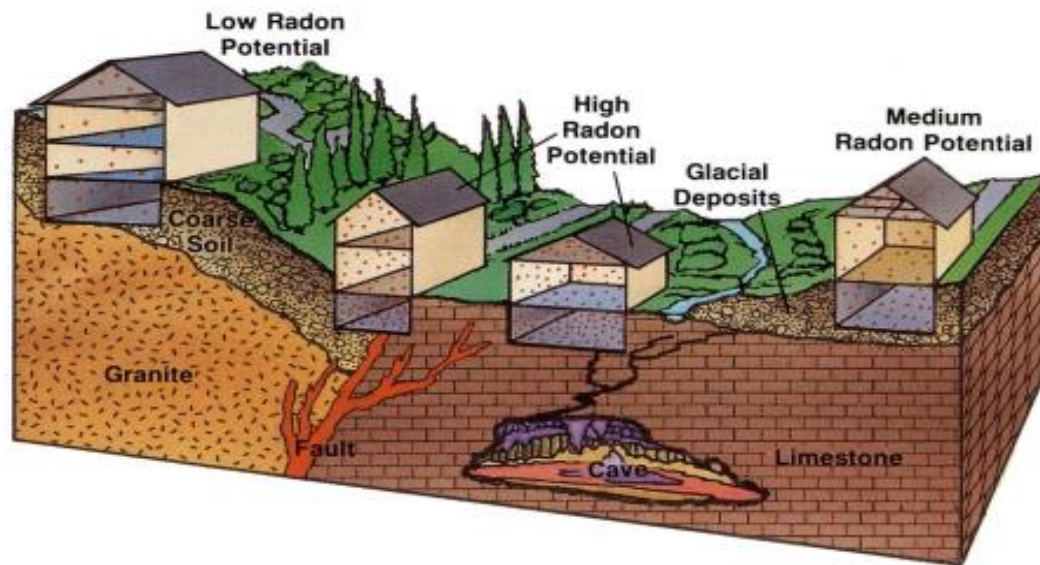
Figure 2.1: Impact of geology and building design on indoor radon levels

Under specific conditions, indoor radon concentrations can exceed 110,000Bq/m³ dramatically higher than outdoor levels. Extended exposure results from lower indoor air pressure, which draws radon into buildings through cracks, joints, and porous materials. Prolonged inhalation at such high levels significantly increases lung cancer risk (Knol, 2005).

Radon mobility fluctuates with soil moisture levels, influencing indoor Concentrations. Porous soils enhance radon diffusion, while moisture saturation can either trap or release radon. Radon recoil from solid surfaces depends on soil porosity, encountering water films and air pockets that either hinder or facilitate movement. Building material permeability also affects indoor radon retention. Fine-grained, dense materials such as cement reduce radon infiltration, whereas coarse-grained materials like sand allow greater radon transport. Cement structures generally provide better radon protection than mud houses, reducing long-term exposure risks (Sun & Furbish, 1995; Chauhan et al., 2008).

2.2.5 Radon Transport and Moisture in Porous Building Materials

Numerical analyses indicate that radon transport through building materials is highly sensitive to moisture content. Material porosity primarily dictates the effect of water on radon concentration and exhalation. Studies suggest that in low-porosity materials such as granite and concrete ($\varphi < 0.2$), radon levels rise rapidly as moisture increases until a volumetric water content of about 30% is reached. At this point, radon emanation becomes the dominant process over molecular diffusion (Sun & Furbish, 1995). In contrast, medium-porosity materials like cement, limestone, and brick ($0.3 < \varphi < 0.45$) exhibit radon concentration increases up to about 10% moisture content before declining, attributed to molecular diffusion within the porous matrix. The relationship between diffusion and emanation coefficients, both heavily influenced by water content, governs radon exhalation. Research shows that radon emanation is more pronounced in saturated conditions than in dry environments. For instance, when transitioning from dry to fully saturated conditions, the emanation coefficient in low-porosity materials such as concrete ($\varphi = 0.12$) increases by 86%. In contrast, in higher-porosity materials, emanation plateaus at water contents between 5% and 10% due to the development of water films along pore surfaces that inhibit additional recoil. Moisture, however, has the opposite effect on radon diffusion (Cosma et al., 2001; Menetrez et al., 1996; Misdaq et al., 1998; Przylibski, 2000).

2.3 Radon-222: Geological Sources, Transport Mechanisms, and Seismic Indicators

2.3.1 Geological and Geochemical Influence on Radon Mobility

Geological and geochemical substrates play an important role in the transport mechanisms that enable radon migration from its uranium source. Processes such as groundwater flow, hydrothermal activity, and high-temperature fluid interactions contribute to the mobilization of uranium, thorium, and radium, leading to uranium

concentration in ore deposits and influencing radon production. Radon emanates from mineral surfaces and traverses rock formations, either dissolved in groundwater or as a free gas. The efficiency of radon migration is dictated by diffusion, advection, porosity, permeability, and structural discontinuities such as fractures. Radon generation within geochemical halos is strongly affected by uranium enrichment processes, which give rise to economically significant ore deposits. The movement of fluids and geochemical interactions that govern uranium mobility are crucial in determining radon release from subsurface uranium-rich formations (Gingrich, 1984).

2.3.2 Radon in Underground Uranium Mines

The predominant sources of radon in underground uranium mines include mine water, backfill mill tailings, broken ore, and emissions from the ore body itself. The factors affecting radon exhalation include uranium grade, radium concentration, porosity, moisture content, and the mineralogical composition of the ore. Additionally, environmental and operational factors such as temperature variations, ventilation effectiveness, and atmospheric pressure fluctuations influence radon dispersion within mine atmospheres (Sahu et al. 2016).

2.3.3 Regional Radon Concentrations and Lithological Influence

Studies conducted in the Bhilangana Valley of the Garhwal region indicate that high radon concentrations in soil, air, and groundwater are strongly correlated with uranium mineralization in gneiss and quartzite rock formations. Structural elements such as shear zones, faults, and thrusts enhance radon mobility. In contrast, lithologies composed predominantly of schists and phyllites demonstrate lower radon emissions, illustrating the substantial influence of rock type on radon distribution (Choubey & Ramola, 1997).

2.3.4 Radon as a Geochemical Tracer and Seismic Activity Indicator

Groundwater geochemistry plays a vital role in radon transport and mobility, impacting its concentration and spatial distribution. Radon primarily migrates via convective and pressure-driven flow in groundwater systems, particularly along faults and fractures. Hydrothermal activity and subsurface physicochemical conditions modulate radon solubility and mobility. Variations in groundwater chemistry, including temperature shifts, redox potential changes, and pH fluctuations, critically affect radon dissolution and exhalation. A comprehensive understanding of these interactions is essential for environmental monitoring, uranium exploration, seismic precursor studies, and groundwater contamination assessments (Ball et al., 1991).

Fluctuations in radon levels, dissolved elemental compositions, and stable isotope ratios in groundwater chemistry are regarded as potential precursors to seismic events. Additional seismic precursors include shear wave splitting, micro-seismic activity, borehole water level changes, and variations in seismic wave velocities. These indicators are often linked to rock volume expansion, which alters subsurface fluid dynamics and geochemical equilibrium (Skelton et al., 2014). Since the 1970s, countries such as the United States, Japan, China, and Italy have actively monitored soil gas emissions and groundwater radon levels for earthquake prediction purposes. Anomalous behavior in noble gases, such as fluctuations in helium/argon ratios and radon concentrations, has been correlated with impending seismic activity. A notable example is the 1966 Tashkent earthquake, where radon levels in deep wells nearly doubled before the event and returned to baseline afterward (Sano et al., 2016).

2.3.5 Radon Degassing and Fault Zones

The release of radon over fault zones is controlled by tectonic activity, fracture fill properties, water saturation levels, and surface permeability. These factors collectively form distinct radon anomalies, manifesting as elongated or isometric degassing zones along permeable fault segments. Elevated radon concentrations in soil gas near fault lines are indicative of enhanced radon transport through fractured bedrock. The upward

migration of fluids and gas bubbles through these fractures further contributes to surface radon emissions (Pulinets et al., 2024; Iwata et al., 2018).

2.3.6 Case Studies of Radon as a Seismic Precursor

Tashkent, 1966: Prior to the April 26, 1966, Tashkent earthquake (magnitude 5.5), radon levels in deep wells (1200–2400 m) exhibited a steady increase, reaching two to three times their baseline values before normalizing post-earthquake. (de Acosta, 2013).

Tohoku-Oki Earthquake, 2011: A study conducted in a Korean limestone cave revealed abnormally high peaks in ^{220}Rn levels preceding the M9.0 Tohoku-Oki Earthquake in February 2011. Researchers noted that while ^{222}Rn levels were influenced by environmental factors, ^{220}Rn appeared to be a more reliable seismic indicator (Hwa Oh & Kim, 2015).

Bohai Bay Basin & Tangshan Earthquake, 1976: Radon fluxes exhibited significant variability, with the Bohai Bay Basin displaying higher values than other seismic regions. Prior to the MS 7.8 Tangshan earthquake, radon concentrations reached 57.67kBq/m³, with a flux of 334.56mBq/m²·s (Chen et al., 2018).

2.3.7 Advances in Radon Monitoring and Seismic Hazard Assessment

Recent developments in radon monitoring technology have led to the establishment of radon surveillance networks in China and Italy, where machine learning algorithms are employed for data analysis. Active fault zones, characterized by extensive surface areas within damage zones, facilitate radon transport by acting as conduits for groundwater movement. Radon mapping has proven to be a valuable tool in assessing fault dynamics and seismic hazards, with strong correlations observed between radon concentration anomalies and tectonic activity (Kawabata et al., 2024).

Active tectonic faults function as primary conduits for crustal degassing, allowing radon to migrate through fractures and fault planes. The permeability of fault structures is dictated by factors such as tectonic creep, fracture fill composition, water saturation, and

overlying sediment permeability. Variations in stress and strain associated with seismic activity drive crustal fluid migration, resulting in elevated radon emissions along fault lines. Numerous studies have reported radon concentrations exceeding levels expected from ^{238}U decay alone in tectonically active regions (Ciotoli et al., 2014; King et al., 1996; Miklyaev et al., 2022).

2.4 Review of Natural Radioactivity in Indoor Air, Water, and Soil

Research on natural radiation levels and radon exposure has been widely explored in various geographical regions, revealing significant findings regarding radiological hazards and health implications. (Kumar et al ., 2024) in their reported elevated levels of natural radiation, attributed primarily to the mineral composition of soil and rock formations, thereby offering crucial insights into the region's radiological profile. Similarly, (Chahal et al., 2024) examined radionuclide concentrations, specifically ^{236}U and ^{232}Th, alongside radon (^{222}Rn) and thoron (^{220}Rn) exhalation rates in Mahendergarh, near the Aravalli range in India. Using NaI (Tl) gamma spectroscopy, they demonstrated that hill soils, influenced by granite and gneiss, exhibited significantly higher radioactivity than field soils.

A separate study by (Kumar & Kumar., 2024) assessed soil samples from villages surrounding the Narora Atomic Power Plant in India. Their results indicated that the levels of radio nuclides ^{226}Ra, ^{232}Th, and ^{40}K exceeded UNSCEAR standards, with the mean gamma dose rates for indoor and outdoor environments surpassing global averages. Additionally, the annual effective dose rate exceeded the 1mSv/year threshold, raising potential radiological concerns. In the context of building materials, (Ambrosino et al., 2024) investigated radon emanation and exhalation properties from volcanic gray tuff in Sant'Agata de' Goti, Campania, Italy. Their study suggested a significant increase in emanation and exhalation rates, potentially linking these materials to an elevated lung cancer risk. Residential radon exposure in Iran has also been comprehensively reviewed

by (Yousefian et al., 2024), who underscored potential health implications associated with raising indoor radon levels, particularly in the Mazandaran province.

In a pioneering study (Chakan et al., 2024) assessed radon levels in groundwater from Kupwara, Kashmir, revealing that 10.6% of samples exceeded UNSCEAR's radon limit, while 1.2% surpassed WHO guidelines. (Rahim et al., 2024) examined uranium levels in groundwater from central districts of Jammu and Kashmir. Their findings indicated that uranium concentrations remained within WHO and USEPA safety limits, suggesting minimal radiological and chemical health risks. Geological factors were identified as key contributors to the region's low radium and thorium levels, ensuring the groundwater's safety for consumption. The radiological assessment of soil samples from Gurugram, India, conducted by (Gurugram et al., 2023), revealed notable radon and thoron exhalation levels, with elevated thoron emissions in the soil. Furthermore, (Singh & Kant., 2023) reported fluctuations in indoor radon, thoron, and their progenies in 150 homes in Gurugram, with peak concentrations observed during winter due to limited ventilation in both modern and mud-constructed dwellings.

(Küçükönder et al., 2023) provided a detailed evaluation of radon activity concentrations in the soil of Kahramanmaraş. Their analysis reported radon levels ranging from 62.87 to 421.90Bq/m³, with an average of 179.36 ± 7.50 Bq/m³ and exhalation rates between 8.44 and 56.68mBq/m²h. The results confirmed that radon levels in the region remained within national and international safety standards, posing no significant radiological threat. Water safety assessments have also been a focal point of recent studies. (Dongre et al., 2023) examined radon concentrations in Shankaraghatta's drinking water, noting that while the levels exceeded USEPA thresholds, the estimated radiation doses remained within WHO and EC safety limits, affirming the water's safety for consumption.

The seasonal dynamics of indoor radon concentrations have been explored by (Belete & Shiferaw., 2022), who found that levels typically peaked during winter and

declined in summer. Their study highlighted the role of environmental factors and construction styles, with older homes experiencing higher radon infiltration due to structural cracks and porous building materials. (Somsunun et al., 2022) investigated the link between indoor radon exposure and lung disease chances in Upper Northern Thailand. Measurements from 192 homes across eight provinces revealed radon levels ranging from 11 to 405Bq/m³. The study identified significant differences in radon concentrations between the homes of lung cancer patients and healthy individuals, supporting an evidence for association of radon exposure with rising cancer risks.

In an earlier study, (Kumar et al., 2021) assessed spring water in Bageshwar, determining that while the water remained radiologically safe for consumption, elevated radon levels and potential uranium-related chemical toxicity could pose health concerns, particularly for infants and children. They emphasized the need for continued monitoring to ensure safe drinking water for vulnerable populations. (Yazzie et al., 2020) conducted an indoor radon survey in 51 homes on the Navajo Nation between November 2014 and May 2015. Their findings indicated an average radon concentration of 60.5Bq/m³, with the highest levels recorded in concrete and cement homes (105.7Bq/m³). This study provided valuable data on radon exposure patterns in indigenous communities.

2.4.1 Subject Specific Literature Survey in Context to Regions with Distinct Geology Locally and Globally

(Cho et al., 2015) described how elevated radon levels in groundwater are significantly influenced by geological factors, notably the proximity to active fault zones such as the Yangsan Fault in Korea and the presence of uranium-bearing lithologies like granite, granitic gneiss, and schist. These fault-related fractures act as conduits, enhancing the vertical migration of radon from deeper mineralized zones into the groundwater system.

The observed variation in radon concentrations within natural springs and bottled waters of the Sub-Himalayan region can be attributed to the region's unique and complex geological framework, as the area is characterized by active fault systems and the

presence of uranium-bearing lithologies, which collectively facilitate the movement of radon into groundwater systems. The comparatively higher radon levels detected in natural springs, in contrast to bottled drinking water, highlight the role of direct hydro geological interaction between groundwater and the fractured, mineral-rich bedrock (Sajid et al., 2024).

The correlation between uranium-rich geological formations and elevated indoor radon concentrations is well demonstrated in several regions of Tanzania, particularly those located in close proximity to active mining sites like Bahi Makulu, situated near the Bahi uranium deposit, exhibited the highest recorded indoor radon concentration of 619 ± 59 Bq/m³. In contrast, significantly lower concentrations, such as 19 ± 3 Bq/m³, were measured in Manyoni town (Ntarisa, 2024).

Radon distribution in groundwater is mainly influenced by geological and hydrogeological conditions, including uranium-rich bedrock and aquifer properties, while deeper, older groundwater shows reduced radon levels due to radioactive decay and groundwater mixing can also lower its concentrations, particularly in central basin areas (Faryabi et al., 2024).

(Stoulos et al., 2024) in Greece have developed advanced analytical approaches, including time series analysis and artificial intelligence based methods, demonstrated statistically significant correlations between radon anomalies and earthquake occurrence. Present in both soil gas and groundwater they have been identified as potential precursors to seismic events. Soil gas radon exhibits a higher sensitivity to surface environmental conditions and can respond rapidly to changes in pressure and radon concentrations in groundwater tend to remain relatively stable due to consistently low temperatures, with significant variations observed in response to seismic or hydrological disturbances.

(Kumar et al., 2018), investigated groundwater radon levels in Udhampur district, Jammu and Kashmir, using RAD7 and Smart RnDuo detectors. RAD7 recorded concentrations

between 1.44 ± 0.31 and 63.64 ± 2.88 Bq L^{-1} with mean 28.73 Bq L^{-1}, while Smart RnDuo measured 0.64 ± 0.28 to 52.65 ± 2.50 Bq L^{-1} with mean: 20.30 Bq L^{-1}.

(Saadoon and Aswood, 2025) in Dhi Qar governorate, southern Iraq, revealed the weak association of physicochemical parameters with radon in water ranging from 0.058-0.802 Bq/L with an average of 0.26 ± 0.17 Bq/L.

(Cadungog et al., 2025) conducted study near active Taal Volcano in the Philippines, using a Liquid Scintillation Counter (LSC) and observed groundwater radon concentrations ranged from 4 to 51 Bq/L, with a mean concentration of 16.84 Bq/L. All observed values were significantly below the World Health Organization's recommended limit of 100 Bq/L.

A comparative study of radon variations in soil and groundwater across Vitia and Peja two geologically similar regions in Kosovo despite sharing same geological features, radon behavior differed notably, shaped by localized environmental and physicochemical conditions that revealed temperature emerged as a key factor, showing a moderate negative correlation with radon in both areas, consistent with reduced gas solubility at higher temperatures. Spatially, higher radon levels in Peja were likely due to more permeable soils and fault-related gas migration, despite similar radium content (Elezaj et al., 2025).

In Garhwal, Himalaya India, the concentrations of uranium in the analyzed drinking water samples were reported by (Panwar et al., 2024) that vary from 0 to 21.57 ppb with a mean value of 1.54 ppb.

A study conducted by (u Din et al., 2025) in Ganderbal, Jammu & Kashmir, analyzed uranium concentrations in 153 water samples, with values ranging from 0.51 to $6.83\,\mu$g L^{-1} and an average of $1.15\,\mu$g L^{-1}. The findings contribute to understanding geochemical behavior, potential environmental contamination, and associated human health risks. Bio kinetic modeling further aids in formulating strategies for managing uranium-contaminated water sources.

(Wagh et al., 2025) in their review study has reported the uranium concentrations across various Indian states such as 0.5- 90.46 ppb with mean 6.51 ppb in Chamba (Himachal Pradesh), 1.7- 12.28 ppb with average 5.89 ppb in Panchkula (Harayana).

(Mittal et al., 2025) reported activity concentrations in soil from the Aravalli hill and mining areas ranging from 25 ± 5 to 39 ± 7 Bq/kg for ^{226}Ra, 51 ± 2 to 67 ± 6 Bq/kg for ^{232}Th, and 435 ± 7 to 743 ± 7 Bq/kg for ^{40}K, with mean values of 28.7, 57.8, and 611 Bq/kg respectively. The radium equivalent activity ranged from 136 to 187 Bq/kg, averaging 154 Bq/kg.

(Thakur et al., 2024) conducted a study in the Budhakedar region of the Garhwal Himalaya to assess indoor radon and thoron concentrations using the portable SMART RnDuo monitor. The measured indoor radon and thoron were found with an arithmetic mean of 100 ± 27 Bq m^{-3}, 76 ± 33 Bq m^{-3} respectively. These findings provide important baseline data for radiological risk assessment in this seismically sensitive region.

Case control studies conducted by (Ngoc et al., 2022) across various European cites provide strong support that exposure to radon within indoor settings is significantly linked to an increased risk of lung cancer and childhood leukemia, particularly among individuals residing in regions where radon concentrations exceed 100 Bq/m^3.

(Serge et al., 2023) evaluated indoor radon and thoron levels in centre and south regions of Cameroon where thoron levels came out to be dominating with 60% of the effective dose contribution, highlighting the importance of thoron in radio- epidemiological studies.

In 2018, a differentiated survey of ^{222}Rn and ^{220}Rn conducted in Wuhan China, using RADUET and passive progeny monitors along with stochastic method observed minimized track heterogeneity on CR-39 detectors thus enhancing the result. Notably ^{220}Rn progeny accounted for over 40% of the total inhalation dose, highlighting its significant contribution in urban indoor environments (Hu et al., 2024).

(Singla et al., 2021) conducted a study on indoor radon and thoron concentrations across 75 dwellings in the Hanumangarh district of Rajasthan and evaluated the annual effective dose to be 0.8 mSv y^{-1}, which falls within the recommended safety limits. Based on these findings, the region was characterized as radiologically safe for the residents.

2.5 Research objectives

- To estimate the indoor radon concentrations in the dwellings of the study area for health hazards.
- Radon monitoring and delineation of active faults in the central Kashmir valley.
- To study the Radium and Radon exhalation rate of the soil samples exhumed from the study area.
- To measure the natural radioactivity in the soils of the study area.

2.6 Research Gap and Novel Approach

This work fills a significant gap by putting forward and effectively employing a novel technique that performs better than existing techniques in determining the relationship between radioactive analysis and its geological associations.
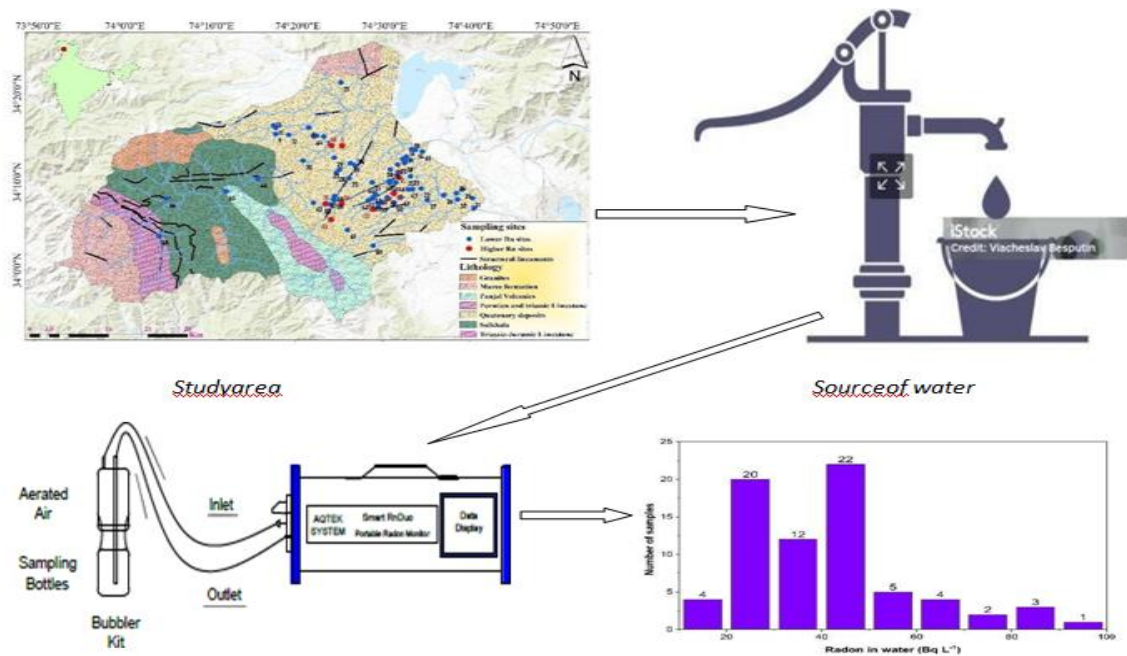
Figure 2.2: Geological map depicting the exploration of tectonic sites, highlighting elevated radon levels with red dots, indicating active fault zones and potential seismic activity

A key breakthrough of this research is the identification of active fault zones through elevated radon concentrations, highlighting a strong correlation between radon anomalies and tectonic activity. Groundwater samples from various sources were analyzed using a Radon Monitor, revealing site-specific variations and identifying active seismic regions. The novelty of this study was further validated when, post-publication, the Meteorological Department and seismological associations successfully identified regional epicenters of two back-to-back earthquakes on August 20, 2024, with magnitudes of 4.9 and 4.8. The GPS coordinates placed the epicenter just 2 km from a key sampling site in Shutloo, Rafiabad, Baramulla, followed by another minor tremor. These findings confirm radon's role as a geochemical tracer for monitoring and predicting seismic activity, reinforcing its potential as an early warning indicator for tectonic movements. Unlike well-documented fault zones such as the Panjal Thrust, Hindu Kush, Zanskar Thrust, and Balapur Faults, this research uncovers previously

unrecognized active seismic zones. By integrating geochemical analysis, tectonic studies, and real-time seismic data, this study provides first-hand evidence supporting radon emissions as a practical tool for earthquake forecasting. It not only addresses a critical research gap but also lays the foundation for future interdisciplinary studies on seismic risk assessment and early warning systems.
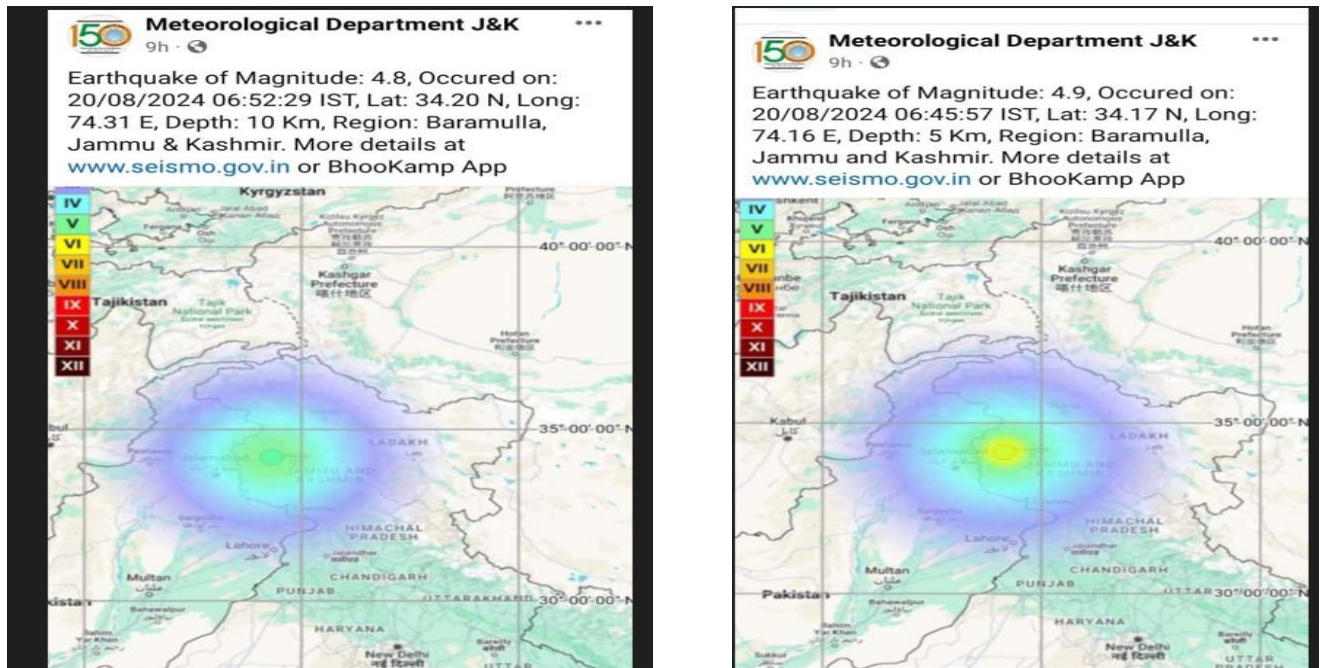
Figure 2.3: Seismic activity map showing epicenters of **4.8 and 4.9 magnitude** earthquakes in **Baramulla, J&K, on August 20, 2024**

References

- Adithya, V. S., Chidambaram, S., Keesari, T., Mohokar, H. V., & Prasanna, M. V. (2019). Occurrence of Uranium in Groundwater Along the Lithological Contacts in Central Tamilnadu, India: An Isotope Hydrogeochemical Perspective. *Exposure and Health*, *11*(4), 277–290. https://doi.org/10.1007/s12403-017-0269-3

- Ambrosino, F., La Verde, G., Gagliardo, G., Mottareale, R., Della Peruta, G., Imparato, C., D'Elia, A., &

- Balaram, V., Rani, A., & Rathore, D. P. S. (2022). Uranium in groundwater in parts of India and world: A comprehensive review of sources, impact to the environment and human health, analytical techniques, and mitigation technologies. *Geosystems and Geoenvironment*, *1*(2), 100043. https://doi.org/10.1016/j.geogeo.2022.100043

- Ball, T. K., Cameron, D. G., Colman, T. B., & Roberts, P. D. (1991). Behaviour of radon in the geological environment: A review. *Quarterly Journal of Engineering Geology*, *24*(2), 169–182. https://doi.org/10.1144/GSL.QJEG.1991.024.02.01

- Baltrocchi, A. P. D., Maggi, L., Dal Lago, B., Torretta, V., Szabó, M., Nasirov, M., Kabilov, E., & Rada, E. C. (2024). Mechanisms of Diffusion of Radon in Buildings and Mitigation Techniques. *Sustainability (Switzerland)*, *16*(1). https://doi.org/10.3390/su16010324

- Belete, G. D., & Shiferaw, A. M. (2022). A Review of Studies on the Seasonal Variation of Indoor Radon-222 Concentration. *Oncology Reviews*, *16A Review*(September), 1–6. https://doi.org/10.3389/or.2022.10570

- Benà, E., Ciotoli, G., Petermann, E., Bossew, P., Ruggiero, L., Verdi, L., Huber, P., Mori, F., Mazzoli, C., & Sassi, R. (2024). A new perspective in radon risk assessment: Mapping the geological hazard as a first step to define the collective radon risk exposure. *Science of the Total Environment*, *912*(December 2023). https://doi.org/10.1016/j.scitotenv.2023.169569

- Blöcher, D. (1988). DNA Double-strand Break Repair Determines the RBE of α-particles. *International Journal of Radiation Biology*, *54*(5), 761–771. https://doi.org/10.1080/09553008814552201

- Brindha, K., & Elango, L. (2013). Occurrence of uranium in groundwater of a shallow granitic aquifer and its suitability for domestic use in southern India. *Journal of Radioanalytical and Nuclear Chemistry*, *295*(1), 357–367. https://doi.org/10.1007/s10967-012-2090-6

- Cadungog, D.G.E., Racadio, C.D.T., Valdez, J.D.G., Racho, J.M.D., Mendoza, N.D.S., Sucgang, R.J., 2025. Radiological investigation of radon in groundwater around the active Taal Volcano (Philippines) and dose evaluation. Environ. Geochem. Health 47, 287. https://doi.org/10.1007/s10653-025-02610-w

- Chakan, M. R., Mir, R. R., Nazir, S., Mohi u Din, M., Simnani, S., & Masood, S. (2024). Radiological assessment of radon in groundwater of the northernmost Kashmir Basin, northwestern Himalaya. *Environmental Geochemistry and Health*, *46*(9), 1–13. https://doi.org/10.1007/s10653-024-02088-y

- Chauhan, R. P., Nain, M., & Kant, K. (2008). Radon diffusion studies through some building materials: Effect of grain size. *Radiation Measurements*, *43*(SUPPL.1). https://doi.org/10.1016/j.radmeas.2008.03.013

- Chen, G., Sun, Z., Nie, F., Li, C., Zhen, Y., & Zhou, Z. (2020). Hydrogeochemical characteristics of the sandstone-hosted uranium mineralization in northern Ordos Basin, China. *Ore Geology Reviews*, *126*(September), 103769. https://doi.org/10.1016/j.oregeorev.2020.103769

- Chen, Z., Li, Y., Liu, Z., Wang, J., Zhou, X., & Du, J. (2018). Radon emission from soil gases in the active fault zones in the Capital of China and its environmental effects. *Scientific Reports*, *8*(1), 1–12. https://doi.org/10.1038/s41598-018-35262-1

- Choubey, V. M., & Ramola, R. C. (1997). Correlation between geology and radon levels in groundwater, soil and indoor air in Bhilangana Valley, Garhwal

Himalaya, India. *Environmental Geology*, *32*(4), 258–262. https://doi.org/10.1007/s002540050215

- Cho, B.-W., Choo, C.O., Kim, M.S., Hwang, J., Yun, U., Lee, S., 2015. Spatial relationships between radon and topographical, geological, and geochemical factors and their relevance in all of South Korea. Environ. Earth Sci. 74, 5155–5168. https://doi.org/10.1007/s12665-015-4526-0

- Chahal, K., Kumar, S., Budhwar, S., Amanjeet, Singh, R., & Singh, B. (2024). An assessment of radionuclides level, radon and thoron exhalation rate in hill and field soil of Mahendergarh district in Haryana, India. *Journal of Radioanalytical and Nuclear Chemistry* , *333*(6), 2649–2659. https://doi.org/10.1007/s10967-024-09494-7

- Ciotoli, G., Bigi, S., Tartarello, C., Sacco, P., Lombardi, S., Ascione, A., & Mazzoli, S. (2014). Soil gas distribution in the main coseismic surface rupture zone of the 1980, M s = 6.9, Irpinia earthquake (southern Italy). *Journal of Geophysical Research: Solid Earth*, *119*(3), 2440–2461. https://doi.org/10.1002/2013JB010508

- Corlin, L., Rock, T., Cordova, J., Woodin, M., Durant, J. L., Gute, D. M., Ingram, J., & Brugge, D. (2016). Health Effects and Environmental Justice Concerns of Exposure to Uranium in Drinking Water. *Current Environmental Health Reports*, *3*(4), 434–442. https://doi.org/10.1007/s40572-016-0114-z

- Cosma, C., Dancea, F., Jurcut, T., & Ristoiu, D. (2001). Determination of 222Rn emanation fraction and diffusion coefficient in concrete using accumulation chambers and the influence of humidity and radium distribution. *Applied Radiation and Isotopes*, *54*(3), 467–473. https://doi.org/10.1016/S0969-8043(00)00286-4

- Darby, S., Hill, D., Auvinen, A., Barros-Dios, J. M., Baysson, H., Bochicchio, F., Deo, H., Falk, R., Forastiere, F., Hakama, M., Heid, I., Kreienbrock, L., Kreuzer, M., Lagarde, F., Mäkeläinen, I., Muirhead, C., Oberaigner, W., Pershagen, G., Ruano-Ravina, A., … Doll, R. (2005). Radon in homes and risk of lung cancer:

collaborative analysis of individual data from 13 European case-control studies. *BMJ*, *330*(7485), 223. https://doi.org/10.1136/bmj.38308.477650.63

- de Acosta, J. (2013). Of earthquakes. *Natural and Moral History of the Indies*, *September 1991*, 157–159. https://doi.org/10.1215/9780822383932-066

- Devaraj, N., Panda, B., Chidambaram, S., Prasanna, M. V., Singh, D. K., Ramanathan, A. L., & Sahoo, S. K. (2021). Spatio-temporal variations of Uranium in groundwater: Implication to the environment and human health. *Science of the total environment*, *775*, 145787.

- Dobrzyńska, M. M., Gajowik, A., & Wieprzowski, K. (2023). Radon – Occurrence and Impact on the Health. *Roczniki Panstwowego Zakladu Higieny / Annals of the National Institute of Hygiene*, *74*(1), 5–14. https://doi.org/10.32394/rpzh.2023.0242

- Dongre, S., Kumar, S., Suresh, S., & Sannappa, J. (2023). Estimation of Inhalation and Ingestion Dose Due to Radon Concentration in Drinking Water Samples of Shankaraghatta Forest Environment, Karnataka, India. *Indian Journal Of Science And Technology*, *16*(5), 367–376. https://doi.org/10.17485/ijst/v16i5.2321

- Elezaj, N., Xhixha, G., Zorko, B., Mustafa, S., Bytyqi, V., Rrakaqi, B., 2025. Temporal variation of radon in soil and water in Kosovo. Radiochim. Acta 113, 471–483. https://doi.org/10.1515/ract-2024-0350

- Evans, H. J. (1992). Alpha-particle after effects. *Nature*, *355*(6362), 674–675. https://doi.org/10.1038/355674a0

- Faryabi, M., Behzad, H.R.M., Shojaheydari, R., 2024. Factors controlling 222Rn activity of groundwater in Jiroft plain, Iran. Int. J. Radiat. Res. 22, 639–646. https://doi.org/10.61186/ijrr.22.3.639

- Giammanco, S., Bonfanti, P., & Neri, M. (2023). Radon on Mt. Etna (Italy): a useful tracer of geodynamic processes and a potential health hazard to populations. *Frontiers in Earth Science*, *11*(May), 1–14. https://doi.org/10.3389/feart.2023.1176051.

- Gingrich, J. E. (1984). Radon as a geochemical exploration tool. *Journal of Geochemical Exploration*, *21*(1–3), 19–39. https://doi.org/10.1016/0375-6742(84)90032-3

- Hwa Oh, Y., & Kim, G. (2015). A radon-thoron isotope pair as a reliable earthquake precursor. *Scientific Reports*, *5*, 220–225. https://doi.org/10.1038/srep13084

- Iwata, D., Nagahama, H., Muto, J., & Yasuoka, Y. (2018). Non-parametric detection of atmospheric radon concentration anomalies related to earthquakes. *Scientific Reports*, *8*(1), 1–9. https://doi.org/10.1038/s41598-018-31341-5

- Kaur, J., Shikha, D., Kapil, C., & Mehta, V. (2024). Assessment of radon gas exposure in drinking water: a case study of Una District, Himachal Pradesh, India. *Journal of Radioanalytical and Nuclear Chemistry* , *0123456789*. https://doi.org/10.1007/s10967-024-09578-4

- Kawabata, K., Tsunomori, F., Kitamura, Y., Lin, Y. Y., Chan, C. H., & Ma, K. F. (2024). Radon concentration in seawater as a geochemical indicator of submarine fault activity in the Yatsushiro Sea, Japan. *Scientific Reports*, *14*(1), 1–9. https://doi.org/10.1038/s41598-024-59006-6

- Khan, M. A., Khattak, N. U., Hanif, M., & Qadir, A. (2023). Assessment of soil-gas radon concentration over lithologies: a case study from district Karak, Khyber Pakhtunkhwa, Pakistan. *Environmental Monitoring and Assessment*, *195*(1). https://doi.org/10.1007/s10661-022-10716-2

- King, C.-Y., King, B.-S., Evans, W. C., & Zhang, W. (1996). Spatial radon anomalies on active faults in California. *Applied Geochemistry*, *11*(4), 497–510. https://doi.org/10.1016/0883-2927(96)00003-0

- Krewski, D., Lubin, J. H., Zielinski, J. M., Alavanja, M., Catalan, V. S., William Field, R., Klotz, J. B., Létourneau, E. G., Lynch, C. F., Lyon, J. L., Sandler, D. P., Schoenberg, J. B., Steck, D. J., Stolwijk, J. A., Weinberg, C., & Wilcox, H. B. (2006). A Combined Analysis of North American Case-Control Studies of

Residential Radon and Lung Cancer. *Journal of Toxicology and Environmental Health, Part A*, *69*(7–8), 533–597. https://doi.org/10.1080/15287390500260945

- Knol, A. (2005). *Trends in the environmental burden of disease in the Netherlands*. 97.

- Küçükönder, E., Gümbür, S., & Alıç, H. (2023). Radon gas measurement in soil samples taken from Kahramanmaras province of Turkey. *International Journal of Environmental Science and Technology*, *20*(7), 7477–7486. https://doi.org/10.1007/s13762-023-04889-7

- Kumar, A., Arora, T., Singh, P., Singh, K., Singh, D., Pathak, P. P., & Ramola, R. C. (2021). Quantification of radiological dose and chemical toxicity due to radon and uranium in drinking water in Bageshwar region of Indian Himalaya. *Groundwater for Sustainable Development*, *12*(October), 100491. https://doi.org/10.1016/j.gsd.2020.100491

- Kumar, A., Singh, P., Singh, D., Singh, K., Kandari, T., Saklani, C. P., & Deep, A. (2024). Assessment of exhalation rates of radon and thoron in soil from the Jaunsar-Bawar region of the Indian Himalayas. *Journal of Radioanalytical and Nuclear Chemistry* , *333*(6), 3147–3158. https://doi.org/10.1007/s10967-024-09407-8

- Kumar, P., & Kumar, M. (2024). Radon emanation factor for soil and external exposure of the public around an atomic power plant narora (U.P.) India. *Journal of Radioanalytical and Nuclear Chemistry* , *0123456789*. https://doi.org/10.1007/s10967-024-09604-5

- Kumar, A., Sharma, S., Mehra, R., Kanwar, P., Mishra, R., Kaur, I., 2018. Assessment of radon concentration and heavy metal contamination in groundwater of Udhampur district, Jammu & Kashmir, India. Environ. Geochem. Health 40, 815–831. https://doi.org/10.1007/s10653-017-0027-2

- Li, J., & Zhang, Y. (2012). Remediation technology for the uranium contaminated environment: a review. *Procedia Environmental Sciences*, *13*(2011), 1609–1615. https://doi.org/10.1016/j.proenv.2012.01.153

- Little, J. B. (1993). Cellular, Molecular, and Carcinogenic Effects of Radiation. *Hematology/Oncology Clinics of North America*, *7*(2), 337–352. https://doi.org/10.1016/S0889-8588(18)30244-2

- Malakootian, M., & Soltani Nejhad, Y. (2017). Determination of radon concentration in drinking water of Bam villages and evaluation of the annual effective dose. *International Journal of Radiation Research*, *15*(1), 81–89. https://doi.org/10.18869/acadpub.ijrr.15.1.81

- Menetrez, M. Y., Mosley, R. B., Snoddy, R., & Brubaker, S. A. (1996). Evaluation of radon emanation from soil with varying moisture content in a soil chamber. *Environment International*, *22*, 447–453. https://doi.org/10.1016/S0160-4120(96)00145-6

- Miklyaev, P. S., Petrova, T. B., Shchitov, D. V., Sidyakin, P. A., Murzabekov, M. A., Tsebro, D. N., Marennyy, A. M., Nefedov, N. A., & Gavriliev, S. G. (2022). Radon transport in permeable geological environments. *Science of The Total Environment*, *852*, 158382. https://doi.org/10.1016/j.scitotenv.2022.158382

- Misdaq, M. A., Khajmi, H., & Ktata, A. (1998). Study of the influence of porosity on the radon emanation coefficient in different building material samples by combining the SSNTD technique with Monte Carlo simulations. *Radiation Physics and Chemistry*, *53*(4), 385–390. https://doi.org/10.1016/S0969-806X(98)00021-8

- Mittal, S., Mehra, R., Gill, K.S., 2025. Assessment of Natural Terrestrial Radionuclides and their Radiological Effects on Human Health in Soil Samples of Aravalli Hill and Mining Areas of Northern Rajasthan. J. Nucl. Eng. Radiat. Sci. 1–10. https://doi.org/10.1115/1.4068724

- Mitchell, E., Frisbie, S., & Sarkar, B. (2011). Exposure to multiple metals from groundwater - A global crisis: Geology, climate change, health effects, testing, and mitigation. *Metallomics*, *3*(9), 874–908. https://doi.org/10.1039/c1mt00052g

- Muhammad, Y. M. Y., Fatah, P. K., & Yaba, S. P. (2023). Measurement of Radon Activity Concentration in Soils Samples of Shaqlawa Region in Erbil City/

Iraqi Kurdistan Using RAD7 Detector. *Zanco Journal of Pure and Applied Sciences*, *35*(2), 58–62. https://doi.org/10.21271/ZJPAS.35.2.7

- Ngoc, L.T.N., Park, D., Lee, Y.-C., 2022. Human Health Impacts of Residential Radon Exposure: Updated Systematic Review and Meta-Analysis of Case–Control Studies. Int. J. Environ. Res. Public Health 20, 97. https://doi.org/10.3390/ijerph20010097

- Ntarisa, A.V., 2024. Review of radon research in Tanzania. J. Eur. Radon Assoc. https://doi.org/10.35815/radon.v5.10728

- Nunes, L. J. R. (2023). *applied sciences The Relationship between Radon and Geology : Sources , Transport and Indoor Accumulation*.

- Orloff, K. G., Mistry, K., Charp, P., Metcalf, S., Marino, R., Shelly, T., Melaro, E., Donohoe, A. M., & Jones, R. L. (2004). Human exposure to uranium in groundwater. *Environmental Research*, *94*(3), 319–326. https://doi.org/10.1016/S0013-9351(03)00115-4

- Panwar, P., Joshi, A., Singh, K.P., Prasad, M., Mehra, R., Sahoo, S.K., Ramola, R.C., 2024. Distribution of uranium and selected toxic heavy metals in drinking water of Garhwal Himalaya, India. J. Radioanal. Nucl. Chem. 333, 2927–2935. https://doi.org/10.1007/s10967-023-08998-y

- Prise, K. M. (1994). Use of Radiation Quality as a Probe for DNA Lesion Complexity. *International Journal of Radiation Biology*, *65*(1), 43–48. https://doi.org/10.1080/09553009414550061

- Przylibski, T. A. (2000). Estimating the radon emanation coefficient from crystalline rocks into groundwater. *Applied Radiation and Isotopes*, *53*(3), 473–479. https://doi.org/10.1016/S0969-8043(99)00145-1

- Puskin, J. S., & Nelson, C. B. (1989). EPA's Perspective on Risks from Residential Radon Exposure. *JAPCA*, *39*(7), 915–920. https://doi.org/10.1080/08940630.1989.10466577

- Prise, K. M. (1994). Use of Radiation Quality as a Probe for DNA Lesion Complexity. *International Journal of Radiation Biology*, *65*(1), 43–48. https://doi.org/10.1080/09553009414550061

- Przylibski, T. A. (2000). Estimating the radon emanation coefficient from crystalline rocks into groundwater. *Applied Radiation and Isotopes*, *53*(3), 473–479. https://doi.org/10.1016/S0969-8043(99)00145-1

- Puskin, J. S., & Nelson, C. B. (1989). EPA's Perspective on Risks from Residential Radon Exposure. *JAPCA*, *39*(7), 915–920. https://doi.org/10.1080/08940630.1989.10466577

- Pugliese, M. (2024). Radon Exhalation Rate: A Metrological Approach for Radiation Protection. *Sensors*, *24*(11). https://doi.org/10.3390/s24113633

- Pulinets, S., Mironova, I., Miklyaev, P., Petrova, T., Shitov, A., & Karagodin, A. (2024). Radon Variability as a Result of Interaction with the Environment. *Atmosphere*, *15*(2). https://doi.org/10.3390/atmos15020167

- Radford, E. P., & Hunt, V. R. (1964). Polonium-210: A Volatile Radioelement in Cigarettes. *Science*, *143*(3603), 247–249. https://doi.org/10.1126/science.143.3603.247

- Rahim, A., Khan, S., & Rani, A. (2024). Toxicology Risk Assessment of Uranium in Drinking water of Ganderbal and Budgam Districts of Jammu. *Water, Air, & Soil Pollution*, *235*(9), 1–12. https://doi.org/10.1007/s11270-024-07345-5

- Ramesh, R. P., Subramanian, M., Lakshmanan, E., Subramaniyan, A., & Ganesan, G. (2021). Human health risk assessment using Monte Carlo simulations for groundwater with uranium in southern India. *Ecotoxicology and Environmental Safety*, *226*(April), 112781. https://doi.org/10.1016/j.ecoenv.2021.112781

- Rani, S., Kundu, R. S., Garg, V. K., Singh, B., Panghal, A., & Dilbaghi, N. (2023). Radon and thoron exhalation rate in the soil of Western Haryana, India. *Environmental Monitoring and Assessment*, *195*(4), 1–15. https://doi.org/10.1007/s10661-023-11046-7

- Rani, S., Kansal, S., Singla, A. K., Nazir, S., & Mehra, R. (2023). Estimation of Annual Effective Dose due to Radon Concentration in Water Samples of Moga District of Northern Punjab, India. *Indian Journal of Pure and Applied Physics*, *61*(6), 423–428. https://doi.org/10.56042/ijpap.v61i6.2412

- Rose, A. W., & Wright, R. J. (1980). Geochemical exploration models for sedimentary uranium deposits. *Journal of Geochemical Exploration*, *13*(2–3), 153–179. https://doi.org/10.1016/0375-6742(80)90005-9

- Sahu, P., Panigrahi, D. C., & Mishra, D. P. (2016). A comprehensive review on sources of radon and factors affecting radon concentration in underground uranium mines. *Environmental Earth Sciences*, *75*(7). https://doi.org/10.1007/s12665-016-5433-8

- Sajid, A., Anjum, M., Younis, H., Salouci, M., Mehboob, K., Haj Ismail, A., 2024. Assessment of Radon Concentration and Health Hazards in Natural Spring Water of a Sub-Himalayan District. Atmosphere (Basel). 15, 940. https://doi.org/10.3390/atmos15080940

- Samet, J. M., Marbury, M. C., & Spengler, J. D. (1987). Health Effects and Sources of Indoor Air Pollution. Part I. *American Review of Respiratory Disease*, *136*(6), 1486–1508. https://doi.org/10.1164/ajrccm/136.6.1486

- Saadoon, A.A., Aswood, M.S., 2025. Measurement of radon gas activity concentration and physiochemical parameters (pH, TDS, conductivity) in marshes water in Dhi Qar governorate – southern Iraq. Int. J. Environ. Anal. Chem. 1–17. https://doi.org/10.1080/03067319.2025.2458145

- Sano, Y., Takahata, N., Kagoshima, T., Shibata, T., Onoue, T., & Zhao, D. (2016). Groundwater helium anomaly reflects strain change during the 2016 Kumamoto earthquake in Southwest Japan. *Scientific Reports*, *6*(November), 1–7. https://doi.org/10.1038/srep37939

- Serge, A.B.M., Didier, T.S.S., Samuel, B.G., Kranrod, C., Omori, Y., Hosoda, M., Saïdou, Tokonami, S., 2023. Assessment of Radiological Risks due to Indoor

Radon, Thoron and Progeny, and Soil Gas Radon in Thorium-Bearing Areas of the Centre and South Regions of Cameroon. Atmosphere (Basel). 14, 1708. https://doi.org/10.3390/atmos14121708

- Singh, K. P., Chandra, S., Prasad, M., Joshi, A., Prasad, G., & Ramola, R. C. (2024). Estimation of radiation dose due to ingestion of radon in water samples of Garhwal Himalaya, India. *Journal of Radioanalytical and Nuclear Chemistry* , *333*(6), 2867–2879. https://doi.org/10.1007/s10967-023-09002-3

- Singh, B., & Kant, K. (2023). Annual effective dose due to inhalation of indoor radionuclides and their progeny measured by track etched techniques using pinhole dosimeter and deposition-based progeny sensors. *Journal of Radioanalytical and Nuclear Chemistry*, *332*(8), 3121–3131. https://doi.org/10.1007/s10967-023-08988-0

- Singh, B., & Kant, K. (2023). Annual effective dose due to inhalation of indoor radionuclides and their progeny measured by track etched techniques using pinhole dosimeter and deposition-based progeny sensors. *Journal of Radioanalytical and Nuclear Chemistry*, *332*(8), 3121–3131. https://doi.org/10.1007/s10967-023-08988-0

- Singla, A.K., Kansal, S., Mehra, R., 2021. Dose distribution to individual tissues and organs due to exposure of alpha energies from radon and thoron to local population of Hanumangarh, Rajasthan, India. J. Radioanal. Nucl. Chem. 327, 1073–1085. https://doi.org/10.1007/s10967-021-07604-3

- Skelton, A., Andrén, M., Kristmannsdóttir, H., Stockmann, G., Mörth, C. M., Sveinbjörnsdóttir, Á., Jónsson, S., Sturkell, E., Gudrúnardóttir, H. R., Hjartarson, H., Siegmund, H., & Kockum, I. (2014). Changes in groundwater chemistry before two consecutive earthquakes in Iceland. *Nature Geoscience*, *7*(10), 752–756. https://doi.org/10.1038/NGEO2250

- Somsunun, K., Prapamontol, T., Pothirat, C., Liwsrisakun, C., Pongnikorn, D., Fongmoon, D., Chantara, S., Wongpoomchai, R., Naksen, W., Autsavapromporn,

N., & Tokonami, S. (2022). Estimation of lung cancer deaths attributable to indoor radon exposure in upper northern Thailand. *Scientific Reports*, *12*(1), 1–10. https://doi.org/10.1038/s41598-022-09122-y

- Stoulos, S. (2024). Radon indoors source potential from soil gas in a temperate climate: impact of infiltration rate and seismicity. *Environmental Science and Pollution Research*, *31*(13), 20277–20292. https://doi.org/10.1007/s11356-024-32334-w

- Stoulos, S., Papadimitriou, E., Karakostas, V., Kourouklas, C., Atac–Nyberg, A., Wyss, R., Bäck, T., Tallini, M., DeLuca, G., 2024. Radon signals in soil gas associated with earthquake occurrence in Greece: review and perspective. J. Radioanal. Nucl. Chem. 333, 6107–6120. https://doi.org/10.1007/s10967-024-09710-4

- Sun, H., & Furbish, D. J. (1995). Moisture content effect on radon emanation in porous media. *Journal of Contaminant Hydrology*, *18*(3), 239–255. https://doi.org/10.1016/0169-7722(95)00002-D

- Talib K. Abed, Mohammed A. Fayad, Ahmed A. Al-Amiery, Hasanain A. Abdul Wahhab, Jabbar K. Mohammed, Hassan Sh. Majdi,Radon gas emission from home appliances: Understanding sources, implications, and mitigation strategies,Results in Engineering,Volume 22,2024,102133,ISSN 2590-1230, https://doi.org/10.1016/j.rineng.2024.102133.

- Thakur, V., Singh, K.P., Joshi, A., Sharma, S., Bourai, A.A., Ramola, R.C., 2024. Comparative study of the radon and thoron concentrations in the indoor environment of the Budhakedar region of the Garhwal Himalaya, India. J. Radioanal. Nucl. Chem. 333, 3239–3248. https://doi.org/10.1007/s10967-024-09351-7

- u Din, M.M., Nazir, S., Simnani, S., Chakan, M.R., Masood, S., Rani, S., Singla, A.K., 2025. Assessment of uranium exposure in drinking water sources across Ganderbal, Jammu and Kashmir: A biokinetic modelling approach. J. Geochemical Explor. 274, 107763. https://doi.org/10.1016/j.gexplo.2025.107763

- Ummah, M. S. (2019). Title. In *Sustainability (Switzerland)* (Vol. 11, Issue 1). http://scioteca.caf.com/bitstream/handle/123456789/1091/RED2017-Eng

- Virk, H. S., Jakhu, R., Bangotra, P., & Singh Virk, H. (2016). Natural Uranium Content in Ground Waters of Mohaliand Fatehgarh Districts of North Punjab (India) for the Assessment of Excess Cancer Risk. *Global Journal of HUMAN-SOCIAL SCIENCE: B Geography*, *16*(4).

- Vogiannis, E. G., & Nikolopoulos, D. (2015). Radon sources and associated risk in terms of exposure and dose. *Frontiers in Public Health*, *2*(JAN), 1–10. https://doi.org/10.3389/fpubh.2014.00207

- Waseem, A., Ullah, H., Rauf, M. K., & Ahmad, I. (2015). Distribution of natural uranium in surface and groundwater resources: A review. *Critical Reviews in Environmental Science and Technology*, *45*(22), 2391–2423. https://doi.org/10.1080/10643389.2015.1025642

- Wagh, G., Bhutekar, D., Kale, A., 2025. Assessing Uranium Contamination in Groundwater : A Comprehensive Review for India 45, 17–30.

- World Health Organization. (2001). *Depleted uranium: sources, exposure and health effects* (No. WHO/SDE/PHE/01.1). World Health Organization.

- WHO. (2007). *Indoor Radon a Public Health Perspective*. 110.

- Wu, Y., Wang, Y., & Xie, X. (2014). Occurrence, behavior and distribution of high levels of uranium in shallow groundwater at Datong basin, northern China. *Science of the Total Environment*, *472*, 809–817. https://doi.org/10.1016/j.scitotenv.2013.11.109

- Yazzie, S. A., Davis, S., Seixas, N., & Yost, M. G. (2020). Assessing the impact of housing features and environmental factors on home indoor radon concentration levels on the Navajo Nation. *International Journal of Environmental Research and Public Health*, *17*(8), 1–18. https://doi.org/10.3390/ijerph17082813

- Yousefian, F., Nasiri, Z., Kordi, M., Marzi, Y. G., Dehghani, R., Mirzaei, N., Janjani, H., Aghaei, M., & Aboosaedi, Z. (2024). Indoor Radon and Its Health

Risk Assessment in Iran: A Comprehensive Review Study. *Indoor Air*, *2024*. https://doi.org/10.1155/2024/2300116

CHAPTER 3

INSTRUMENTATION TECHNIQUES AND METHODS

3.1 Overview

This chapter presents the tools and instrumentation techniques employed for evaluating natural radioactivity in the study area. Adhering to standard protocols is essential to detect the accuracy and precision of Rn-222 and its daughter concentration measurements, thereby assessing potential health risks to residents. Radon in indoors is impacted by several variables, like ventilation conditions, house type, geological characteristics, seasonal variations, and meteorological parameters (Al-Sharif & Abdelrahman, 2001). Taking these variables into account, a systematic approach was followed from sampling to evaluation to investigate the radon levels in varying environmental conditions using both active and passive measurement techniques. The key distinction between these methods lies in their temporal coverage: passive methods provide an average radon concentration over an extended period, whereas active techniques enable continuous on-site monitoring.

To achieve the objectives of the study, a pinhole dosimeter was used as a passive measurement tool, collecting data over a year in three distinct four-month-long seasons. The Smart RnDuo Radon Monitor served as an active measurement device for determining radon concentrations in water on-site, as well as for assessing radon and thoron exhalation rates in the study area. For the analysis of radium, thorium, and potassium concentrations, NaI gamma spectrometry was utilized. Since uranium is the primary source of radon and holds significant radiochemical and toxicological relevance, particularly in underground water, its concentration in the Leh-Ladakh valley of Northwestern Himalayas, India, was evaluated using the LED Fluorimeter Quantalase.

The contents described below of this chapter provide a deep discussion of these methodologies, ensuring a thorough understanding of the measurement techniques employed in this study.

3.2 Active Measurement Methods

3.2.1 Geiger-Mueller (GM) Counter

The (GM) Counter was utilized to assess the ambient gamma radiation at each site. The detector used in the study has a (DER) of 0.01μSv/h to 100mSv/h. To ensure measurement accuracy, readings were averaged over five minutes at each sampling site, with the survey monitor placed 1 meter above ground level to evaluate gamma field strength reliably.

3.2.2 Scintillation Detector

The Smart RnDuo (figure 3.1) a state-of-the-art, portable radon/thoron measurement device, was employed for continuous monitoring of ^{222}Rn and ^{220}Rn concentrations in air, water, and soil. Developed by (BARC), Mumbai, India, this detector operates on the method of scintillation counting. When α emitted progenies hit with the ZnS-Ag coating inside the detection chamber, they generate scintillations, which are then detected and converted into counts by a (PMT). The built-in algorithm processes these counts and displays the ^{222}Rn and ^{220}Th concentrations on the device display. To maintain accurate measurements, the instrument was calibrated at BARC using certified radon and thoron sources (Models RN-1025 and TH-102) supplied by Pylon Electronics Inc., Canada, within a 0.05 m³ calibration chamber. One of the key strengths of this detector is its robustness against humidity and minor gas interferences, which enhances its sensitivity and measurement accuracy. The device offers detection sensitivities of 1.2 CPH (Bq/m³) for radon and 0.8 CPH (Bq/m³) for thoron, with an alpha particle detection efficiency close to 75%.
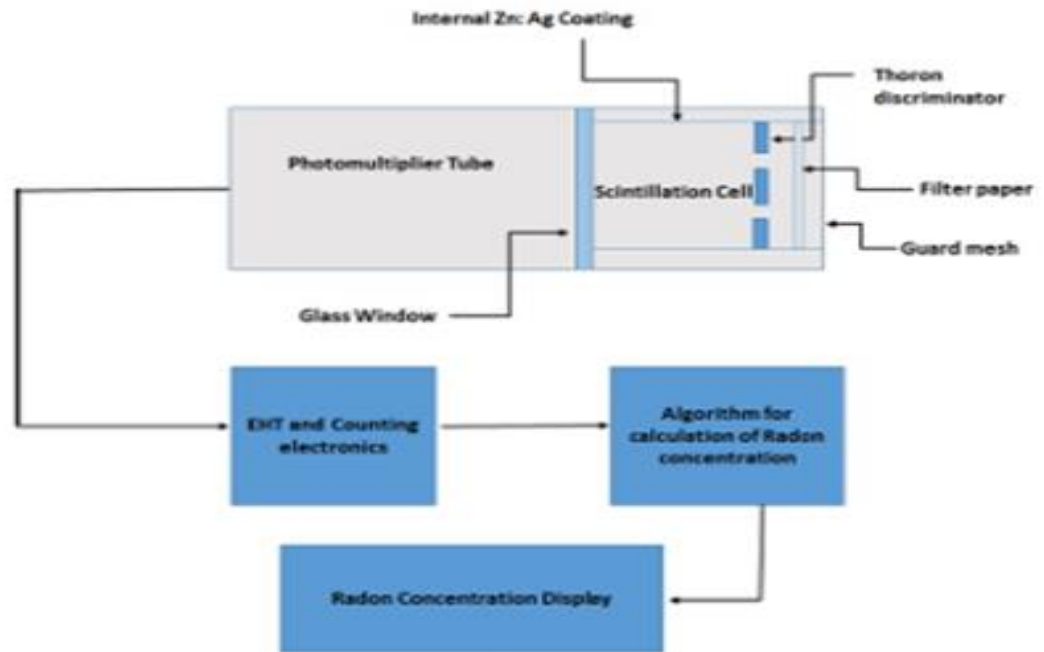
Figure 3.1: Schematic diagram of RnDuo Monitor

3.3 Evaluation of Exhalation Emissions

To determine the radon and thoron exhalation rates in soil samples, the Smart Radon Monitor was utilized in conjunction with an exhalation chamber, following established procedural guidelines (Hidayath et al., 2023). Proper site selection was crucial for obtaining accurate measurements, with soil samples being collected from areas with minimal humidity and moisture content. To prevent interference with the detector's Lucas cell, sampling was primarily conducted during dry seasons, as moisture can significantly impact alpha count readings (Kaur et al., 2023).

3.3.1 Radon Mass Exhalation Rate

The radon mass exhalation rate or emanation flux describes the amount of radon released from the soil per unit mass and per unit time, serving as a direct method for assessing radon flux density. Each dry soil sample was placed inside an accumulation chamber, where the detector was operated in diffusion mode for one-hour cycles to evaluate its radon emission potential. The diffusion delay ensured minimal interference from thoron and its decay products.

For mass exhalation rate measurements, approximately 500 grams of soil were used within the chamber, and the detector setup was run continuously for 24 hours, as illustrated in Figure 3.2. The recorded data was later processed using linear fitting models in ORIGIN software to compute the radon mass exhalation rate (Kumar et al., 2020).

Figure 3.2: Smart RnDuo monitor analyzing radon mass exhalation

The Rn-222 concentration inside the chamber at any given time **t**, denoted as **C(t)**, follows the equation

$$C(t) = \left(\frac{M\chi e}{\rho}\right)t + Co \qquad\qquad 3.1$$

Here, χ_e denotes the radon mass exhalation rate (Bq/kg/h), M is the sample mass, ρ represents the effective volume (m³), including detector, sample pores, and chamber air and C_0 is the initial radon concentration, generally taken as zero.

χ_e is determined from the slope of the equation

=Slope (ρ/M)

Where the slope is derived from c(t)/t using linear fitting models.

3.3.2 Surface Exhalation flux Density

The surface exhalation was measured using the flow mode setup of the detector, as per standard guidelines. Due to its limited diffusion length thoron does not disperse uniformly in the accumulation chamber, necessitating a specialized approach. The detector is equipped with an inbuilt pump which continuously circulates thoron-containing air into the Lucas cell for analysis. The detector registers the alpha emissions from thoron and its progeny, displaying the corresponding counts (Kumar et al., 2023).Figure 3.3 below shows the on-site estimation of the thoron flux density. To achieve equilibrium concentration C(t), the measurement process spanned one hour, divided into four cycles of 15 minutes each. Each cycle comprised of

- 5 minutes of active sampling, allowing thoron and background air to enter the detector,
- 5 minutes of decay phase, during which thoron levels decrease,
- 5 minutes of background counting, ensuring accurate readings.

Within a closed-loop accumulation chamber, (ψ_s) was calculated using the equation

$$\psi s = C(t)\rho\lambda/A \qquad\qquad 3.2$$

Where ψ_s represents the thoron surface exhalation rate (Bq/m²/s), A is the surface area of the chamber (m²), ρ indicates the effective volume (m³), including the chamber's residual space, detector volume, pipe, and lid, C(t) denotes the thoron concentration inside the chamber at time t (Bq/m³) and λ is the decay constant of thoron (0.0126 s⁻¹) reflecting its 55-second half-life.

Figure 3.3: Field/ on-site estimation of the thoron flux density

3.4 Measurement of Rn-222 in Water

To obtain the radon gas levels, samples were collected across various underground water resources, ensuring they were potable and widely used for drinking. The depth of each source and its GPS coordinates were recorded for precise location tracking. Special care was taken during sampling to prevent radon loss, as it is a volatile gas. The samples were gathered in 60 ml bottles using a monitor bubble kit, with the bottles sealed underwater to avoid aeration. Measurements were conducted immediately on-site (in situ) to minimize radon escape.

The Smart RnDuo Radon Monitor was employed for radon analysis, utilizing a scintillation-based radioactive decay algorithm for accurate readings. The device, resistant to humidity effects, was calibrated annually to maintain precision. Before each measurement, the detector's built-in pump was run in open-loop mode for five minutes to remove residual gases. The water sample was then connected to the monitor via a bubbler attachment, and radon concentration was measured over 60 minutes in 4 cycles comprising of 15 minutes each. The detector's sensitivity enabled the detection of radon levels ranging from 8Bq/m³ to 50MBq/m³, achieving 95% accuracy within 40 minutes. The study was conducted by utilizing the facilities at the Radiation Lab, Department of Physics, University of Kashmir ensuring reliable and precise analysis. Figure 3.4 shows the setup of in-situ measurement of radon in water.
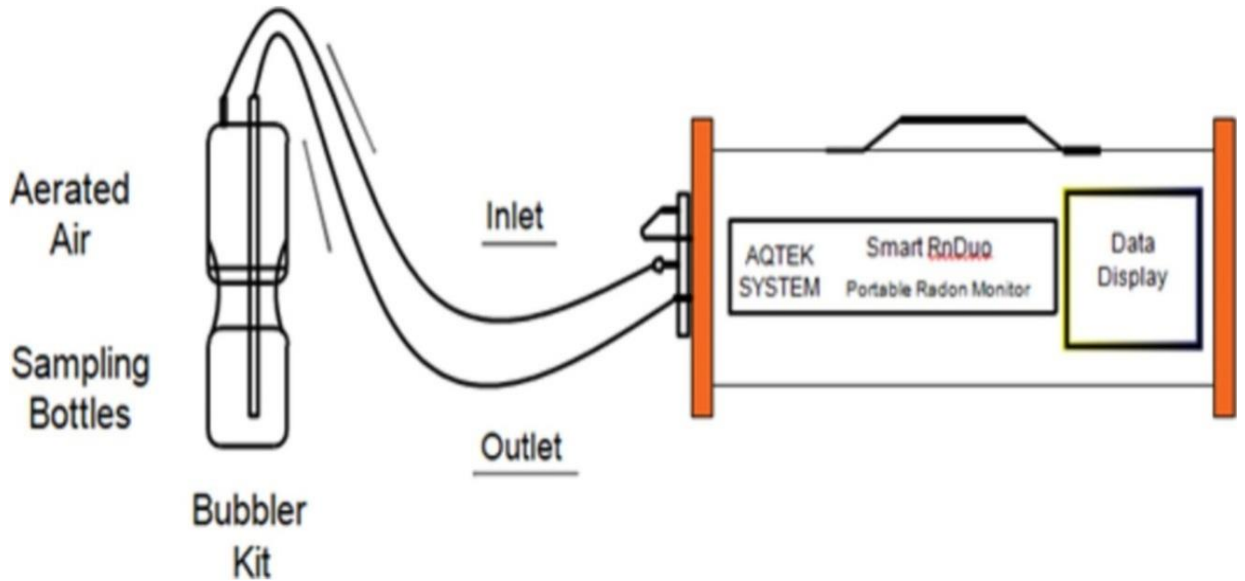
Figure 3.4: In-situ measurement of radon in water using a bubbler

The final radon concentration in water was determined using a standard formula, incorporating the air-water partition coefficient and volume ratios, and is given as (Pandith et al., 2024).

$$Ca = Cw \ (K + Ta/Tw) \hspace{3cm} 3.3$$

Where the symbols with their corresponding values are discussed in detail in chapter 4 and 5

3.5 Methodology for Radon and Thoron Measurement

Measurement Techniques for Indoor Radon

Radon measurements can be conducted using both passive and active techniques, each with distinct advantages. Short-term methods are generally preferred due to their quick results, making them suitable for dosimetric analysis. Considering the seasonal fluctuations in indoor radon levels and its potential hazards on the people of the studied

area, pinhole dosimetry technique was employed for radon and thoron analysis. This technique involved the use of (SSNTDs) to measure the activity concentrations of these gases.

The domain of SSNTDs was initiated at AERE, Harwell (1958). These detectors are available in various materials, both naturally occurring and synthetic (Durrani & Bull, 2013). Several types of plastic track detectors exist, including CR-39, Lexan, Makrofol, CN-85, and LR-115, which record alpha particles within a specific energy range. In this study, LR-115 Type-II films, also known as cellulose nitrate (chemical formula $C_6H_8O_9N_2$), were selected due to their efficiency. These films consist of a 12 μm thick active red layer and were installed in a single-entrance pinhole dosimeter along with progeny sensors.

The process of track formation is effectively described by the ion explosion spike theory introduced by (Fleischer et al., 1965). Based on this model, as a positively charged particle passes through the non conducting detector material, it strips orbital electrons from atoms, leaving behind a narrow damage trail. These latent tracks, measuring 1μm to 15 μm in diameter, are not visible to the naked eye. To visualize them, the films undergo a chemical etching process and are later analyzed using optical microscopy or spark counters.

Pin-Hole Dosimeter: Design and Working Principle

The pinhole dosimeter consists of two interchangeable cylindrical chambers distanced by a pinhole-based radon (^{222}Rn) and thoron (^{220}Rn) discriminating plate, with dimensions of 3.1 cm radius and 4.1 cm length (Saini et al., 2016). A single gas entrance face ensures uniform radon entry, eliminating uncertainties encountered in previous double-entry dosimeters, which often yielded negative thoron values. The discriminating plate comprises four pinholes, each with a 0.5 mm radius and 2 mm length, as shown in figure 3.5. The gas enters the Rn+Th portion of dosimeter through a filter paper, which prevents the ingress of progenies. With its brief 55.6-second half-life, most thoron disintegrates

before entering the second chamber, ensuring that only radon is detected there (Sajwan et al., 2021). The detector films placed in their respective chambers register tracks from both these gases, whereas those in the radon chamber register tracks from radon alone.

Dosimeters were located 1.5–2 meters above ground level and kept 10–15 cm from walls, the setup aimed to reduce thoron interference which accumulates near walls due to its short half-life (de With et al., 2016; Mayya et al., 2012). Each set of detectors was deployed for 120 days per season before being replaced with a new set. To prevent electric field-induced variations in decay product deposition, the chamber interiors were coated with nickel powder, ensuring a uniform deposition environment (Sahoo et al., 2013).
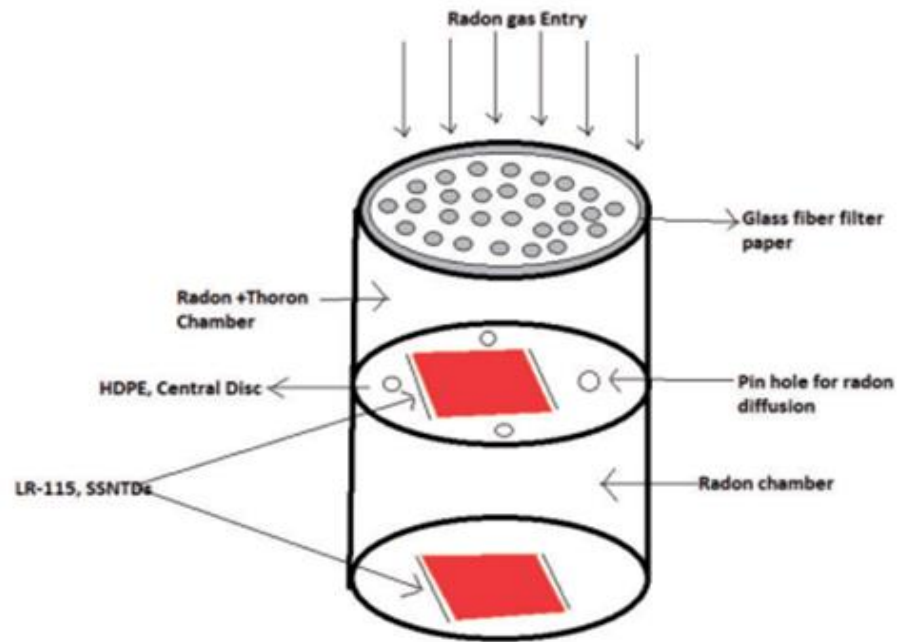
Figure 3.5: pinhole-based twin cup dosimeter

Assessment of Rn-222, Rn-220 Activity Concentrations

The decay of these radioactive gases produces alpha tracks on the detector films, which are converted into activity concentrations using the following equations:

$$C_r = \frac{T_{Kr} - B_g}{P.Q_r} \qquad\qquad 3.4$$

$$C_t = \frac{T_{K(r+T)} - T_{Kr} - B_g}{P.Q_T} \qquad\qquad 3.5$$

Here T_{Kr} represents radon progeny tracks, $T_{K(r+T)}$ represents total tracks from thoron progeny, B_g represent background tracks. P represents exposure time (days), and Q_r and Q_T are the calibration factors.

The Q_r for (^{222}Rn) in its respective portion is 0.0170 tracks cm^{-2} (Bq m^{-3} d)$^{-1}$, while for thoron (^{220}Rn), it is 0.010 tracks cm^{-2} (Bq m^{-3} d)$^{-1}$ (Eappen et al., 2008). The small Q_t value attributed to thoron is due to its short diffusion length, causing nearly 44% decay before reaching the chamber.

Direct Progeny Sensing Detectors

To obtain gas-independent concentrations, (DRPS) and (DTPS) were used. As displayed in figure 3.6, these detectors employ LR-115 Type-II films combined with selective aluminized Mylar absorbers, allowing precise alpha detection (Kumar et al., 2022).DTPS, uses a 50μm aluminized Mylar absorber to selectively record 8.78MeV alpha emissions from ^{212}Po while filtering out lower-energy radon progeny. DRPS, uses a 37μm absorber (25μm aluminized Mylar + 12μm LR-115 film) to detect 7.69MeV alpha emissions from ^{214}Po and also records 8.78MeV alpha emissions from ^{212}Po, requiring a correction factor (Campi, 2004) and is given by

Tracks only Rn Progeny alone (DRPS) = Tracks DRPS All- $\frac{\varepsilon_{RT}}{\varepsilon_{TT}}$ Tracks Total (DTPS)

3.6

This equation gives the tracks (tracks DRPS only due to radon progeny) recorded on the DRPS using the track registration efficiency. The DRPS and DTPS should be used in conjunction to achieve radon and thoron progeny distinction. ε_{TT} is used to denote the registration efficiency of thoron progeny on DTPS and is equal to 0.083 ± 0.004 per emitted alpha particle, whereas ε_{RT} is used to denote the registration efficiency of radon progeny on DRPS and is equal to 0.001 ± 0.0004 per emitted alpha particle.
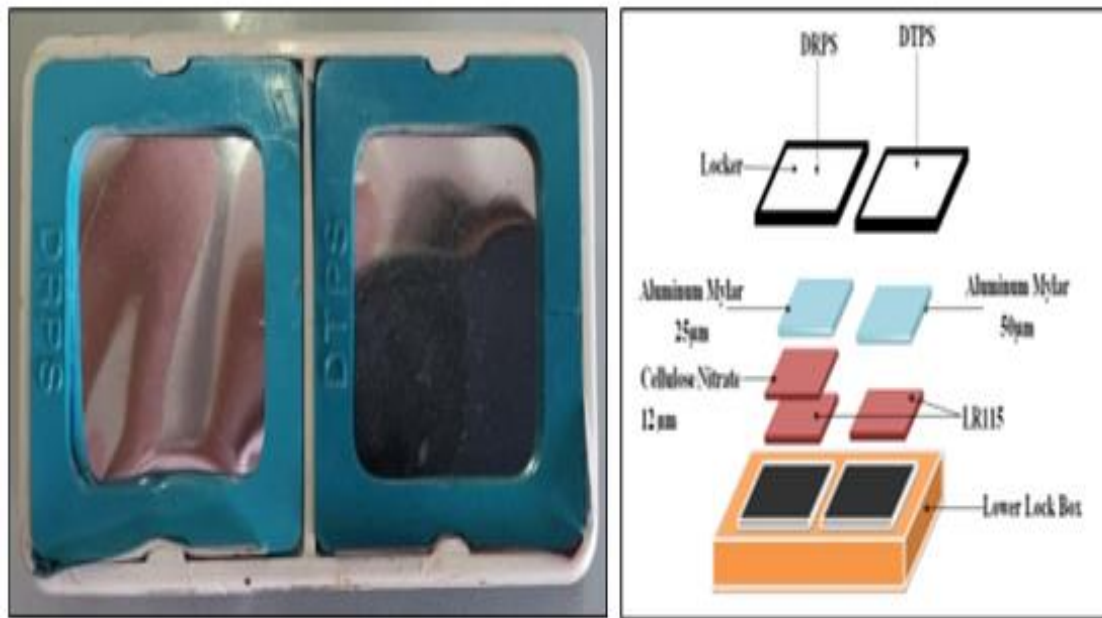
Figure 3.6: DRPS/DTPS progeny sensors embedded with aluminized mylars

Equilibrium Equivalent Progeny Concentration and Factors

The (EERC) and (EETC) were determined using

$$\text{EETC (Bqm}^{-3}) = \frac{\text{All Tracks DTPS}}{\text{KST}} * \text{exposure time (days)} \qquad 3.7$$

$$\text{EERC (Bqm}^{-3}) = \frac{\text{All Tracks DRPS}}{\text{KSR}} * \text{exposure time (days)} \qquad 3.8$$

Here, KST and KSR represent the calibration coefficients, with values of 0.94 tracks cm^{-2} day^{-1} per Bq m^{-3} for DTPS and 0.09 tracks cm^{-2} day^{-1} per Bq m^{-3} for DRPS, (Semwal et al., 2023).

Calibration and detection limits for Progeny Sensors

The sensitivity and calibration of the sensors depend on track registration efficiency, which relates detected track density to deposited progeny atoms, and deposition velocity, influencing progeny adherence to the detector surface (Kaushal et al., 2022). Calibration is conducted under controlled indoor and laboratory conditions to ensure precision (Sahoo et al., 2024).The equilibrium factor (F) of radon and thoron represents the ratio of progeny activity to gas concentration, expressed by equation 3.9 and 3.10 respectively.

$$F_R = EERC/C_{Rn} \qquad 3.9$$

$$F_T = EETC/C_{Th} \qquad 3.10$$

Both are unit less since Concentrations are measured in Bq/m^{-3}. Regarding detection thresholds, the (DTPS) has a sensitivity of 0.1Bq/m³, while the (DRPS) detects concentrations as low as 1Bq/m³ (Mishra et al., 2014).

3.6 Chemical Etching and Counting Process

After retrieval from the dosimeters, LR-115 detector films undergo chemical etching and track counting for analysis. This process involves two essential components: a constant temperature etching bath for precise chemical processing and a spark counter for efficient track density measurement. Both are crucial for ensuring accurate and reproducible results.

Constant Temperature Etching Bath

The constant temperature bath (Model PSI-CTB1), developed by Pollitech Instruments Pvt. Ltd. (Figure 3.7), is specifically designed for the controlled chemical etching of LR-115 films. This system comprises a temperature sensor, an electrical water heater, three etching containers, a circulating pump, and a double-distilled water bath with glass wool insulation. The integrated electronic controls ensure stable temperature conditions, preventing fluctuations that might affect the etching rate.

Upon retrieval, the detector films are subjected to chemical etching in the laboratory to enhance the visibility of alpha tracks recorded during exposure. The standardization of chemical etching parameters is crucial for consistent processing. The films are immersed in a 2.5N sodium hydroxide solution at a constant temperature of 60 degree centigrade for 90 minutes without stirring. Since the etching reaction occurs at the solid–liquid interface, damaged areas in the film dissolve preferentially, leaving behind well-defined latent tracks. For the tracks to be properly formed, the etching rate along the track path must exceed that of the surrounding bulk material. Once the process is complete, the films are rinsed with distilled water to remove any residual etching solution and dried before further analysis. This careful standardization ensures that the tracks are clearly distinguishable and suitable for subsequent counting (Eappen & Mayya, 2004).

Figure 3.7: Constant temperature etching bath employed for etching of SSNTD LR-115 Detectors

Spark Counter for Track Density Measurement

The spark counting technique is widely recognized for its efficiency in determining track densities in plastic detectors. This method, initially developed by Cross & Tommasino (1970), provides a rapid and cost-effective alternative to optical microscopy, making it particularly suitable for large-scale radon studies. The Model PSI-SC1 Spark Counter is employed for automated track counting in LR-115 Type-II films.

This spark counter is an advanced microcontroller-based device equipped with a programmable high-voltage module (ranging from 100V to 999V), a counting circuit, and a digital keypad for voltage adjustments. To ensure accuracy, the spark counter undergoes a precise calibration process by setting a pre-spark voltage of 900V, a gate duration of 6 seconds, and a count voltage of 300V. Track counting is performed over a voltage range of 300V to 900V in 20V increments, generating a plateau curve between 420V and 560V, which defines the optimal operational voltage. Based on this curve, an

operational voltage of 450V was selected for the study. Figure 3.8 below shows the track counting process via a spark counter. The mechanism of the spark counter is based on dielectric breakdown. The etched LR-115 detector is placed between two electrodes, forming a capacitor-like structure. The detector is covered with an aluminized Mylar sheet to enhance conductivity, with a weighted component ensuring firm contact. When high voltage is applied, sparks pass through the track holes, vaporizing the thin aluminum coating on the mylar and generating electrical pulses. These pulses are electronically recorded, providing a direct measure of the etched track density. To prevent repeated sparking at the same location, the vaporization process ensures that the spark jumps randomly across different holes until all tracks are counted. This automated and highly efficient counting technique makes the spark counter an indispensable tool for large-scale radiological studies, offering a high degree of accuracy, reliability, and cost-effectiveness.

Figure 3.8: Alpha track counting analysis using a spark counter (Radiation lab Khalsa College).

3.7 LED Fluorimetry for Uranium Analysis

Uranium levels were analyzed using an LED fluorimeter (Model LF-2a), a rapid and highly sensitive method for detecting trace uranium concentrations. This technique is based on the fluorescence principle, where uranyl complexes emit light upon excitation (Singh et al., 2024). The photo-multiplier tube (PMT) in the fluorimeter captured these emissions and converted them into electrical signals, which were measured to determine uranium concentration (Prasad et al., 2024). To enhance fluorescence, a 5% sodium pyrophosphate solution was added to the samples. A 7mL quartz cuvette with a 20 mm optical path length was used to ensure precise measurements. The calibration of uranium

analysis via LED fluorimetry follows a systematic protocol to ensure precision and repeatability. Standard uranium solutions spanning 0–1000 µg/L are prepared using uranyl acetate dihydrate in nitric acid-acidified distilled water to maintain solubility. A 5% sodium pyrophosphate solution, serving as the fluorescence reagent, facilitates complexation with uranyl ions to enhance signal response. Calibration involves measuring the fluorescence of distilled water and uranium standards mixed with the reagent, generating a calibration curve that correlates fluorescence intensity to uranium concentration (Negi et al., 2024; Panwar et al., 2024 ; Sharma et al., 2017). Uranium concentration was determined using a fluorimeter capable of detecting levels between 0.1 and 1000 ppb, with a detection limit of 0.05 ppb, obtained by averaging 1000 pulses from the UV LED excitation source (Mehta et al., 2024). Before analysis, a 45µm filter paper was used to eliminate impurities and minimize discrepancies. All measurements were conducted following BARC-recommended protocols to ensure accuracy and reliability (Monica et al., 2018). The calibration process was carefully performed, ensuring consistency in uranium detection across different samples (Mahajan & Kale, 2024).
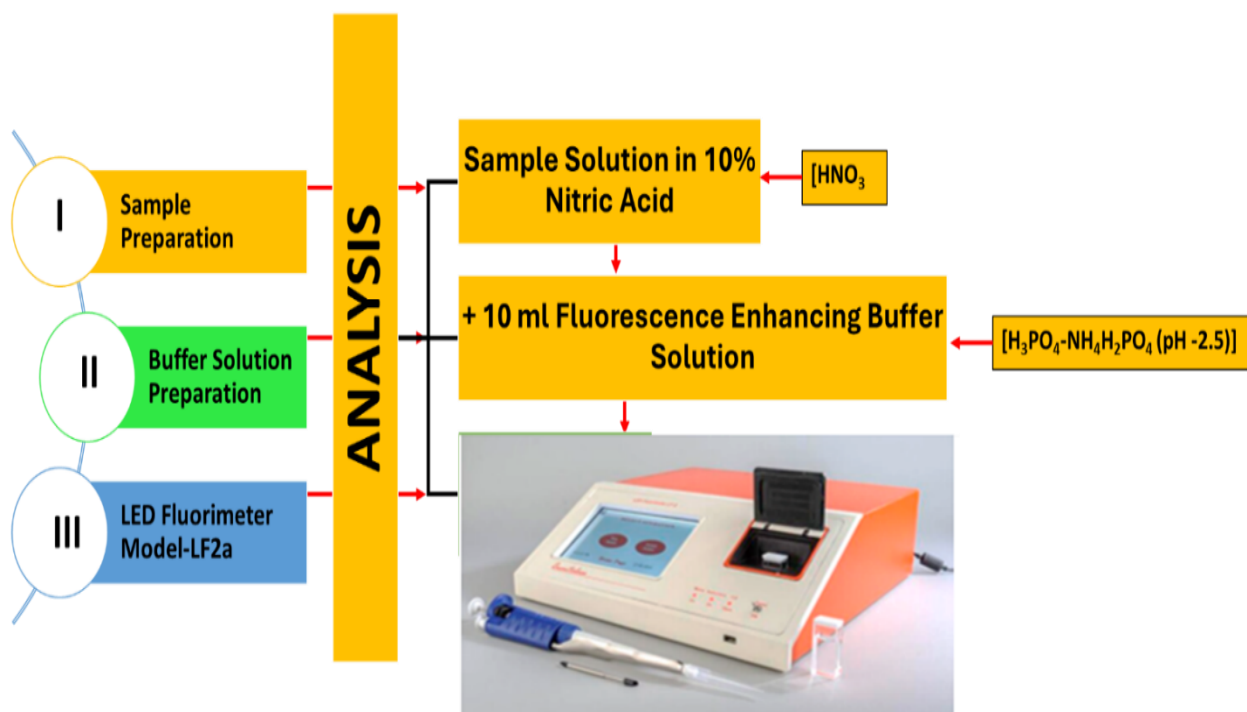
Figure 3.9: Flowchart of uranium analysis

3.8 Radiological and Chemical Risk Assessment

The possible radiological hazard from uranium presence in drinking water is evaluated through the estimation of Excess Cancer Risk (USEPA, 2003). It is determined by the following equation

$$\text{ECR} = \text{Uranium Activity (Bq/L)} \times R_F \qquad\qquad 3.11$$

Here, RF denotes the result of multiplying the cancer risk coefficient (R_c) by the average individual uranium intake (U_{in})

$$R_F = R_c \times U_{in} \qquad\qquad 3.12$$

The cancer risk constant (R_c) for uranium is estimated as 1.19×10^{-9} Bq^{-1} for mortality. The per capita uranium intake (U_{in}) is calculated based on an average human lifespan of 23,250 days and an average daily water consumption rate of 4.05 L/day:

$$U_{in} = 23{,}250 \text{ days} \times 4.05 \text{ l/day} \qquad\qquad 3.13$$

Assessment of Chemo toxic Risk

The toxic risk from uranium in water is assessed using the Lifetime Average Daily Dose (LDAv), which estimates long-term intake per body weight. It is determined using the formula

$$LD_{Av} \text{ (µg/kg/day)} = (A_c \times W_{intake} \times D_L \times E\upsilon) / (B_{Wt} \times C_{T \times 365}) \qquad\qquad 3.14$$

- A_c = Activity concentration of uranium (µg/L)
- W intake = Water intake rate (4.05 L/day)
- D_L = Lifetime duration exposure (63.7 years or 23,250 days)
- $E\upsilon$ = frequency period of exposure (365 days/year)
- B_{Wt} = Normal body weight (70 kg)
- C_T = Averaging time for carcinogenic risk (63.7 years or 23,250 days)

Evaluation of Hazard Quotient

The Hazard Quotient ($_{HZ}Q$) is used to estimate the possible non-cancer health risks linked to uranium consumption through drinking water. It is calculated as follows

$$_{HZ}Q = LDAv_{/DF} \qquad\qquad 3.15$$

Where $_{DF}$ represents the reference dose, defined as the maximum daily intake a person can tolerate without adverse effects. According to WHO (2004) and USEPA (2003) guidelines, the reference dose for uranium exposure is 2.26 µg/kg/day, which has been adopted in this study.

Age-Based Uranium Ingestion Dose Assessment

The uranium intake dose across various age groups was determined based on IAEA dose conversion factors combined with age-specific water consumption rates. The calculation follows the methodology outlined by (UNSCEAR, 2000).

$$A_D \text{ Ingestion} = U_C \times IW \times F_{ING \times 365} \qquad\qquad 3.16$$

Where U_C = Uranium concentration in water (Bq/L), IW = Daily water intake (varies with age), F_{ING} = Dose conversion factor for uranium ingestion (4.5×10^{-8} Sv/Bq, as per UNSCEAR, 2000).

3.9 Gamma Spectrometry Analysis for Natural Radioactivity

3.9.1 Collection and Preparation of Soil Samples

Soil specimens for radionuclide analysis were obtained from the study area at a depth ranging between 20 and 30 cm beneath the surface. To maintain sample integrity, unwanted debris such as stones and gravel were carefully removed prior to further processing. Initially, moisture was reduced by sun-drying, followed by oven-drying at 100°C for eight hours to ensure complete dehydration. The dried soil was then pulverized using a mortar and pestle and sieved through a 150µm mesh to standardize particle size. Approximately 150 g of each prepared sample was placed in a sealed 150mL Sunpet

container and stored for 28 to 30 days to achieve secular equilibrium, preparing the samples for accurate radionuclide measurement (Mehra et al., 2021).

3.9.2 NaI (Tl) Gamma Spectrometry Evaluation

Radionuclide concentrations of ^{226}Ra, ^{232}Th, and ^{40}K were determined utilizing a high-efficiency, low-resolution gamma spectrometer (ATOMTEX AT-1315), equipped with a 63×63 mm² NaI(Tl) scintillation detector coupled to a multi-channel analyzer (MCA), as depicted in Figure 3.11. The measurements were conducted at NIT Jalandhar, where the NaI(Tl) crystal detector, paired with a photomultiplier tube (PMT) operating at high voltage, was selected for its rapid response, non-destructive nature, and high sensitivity in detecting radiation (Kaur et al., 2021). The system's minimum detection limits were established at 3 Bq/kg for both ^{226}Ra and ^{232}Th, and 20 Bq/kg for ^{40}K. Each sample was analyzed for duration of no less than four hours to ensure precise quantification of natural radioactivity levels (Sharma et al., 2023).

Activity concentrations were derived from characteristic peak areas in the gamma energy spectrum, taking into account variables such as sample mass, geometry, counting time, detector efficiency, and instrumental response (Gusain et al., 2009; Yadav et al., 2014). Prior to sample measurement, energy and efficiency calibrations of the spectrometer were performed using a ^{137}Cs point source at the 661 keV gamma emission line (Rahim et al., 2023). Calibration protocols adhered to IAEA (2003) standards employing certified reference materials: ^{40}K (RGK-40), ^{238}U (RGU-238), and ^{232}Th (RGTh-232). To reduce background radiation, a lead shielding enclosure was utilized (Ravisankar et al., 2012).

Gamma emissions at specific energies—1460 keV for ^{40}K, 1764 keV for ^{214}Bi (proxy for ^{226}Ra), and 2610 KeV for ^{208}Tl (proxy for ^{232}Th)—were analyzed to quantify respective radio nuclides (Singh et al., 2025). Data acquisition and processing were facilitated by the SPTR-ATC software, which incorporated sample parameters such as mass, measurement duration, and geometry, alongside corrections for self-attenuation effects, thereby improving measurement accuracy.

3.9.3 Radium Equivalent Activity Calculation

Since natural radio nuclides are heterogeneously distributed, and most radiological concerns arise from radium and its decay products within the ^{238}U series, an integrated evaluation of radiation exposure is necessary. Instead of assessing individual radionuclide concentrations, the (Ra_{equ}) is evaluated using the following equation

$$Ra_{equ} = LR_a + 1.43L_{Th} + 0.077L_k \qquad\qquad 3.17$$

Figure 3.10 Schematic diagram of NaI gamma spectrometer

References

- Al-Sharif, A., & Abdelrahman, Y. S. (2001). Factors Affecting Radon Concentration in Houses. *Turkish Journal of Physics*, *25*(2), 153–158.

- Campi, F. (2004). Uncertainty evaluation of radon measurements with LR115 detector and spark counter. *Radiation Protection Dosimetry*, *111*(1), 59–64. https://doi.org/10.1093/rpd/nch361

- Cross, W. G., & Tommasino, L. (1970). A rapid reading technique for nuclear particle damage tracks in thin foils. *Radiation Effects*, *5*(1), 85–89. https://doi.org/10.1080/00337577008235000

- de With, G., de Jong, P., & Donk, J. J. (2016). Thoron Mitigation from Building Materials with Surface Barriers. *Health Physics*, *111*(5), 420–426. https://doi.org/10.1097/HP.0000000000000566

- Durrani, S. A., & Bull, R. K. (2013). *Solid state nuclear track detection: Principles, methods and applications* (Vol. 111). Elsevier.

- Eappen, K. P., Sahoo, B. K., Ramachandran, T. V., & Mayya, Y. S. (2008). Calibration factor for thoron estimation in cup dosimeter. *Radiation Measurements*, *43*(SUPPL.1), 418–421. https://doi.org/10.1016/j.radmeas.2008.03.019

- Eappen, K. P., & Mayya, Y. S. (2004). Calibration factors for LR-115 (type-II) based radon thoron discriminating dosimeter. *Radiation Measurements*, *38*(1), 5–17.

- Fleischer, R. L., Price, P. B., & Walker, R. M. (1965). Tracks of Charged Particles in Solids. *Science*, *149*(3682), 383–393. https://doi.org/10.1126/science.149.3682.383

- Gusain, G. S., Badoni, M., Prasad, G., Prasad, Y., Ramachandran, T. V., & Ramola, R. C. (2009). Studies of natural radionuclides and dose estimation from soil samples of Kumaun Himalaya, India. *Indian Journal of Physics*, *83*(8), 1215–1220. https://doi.org/10.1007/s12648-009-0104-1

- Hidayath, M., Lavanya, B. S. K., Naveena, M., & Chandrashekara, M. S. (2023). Studies on Radon Exhalation Rate and Activity of Radioactive Elements in Soil Samples and their Radiological Hazards to the Population of Davanagere District, Karnataka, India. *Journal of the Geological Society of India*, *99*(4), 525–532. https://doi.org/10.1007/s12594-023-2340-y

- Kaur, J., Shikha, D., Mehta, V., & Chauhan, R. P. (2023). Assessment of Radionuclide Concentration and Exhalation Rates in some NORMs and TENORMs of Shivalik Region. *Indian Journal of Pure and Applied Physics*, *61*(6), 520–525. https://doi.org/10.56042/ijpap.v61i6.2435

- Kaur, M., Kumar, A., Mehra, R., Mishra, R., & Bajwa, B. S. (2021). Measurement of radionuclide contents and 222Rn/220Rn exhalation rate in soil samples from sub-mountainous region of India. *Arabian Journal of Geosciences*, *14*(9). https://doi.org/10.1007/s12517-021-07103-5

- Kaushal, A., Joshi, M., Sarin, A., Sharma, N., 2022. Dosimetry of indoor alpha flux belonging to seasonal radon, thoron and their EECs. Environ. Monit. Assess. 194, 119. https://doi.org/10.1007/s10661-021-09746-z

- Kumar, M., Sahoo, B., Kumar, R., & Sharma, N. (2020). Estimation of radon exhalation rate from a brick wall during various stages of construction by measuring exhalation rates from various building materials. *Radiation Protection and Environment*, *43*(1), 31. https://doi.org/10.4103/rpe.RPE_38_19

- Kumar, A., Kansal, S., Rani, S., Nazir, S., & Mehra, R. (2023). *Estimation of Exhalation Rates of Radon / Thoron in Soil in Hanumangarh District*. *61*(June), 435–442. https://doi.org/10.56042/ijpap.v61i6.2414

- Kumar, R., Kumar, S., Kumar, P., Kumar, A., Vats, K., & Rawat, R. B. S. (2022). The Study Of Radon/Thoron And Progeny Concentration In The District Haridwar, Uttarakhand, India Using SSNTDS. *Journal of Survey in Fisheries Sciences*, *9*(1). https://doi.org/10.53555//sfs.v9i1.1769

- Mahajan, R. R., & Kale, A. (2024). *Chemo-Radiological Assessment of Groundwater Potability in the North- western Region of Maharashtra , India*

Chemo-Radiological Assessment of Groundwater Potability in the North- western Region of Maharashtra , India. October.

- Mayya, Y. S., Mishra, R., Prajith, R., Gole, A. C., Sapra, B. K., Chougaonkar, M. P., Nair, R. R. K., Ramola, R. C., Karunakara, N., & Koya, P. K. M. (2012). Deposition-based passive monitors for assigning radon, thoron inhalation doses for epidemiological studies. *Radiation Protection Dosimetry*, *152*(1–3), 18–24. https://doi.org/10.1093/rpd/ncs196

- Mehra, R., Kaur, S., Chand, S., Charan, C., & Mehta, M. (2021). Dosimetric assessment of primordial radionuclides in soil and groundwater of Sikar district, Rajasthan. *Journal of Radioanalytical and Nuclear Chemistry*, *330*(3), 1605–1620. https://doi.org/10.1007/s10967-021-07998-0

- Mishra, R., Sapra, B. K., & Mayya, Y. S. (2014). Multi-parametric approach towards the assessment of radon and thoron progeny exposures. *Review of Scientific Instruments*, *85*(2). https://doi.org/10.1063/1.4865165

- Monica, S., 2018. Assessment of age-dependent uranium intake due to drinking water in Neendakara, Kollam district Kerala. Int. J. Sci. Res. Phys. Appl. Sci. 6, 31-44.. https://doi.org/10.26438/ijsrpas/v6i3.3134

- Negi, R.S., Prasad, M., Aswal, R.S., Negi, J.S., Shrivastava, U., Panwar, P., Kaintura, S.S., Uniyal, S.C., Ramola, R.C., 2024. LED fluorimetric analysis of uranium in potable groundwater and associated health concerns. J. Radioanal. Nucl. Chem. https://doi.org/10.1007/s10967-024-09770-6

- Pandith, T. A., Gewali, J. P., Simnani, S., Nazir, S., Singh, K. P., & Chakan, M. R. (2024). Exploring tectonic sites with radon from groundwater sources and dose evaluation in various age groups in Baramulla, J&K, India. *Groundwater for Sustainable Development*, *26*(June), 101232. https://doi.org/10.1016/j.gsd.2024.101232

- Panwar, P., Joshi, A., Singh, K.P., Prasad, M., Mehra, R., Sahoo, S.K., Ramola, R.C., 2024. Distribution of uranium and selected toxic heavy metals in drinking water of Garhwal Himalaya, India. J. Radioanal. Nucl. Chem. 333, 2927–2935.

https://doi.org/10.1007/s10967-023-08998-y

- Pandith, T. A., Gewali, J. P., Simnani, S., Nazir, S., Singh, K. P., & Chakan, M. R. (2024). Exploring tectonic sites with radon from groundwater sources and dose evaluation in various age groups in Baramulla, J&K, India. *Groundwater for Sustainable Development*, *26*(June), 101232. https://doi.org/10.1016/j.gsd.2024.101232

- Prasad, M., Utpal, R. S. A., Abhishek, S., Pooja, J., Pargin, P., 2024. Levels and effects of uranium in groundwater sources of Shivalik hills , outer Himalaya , India. J. Radioanal. Nucl. Chem. 333(5), 2495–2504. https://doi.org/10.1007/s10967-023-08906-4

- Rahim, A., Khan, S., Rani, A., Abida, K., Mehra, R., & Chand, S. (2023). Estimation of 226Ra, 232Th and 40K activity from the Soil Samples of Ganderbal and Budgam Districts of Jammu and Kashmir, India. *Journal of the Geological Society of India*, *99*(12), 1767–1775. https://doi.org/10.1007/s12594-023-2531-6

- Ravisankar, R., Vanasundari, K., Chandrasekaran, A., Rajalakshmi, A., Suganya, M., Vijayagopal, P., & Meenakshisundaram, V. (2012). Measurement of natural radioactivity in building materials of Namakkal, Tamil Nadu, India using gamma-ray spectrometry. *Applied Radiation and Isotopes*, *70*(4), 699–704. https://doi.org/10.1016/j.apradiso.2011.12.001

- Saini, K., Sahoo, B. K., & Bajwa, B. S. (2016). *Case Study Report I ndoor and Built Estimation of indoor radon , thoron and their decay products ' concentrations along with annual inhalation dose in dwellings of Punjab , India*. *0*(0), 1–10. https://doi.org/10.1177/1420326X16676305

- Sajwan, R. S., Joshi, V., Kumar, N., Dutt, S., Rawat, K., Prasad, M., & Ramola, R. C. (2021). Study of radiation exposure due to indoor radon, thoron and progeny in Ghuttu, Tehri Garhwal, India. *Journal of Radioanalytical and Nuclear Chemistry*, *330*(3), 1497–1507. https://doi.org/10.1007/s10967-021-07937-z

- Sahoo, B. K., Sapra, B. K., Kanse, S. D., Gaware, J. J., & Mayya, Y. S. (2013). A new pin-hole discriminated 222Rn/220Rn passive measurement device with

single entry face. *Radiation Measurements*, *58*(January), 52–60. https://doi.org/10.1016/j.radmeas.2013.08.003

- Sahoo, B. K., Mishra, R., Khan, A., & Sapra, B. K. (2024). Radon Inhalation Dose Monitoring. In *Handbook on Radiation Environment, Volume 2* (pp. 623–654). Springer Nature Singapore. https://doi.org/10.1007/978-981-97-2799-5_21

- Semwal, P., Agarwal, T. K., Joshi, M., Kumar, A., Singh, K., & Ramola, R. C. (2023). Effective dose estimation of radon, thoron and their progeny concentrations in the environs of Himalayan belt, India. *International Journal of Environmental Science and Technology*, *20*(4), 4127–4138. https://doi.org/10.1007/s13762-022-04118-7

- Sharma, R. L., Mahur, A. K., Mehra, R., Chand, S., Ali, S. A., Gupta, D. Sen, & Singh, H. (2023). Natural Radioactivity, Radon Exhalation Rates and Radiation Doses in the Soil Samples Collected from the Vicinity of Kolaghat Thermal Power Plant, West Bengal, India. *Indian Journal of Pure and Applied Physics*, *61*(8), 653–658. https://doi.org/10.56042/ijpap.v61i8.2795

- Singh, P., Kaur, B., & Bajwa, B. S. (2024). Analysis of uranium and radon concentration in water of north-west Punjab, India. *Journal of Radioanalytical and Nuclear Chemistry*. https://doi.org/10.1007/s10967-024-09885-w

- Singh, K. P., Chandra, S., Prasad, M., Panwar, P., Joshi, A., Sharma, S., Kimothi, S., Prasad, G., Mehra, R., & Ramola, R. C. (2025). Measurement of natural radionuclides and health risk assessment in soil samples of the Main Central Thrust region in Garhwal Himalaya, India. *Environmental Monitoring and Assessment*, *197*(2). https://doi.org/10.1007/s10661-024-13569-z

- Sharma, S., Kumar, A., Mehra, R., Mishra, R., 2017. Ingestion doses and hazard quotients due to intake of Uranium in drinking water from Udhampur District of Jammu and Kashmir State, India. Radioprotection 52, 109–118. https://doi.org/10.1051/radiopro/2017009

- USEPA (United States Environmental Protection Agency) 2003. Current drinking water standards, Ground water and drinking water protection agency, United States Environmental Protection Agency.

- UNSCEAR (United Nations Scientific Committee on the Effect of Atomic radiation) (2000). United Nations general assembly. Vol. 1, Annex B, United Nations 84–140.

- WHO (2004). Guidelines for drinking-water quality, vol 1, 3rd edn. World Health Organization, Geneva.

- Yadav, M., Rawat, M., Dangwal, A., Prasad, M., Gusain, G. S., & Ramola, R. C. (2014). Levels and effects of natural radionuclides in soil samples of Garhwal Himalaya. *Journal of Radioanalytical and Nuclear Chemistry*, *302*(2), 869–873. https://doi.org/10.1007/s10967-014-3277-9

CHAPTER 4

TECTONIC ACTIVITY AND DOSE ASSESSMENT VIA GROUND WATER MONITORING OF RADON IN BARAMULLA, KASHMIR, INDIA

4.1 Introduction

Human health depends critically on the quality of the water, a worry that has sparked international efforts to carefully evaluate many aspects of water quality (Singh, P. et. al., 2021).The huge barriers are caused by contamination from both natural and man-made causes which has an adverse effect on public health as a whole. The sources of contaminants whether they are the result of natural minerals or human activity are crucial in defining how much water quality is deteriorating. It turns out that the mineral makeup of drinking water plays a significant role, even aside from bacteriological issues (Rafiq, M. et. al., 2023; Singh, K. P. et. al., 2023; Sarin, A. et. al., 2021). The undesirable existence of heavy elements like lead and arsenic, as well as some radioactive elements that are over allowable thresholds, constitutes a real threat to human health. All sources of groundwater include Radon (Rn-222), an odorless and colorless gas that is released when Radium (Ra-226) decays from the uranium decay chain. Its short half-life (3.82 days) and water solubility lead to varying amounts (Xinwei, L., 2006). Consuming or breathing in water with high radon levels might be harmful to one's health. Research and management strategies that are comprehensive are necessary to reduce these hazards (Kumar, A. et. al., 2022). The serious health consequences linked to low water quality are highlighted by the ominous threat of high concentrations of radioactive sources such as uranium and radon (Ganesh, D. et. al., 2020; Najam, L. A. et. al., 2018; Yousuf, R. M. et. al., 2009; Ravikumar, P. et. al., 2014). Because of the possible health effects, it is critical to comprehend whether drinking water contains radioactive contamination. The migration of pollutants from nearby rocks and soil is closely related to the quality of groundwater. Radon levels in soil and water can be influenced by the concentrations of uranium and radium in geological formations, which can reflect regional variations (W H O, 2017; Yu, K. N. 1994). Geo hydrology (fault-lineament (FL) and fracture-joint (FJ) type source of water is a key factor in the occurrence of increased radon levels in groundwater.

However, the presence of active thrusts, faults, and displacement of cracks enables the upward migration of radon gas (Singh, K. P. et. al., 2023). On the other hand, relatively low radon values in the groundwater sources were observed in sedimentary rocks or soil regions (Prasad, M. et. al., 2018). Dissolved radon poses a dual threat to residents, impacting the gastrointestinal system upon ingestion and infiltrating the respiratory system when released during routine household activities. The level of risk is determined by the movement of radon from the soil matrix to the surrounding environment, where diffusion and advection play a crucial role until it either decays or is discharged into the atmosphere. This combined danger underscores the importance of residents being vigilant about their health in the face of potential exposure (Kumar, A. et. al., 2022; Abojassim, A. et. al., 2017; Baltrenas, P. et. al., 2020; Gupta, M. et. al., 2011; Nazir, S. et. al., 2021; Xie, D. et. al., 2017).

Global awareness of the health risks associated with naturally occurring radioactive elements in water, such as radon, has developed. Waterborne radon is the second main cause of lung cancer in the United States, contributing to 14,000 of these deaths. It also causes 25,000 premature deaths annually (Vipin K. P. et. al., 2019). Various levels of contamination and reference values have been proposed by regulatory agencies, including the World Health Organization (WHO), the United Nations Scientific Committee on the Effects of Atomic Radiation (UNSCEAR), and the US Environmental Protection Agency (USEPA), for radon in water and annual radiation exposure through ingestion (UNSCEAR, 2008; Hess, C. et. al., 1985; USEPA., 2000; UNSCEAR., 2000). Key elements impacting indoor radon levels include meteorological factors, geological composition, building materials, construction methodologies, and the degree of ventilation in enclosed areas. Radon levels in water fluctuate due to factors like radioactive elements, rock features, water movement, and contact duration. Groundwater typically exhibits elevated radon levels because of its extended interaction with geological features (Thivya, C. et. al., 2017; Diana, A.S. et. al., 2020; Adithya, V.S.P.et. al., 2021;Singh, K.P. et. al., 2023; Kumar, A., 2022). Radon emission and the existence of tectonic faults are strongly correlated, according to recent studies. Even from deep

geological layers, these faults provide efficient routes for radon transport. The present study aims to protect the environment and public health from the harmful effects of radiation caused by radon. In order to pinpoint locations in the research region with elevated radon levels, a precise pathway must be created first. A crucial component of the research project, this strategic mapping establishes the framework for carrying out careful observation and focused interventions (Grzywa, C. A. et. al., 2020; Siročić, A. P. et al., 2020). In the study area, varying concentrations of radon-inducing radiation have been observed among different age groups due to differences in water consumption rates relative to body mass. Doses have been estimated for each age group, revealing that the ingestion dose predominates over the inhalation dose when water is the sole source of radon exposure (Sarin, A. et. al., 2021; Pant, D. et al., 2019).

As per the International Agency for Research on Cancer (IARC), cancer can be triggered by ionizing radiation in individuals of any age. Ionizing radiation, which increases the risk of cancer and can cause detrimental alterations to human cells, is released when radon gas and its metabolites decay. Cancer is caused by a series of genetic alterations known as carcinogenesis, which result in cell mutations. It is important to know the effects of indoor radon exposure on human health because individuals spend a lot of time indoors. To safeguard people against radiation-induced cancer, one needs to evaluate the risks and take action to reduce indoor radon levels (Robertson, A. et al., 2013, Giraldo, O. A. et al., 2020). Numerous studies have been conducted across India on the concentration of radon in water samples (Singh, K.P. et. al., 2023; Yadav, M. et. al., 2023). However, no such research has been done in the Baramulla region of the Indian state of Jammu and Kashmir. The objective of this study is to assess the groundwater radon activity and determine the associated ingestion and inhalation doses as well as the excess lifetime cancer risk (ELCR) for residents of the study area. The results of this study may be helpful for health risk assessment, uranium exploration, concealed thrusts, and fault allocation (Prasad, M. et. al., 2018, Ezzulddin, S. K. et. al., 2020; Nagaraja, K., 2006; Seminsky, K. Z. et. al., 2019).

4.2 Materials and Methods

Study Area

Based on its geological and geographical significance, the study has been carried out in the Baramulla district of Jammu and Kashmir, India as shown in **Figure 4.1**,located between 34.54° and 34.24° North latitude and 73.54° and 74.41° East longitude. Baramulla has borders with Budgam, Pounch, Bandipora, Kupwara, and Srinagar. Tectonically, the area is special, positioned on the edge of the Lesser Himalayan Pir Panjal range. While rivers and its tributaries supply gravel, sand, and bajri, mining operations in Baramulla rely on gypsum and slate. Geological conditions in the district are enhanced by sediments from the Proterozoic, Paleozoic, and Quaternary eras, which have a significant impact on both the terrain and mineral resources (Chapters ii and iii of the district survey report 2017). Baramulla has a distinct climate, ecology, and biodiversity because of its diverse landscape, which is shaped by the Pir Panjal range and includes hills, valleys, and river networks (GSI, NER, 2012).
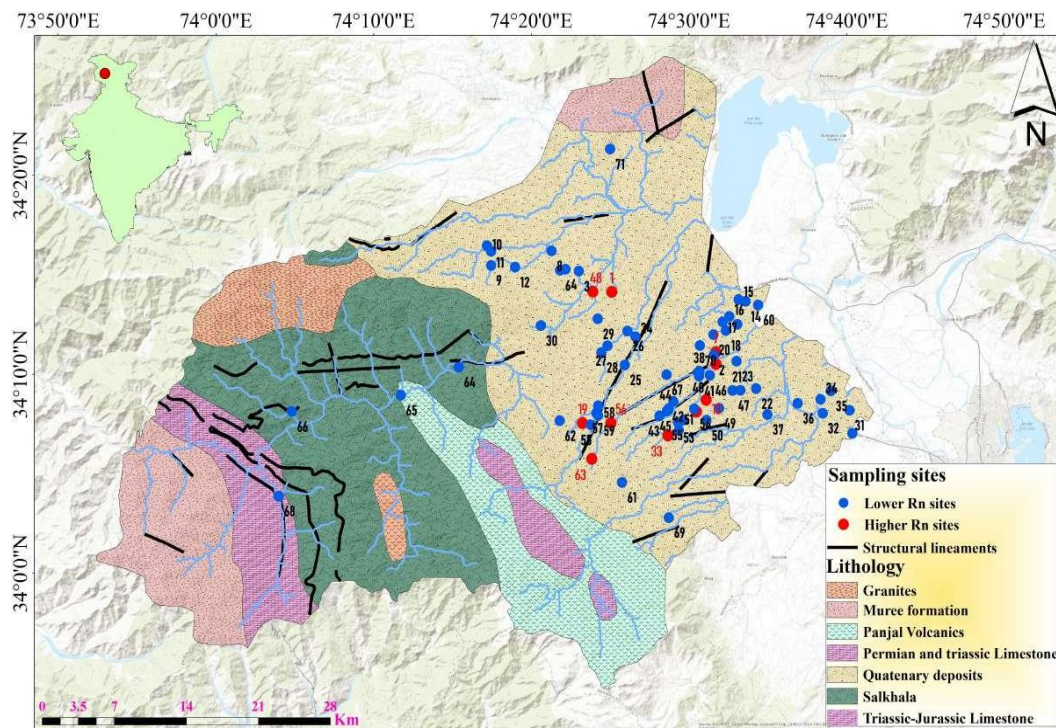
Figure 4.1: Geological map of the study area (Source; Geological Survey of India) (Raju, S., 2020)

96

Sample Collection

A total of s73 water samples were gathered for this study from various locations within the Baramulla district. The water was collected from groundwater sources such as drinking springs, hand pumps (tube wells), and wells. The **GPS device (GPS Map78s from Garmin Inc.)** was used to record the locations from where each sample was taken and the gamma radiation was also measured using a PM 1405 survey meter (Polimaster Inc.).The study is totally different from the others previously published concerning the location of the sites, geological formations, and also from sample-wise distributions. So, the care was taken to document information about where the groundwater came from.

The samples were collected from 20 August to 10 November of the year 2023.To collect the samples, a specific method was followed that is described in the Bhabha Atomic Research Center (BARC) radon handbook and manual of the instruments (Operational Manual, 2015). Care has been taken to ensure that the sampling bottles didn't make any air bubbles during sampling. A 60-ml glass bottle was used for the collection of the samples. Firstly, the bottle was submerged underwater and then filled without letting any air inside it and it was done using a tube to transfer the water carefully as shown in **Figure 4.2**. The process was repeated several times, making sure there was no air left in the bottle. Finally, the bottles were tightly sealed underwater to avoid any leaks (Sahoo, B. K. et. al., 2013; Kanse, S. D. et. al., 2016; Gaware, J. J. et. al., 2011; Singh, K.P. et. al., 2023).
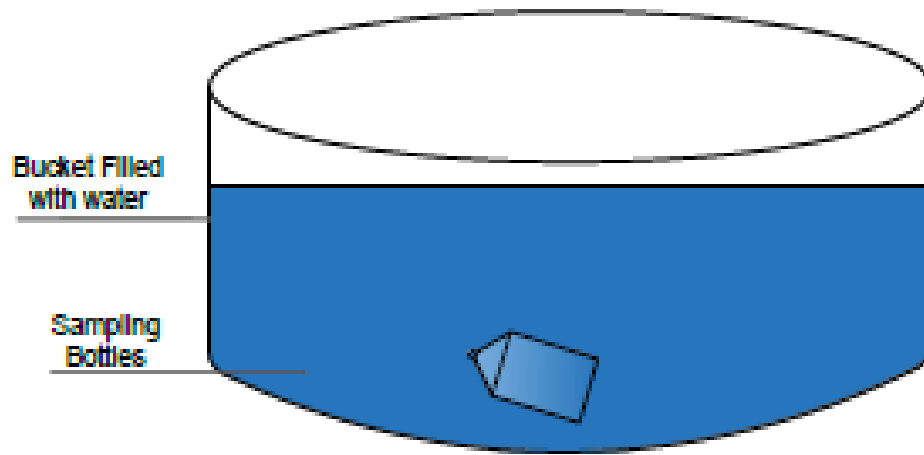
Figure 4.2: Method used to collect the water samples from the study area

Assessment of Radon in Water Samples

Using a sophisticated **RnDuo monitor** from **AQTEK Systems**, India, the amount of radon in water samples was evaluated. Since this monitor uses scintillation cell technology, it is more effective and not impacted by humidity than other radon monitors which use different detectors. Employing a radioactive decay mechanism, the monitor's integrated processor converts inputs into radon activity concentrations. It can detect up to 50 MBqm^{-3} of radon and as low as 8 Bqm^{-3} at 1 sigma confidence for 1 hour counting time. Its response time is 20 minutes for attaining 63% of radon and 40 min for attaining 95% of radon gas with a sensitivity of 1.2 CPH/(Bq/m^3). The overall calibration accuracy of the detector is approximately ± 5%.The Bhabha Atomic Research Center in Mumbai calibrates the monitor each year (Gaware, J. J. et. al., 2011; Rani, S. et. al., 2021; Rani, S. et. al., 2023).We ensured a minimal delay between sample collection and radon counting to prevent radon loss due to its radioactive nature. The measurement setup involved attaching the sampled bottle to the smart radon monitor, as shown in **Figure 4.3**.

Initially, a pump was attached to the system, and measurements were done directly where the samples were gathered (Rani, S. et. al., 2023). A radon detector runs four cycles of

fifteen minutes for a total of an hour and to remove the remaining gases, the pump runs in an open loop mode for five minutes before each sample measurement.
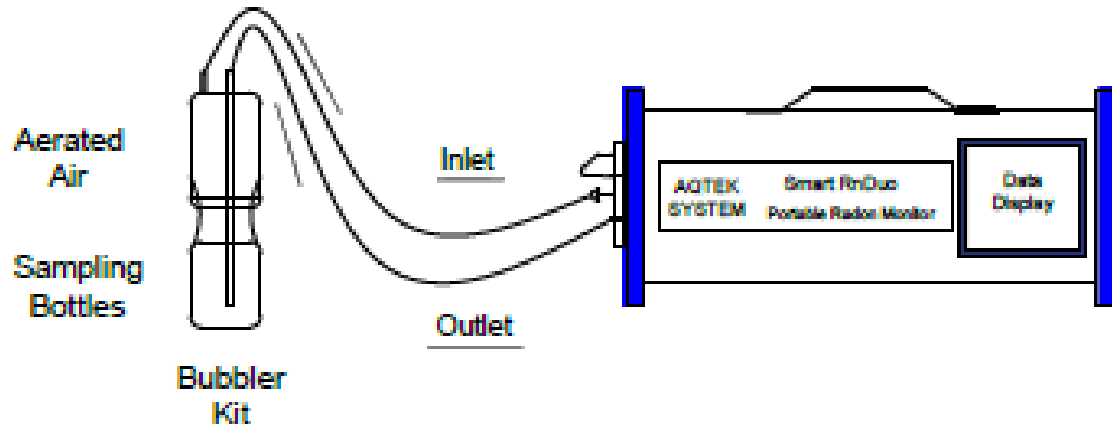
Figure 4.3: Measurement Setup for the analysis of radon in collected water samples

Calculation and Formulation Used

The following equation was employed to get the radon concentration in the collected water samples (Gaware, J. J. et. al., 2011).

$$RC_w = RC_a \times \left(K + \frac{V_a}{V_w} \right) \tag{4.1}$$

Where RC_w is the concentration of radon in water, RC_a is the concentration of radon in air, K is the partition coefficient of radon in liquid with respect to air (0.25), and V_a and V_w represent the volume of air and water respectively.

Radiological Dose Assessment Due to Radon in Water

There are two ways that radon can enter our bodies through water, either through consumption or inhalation of radon gas released into the indoor air from household water. Human respiratory problems are linked to inhalation of radon. When radon is emitted indoors or when it is present in water, we are exposed to radiation. The annual radiation dosage from radon in water was determined for newborns, children, and adults to get an idea of how this impacts different age groups.

A) **The effective (annual) ingestion dose** to residents of the studied area due to radon in drinking water has been assessed for different age groups as per (UNSCEAR., 2000).

B) $\quad D_{Ing} = RC_W \times A_{DWC} \times H_{Ing}$ (4.2)

Where D_{ing} is the ingestion dose due to Rn-222 (μSvy^{-1}), RC_W is the concentration of Rn-222 in water(Bqm^{-3}), A_{DWC} is the average daily water consumption (0.7 L for infants, 1.5 L for children, 3 L for adults and so on)(Sharma, S. et. al. 2017).For humans, the dose conversion factor (H_{ing}) due to ingested radon is 23 $nSvBq^{-1}$, 5.9 $nSvBq^{-1}$, and 3.5 $nSvBq^{-1}$ respectively (UNSCEAR., 2000).

C) **The effective (annual) inhalation dose** was calculated using (UNSCEAR., 2000)

D) $\quad D_{Inh} = RC_W \times \eta_{\frac{a}{w}} \times I_{ot} \times E \times H_{Inh}$ (4.3)

Where RC_W is the radon concentration in water, $\eta_{a/w}$ is the ratio of radon in the air to radon in water ($=10^{-4}$), E is the equilibrium factor between radon and its progenies ($=0.4$), I_{Ot} is the average indoor occupancy time per individual ($=7000$ hy^{-1}), and the dose conversion factor of radon inhalation for infants, children, and adults are $33nSv$ $(Bqhm^{-3})^{-1}$, $31.4nSv$ $(Bqhm^{-3})^{-1}$, and $28.3nSv$ $(Bqhm^{-3})^{-1}$ respectively (Kumar, A.et. al., 2021).

E) **The annual effective mean dose** for different organs especially the stomach and lungs were calculated by using UNSCEAR relations.

F) $\quad M_{Eff} = W_{TF} \times D_{(Ing, \ Inh)}$ (4.4)

Where W_{TF} is the tissue weighting factor (0.12 for the lungs and stomach, 0.05 for the liver and kidney, etc.,) and D is the effective ingestion and inhalation dose measured separately (UNSCEAR. 2000; Sharma, S. et. al., 2019).

G) **Excess lifetime cancer risk (ELCR)**

The Excess lifetime cancer risk (ELCR) was calculated by the following relation (Abojassim, A.et. al., 2017; Faweya, E. B. et. al., 2019; Taskin, H. et. al., 2009)

$$ELCR = D_{(Ing, \ Inh)} \times L_E \times R_F \quad (4.5)$$

Where D (ingestion, inhalation) is the annual effective dose due to ingestion and inhalation of water(μSvy^{-1}), L_E is the average duration of life for the country (70 years) and R_f is a risk factor (0.05 Sv^{-1}) as described in the ICRP report 2010.

4.3 Results and Discussions

4.3.1 Assessment of Physiochemical Parameters

In this study, groundwater samples were collected from different locations using hand pumps, wells, and springs for about 10 to 15 minutes. Precautions were taken during collection, using pre-cleaned polypropylene bottles. Environmental factors such as temperature, pH, conductivity, and TDS on-site were tested using the Benchtop conductivity/TDs master kit. Examination of the physicochemical characteristics of groundwater at the seventy-three study locations showed significant deviations from established water quality standards, with noticeable variations in the concentration of each parameter (Bilewu, O. F. et. al., 2022). A descriptive statistical analysis was done as highlighted in **Table 4.1**.

Table 4.1 Statistical analysis of collected groundwater samples

Statistical Parameters	PH Values	Temperature (^{o}C)	Conductivity (μS/cm)	TDS (mg/L)
Mean	7.59	13.63	907.06	465.14
Standard Error	0.04	0.16	59.51	31.12
Median	7.60	14.00	786.00	395.00
Mode	7.60	14.00	1132.00	290.00
Standard Deviation	0.32	1.33	508.45	265.87
Sample Variance	0.10	1.76	258523.00	70688.87
Kurtosis	0.15	-0.05	3.67	2.98
Skewness	-0.20	-0.31	1.76	1.67
Range	1.65	6.00	2801.00	1415.00
Minimum	6.85	10.50	186.00	95.00

Maximum	8.50	16.50	2987.00	1510.00

A total number of 73 water samples from various groundwater sources, such as hand pumps, wells, and springs, were taken for the analysis of the radon concentrations in this study. In particular, 11 samples were collected from wells, 16 from springs, and 46 samples from the hand pump averaging 41.3 ± 1.0 BqL^{-1}(from all sources), the radon levels ranged from $19 \pm 0.7$to 93 ± 0.4 Bq L^{-1}. Importantly, not a single sample went above the 100 Bqm^{-3} in this study as suggested limit recommended by WHO (WHO, 2017).

Table 4.2 Description of sampling locations, GPS Coordinates, Gamma field strength (GFS), water sample type, and measured radon concentration in water (RC$_W$) samples analyzed in the study area

Sample Code	Latitude (^{o}N)	Longitude (^{o}E)	Water Source	Depth(meters)	GFS (nSv/h)	RC$_W$ (BqL^{-1})
1	34.19	74.53	Tube Well	7.62	127	50 ± 1.2
2	34.26	74.39	Well	6.09	146	25 ± 0.8
3	34.26	74.37	Spring	7.62	136	22 ± 0.8
4	34.26	74.37	Tube Well	5.28	139	19 ± 0.7
5	34.27	74.36	Tube Well	10.67	142	21 ± 0.8
6	34.26	74.29	Tube Well	42.68	138	37 ± 0.9
7	34.28	74.29	Spring	0.6	146	31 ± 0.9
8	34.27	74.29	Spring	1.52	150	34 ± 0.9
9	34.26	74.32	Well	3.35	119	40 ± 1
10	34.23	74.56	Tube Well	6.09	137	22 ± 0.8
11	34.23	74.55	Well	9.14	142	21 ± 0.7
12	34.22	74.54	Tube Well	7.62	153	60 ± 0.8
13	34.22	74.54	Well	13.84	151	25 ± 0.8
14	34.21	74.54	Tube Well	16.76	157	26 ± 0.8
15	34.21	74.53	Well	6.09	154	34 ± 0.9

16	34.16	74.56	Tube Well	22.86	137	43 ± 1.1
17	34.16	74.57	Tube Well	9.14	135	49 ± 1.2
18	34.18	74.55	Tube Well	12.19	207	48 ± 1.2
19	34.2	74.45	Tube Well	82.31	143	31 ± 0.9
20	34.18	74.43	Tube Well	76.21	141	27 ± 0.9
21	34.21	74.44	Tube Well	73.17	132	34 ± 0.9
22	34.2	74.42	Tube Well	79.26	147	48 ± 1.2
23	34.19	74.41	Tube Well	82.31	135	40 ± 1.1
24	34.22	74.41	Tube Well	54.87	146	47 ± 1.2
25	34.21	74.35	Tube Well	21.34	148	52 ± 1.2
26	34.24	74.42	Tube Well	16.76	130	60 ± 1.3
27	34.14	74.67	Well	4.57	113	19 ± 0.7
28	34.14	74.64	Tube Well	4.57	114	39 ± 1
29	34.15	74.64	Tube Well	30.48	142	42 ± 1.1
30	34.16	74.65	Tube Well	27.43	149	39 ± 1.1
31	34.15	74.62	Well	5.48	178	29 ± 0.9
32	34.14	74.58	Tube Well	13.71	179	22 ± 0.9
33	34.17	74.51	Tube Well	13.71	136	25 ± 0.8
34	34.17	74.51	Spring	30.48	149	28 ± 0.9
35	34.17	74.51	Natural spring	2.43	166	31 ± 0.9
36	34.15	74.49	Tube Well	45.73	158	29 ± 0.9
37	34.14	74.47	Spring	5.48	150	50 ± 1.1
38	34.14	74.48	Tube Well	76.21	157	45 ± 1.1
39	34.14	74.48	Tube Well	91.46	145	45 ± 1.1
40	34.17	74.52	Tube Well	12.19	138	57 ± 1.3
41	34.18	74.53	Tube Well	13.71	168	72 ± 1.4
42	34.19	74.53	Tube Well	16.76	171	74 ± 1.4
43	34.16	74.55	Tube Well	48.78	173	45 ± 1.1
44	34.14	74.53	Tube Well	100.69	155	35 ± 1

45	34.13	74.52	Tube Well	82.31	137	28 ± 0.9
46	34.13	74.49	Tube Well	60.97	197	27 ± 0.9
47	34.13	74.5	Spring(Joshi Nag)	3.35	139	44 ± 1.1
48	34.13	74.49	Spring(Gorivan)	2.13	138	59 ± 1.3
49	34.13	74.48	Tube Well	12.19	154	65 ± 1.3
50	34.14	74.51	Tube Well	18.29	140	65 ± 1.3
51	34.15	74.52	Tube Well	18.29	133	81 ± 1.5
52	34.13	74.39	Tube Well	51.82	138	89 ± 1.5
53	34.13	74.4	Spring	2.43	145	41 ± 1.1
54	34.14	74.4	Tube Well	48.78	158	48 ± 1.2
55	34.15	74.41	Tube Well	53.35	141	50 ± 1.2
56	34.14	74.41	Spring	3.35	149	46 ± 1.2
57	34.23	74.57	Well	13.71	172	31 ± 0.8
58	34.08	74.43	Spring	3.65	268	24 ± 0.8
59	34.13	74.37	Tube Well	82.31	187	33 ± 0.9
60	34.18	74.26	Spring	4.57	139	45 ± 1.2
61	34.15	74.2	Tube Well	56.4	171	56 ± 1.2
62	34.25	74.4	Tube Well	38.1	183	60 ± 1.2
63	34.14	74.08	Spring	2.74	189	27 ± 0.8
64	34.17	74.48	Tube Well	73.17	163	41 ± 1.1
65	34.33	74.46	Tube Well	28.96	149	26 ± 0.8
66	34.07	74.07	Spring	3.96	164	27 ± 0.9
67	34.05	74.48	Spring	3.04	207	45 ± 1.1
68	34.2	74.51	Tube Well	48.78	151	42 ± 1.1
69	34.36	74.42	Tube Well	38.1	147	21 ± 0.7
70	34.13	74.42	Spring	5.57	159	89 ± 1.5
71	34.12	74.67	Well	6.09	167	20 ± 0.7
72	34.21	74.55	Well	9.75	168	19 ± 0.7
73	34.1	74.4	Tube Well	64.02	207	93 ± 1.5

The frequency trend displayed in **Figure 4.4**, provides insight on how the radon concentration varies over time in the groundwater samples. 36 samples of ground water were in the level 20-40 BqL^{-1}whereas26 water samples collected were having concentrations in the range 40-60Bq L^{-1}.Only a few samples(N = 4) were recorded with concentrations between 80-100 Bq L^{-1}. These samples were taken from hand pumps or tube wells except one (N = 1) from the spring source. This finding points to a relationship between regions with high radon levels and those with tectonic activity, as shown in **Table 4.3**. One can figure out the range of radon concentrations in the samples by examining the distribution curve. This enables one to look for possible clusters or outliers that may indicate localized sources or environmental variables impacting groundwater radon levels.
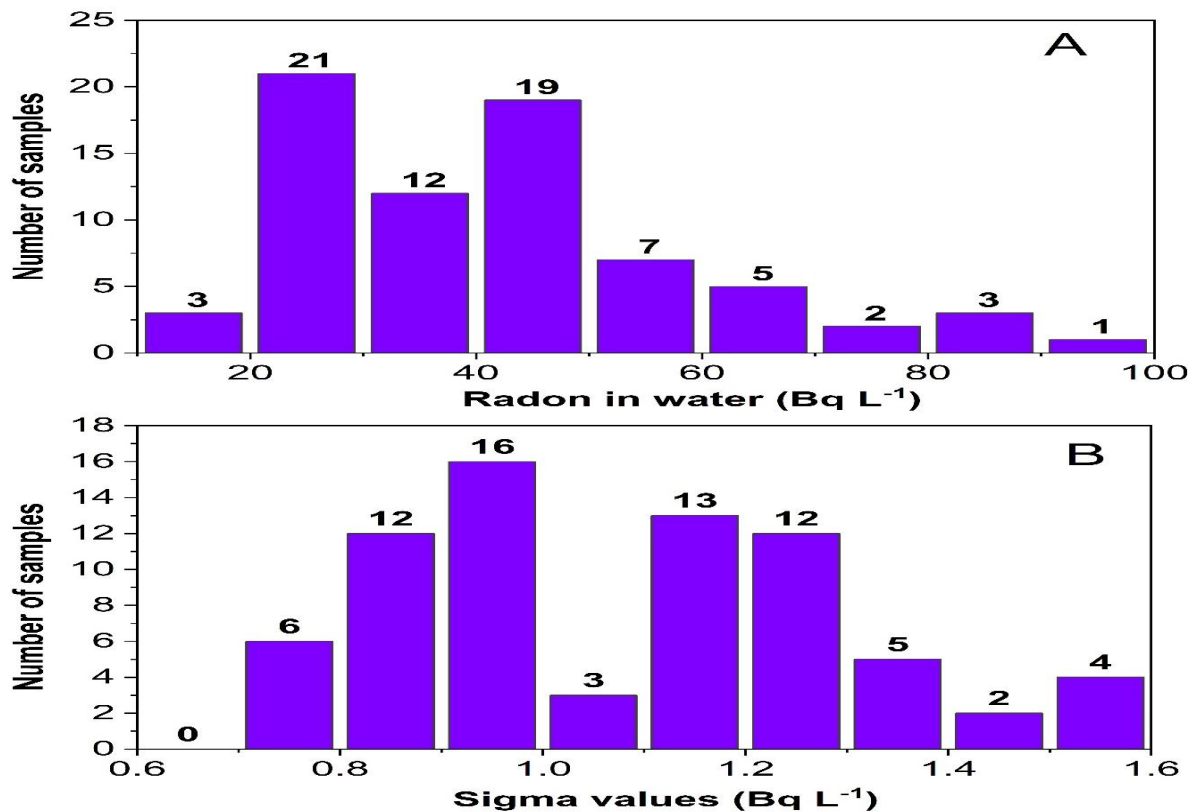
Figure 4.4: Frequency distribution of radon concentration in groundwater along with the sigma values

The distribution of the sigma values occurs in the measurement of radon concentration in water samples is also plotted in the Figure and it was found that the 34 samples were within the values of 1 Bq L^{-1}. In addition to supporting the assessments of the study area's geological and environmental health, this investigation helps to understand the regional distribution and variability of radon concentrations.

Table 4.3 Showing elevated radon concentrations around neo-tectonic fault zones

Sample Code	Latitude (ºN)	Longitude (ºE)	Water source	GFS nSv/h	RC_W BqL^{-1}
1	34.24	74.42	Tube well	130	60
2	34.18	74.53	Tube well	168	72
3	34.19	74.53	Tube well	171	74
4	34.15	74.52	Tube well	133	81
5	34.13	74.39	Tube well	138	89
6	34.12	74.48	Tube well	154	65
7	34.14	74.51	Tube well	140	65
8	34.24	74.40	Tube well	183	60
9	34.13	74.42	Spring	159	89
10	34.10	74.40	Tube well	207	93

4.3.2 Radon in Water as a Tracer: An Earthquake Station with Evidence of Active Tectonics in the Study Area

This study examines the relationship between active tectonics and radon anomalies (Rößler, F. A., and Villert, J., 2017), with particular reference to the 2005 Kashmir earthquake along the Main Boundary Thrust (Ahmad, B. et. al., 2014). Historical earthquakes that happened between 1555 and 1885 served as the inspiration for the research, which focuses on the Kashmir intermountain basin (Bali, B. S. et. al., 2020; Bilham, R., 2019; Karmakar, S., 2008; Rajendran, C. P. et. al., 2020).The water samples were collected in a manner that the tectonic disturbed locations were covered completely (as per accessibility) and then the radon concentrations in these locations were measured

to check the variation level. Ground-penetrating radar (GPR) and electrical resistivity are two of the novel techniques that the current study cites and that the local geologists previously employed to locate active faults and neo tectonic structures (Sana, H. et. al., 2021, Singh, B. et. al., 2021). The results of the study effectively established a relationship between radon anomalies and active tectonic processes in the study region, indicating the existence of hidden surface ruptures, structural discontinuities, and active faults. The findings suggested that the radon concentrations were higher in the active zones of the region rather than in other sampled sites. Table 3 showed the region of active neo-tectonic zones of the study area has higher values of these radon concentrations in all of the ten (N=10) samples collected while all other sites have low values of radon concentrations when compared. Following the study, there have been ongoing reports of small-scale seismic activity at multiple locations in the valley. These reports are mainly characterized by localized epicenters, as Google sources confirmed.

4.4 Dose Assessment Due to Radon in Water

The research evaluated the annual effective doses of radon exposure via ingestion and inhalation in adults, children, and infants. **Tables 4.4** and **Table 4.5** provide a statistical description of the results. Across all age groups, the annual effective inhalation dose was found to be higher than the 100 μSvy^{-1} limit recommended by the World Health Organization (WHO) but still significantly lower than the 1000 μSvy^{-1} limit recommended by the United Nations Scientific Committee on the Effects of Atomic Radiation (UNSCEAR)(WHO, 2017; UNSCEAR, 2000).

Additionally, the mean annual effective dose for all age groups was within the 3–10 $mSvy^{-1}$ suggested by the International Commission on Radiological Protection (ICRP, 2010). The analysis showed that radon exposure was likely to cause an excess of 0.52 to 3 cancer cases per thousand people over the course of a lifetime, with infants being more sensitive. Notably, the average values for every age group remained below the UNSCEAR-suggested upper limit of 1.45×10^{-3}(UNSCEAR, 2008).

Furthermore, the annual effective ingestion dose in infants was found to be between 108.48 and 533.31 μSvy^{-1}, with a mean value of 236.26 μSvy^{-1}, significantly exceeding

the WHO recommended limit of 100 μSvy^{-1}(WHO, 2017). Similarly, children and adults showed ingestion doses ranging from 60.87 to 298.24 μSvy^{-1} (mean 132.12 μSvy^{-1}) and 72.64 to 357.09 μSvy^{-1} (mean 158.19 μSvy^{-1}), respectively, also surpassing the WHO limit.

These results are explained by a number of factors, such as differences in the size and shape of the lungs, newborns' faster breathing rates (ATSDR, 2009), and smaller age groups' greater dose conversion factors. There are no significant correlations were found between electrical conductivity, temperature, depth to water levels, and ^{222}Rn activity. The position of lineaments, however, is consistent with the preponderance of significant ^{222}Rn activity found in groundwater. Additionally, the radium level in the host rock, and the rock's emanation coefficient, all significantly may influence the presence of radon in groundwater. When radon is inhaled, short-lived radioactive offspring accumulate on the surface of the respiratory tract and may effectively deliver doses to the bronchial epithelium (Ciotoli, G., 2017). Soft bodily organs are more sensitive to the deep effects of radiation exposure from progenies of radon because of their small size and developing physiology, especially in infants. Furthermore, enhanced particle penetration into other organs due to the deposition sequence of radon progenies in the respiratory tract, which follows the principles of Brownian motion, increases radiation exposure (Sharma, S.et.al., 2018; Kaur, M. et. al., 2019).

Table 4.4 Showing results of annual effective ingestion dose, mean annual effective ingestion dose, and excess lifetime cancer risk estimation for infants, children, and adults respectively

Statistical Analysis	Infants			Children			Adults		
	D_{ing} ($\mu Sv\ y^{-1}$)	M_{Eff} ($\mu Sv\ y^{-1}$)	ELCR $\times 10^{-3}$	D_{ing} ELCR ($\mu Sv\ y^{-1}$)	($\mu Sv\ y^{-1}$)	$\times$	M_{Eff} D_{ing} ELCR ($\mu Sv\ y^{-1}$)	D_{ing} ($\mu Sv\ y^{-1}$)	M_{Eff} $\times$

			10^{-3}			10^{-3}			
Mean	236.26	28.35	0.83	132.12	15.85	0.46	158.19	18.98	0.55
SE	12.08	1.45	0.04	6.75	0.81	0.02	8.09	0.97	0.03
Median	228.92	27.47	0.80	128.02	15.36	0.45	153.28	18.39	0.54
Mode	256.59	30.79	0.90	143.49	17.22	0.50	171.81	20.62	0.60
S D	102.47	12.30	0.36	57.30	6.88	0.20	68.61	8.23	0.24
S V	10500.04	151.20	0.13	3283.62	47.28	0.04	4707.35	67.79	0.06
Kurtosis	0.89	0.89	0.89	0.89	0.89	0.89	0.89	0.89	0.89
Skewness	1.07	1.07	1.07	1.07	1.07	1.07	1.07	1.07	1.07
Range	424.82	50.98	1.49	237.57	28.51	0.83	284.45	34.13	1.00
Minimum	108.49	13.02	0.38	60.67	7.28	0.21	72.64	8.72	0.25
Maximum	533.31	64.00	1.87	298.24	35.79	1.04	357.09	42.85	1.25

S E = Standard Error, S D = Standard Deviation, and S V = Sample Variance

Table 4.5 The statistical description of annual effective inhalation dose, mean annual effective inhalation dose, and excess lifetime cancer risk estimation in infants, children, and adults respectively

Statistical Analysis	**Infants**			**Children**			**Adults**		
	D_{inh} (μSv y^{-1})	M_{Eff} (μSv y^{-1})	ELCR $\times 10^{-3}$	D_{inh} (μSv y^{-1})	M_{Eff} (μSv y^{-1})	ELCR $\times 10^{-3}$	D_{inh} ELCR (μSv y^{-1})	M_{Eff} (μSv y^{-1}) $\times 10^{-3}$	
Mean	379.67	45.56	1.33	361.26	43.35	1.26	325.59	39.07	1.14
S E	19.41	2.33	0.07	18.46	2.22	0.06	16.64	2.00	0.06
Median	367.87	44.14	1.29	350.03	42.00	1.23	315.47	37.86	1.10
Mode	412.34	49.48	1.44	392.34	47.08	1.37	353.61	42.43	1.24
S D	164.66	19.76	0.58	156.68	18.80	0.55	141.21	16.95	0.49

S V	27114.35	390.45	0.33	24548.82	353.50	0.30	19940.87	287.15	0.24
Kurtosis	0.89	0.89	0.89	0.89	0.89	0.89	0.89	0.89	0.89
Skewness	1.07	1.07	1.07	1.07	1.07	1.07	1.07	1.07	1.07
Range	682.67	81.92	2.39	649.57	77.95	2.27	585.44	70.25	2.05
Minimum	174.34	20.92	0.61	165.88	19.91	0.58	149.51	17.94	0.52
Maximum	857.01	102.84	3.00	815.46	97.85	2.85	734.95	88.19	2.57

Radon concentrations from other parts of the world and local parts of India were cited here for reference with the current study to compare local and global variations in radon concentration in **Table 4.6.**

Table 4.6 The Global and Local radon concentrations as reported by various authors

Sources	Country	Range (Bq L^{-1})	References
Ground	Brazil	0.95-36	[Althoyaib,S.S.et.al., 2014]
Well	Turkey	0.70-31.70	[Althoyaib, S.S. et. al., 2014]
Well	Mexico	1.78-39.75	[Althoyaib, S.S. et. al., 2014]
Ground	Italy	1.80-52.70	[Althoyaib, S.S. et. al., 2014]
Well	Saudi Arabia	1.45-9.15	[Althoyaib, S.S. et. al., 2014]
Ground	Qatar	2.7-13.4	[Manawi, Y.et.al., 2023]
Drinking	Siwalik Himalaya	0.4 - 28	[Kaur, M. et.al., 2019]
Drinking	Mizoram	0.30 - 32.53	[Hmingchungnunga,2018]
Public supply	Tehran	27.70-74.30	[Alirezazadeh, N., 2005]
Ground	Northwest India	0.58 -3.6	[Diana A. S., 2020]
Ground	South India	0.25 – 7.1	[Adithya, V.S.P., 2021]

Drinking	Garhwal Himalaya	1.1-183.9	[Singh, K. P. et. al.,2023]
Ground	Lolab Valley Himalaya (Kashmir)	3.27 -59.50	[Rafiq, M.,2023]
Ground	Baramulla (J&K)	18.86-92.75	[Current study]

4.5 Correlation Study

A small correlation (shown in **Figure 4.5)** between radon concentrations and the depth of groundwater sources was found in the study (Pearson's r value of 0.076, R-square value of 0.005). It was observed that for a few samples bearing equal depth varied radon concentration was observed which may be attributed to the variation in radioactive content of groundwater source from its decay in nearby rock and soil at that site. By emphasizing the effect of nearby decay processes in rocks and soil formations, this relation illustrates the complex relationship between radon gas distribution and geological dynamics. The results provide insight into how radon levels are dependent on geological substrates and how important geological factors are in determining radon concentrations.

After doing statistical analysis, the study revealed that at different site locations, there was a slight correlation between the gamma field strength (GFS) and radon concentration (Rn-222) as shown in **Figure 4.6**. A portable Geiger-Muller (GM) counter radiation monitor (PM 1405, Polimaster Inc., USA) was used to measure gamma field strength (GFS) to assess surface contamination. The detector has a dose equivalent range (DER) of 0.01 μSv h^{-1} to 100 mSv h^{-1}. At each site, a 5-minute average with an error below 10 percent was considered for an accurate precision. For measuring gamma field strength (GFS) was recorded by raising the detector one meter above the ground level and leaving it for an average of five minutes. The R-square value of 0.01 and Pearson's coefficient of 0.02 both indicate this weak association. It indicates that surface-level radioactivity mostly affects the gamma field intensity measured above ground, but the radioactivity of nearby rocks influences the quantity of radon in water. The difference is explained by the thick layer of the clay materials shielding characteristics, which keep deeper radioactivity from significantly affecting surface-based observations of gamma field strength. The

correlation does not have any special significance but an idea of how much degree of amount of contribution to surface evaluated Gamma field with the corresponding underground radon water source attributed to uranium enriched sites. However, the elevated values of radon in any sites suggested that there may be a chance of uranium in those sites.
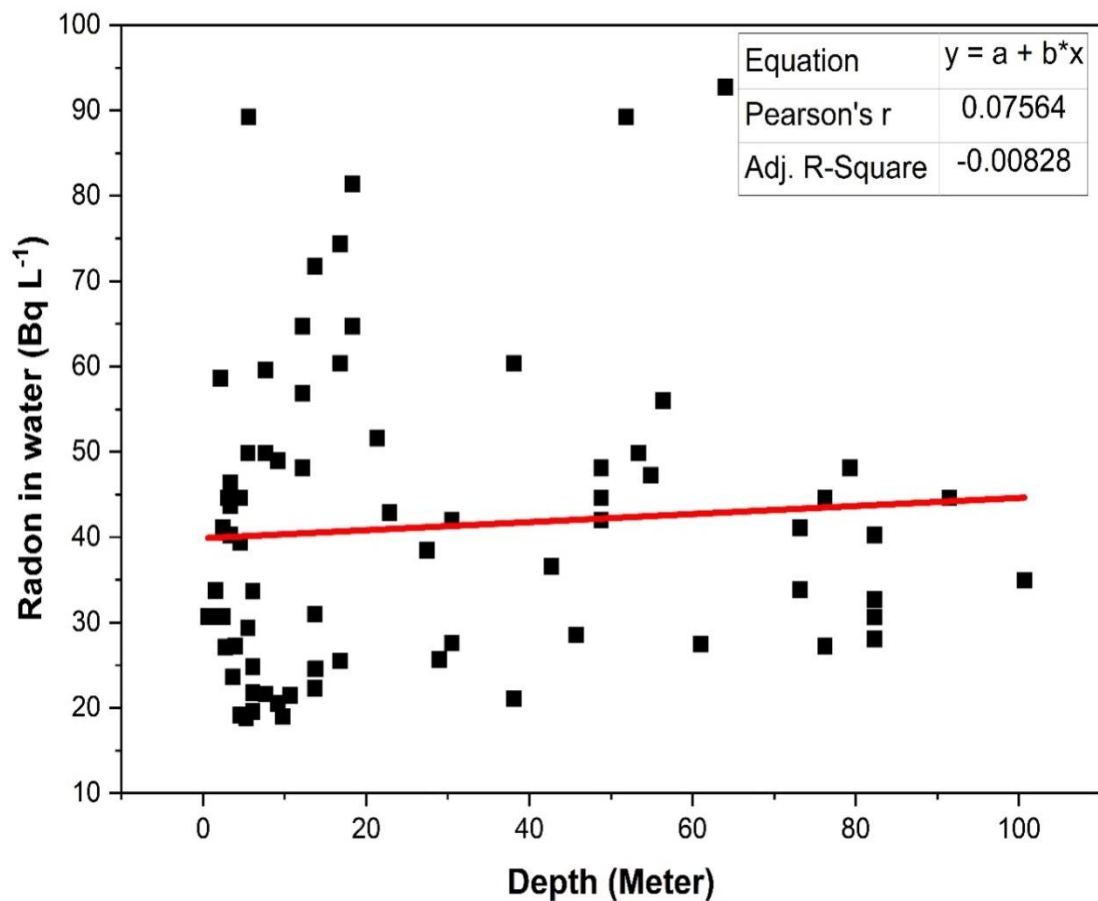
Figure 4.5: Correlation of Rn-222 concentration (BqL^{-1}) with depth in meters
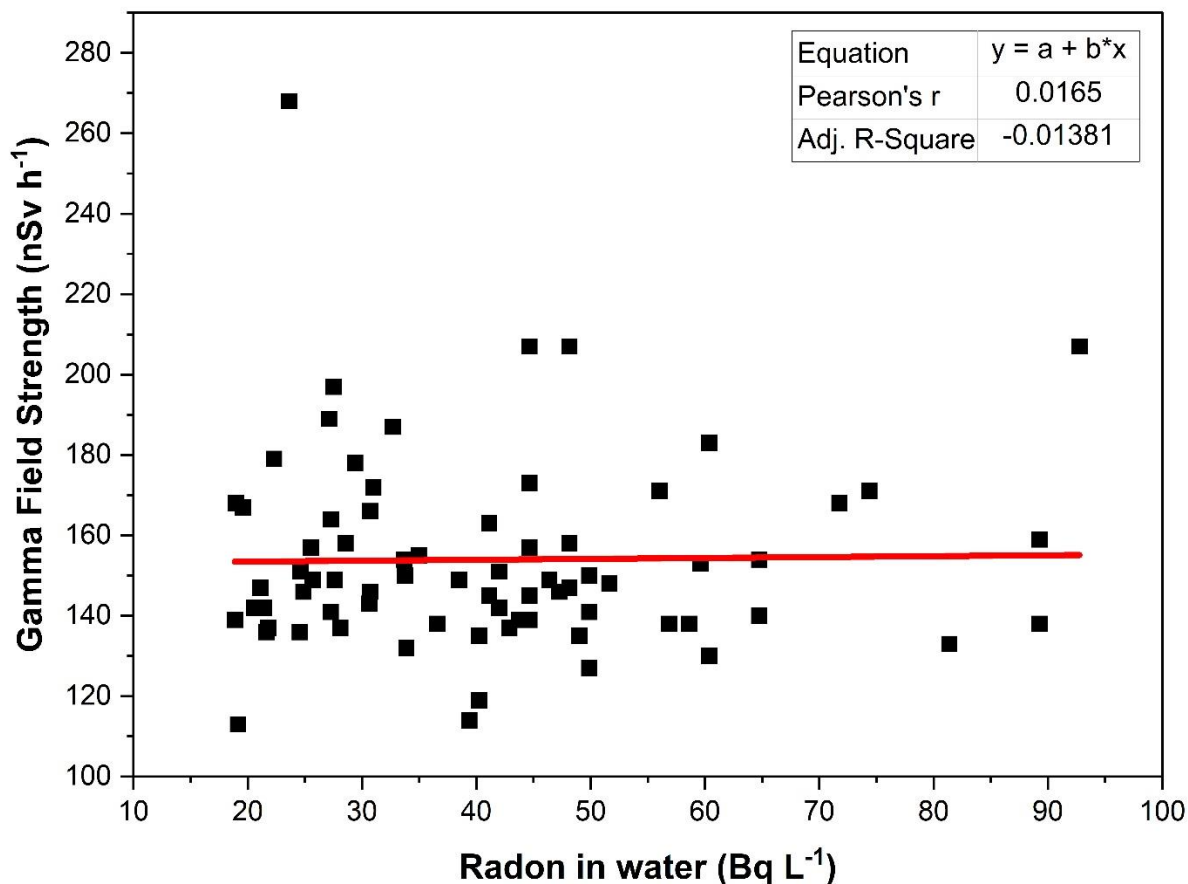
Figure 4.6: Correlation of Gamma filed strength and the Rn-222 concentration

4.6 Conclusions

Seventy-three drinking water samples from the entire Baramulla district were analyzed to determine the amount of dissolved radon. The results show that the radon concentration ranges from 19 ± 0.7 to 93 ± 1.5 Bq L^{-1}, with an arithmetic mean of 41.3 ± 1.0 Bq L^{-1}. The radiation dose that the general public would receive from drinking water polluted by radon gas was estimated for a trio of ages: adults, children, and newborns. In all age categories, the measured values through inhalation were significantly greater than the suggested limit of $100 \mu Svy^{-1}$. Similarly, through ingestion, the values are higher in all cases for newborns and in a few cases for adults and children.

Aquifer characteristics, the neo-tectonically active geology of the district, and the type of water source were all taken into account when the results of the study were analyzed. It was found that children receive the maximum doses due to higher values of radon concentration in their drinking water, and the doses decreased with increased age. However, the calculated yearly effective mean dose for each sample in this investigation was significantly less than the recommended 3–10 mSvy^{-1} limit for radon in water as per the ICRP report. From geological and epidemiological context, the results of the research provide valuable insights and reference data for future researchers.

References

- Abojassim, A., Mraity, H., Husain, A., Wood, M. (2017). Estimation of the excess lifetime cancer risk from radon exposure in some buildings of Kufa Technical Institute, Iraq. Nuclear Physics and Atomic Energy. 18. 276-286. 10.15407/jnpae2017.03.276. JO - Nuclear Physics and Atomic Energy

- Adithya, V. S. P., Chidambaram, S., Prasanna, M. V., Venkatramanan, S., Tirumalesh, K., Thivya, C., & Thilagavathi, R. (2021). Health Risk Implication and Spatial Distribution of Radon in Groundwater Along the Lithological Contact in South India. *Archives of Environmental Contamination and Toxicology*, *80*(1), 308–318. https://doi.org/10.1007/s00244-020-00798-9

- Alirezazadeh, N. (2005). Radon concentrations in public water supplies in Tehran and evaluation of radiation dose. *Iranian Journal of Radiation Research*, *3*(2), 79–83.

- Althoyaib, S. S., & El-Taher, A. (2014). Measurement of Radon and Radium Concentrations in Well Waterfrom Al-Jawa Saudi Arabia. *Journal of Natural Sciences and Mathematics*, *7*(2), 179–192. https://doi.org/10.12816/0009441

- Baltrėnas, P., Grubliauskas, R., & Danila, V. (2020). Seasonal Variation of Indoor Radon Concentration Levels in Different Premises of a University Building. *Sustainability*, *12*(15), 6174. https://doi.org/10.3390/su12156174

- Bilewu, O. F., Ayanda, I. O., & Ajayi, T. O. (2022). Assessment of Physicochemical Parameters in Selected Water Bodies in Oyo and Lagos States. *IOP Conference Series: Earth and Environmental Science*, *1054*(1), 012045. https://doi.org/10.1088/1755-1315/1054/1/012045

- Ciotoli, G., Voltaggio, M., Tuccimei, P., Soligo, M., Pasculli, A., Beaubien, S. E., &Bigi, S. (2017). Geographically weighted regression and geostatistical techniques to construct the geogenic radon potential map of the Lazio region: A methodological proposal for the European Atlas of Natural Radiation. *Journal of Environmental Radioactivity*, *166*, 355–375. https://doi.org/10.1016/j.jenvrad.2016.05.010

- Ezzulddin, S. K., & Mansour, H. H. (2020). Radon and radium activity concentration measurement in drinking water resources in Kurdistan Region-Iraq. *Journal of Radioanalytical and Nuclear Chemistry*, *324*(3), 963–976. https://doi.org/10.1007/s10967-020-07177-7

- Faweya, E. B., Olowomofe, G. O., Akande, H. T., Faweya, O., & Adesakin, G. E. (2019). Evaluation of radon exhalation rate and excessive lifetime cancer risk in Dumpsites in Ondo city Southwestern Nigeria. International Journal of Radiation Research, 17(3),371-382 https:// doi.org/ 10.18869/acadpub.ijrr.17.3.371

- Ganesh, D., Kumar, G. S., Najam, L. A., Raja, V., Neelakantan, M. A., & Ravisankar, R. (2020). uranium quantification in groundwater and health risk from its ingestion in and around Tiruvannamalai, Tamil nadu, India. *Radiation Protection Dosimetry*, *189*(2), 137–148. https://doi.org/10.1093/rpd/ncaa024

- Gaware, J. J., Sahoo, B. K., Sapra, B. K., & Mayya, Y. S. (2011). Development of online radon and thoron monitoring systems for occupational and general environments. BARC News Letter 318:45–51

- Giraldo-Osorio, A., Ruano-Ravina, A., Varela-Lema, L., Barros-Dios, J. M., & Pérez-Ríos, M. (2020). Residential Radon in Central and South America: A Systematic Review. *International Journal of Environmental Research and Public Health*, *17*(12), 4550. https://doi.org/10.3390/ijerph17124550

- Grzywa-Celińska, A., Krusiński, A., Mazur, J., Szewczyk, K., & Kozak, K. (2020). Radon—The Element of Risk. The Impact of Radon Exposure on Human Health. *Toxics*, *8*(4), 120. https://doi.org/10.3390/toxics8040120

- GSI, NER (2012). Briefing Book https://www.gsi.gov.in/webcenter/ShowProperty

- Gupta, M., Mahur, A. K., Sonkawade, R. G., & Verma, K. D. (2011). Monitoring of indoor radon and its progeny in dwellings of Delhi using SSNTDs. *Advances in Applied Science Research*, *2*(5), 421–426. www.pelagiaresearchlibrary.com

- Hess, C. T., Michel, J., Horton, T. R., Prichard, H. M., & Coniglio, W. A. (1985). The occurrence of radioactivity in public water supplies in the United States. Health Physics, 48(5), 553-586.

- Hmingchungnunga, -, Vanramlawma, -, Remlalsiama, -, Laldingngheta, -, Chhangte, L. Z., Pachuau, Z., Zoliana, B., Rosangliana, -, Sahoo, B. K., & Sapra, B. K. (2018). Assessment of radon content in water using SMART RnDuo in Mizoram, Northeast India. *Proceedings of the Mizoram Science Congress 2018 (MSC 2018) - Perspective and Trends in the Development of Science Education and Research*. https://doi.org/10.2991/msc-18.2018.32

- ICRP, (2010). International Commission on Radiological Protection for Protection against Lung Cancer Risk from Radon and Progeny and Statement on Radon. ICRP publication, P. 115.

- Kanse, S.D., Mishra, R., Gaware, J.J., Sahoo, B.K., Rout, R.P., Prajith, R., Agarwal, T.K., Sapra, B.K.,(2016). Handbook on radon transport models and measurement methods. Radiological physics and advisory division, Bhabha Atomic Research Centre, Mumbai.

- Kaur, M., Kumar, A., Mehra, R., & Mishra, R. (2019). Age-dependent ingestion and inhalation doses due to intake of uranium and radon in water samples of Shiwalik Himalayas of Jammu and Kashmir, India. *Environmental Monitoring and Assessment*, *191*(4), 224. https://doi.org/10.1007/s10661-019-7361-z

- Singla, A. K., Kansal, S., & Mehra, R. (2021). Quantification of radon contamination in drinking water of Rajasthan, India. *Journal of Radioanalytical and Nuclear Chemistry*, *327*(3), 1149–1157. https://doi.org/10.1007/s10967-021-07599-x

- Singla, A. K., Kanse, S., Kansal, S., Rani, S., & Mehra, R. (2023). A comprehensive study of radon in drinking waters of Hanumangarh district and the assessment of resulting dose to local population. *Environmental Geochemistry and Health*, *45*(2), 443–455. https://doi.org/10.1007/s10653-022-01304-x

- Manawi, Y., Ahmad, A., Subeh, M., Hushari, M., Bukhari, S., & Al-Sulaiti, H.

(2023). Evaluation of the Radon Levels in the Groundwater Wells of Qatar: Radiological Risk Assessment. *Water*, *15*(22), 4026. https://doi.org/10.3390/w15224026

- Nagaraja, K., Prasad, B. S. N., Chandrashekara, M. S., Paramesh, L., & Madhava, M. S. (2006). Inhalation dose due to radon and its progeny at Pune. *Indian Journal of Pure and Applied Physics*, *44*(5), 353–359.

- Najam, L. A., Ebrahiem, S. A., Abbas, S. A., & Mahdi, H. A. (2018). Assessment of radon gas concentrations levels and radiation hazards in the dwellings of Baghdad province, Iraq. *Rasayan Journal of Chemistry*, *11*(1), 37–40. https://doi.org/10.7324/RJC.2018.1111696

- Nazir, S., Sahoo, B. K., Rani, S., Masood, S., Mishra, R., Ahmad, N., Rashid, I., Zahoor Ahmad, S., & Simnani, S. (2021). Radon mapping in groundwater and indoor environs of Budgam, Jammu and Kashmir. *Journal of Radioanalytical and Nuclear Chemistry*, *329*(2), 923–934. https://doi.org/10.1007/s10967-021-07856-z

- Pant, D., Keesari, T., Rishi, M., Sharma, D. A., Thakur, N., Singh, G., Sangwan, P., Jaryal, A., Sinha, U. K., & Tripathi, R. M. (2020). Spatiotemporal distribution of dissolved radon in uranium impacted aquifers of southwest Punjab. *Journal of Radioanalytical and Nuclear Chemistry*, *323*(3), 1237–1249. https://doi.org/10.1007/s10967-019-06656-w

- Prasad, M., Kumar, G. A., Sahoo, B. K., & Ramola, R. C. (2018). A comprehensive study of radon levels and associated radiation doses in Himalayan groundwater. *Acta Geophysica*, *66*(5), 1223–1231. https://doi.org/10.1007/s11600-018-0135-0

- Singh, K. P., Chandra, S., Panwar, P., Joshi, A., Prasad, G., Gusain, G. S., & Ramola, R. C. (2023). Measurement of radon concentration in soil gas and radon exhalation rate from soil samples along and across the Main Central Thrust of Garhwal Himalaya, India. *Environmental Geochemistry and Health*, *45*(11), 8771–8786. https://doi.org/10.1007/s10653-023-01758-7

- Rößler, F. A., Villert, J., (2017). On-site determination of the radon concentration in water : sampling & on-line methods.

- Rafiq,M., Masood, S., Nazir, S., Mohi, M., & Kumar, A. (2023). A Study of Radon Concentration in Drinking Water of Lolab valley, Kashmir Himalaya. *Indian Journal of Pure & Applied Physics*, *61*(June), 515–519. https://doi.org/10.56042/ijpap.v61i6.2433

- Rajendran, C. P., Singh, T., Mukul, M., Thakkar, M., Kothyari, G. C., John, B., & Rajendran, K. (2020). Paleoseismological Studies in India (2016-2020): Status and Prospects. *Proceedings of the Indian National Science Academy*, *86*. https://doi.org/10.16943/ptinsa/2020/49787

- Raju, S., (2020). Geological Survey of India. Proceedings of the Indian National Science Academy, 86(1), 651–674.

- Rani, S., Kansal, S., Singla, A. K., & Mehra, R. (2021). Radiological risk assessment to the public due to the presence of radon in water of Barnala district, Punjab, India. *Environmental Geochemistry and Health*, *43*(12), 5011–5024. https://doi.org/10.1007/s10653-021-01012-y

- Rani, S., Kansal, S., Kumar, A., Nazir, S., and Mehra, R.(2023). Estimation of Annual Effective Dose Due to Radon Concentration in Water Samples of Moga District of Northern Punjab, India. Indian Journal of Pure & Applied Physics, *61*, 423–428. https://doi.org/10.56042/ijpap.v61i6.2412

- Ravikumar, P., & Somashekar, R. K. (2014). Determination of the radiation dose due to radon ingestion and inhalation. *International Journal of Environmental Science and Technology*, *11*(2), 493–508. https://doi.org/10.1007/s13762-013-0252-x

- Robertson, A., Allen, J., Laney, R., & Curnow, A. (2013). The Cellular and Molecular Carcinogenic Effects of Radon Exposure: A Review. *International Journal of Molecular Sciences*, *14*(7), 14024–14063. https://doi.org/10.3390/ijms140714024

- Sahoo, B. K., Sapra, B. K., Kanse, S. D., Gaware, J. J., & Mayya, Y. S. (2013). A

new pin-hole discriminated 222Rn/220Rn passive measurement device with single entry face. *Radiation Measurements*, *58*, 52–60. https://doi.org/10.1016/j.radmeas.2013.08.003

- Sana, H., Taborik, P., Valenta, J., Bhat, F. A., Flašar, J., Štěpančíkova, P., & Khwaja, N. A. (2021). Detecting active faults in intramountain basins using electrical resistivity tomography: A focus on Kashmir Basin, NW Himalaya. *Journal of Applied Geophysics*, *192*, 104395. https://doi.org/10.1016/j.jappgeo.2021.104395

- Sarin, A., Kaushal, A., Bajwa, B. S., & Sharma, N. (2021). Quantification of doses and health risks to organs and tissues corresponding to different age groups due to radon in water. *Journal of Radioanalytical and Nuclear Chemistry*, *330*(3), 643–655. https://doi.org/10.1007/s10967-021-08050-x

- Seminsky, K. Z., & Seminsky, A. K. (2019). Radon concentration in groundwater sources of the Baikal region (East Siberia, Russia). *Applied Geochemistry*, *111*, 104446. https://doi.org/10.1016/j.apgeochem.2019.104446

- Sharma, S., Kumar, A., Mehra, R., & Mishra, R. (2017). Ingestion doses and hazard quotients due to intake of Uranium in drinking water from Udhampur District of Jammu and Kashmir State, India. *Radioprotection*, *52*(2), 109–118. https://doi.org/10.1051/radiopro/2017009

- Sharma, S., Kumar, A., & Mehra, R. (2018). Age-dependent inhalation dose due to exposure of short lived progeny of radon and thoron for different age groups in Jammu & Kashmir, Himalayas. *Radiation Protection Dosimetry*, *182*(4), 427–437. https://doi.org/10.1093/rpd/ncy084

- Sharma, S., Kumar, A., Mehra, R., & Kaur, R. (2019). Ingestion and inhalation doses due to intake of radon in drinking water samples of Amritsar province, Punjab, India. *Radiation Protection Dosimetry*, *187*(2), 230–242. https://doi.org/10.1093/rpd/ncz157

- Sharma, D. A., Keesari, T., Rishi, M. S., Thakur, N., Pant, D., Sangwan, P., Sahoo, B. K., & Kishore, N. (2020). Distribution and correlation of radon and

uranium and associated hydrogeochemical processes in alluvial aquifers of northwest India. *Environmental Science and Pollution Research*, *27*(31), 38901–38915. https://doi.org/10.1007/s11356-020-10015-8

- Ptiček Siročić, A., Stanko, D., Sakač, N., Dogančić, D., & Trojko, T. (2020). Short-Term Measurement of Indoor Radon Concentration in Northern Croatia. *Applied Sciences*, *10*(7), 2341. https://doi.org/10.3390/app10072341

- Singh, P., Singh, P., Sahoo, B. K., & Bajwa, B. S. (2016). A study on uranium and radon levels in drinking water sources of a mineralized zone of Himachal Pradesh, India. *Journal of Radioanalytical and Nuclear Chemistry*, *309*(2), 541–549. https://doi.org/10.1007/s10967-015-4629-9

- Bali, B. S., & Wani, A. A. (2021). Analysis of neotectonic structures in the piedmont region of Pir Panjal Range NW Himalaya by integrating geomorphic indicators coupled with geophysical transects (GPR). *Natural Hazards*, *105*(3), 2869–2882. https://doi.org/10.1007/s11069-020-04428-4

- Singh, K. P., Chandra, S., Prasad, M., Joshi, A., Prasad, G., & Ramola, R. C. (2024). Estimation of radiation dose due to ingestion of radon in water samples of Garhwal Himalaya, India. *Journal of Radioanalytical and Nuclear Chemistry*, *333*(6), 2867–2879. https://doi.org/10.1007/s10967-023-09002-3

- Singh, P., Nautiyal, O. P., Joshi, M., Kumar, A., Ahamad, T., & Singh, K. (2021). Assessment of physicochemical and radon-attributable radiological parameters of drinking water samples of Pithoragarh district, Uttarakhand. *Journal of Radioanalytical and Nuclear Chemistry*, *330*(3), 1559–1570. https://doi.org/10.1007/s10967-021-08056-5

- Taskin, H., Karavus, M., Ay, P., Topuzoglu, A., Hidiroglu, S., & Karahan, G. (2009). Radionuclide concentrations in soil and lifetime cancer risk due to gamma radioactivity in Kirklareli, Turkey. *Journal of Environmental Radioactivity*, *100*(1), 49–53. https://doi.org/10.1016/j.jenvrad.2008.10.012

- Thivya, C., Chidambaram, S., Thilagavathi, R., Tirumalesh, K., Nepolian, M., & Prasanna, M. V. (2017). Spatial and temporal variations of radon concentrations

in groundwater of hard rock aquifers in Madurai district, India. *Journal of Radioanalytical and Nuclear Chemistry*, *313*(3), 603–609. https://doi.org/10.1007/s10967-017-5300-4

- UNSCEAR, (2008). United Nations Scientific Committee on the Effects of Atomic Radiation, Sources and Effects of Ionizing Radiation (New York: United Nations)

- USEPA., (2000). Radionuclide notice of data availability: technical support document. United States Environmental Protection Agency.

- UNSCEAR., (2000). Sources and Effects of Ionizing Radiation Report to the General Assembly with Scientific Annexes, United Nations. Annexure B, Vol. I, 97–105.

- UNSCEAR., (2000). Sources and effects of ionizing radiation: sources annex B. Exposures from natural radiation sources, 27–28

- Vipin Kumar, P., Gudennavar, S. B., Chandrashekara, M. S., Bubbly, S. G., & Hamsa, K. S. (2019). Radon in groundwater of magadi taluk, ramanagara district in Karnataka. *Radiation Protection Dosimetry*, *183*(4), 514–521. https://doi.org/10.1093/rpd/ncy176

- World Health Organization., (2017). Guidelines for Drinking Water. World health statistics 1–116

- Xie, D., Liao, M., Wang, H., & Kearfott, K. J. (2017). A study of diurnal and short-term variations of indoor radon concentrations at the University of Michigan, USA and their correlations with environmental factors. *Indoor and Built Environment*, *26*(8), 1051–1061. https://doi.org/10.1177/1420326X16660755

- Xinwei, L. (2006). Analysis of radon concentration in drinking water in Baoji (China) and the associated health effects. *Radiation Protection Dosimetry*, *121*(4), 452–455. https://doi.org/10.1093/rpd/ncl048

- Yadav, M., Singh, K. P., Dutt, S., Mehta, V., Kaur, J., & Ramola, R. C. (2024). Risk assessment due to ingestion of uranium and radon in the drinking water

samples of the Budhakedar region in Garhwal Himalaya, India. *Journal of Radioanalytical and Nuclear Chemistry*, *333*(6), 3065–3074. https://doi.org/10.1007/s10967-023-09262-z

- Yousuf, R. M., Husain, M. M., & Najam, I. A. (2009). Measurement of radon-222 concentration levels in spring water in Iraq. Jordan Journal of Physics, 2.

- Yu, K. N., Guan, Z. J., Stokes, M. J., & Young, E. C. M. (1994). A preliminary study on the radon concentrations in water in Hong Kong and the associated health effects. *Applied Radiation and Isotopes*, *45*(7), 809–810. https://doi.org/10.1016/0969-8043(94)90133-3

CHAPTER 5

RADON QUANTIFICATION AND AGE-BASED DOSE ASSESSMENT IN DRINKING WATER OF PATTAN, KASHMIR

5.1 Introduction

Radon is a radioactive gas that can be recognized in soil, water, and the air. As such, it poses significant health risks to the general public (Chakan et al., 2023; Ahamad et al., 2023). Processes by ingesting or breathing in its radioactive decay progenies, such as ^{218}Po, ^{214}Pb, ^{214}Bi, and ^{214}Po, increase the risk of internal radiation exposure and raise the chance of internal organ disorders, particularly those of the stomach and gastrointestinal tract (Thu & Van, 2020; Sharma et al., 2019; Ali, 2005). Radon exposure may arise from a number of sources, such as uranium and radium found in rocks, soil, natural gas, construction materials, water supplies, and outdoor air (Barca et al., 2021). The amount of radon released and the rate of water discharge are influenced by factors such as temperature, pressure, relative humidity, and grain size (Singh et al., 2021). Different amounts of radon exposure have been reported in areas such as India, where radioactive pollution is a result of both coal and non-uranium mining (Khutia et al., 2023; Tufail, et.al., 1988; Rao, et. al., 2001). Radon levels in water vary significantly with geological characteristics, including bedrock, porosity, permeability, fractures, and the type of soil. Since water moves through uranium-containing rocks, groundwater usually contains higher radon concentrations than surface water. In particular, granite aquifers typically have higher radon concentrations (Rani et al., 2023; Xinwei, 2006). Inhaling and ingesting the high values of radon gas causes lung cancer because of releasing alpha particles by its short-lived offspring (Nunes et al., 2022; Singh, K.P. et al., 2024). Furthermore, radon and its offspring can cause alterations in cellular and molecular structures, raising the risk of lung, stomach, and other organ malignancies (Binesh et al., 2010; Kumar et al., 2018).

Studies carried out in the USA claim that 21,000 lung cancer deaths annually are due to radon gas exposure in homes (Neri A. et al., 2013). A global groundwater survey found that the mean concentration of Rn-222 was approximately 183 Bq/L (Panghal et al., 2017). The linear no-threshold theory (LNT) is backed by scientific research that shows a linear relationship between radon exposure and harmful health effects, particularly lung cancer. The International Commission on Radiological Protection (ICRP) stresses that radiation exposure, even at low doses, can cause genetic abnormalities in cells, which can lead to cancer (Grzywa-Celińska et al., 2020). There is a clear link between indoor radon levels and the possibility of lung cancer, based on multiple studies carried out in Europe, North America, and China. These investigations found that, after smoking, radon is the second most common cause of lung cancer (Belete & Shiferaw, 2022). Knowing that ionizing radiation is carcinogenic, the production of radon gas in the soil and its migration into buildings through cracks and gaps represent a serious health threat (Singh, K.P. et al., 2023; Ahamad et al., 2024).

As the amount of time spent indoors rises, it becomes more important to measure indoor radon exposure. Due to epidemiological conclusions, international bodies have lowered acceptable indoor radon levels. This has spurred more research and worldwide surveys to monitor and reduce indoor radon concentrations (Nazir et al., 2021; Althoyaib & El-Teher, 2015). The distribution of radioactive elements in the environment leads to food chain pollution in addition to exposing the general public to ionizing radiation. As a super predator, this is hazardous to individuals. Radioactive elements can contaminate humans through ingestion, inhalation, or contact with the skin and mucous membranes (Hazou et al., 2022). Based on the literature, inhalation accounts for the majority of the dose rather than ingestion. This is generally true if we also consider the inhalation of radon released from indoor construction materials. However, if water is the sole source of radon that can be inhaled, then ingesting more radon will result in a dose that is greater than breathing in it (Sharma et al., 2019).

Beyond health risks, assessing radon concentrations has many other beneficial uses. Field estimates of radon in natural water and soil sources, like uranium deposits, can be helpful

for radiation assurance. Other approaches include constantly monitoring radioactivity in drinking, mining, and thermal water and searching for changes in radon levels in water and soil that may be related to seismic activity (Pant et al., 2020). Because of its relationship to geological formations, it can be used as an environmental tracer to determine contamination in soils and aquifers and aid in the prediction of earthquakes. Assessing groundwater flow velocities and researching processes of groundwater/surface water interaction are facilitated by the monitoring of radon concentrations (Rößler &Villert, 2017). To measure radon concentrations, measurement methods like the CR-39, RAD7, and Lucas Cell are often used (Dongre et al., 2023; El-Araby, et.al., 2019;Duggal, V, et. al., 2020). These methods give researchers the ability to measure radon levels in different environments and create strategies to minimize risk (Giraldo-Osorio et al., 2020). Programs to track indoor radon levels and take action to reduce related risks to health have been established by nations worldwide. However, due to several factors, including chemical forms, attachment to aerosols, and deposition and retention in live creatures, accurately determining radiation doses from radon and its progeny remains a major difficulty (Nsiah-Akoto et al., 2011; Park et al., 2018; Kumar et al., 2019; Singh et al., 2005).

This study, conducted in the Pattan region of Baramulla District, Jammu and Kashmir, is the first attempt to quantify the amount of radon in the study area's underground water source and evaluate its health implications. To understand the impacts of natural radiation on public health, efforts have also been made to identify high natural radiation levels. Furthermore, a study was conducted to examine the relationship between radon content and physicochemical parameters, especially pH, conductivity, and TDS, in underground water (Bilewu et al., 2022). The study will be a valuable source of information to raise public awareness about the chemical distribution of different elements in the underground water in the area under investigation, as the residents of the study area use the underground water for drinking.

5.2 Materials and Methods

Study Area

The location of the Pattan region, which forms a part of Baramulla Jammu and Kashmir, is 34.11°N to 34.23°N and 74.49°E to 74.61°E. The average elevation is 5,095 feet or 1,553 meters. Lying precisely in the middle of the Kashmir valley, Pattan is one of the region's historic capitals. **Figure 5.1** shows the sampling map of the study region. In the Baramulla areas, the topography and nearby surface water bodies have significant effects on groundwater flow (Raju, 2020).

The Pattan region lies to the northwest of the Kashmir Valley, situated between the Pir Panjal and the Great Himalayan ranges. The region's distinct geological constitution is shaped by a range of deposits, notably more recent sediments and transformed Precambrian rocks. A significant portion of the valley is lined with sediments from the Pliocene and Pleistocene epochs, which are associated with the Karewa Group. Among different Paleosol sections, the most common clay minerals consist of elite and chlorite, followed by kaolinite and smectite (Mir, et. al., 2023; Alam, et. al., 2015). Abundant mineral oxides are Fe_2O_3, Cao, SiO_2, Na_2O, K_2O, and MgO. The origins of these sediments are lacustrine, glacio-fluvial, and fluvial. The Kashmir Valley receives a lot of precipitation in the winter and spring due to western disturbances, which influence the climate of the area. The Pir Panjal has a significant impact in shaping the environmental conditions and topography of the valley (Tauseef et al., 2022; Changotra, 2017; Reviews, 2015).The reason behind selecting the particular region was in addition to geo-heritage sites and agrochemical active areas, the residents of the area solely rely on groundwater for drinking purposes.
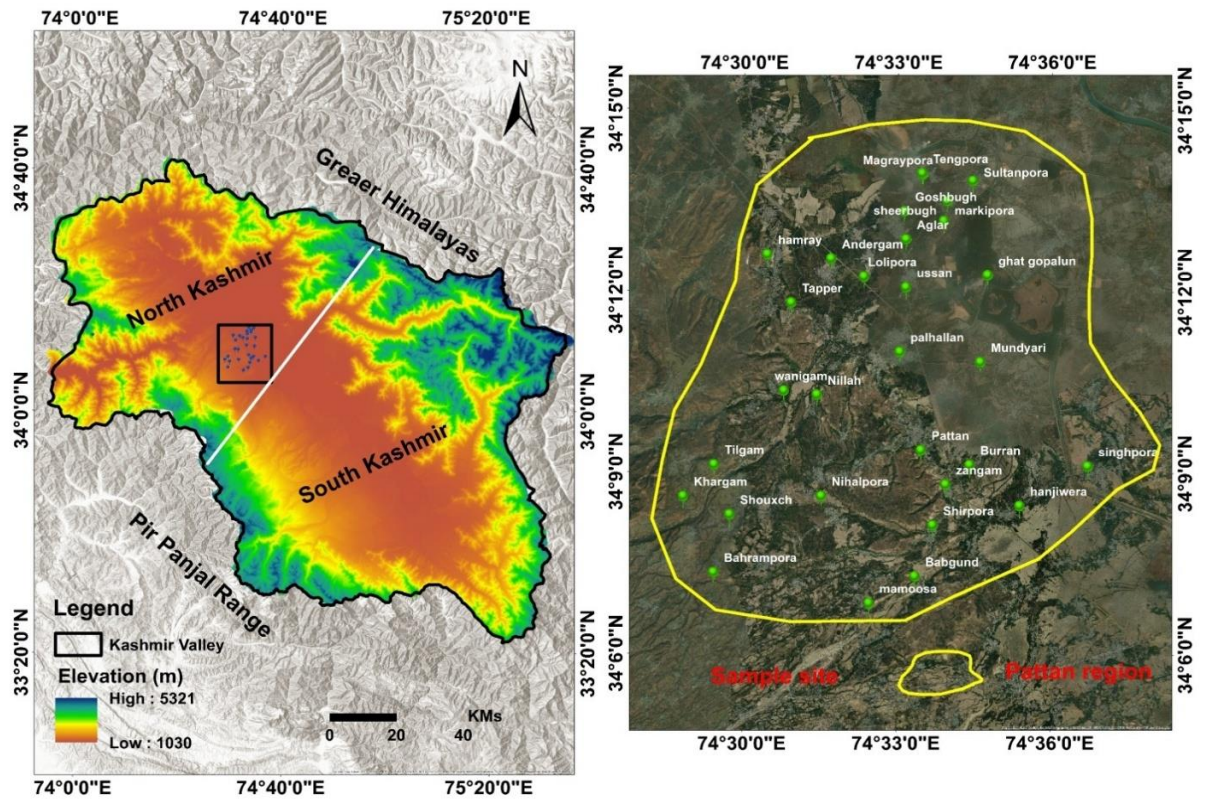
Figure 5.1: Location map of the study area with sample sites

Sample Collection Methods

To analyze the radon concentration, a total of 31 samples were taken from various underground water sources located in 31 villages within the study region. It was ensured that the water sample extracted from several groundwater sources was potable and mostly utilized for drinking by the research area's residents. Every groundwater source's depth was recorded, and each sampling location's GPS coordinates were obtained using (GPSMAP 78S, Garmin Inc). The procedure for measuring radon concentration was carried out by the guidelines provided by the Bhabha Atomic Research Centre (BARC) in their "Radon Handbook" (Sapra et al., 2010 a; Singla et al., 2023). The water samples were collected using glass bottles (60 milliliters) provided with a monitor bubble kit. During the sampling and storage procedures, every precaution was taken to ensure that the water sample did not come into contact with the air. As radon is a volatile gas that can

128

easily escape, the sampling bottle was held under water and the lid cap was fastened inside the water column in a way that prevented any form of aeration from entering the bottle, as displayed in **Figure 5.2**. To avoid any loss of radon gas, measurements were done right away (in situ) after every sample collection (Sapra et al., 2010 b; Sahoo et al., 2013).
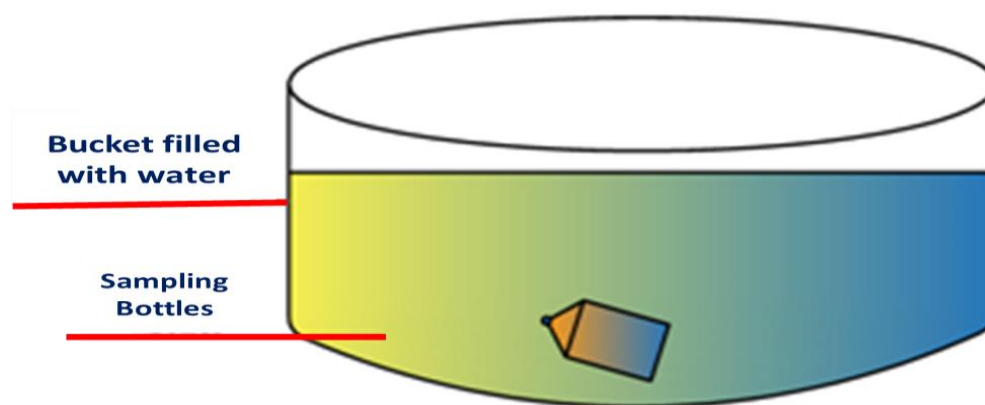
Figure 5.2: Collection technique for water sample analyzed in the present study

 Analysis of Rn-222 Activity

A smart RnDuo radon monitor (AQTEK System, India) was used to measure the amount of radon in a water sample. The Smart RnDuo is a continuous radon monitor that is portable, active and used commercially. The setup includes a radon detector and a water bubbler kit. One of the key benefits of using this detector is that its microcontroller is equipped with a radioactive decay algorithm that uses a scintillation process to convert observed counts to activity concentration (Singla et al., 2021). This algorithm is also immune to humidity effects. Bhabha Atomic Research Center, India calibrates the detector once a year. Before every measurement, the gases were released by running the pump in open-loop mode for five minutes. After that, the sampling bottle was linked to the RnDuo monitor and the bubbler attachment using tubing that bubbled with the monitor (**Figure 5. 3**). The built-in pump operated for approximately five minutes. Radon was measured in situ over one hour in four cycles of fifteen minutes each (Rani et al.,

2023).The detector can detect radon in a range from 8 Bq/m³ to 50 M Bq/m³ with a one-hour counting time at 1-sigma confidence. It has a sensitivity of 1.2 CPH/ (Bq/m³) and achieves 63% of the target radon concentration in 20 minutes and 95% in 40 minutes. The monitor's calibration accuracy is about ±5%. For this analysis, the laboratory facilities were provided by the Radiation Lab, Department of Physics, University of Kashmir, Srinagar, India.
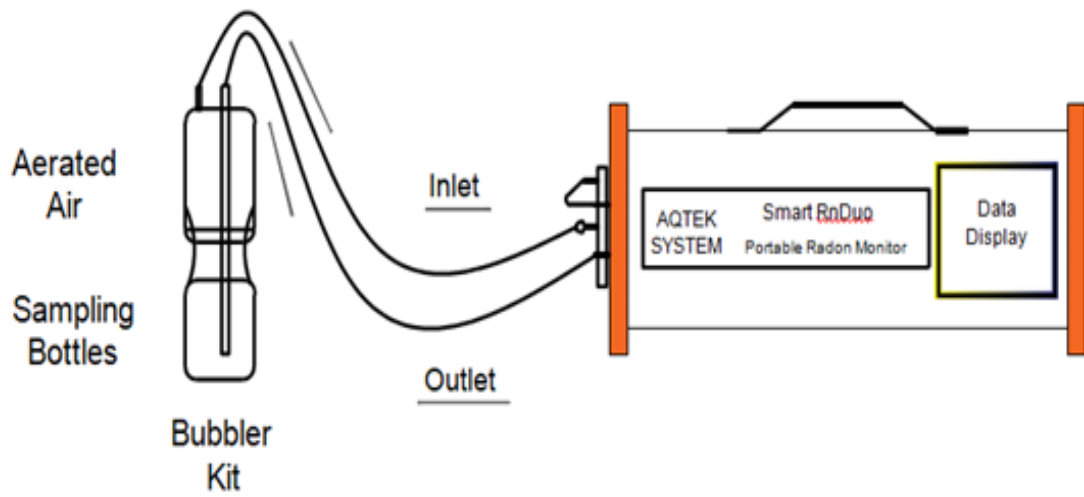
Figure 5.3: In-situ measurement setup for the analysis of radon in water samples

Evaluation of the Radon Content in Water

The radon content of the water was calculated using the following formula (Gaware et al., 2011).

$$C_a = C_w \times \left(k + {}^{T_a}/_{T_w}\right) \qquad (5.1)$$

Where k is the partition coefficient between air and water (0.25), T_a and T_w represent the volume of air and water respectively (Ta/Tw = 3.25) (Chakan, et. al., 2023). C_a (Bq/m³) is radon concentration in air and C_w (Bq/m³) represents radon concentrations in water

Radiation Dose Assessment by Ingestion and Inhalation

The parameters given in the United Nations Scientific Committee on the Effects of Atomic Radiation (UNSCEAR, 2000) report have been utilized for calculating the

annual effective dose exposure resulting from radon ingestion and inhalation from water sources.

(a) The **ingestion dose** due to radon in water has been given by (UNSCEAR, 2000).

$$D_g = C_w \times AW_i \times 365 \times F_{ing}$$ (5.2)

where C_w is the concentration of Rn-222 in water (Bq/m³), D_g is the ingestion dose of Rn-222(μSv/y), and AW_i is the daily consumption of water, aged in increments for newborns (0.7 L/d), children (1.5 L/d), and adults (3.2 L/day)(Sharma et al., 2017). The factor that converts doses (F_{ing}): its values for newborns, children, and adults are 23nSv/Bq, 5.9nSv/Bq, and 3.5nSv/Bq respectively.

(b) UNSCEAR 2000 provides the **inhalation dose** associated with radon consumption in drinking water

$$D_{ih} = C_w \times \beta_{\alpha/\omega} \times O_{ti} \times Z_{Rn-222} \times F_{ih}$$ (5.3)

where D_{ih} is the inhalation dose from Rn-222(μSv/y), C_w is the radon concentration in water (Bq/m³), $\beta_{\alpha/\omega}$ is the ratio of radon in air to radon in water (= 10⁻⁴), O_{ti} is the average occupancy time indoors (= 7000 h/y), Z_{Rn-222} is the equilibrium factor between radon and its progenies (= 0.4), and F_{ih} is the dose conversion factor for infants (33nSv/(Bq h/m³)⁻¹, children (31.4 nSv/(Bq h/m³)⁻¹ and adults (28.3 nSv/(Bq h/m³)⁻¹ (Rani et al., 2021).

(c) The formula below was used to calculate the mean total **annual effective dose** for each of the organs (Belete & Shiferaw, 2022; Rößler &Villert, 2017)

$$M_E = W_T \times D_T \times (g, ih)$$ (5.4)

The total dose by ingestion and inhalation is represented by $D_T \times (g, ih)$, taken collectively, and the tissue weighting factor for each organ is represented by W_T, for the stomach and lungs (0.12) (Khutia et al.,2023; Holm, 2006).

5.3 Results and Discussions

Analysis of Physicochemical Characteristics

Approximately one liter of water samples was collected in polythene containers after staged water was removed for physicochemical examination when the source had sufficiently produced water. Physicochemical properties like pH, temperature, electrical conductivity, and total dissolved solids are assessed in 0.5-liter water samples (Braga et al., 2022; Sagar et al., 2015). Measuring these parameters has an important aspect for living species, such as drastic temperature changes that can be dangerous to aquatic species and the evaluation of PH can be useful in determining the corrosive nature of water, with lower values indicating a high corrosive nature of water. For the measurement of these parameters, a conductivity/TDS master kit was employed, and an effective variation in the concentration of each parameter was observed (Srilatha et al., 2014; Bilewu et al., 2022). The statistical description of each parameter is described in **Table 5.1**.The temperature and pH values range from 10.2 – 16.5 ⁰C and 6.6 – 8.2 (mean of 13.78 ⁰C and 7.35) respectively. However, the Electric Conductivity (EC) and Total dissolved solids (TDS) range from 349 – 1136 and 176 to 561.8 (mean of 707.74 and 352.65) respectively.

Table 5.1 Statistical description of physicochemical parameters

Statistical values	Temperature(°C)	PH	EC (mS)	TDS
Mean	13.78	7.35	707.74	352.65
Standard Error	0.29	0.07	37.54	18.76
Median	14	7.4	719	359
Mode	12.5	7.4	-	-
Standard Deviation	1.65	0.41	209.03	104.49
Range	6.3	1.6	787	10918.73
Minimum	10.2	6.6	349	176
Maximum	16.5	8.2	1136	561.8

Assessment of Surface Contamination

Utilizing a portable Geiger Muller (GM) counter radiation monitor (PM 1405, Polimaster Inc., USA), the ambient gamma radiation at each site location was measured to evaluate surface contamination (Chakan et al., 2023). The dose equivalent range (DER) of the stated detector is 0.01 μSv/h to100 mSv/h. An average of five minutes was taken to check out the accuracy of the gamma field strength at each site location, with the survey monitor placed one meter above the ground (Hidayath et. al., 2022).

Assessment of Radon in Water Samples

In the present study, all thirty-one water samples were collected from natural springs, hand pumps, and wells in the Pattan area of the Baramulla district to measure the presence of radon and to figure out how the local population would be affected. From the thirty-one samples, twelve are taken from wells, three from natural springs, and sixteen are from hand pumps. **Table 5.2** shows an analysis of site location, GPs coordinates, depth in meters, water source, gamma field strength, and radon concentration (in water) with sigma deviations associated with each value.

Table 5.2 Complete data set of the study including Gamma Field Strength (GFS) along with their latitude and longitude

Site location	Latitude (°N)	Longitude (°E)	Depth (m)	water sources	GFS (nSv/h)	C_w (Bq/L)
Bahrampora	34.12	74.49	82.31	Hand pump	132	49.87 ± 1.27
Mamoosa	34.11	74.54	3.04	Spring	207	27.46 ± 0.91
Babgund	34.12	74.55	67.07	Hand pump	162	58.62 ± 1.29
Shirpora	34.13	74.56	73.17	Hand pump	147	47.25 ± 1.15
Shouxch	34.14	74.49	4.26	Spring	153	41.12 ± 1.10
Sultanpora	34.23	74.57	53.35	Hand pump	168	27.69 ± 0.89
Hamray	34.21	74.50	64.02	Hand pump	127	42.00 ± 1.07
Lolipora	34.20	74.53	13.41	Well	134	19.98 ± 0.77

Magraypora	34.23	74.55	8.53	Well	165	27.895 ± 0.91
Tengpora	34.23	74.56	4.57	Well	173	28.15 ± 0.88
Goshbugh	34.22	74.55	10.67	Well	153	27.47 ± 0.89
Chanderhama	34.21	74.05	18.29	Hand pump	159	27.87 ± 0.88
Andergam	34.21	74.53	6.7	Well	171	24.09 ± 0.82
Aglar	34.21	74.55	9.14	Well	162	27.59 ± 0.87
Khargam	34.14	74.48	73.17	Hand pump	182	48.12 ± 0.87
Tilgam	34.15	74.49	53.35	Hand pump	124	48.12 ± 1.20
Wanigam	34.17	74.51	3.65	Spring	167	25.34 ± 0.88
Palhallan	34.18	74.55	21.34	Hand pump	179	36.89 ± 1.23
Ussan	34.20	74.55	16.76	Well	143	25.50 ± 0.86
Ghatgopalun	34.20	74.58	18.29	Hand pump	157	36.98 ± 0.96
Nillah	34.17	74.52	15.24	Well	138	68.25 ± 1.19
Tapper	34.20	74.52	67.07	Hand pump	149	72.62 ± 1.19
Hanjiwera	34.14	74.59	25.91	Hand pump	147	28.51 ± 0.91
Zangam	34.15	74.57	62.5	Hand pump	155	74.37 ± 1.21
Burran	34.15	74.57	10.36	Well	187	61.25 ± 1.23
Pattan	34.16	74.56	13.71	Well	121	27.75 ± 0.87
Mundyari	34.18	74.58	7.62	Well	140	27.70 ± 0.93
Nihalpora	34.14	74.53	54.87	Hand pump	186	36.05 ± 1.02
Singhpora	34.15	74.61	16.76	Hand pump	159	20.96 ± 0.72
Sheerbugh	34.22	74.57	12.4	Well	141	24.71 ± 0.85
Markipora	34.22	74.56	13.26	Hand pump	153	26.96 ± 0.92

Distribution Plot of Radon Concentration

The frequency distribution of radon concentration for all 31 samples is displayed in **Figure 5.4**. Out of 31 samples, 4 (3 wells and 1 hand pump) samples have radon

134

concentrations range 15 to 25 Bq/L, 13 (7 wells,4 hand pumps, and 2 springs)samples fall within a maximum range of 25 and 35 Bq/L,5 (4 hand pumps and 1 spring) samples are occupied and fall within the range of 35–45 Bq/L, 4 (hand pumps only) samples have fallen within the range of 45–55 Bq/L, 2 (1 well and 1 hand pump) samples and 3 (1 well and 2 hand pumps) samples fall into the range of 55–65 Bq/L and 65–75 Bq/L, respectively. From the above radon concentration (**Table 5.2**), quartiles Q1 (25% or lower half median of the data lies below 27.46), Q2 (50% of the data median lies below 28.15), Q3 (75% or upper half median lies below 47.68), and Q4 (74.37 is the maximum of this data point) have been calculated and depicted below.

Quartiles	Q1	Q2	Q3	Q4
Values	27.468	28.154	47.6875	74.375
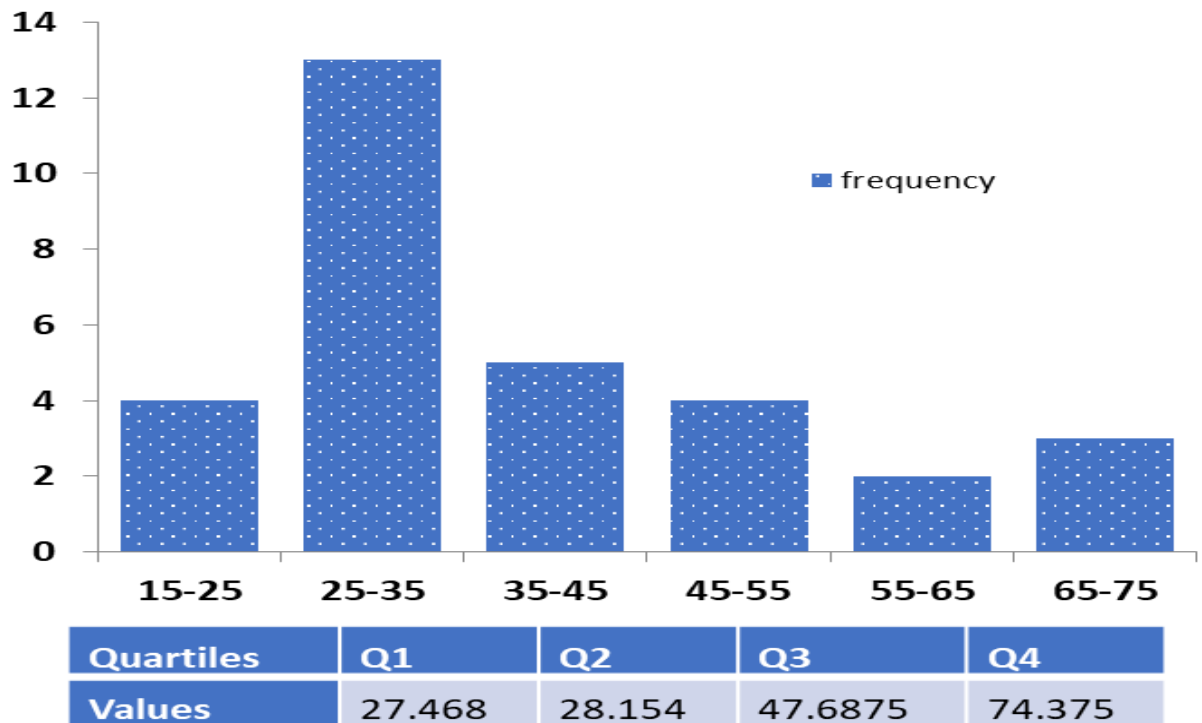
Figure 5.4: Frequency distribution of samples with their radon (Rn-222) concentration

Statistical Correlational Analysis of Depth Parameter with Radon Concentration

The radon concentration and the depth of the underground water sources displayed a significant positive correlation (**Figure 5.5**, R = 0.59), which is in some ways incompatible with the literature that outlines depth as a parameter that is weakly

correlated with the radon concentration as radon is solely dependent on the geology and decays in nearby rock and soil (Khan and Azam., 2012). As intensive sampling is taken into consideration, the study area's overall unique geology may be one of the possible reasons for this.

Correlation of Gamma Field vs. Radon Concentration

Since the ambient gamma radiation shows a better correlation with the increased radon values, in this study, the radon concentration is not too high so the weak correlation may be attributed to contributing factors such as cosmic and terrestrial sources like uranium, thorium, and potassium for natural background radiation (Remlalsiama et.al., 2022). A negative correlation of -0.063 was observed between the radon concentration and gamma field strength, as highlighted in **Figure5.6** below.
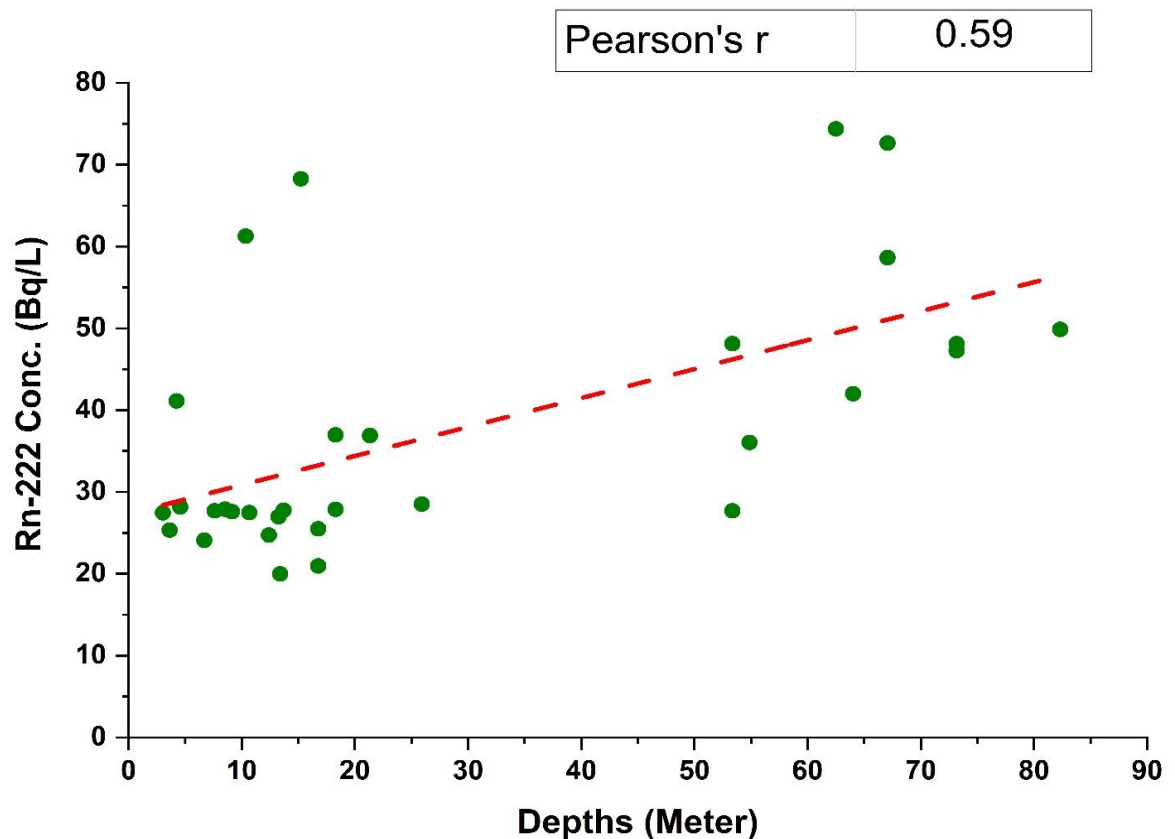
Figure 5.5 Correlation of radon (Rn-222) concentration with depth
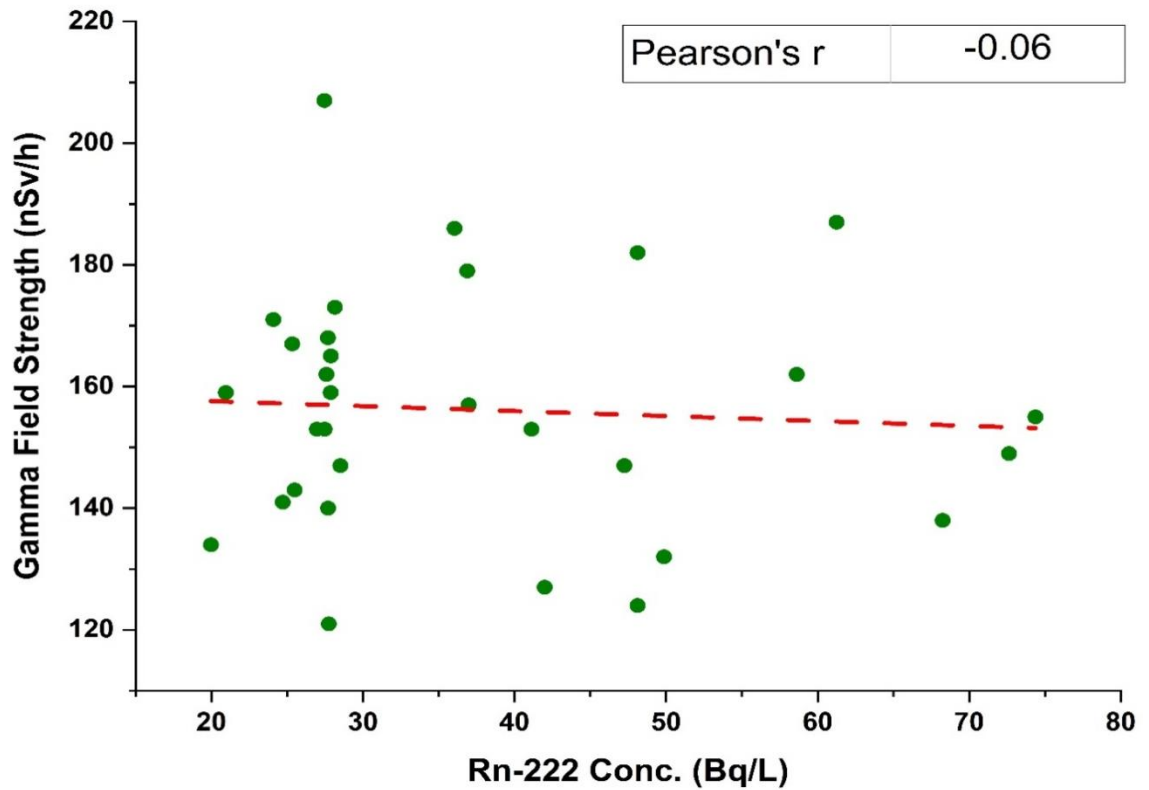
Figure 5.6: Correlation of gamma field with radon (Rn-222) concentration

Correlation Analysis of PH and Temperature with Radon

Temperature changes may impact the pressure in the soil, which can influence radon mobility. Lower temperatures additionally lead to more condensation, which may inhibit radon diffusion. Salinity and temperature are two variables that affect radon's solubility in water. Radon is generally more soluble in cooler, less salinized water (Nunes et al., 2022) but in this case, the study found the opposite results may be due to higher TDS values, mineralogy, and depth of the aquifer material (Srilata, et. al., 2014). **Figures 5.7a and b** depict the statistical relationship between temperature and pH with radon. Significantly a weak correlation of (R=0.031) was observed between temperature of the water sources and radon concentration and a negative correlation of -0.12 was observed between pH Vs radon (**Figure 5.7**).
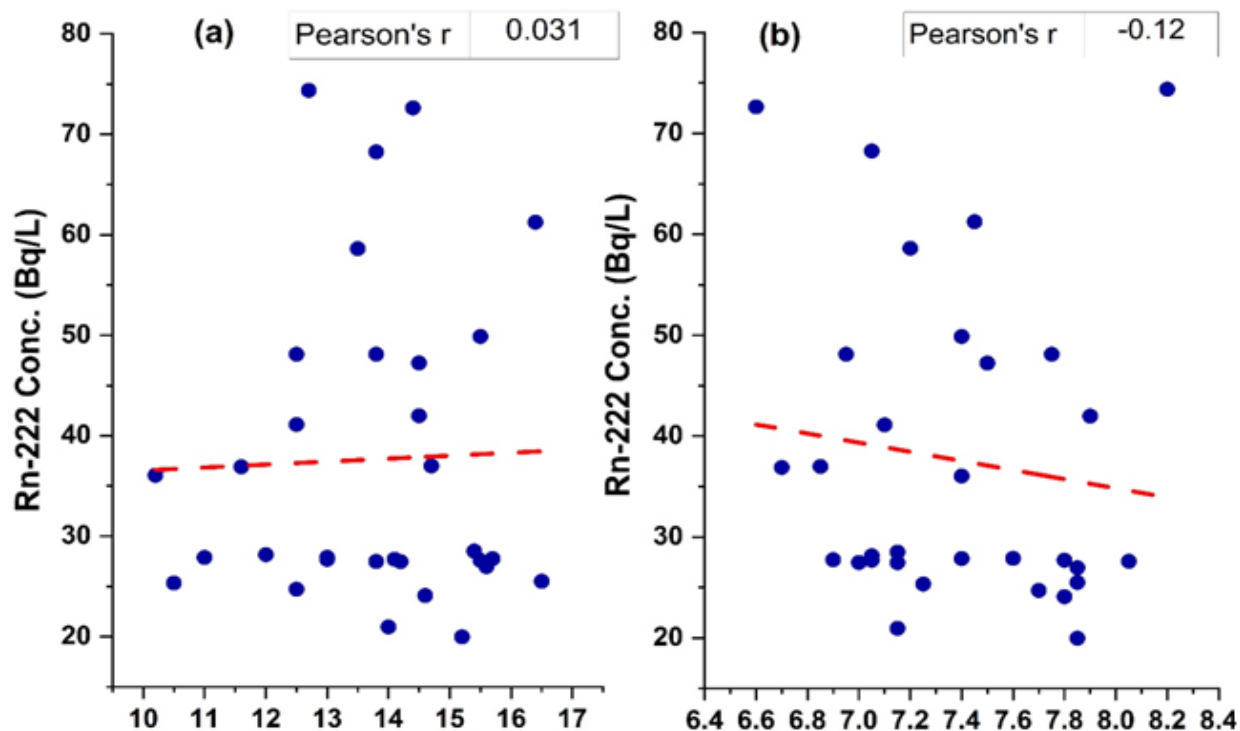
Figure 5.7 (a) Correlation of radon with temperature   **(b)** Correlation of Radon with pH

5.4 Assessment of the Radiological Dose

Groundwater and water supply systems may become exposed to radon, especially in regions with high soil uranium concentrations. People who might be exposed to high amounts of radon through their water supply face the danger of being affected by this. Since many epidemiological investigations have demonstrated that radon exposure is the second-leading cause of lung cancer after smoking, the link between radon exposure and lung cancer is well-established (Nunes et al., 2023). Keeping this context in mind, the current study aims to assess the dosages for ingestion and inhalation across various age groups of newborns, kids, and adults as represented in **Table 5.3**. The inhalation dose for various age groups taken into consideration exceeds the ingestion dose and was observed

to be in the range of 184.69 to 687.22μSv/y for infants, with a mean value of 347.9222μSv/y. For children and adults, doses were found to be 175.73 – 653.90μSv/y and 158.38–589.34 μSvy^{-1}, with mean values of 331.05μSv/y and 298.36μSv/y respectively. The ingestion doses for infants, children, and adults lie in the range 117.23 - 436.2022μSv/y, 64.86-241.34μSv/y, 80.45-299.35μSv/y with mean values of 220.83μSv/y, 122.18μSv/y, and 151μSv/y respectively.

The total of effective doses via inhalation and ingestion for all age groups exceeds the recommended limit of 100μSv/y as set by WHO. The total effective dose of radon for various organs was also computed, and the results show that it is significantly lower than the ICRP-recommended limits of 3–10mSv/y. **Table 5.4** shows the total effective dose contribution (mSv/y) to different organs among age groups via inhalation and ingestion doses. Results make it clear that younger age groups are exposed to higher inhalation and ingestion doses than adults. This is because children's lungs continue to grow, and they breathe faster than adults, making them more susceptible to radiation exposure. In addition, there is evidence in the literature that suggests that small age groups are more exposed to radiation because they spend more time indoors, which is supported by the greater dose conversion factors in newborns (Singla, et al., 2023).

Table 5.3 Statistical description of annual effective inhalation and ingestion doses (µSv/y) among different age groups

Statistical parameter	Radon Content	D$_{ih}$			D$_g$			D$_T$ (g,ih)		
		Infants	Children	Adults	Infants	Children	Adults	Infants	Children	Adults
	Bq/L	µSv/y	µSv/y	µSv/y	µSv/y	µSv/y	µSv/y	µSv/y	µSv/y	µSv/y
Mean	37.65	347.92	331.05	298.36	220.83	122.18	151.55	568.76	453.23	449.92
Standard Error	2.8	25.92	24.67	22.23	16.45	9.1	11.29	42.38	33.77	33.53
Median	28.15	260.14	247.52	223.09	165.12	91.35	113.31	425.26	338.88	336.41
Mode	48.12	444.67	423.11	381.34	282.25	156.16	193.7	726.92	579.28	575.04
Standard Dev	15.62	144.37	137.37	123.8	91.63	50.7	62.88	236.01	188.07	186.69
Sample Var	244.12	20843.2	18871.04	15328.85	8397.62	2570.69	3955.05	55700.88	35371.8	34856.49
Kurtosis	0.18	0.18	0.18	0.18	0.18	0.18	0.18	0.18	0.18	0.18
Skewness	1.11	1.11	1.11	1.11	1.11	1.11	1.11	1.11	1.11	1.11
Minimum	19.98	184.69	175.73	158.38	117.23	64.86	80.45	301.92	240.6	238.84
Maximum	74.37	687.22	653.9	589.34	436.2	241.34	299.35	1123.43	895.25	888.7

Table 5.4 The mean total effective dose contribution (mSv/y) to lung and stomach among age groups via inhalation and ingestion doses

Statistical Analysis	Infants (mSv/y)	Children(mSv /y)	Adults (mSv/y)
Mean	0.07	0.05	0.05
Standard Error	0.01	0.01	0.01
Median	0.05	0.04	0.04
Mode	0.09	0.07	0.07
Standard Deviation	0.03	0.02	0.02
Kurtosis	0.19	0.18	0.18
Skewness	1.11	1.11	1.11
Minimum	0.04	0.03	0.03
Maximum	0.14	0.11	0.11

5.5 Comparative Analysis of Radon Concentration in the Different Countries

Figure 5.8 shows a range of measurements for several types of water sources from different countries, as well as radioactivity levels in (Bq/L). These metrics are critical in determining the safety and quality of drinking water, groundwater, and well water in various places. In India, drinking water and groundwater have different levels of radioactivity, with drinking water ranging from 0.87 to 32.10Bq/L (Singh, J, et. al., 2009) and groundwater ranging from 11.7 to 381.2Bq/L (Ravikumar, et. al., 2014). This shows a wide spectrum of contamination across the country's water sources, emphasizing the possible risk to health connected with radioactive exposure. Similarly, radioactivity levels in Brazil's groundwater and well water range from 0.95 to 36Bq/L (Marques,et. al., 2004)and 1.6 to 215 Bq/L (Corrêa,et. al., 2014), respectively.

The study highlights the significance of monitoring and controlling water sources to ensure population safety. Radioactivity levels in well water vary between Turkey and Mexico, with values ranging from 0.70 to 31.70Bq/L in Turkey (Yalim, et. al., 2007) and 1.78 to 39.75Bq/L in Mexico (Villalba, et. al., 2005). This highlights the necessity for comprehensive water management methods to handle potential pollution concerns and protect public health. Italy has a wide range of radioactivity levels in groundwater, ranging from 1.80 to 52.70Bq/L (D'Alessandro, W., & Vita, F., 2003). Such fluctuations illustrate the complexities of groundwater pollution, emphasizing the need for continuing monitoring and treatment. In Poland, radioactivity levels in drinking water range from 0.42 to 10.52Bq/L (Bem, et. al., 2014),

indicating that contamination is lower than in some of the other countries shown in **Figure 5.8**. Even within this range, there may be specific areas of concern that require treatment. China's groundwater radioactivity ranges from 11.0 to 36.00Bq/L (Wen, et. al., 2014), showing probable heterogeneity in contamination sources and levels across the country.

Saudi Arabia's groundwater and drinking water have variable levels of radioactivity, with groundwater ranging from 0.76 to 100Bq/L (Albharbi, et. al., 2015)and drinking water from 0.89 to 35.44Bq/L (Albharbi, et. al., 2015). These findings emphasize the need to enforce strict water quality rules and monitoring measures to protect human health. Finally, in India found a wide range of radioactivity in groundwater, with readings ranging from 19.88 to 74.37Bq/L (Alabdula, et. al., 1999). This emphasizes the continual need for scientific study and monitoring to assess and solve water quality issues, especially in areas where contamination levels may pose serious health hazards. Overall, the facts in the table highlight the global necessity of providing safe and clean water sources for human use, as well as the vital role that continuing monitoring and regulation play in accomplishing this aim.
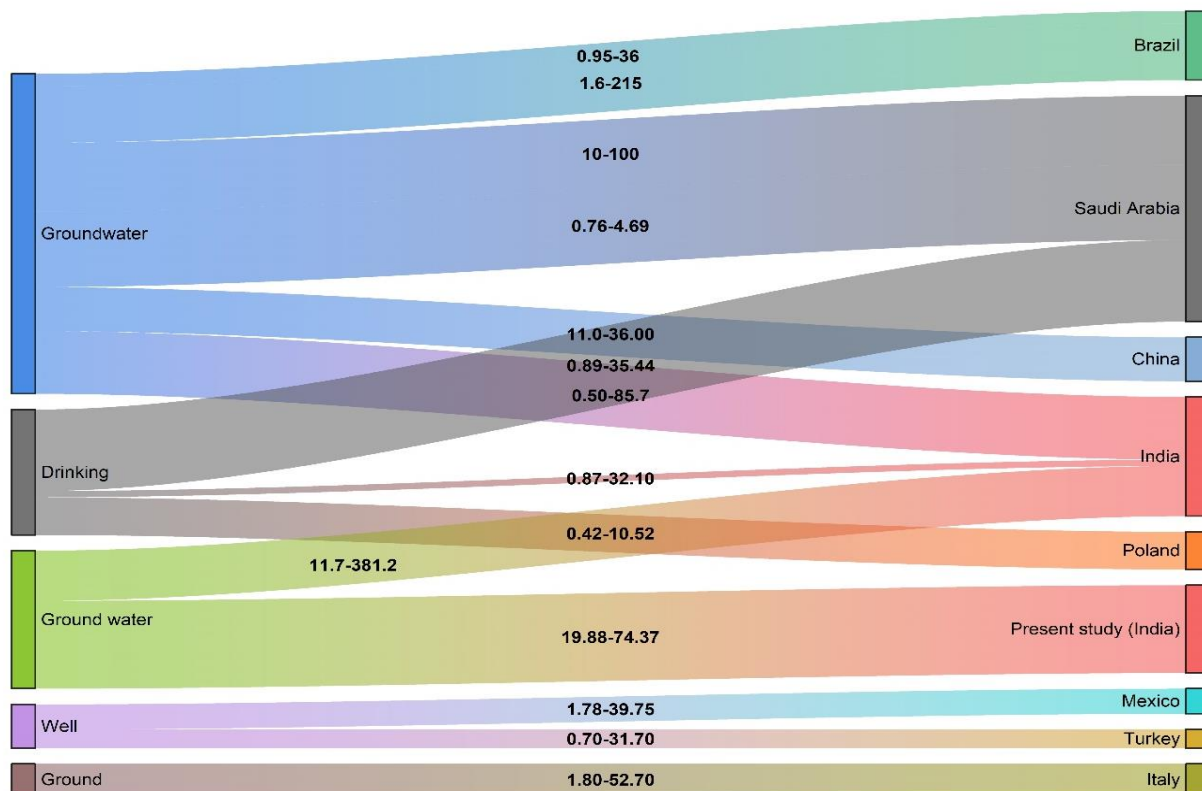
Figure 5.8 Comparative analysis of global radon concentration with the current study (Alharbi et al., 2015)

5.6 Conclusion

In the present study, the average concentration of radon in water sources is 37.65Bq/L, with a range of 19.88 to 74.37Bq/L. These levels, which indicate moderate contamination, are above the USEPA recommendation of 11Bq/L but still fall within the WHO limit of 100Bq/L. Even though the levels are higher than the WHO's 100μSv/y dose limit, they fall within the 3–10mSv/y ICRP safety range. The study area has very important significance due to the excessive use of agricultural pesticides, which may raise the level of natural radioactivity. The levels of radon in water samples from various areas throughout the region should be known, as they may provide crucial information regarding hidden uranium reserves. The solubility of radon might be affected by variations in water quality, as revealed by the analysis of 31 samples taken from hand pumps, springs, and wells. Radon levels and gamma radiation possess a weak correlation, which indicates that uranium and thorium deposits, other external cosmic and terrestrial factors may influence local radiation levels. Radon concentration and water temperature or pH showed minimal correlation, indicating that radon mobility can be affected by local geological features and mineral content. The annual effective dose for body organs, such as the lungs and stomach due to radon ingestion and inhalation in drinking water samples from the study area has been examined to find out whether these dosages have any effect on the residents of the study area directly using underground water. In our study, children and infants are particularly prone to radon exposure, which can have long-term health effects, such as lung cancer, because of higher doses to their sensitive organs. Regular monitoring, local water treatment, raising public and awareness in radon-prone areas are all instructed to protect public health. Mitigation remediation for minimizing the radon levels in water includes proper aeration by the diffused bubble, packed tower method and adsorption by granular activated Carbon as well. The present study is helpful in strengthening the baseline radon data and the presence of radon indicates that ongoing monitoring and potential mitigation are important.

References

- Ahamad, T., Nautiyal, O. P., Joshi, M., Singh, P., Rana, A. S., Bourai, A. A., Sajwan, R. S., & Ramola, R. C. (2024). Seasonal variability of 222Rn and 220Rn equilibrium factors in indoor environment of Kumaun Himalaya, India. *Journal of Radioanalytical and Nuclear Chemistry*, *333*(6), 2881–2890. https://doi.org/10.1007/s10967-023-09101-1

- Ahamad, T., Nautiyal, O. P., Joshi, M., Singh, P., Sajwan, R. S., Rana, A. S., & Bourai, A. A. (2024). Measurement of indoor radioactivity and dose derived from 222Rn, 220Rn and EECs by using SSNTD based technique. *Radiation Protection Dosimetry*, *200*(11–12), 1011–1017. https://doi.org/10.1093/rpd/ncad321

- Alabdula'aly, A. I. (1999). Occurrence of radon in the central region groundwater of Saudi Arabia. *Journal of Environmental Radioactivity*, *44*(1), 85–95. https://doi.org/10.1016/S0265-931X(98)00063-0

- Alam, A., Ahmad, S., Bhat, M. S., & Ahmad, B. (2015). Tectonic evolution of Kashmir basin in northwest Himalayas. *Geomorphology*, *239*, 114–126. https://doi.org/10.1016/j.geomorph.2015.03.025

- Althoyaib, S. S., & El-Taher, A. (2015). Natural radioactivity measurements in groundwater from Al-Jawa, Saudi Arabia. *Journal of Radioanalytical and Nuclear Chemistry*, *304*(2), 547–552. https://doi.org/10.1007/s10967-014-3874-7

- Alharbi, W., Abbady, A. G. E., & El-Taher, A. (2015). Radon Concentrations Measurement for groundwater Using Active Detecting Method. *American Scientific Research Journal for Engineering, Technology, and Sciences*, *14*(1), 1–11. http://asrjetsjournal.org/

- Alirezazadeh, N. (2005). Radon concentrations in public water supplies in Tehran and evaluation of radiation dose. *Iranian Journal of Radiation Research*, *3*(2), 79–83.

- Barca, D., Bjosvik, L. L., Edman, G., Eliasson, U. H., Gervino, G., Philemark, C., & Due Svendson, B. E. (2021). Indoor Radon Concentration and Risk Estimation: the EURA PROJECT. *Journal of Human, Earth, and Future*, *2*(4), 323–333. https://doi.org/10.28991/HEF-2021-02-04

- Belete, G. D., & Shiferaw, A. M. (2022). A Review of Studies on the Seasonal Variation of Indoor Radon-222 Concentration. *Oncology Reviews*, *16*. https://doi.org/10.3389/or.2022.10570

- Bem, H., Plota, U., Staniszewska, M., Bem, E. M., & Mazurek, D. (2014). Radon (222Rn) in underground drinking water supplies of the Southern Greater Poland Region. *Journal of Radioanalytical and Nuclear Chemistry*, *299*(3), 1307–1312. https://doi.org/10.1007/s10967-013-2912-1

- Bilewu, O. F., Ayanda, I. O., & Ajayi, T. O. (2022). Assessment of Physicochemical Parameters in Selected Water Bodies in Oyo and Lagos States. *IOP Conference Series: Earth and Environmental Science*, *1054*(1), 012045. https://doi.org/10.1088/1755-1315/1054/1/012045

- Binesh, A., Mohammadi, S., Mowlavi, A. A., & Parvaresh, P. (2010). *Evaluation of the radiation dose from radon ingestion.pdf*. *2*(November), 174–178.

- Braga, F. H. R., Dutra, M. L. S., Lima, N. S., Silva, G. M., Miranda, R. C. M., Firmo, W. C. A., Moura, A. R. L., Monteiro, A. S., Silva, L. C. N., Silva, D. F., & Silva, M. R. C. (2022). Study of the Influence of Physicochemical Parameters on the Water Quality Index (WQI) in the Maranhão Amazon, Brazil. *Water*, *14*(10), 1546. https://doi.org/10.3390/w14101546

- Chakan, M.R., Masood, S., Nazir, S., Mohi, M., & Kumar, A. (2023). A Study of Radon Concentration in Drinking Water of Lolab valley, Kashmir Himalaya. *Indian Journal of Pure & Applied Physics*, *61*(June), 515–519. https://doi.org/10.56042/ijpap.v61i6.2433

- Changotra, S. (2017). Mineral Distribution of Jammu and Kashmir. *International Journal of Science and Research,6(10),* 1997–2001. https://doi.org/10.1007/s12517-022-09806-9

- Corrêa, J. N., Paschuk, S. A., Kappke, J., Perna, A. F. N., França, A. C., Schelin, H. R., & Denyak, V. (2014). Measurements of 222Rn activity in well water of the Curitiba metropolitan area (Brazil). *Radiation Physics and Chemistry*, *104*, 108–111. https://doi.org/10.1016/j.radphyschem.2014.01.006

- D'Alessandro, W., & Vita, F. (2003). Groundwater radon measurements in the Mt. Etna area. *Journal of Environmental Radioactivity*, *65*(2), 187–201. https://doi.org/10.1016/S0265-931X(02)00096-6

- Dongre, S., Kumar, S., Suresh, S., & Sannappa, J. (2023). Estimation of Inhalation and

Ingestion Dose Due to Radon Concentration in Drinking Water Samples of Shankaraghatta Forest Environment, Karnataka, India. *Indian Journal Of Science And Technology*, *16*(5), 367–376. https://doi.org/10.17485/IJST/v16i5.2321

- Duggal, V., Sharma, S., & Mehra, R. (2020). Risk assessment of radon in drinking water in Khetri Copper Belt of Rajasthan, India. *Chemosphere*, *239*, 124782. https://doi.org/10.1016/j.chemosphere.2019.124782

- El-Araby, E. H., Soliman, H. A., & Abo-Elmagd, M. (2019). Measurement of radon levels in water and the associated health hazards in Jazan, Saudi Arabia. *Journal of Radiation Research and Applied Sciences*, *12*(1), 31–36. https://doi.org/10.1080/16878507.2019.1594134

- Gaware, J., Sahoo, B., Sapra, B., & Mayya, Y. (2011). Indigenous development and networking of online radon monitors in the underground uranium mine. *Radiation Protection and Environment*, *34*(1), 37. https://doi.org/10.4103/0972-0464.93943

- Giraldo-Osorio, A., Ruano-Ravina, A., Varela-Lema, L., Barros-Dios, J. M., & Pérez-Ríos, M. (2020). Residential Radon in Central and South America: A Systematic Review. *International Journal of Environmental Research and Public Health*, *17*(12), 4550. https://doi.org/10.3390/ijerph17124550

- Grzywa-Celińska, A., Krusiński, A., Mazur, J., Szewczyk, K., & Kozak, K. (2020). Radon—The Element of Risk. The Impact of Radon Exposure on Human Health. *Toxics*, *8*(4), 120. https://doi.org/10.3390/toxics8040120

- Hazou, E., Patchali, T. E., Konzou, E., Kola, P., Zorko, B., Ndontchueng Moyo, M., & Tchakpele, P. K. (2022). Radiological Assessment and Statistical Approaches of Natural Radionuclides in Soil Samples Related to Phosphate Ore Activities in the site of Dagbati, Southern Region of Togo. *Water, Air, & Soil Pollution*, *233*(7), 237. https://doi.org/10.1007/s11270-022-05700-y

- Hidayath, M., Chandrashekara, M. S., Rani, K. S. P., & Namitha, S. N. (2022). Studies on the concentration of 226Ra and 222Rn in drinking water samples and effective dose to the population of Davanagere district, Karnataka state, India. *Journal of Radioanalytical and Nuclear Chemistry*, *331*(4), 1923–1931. https://doi.org/10.1007/s10967-022-08240-1

- Holm, L. E. (2006). Evolution of ICRP's recommendations. *Nuclear Plant Journal*, *24*(3), 32-+.

- Khan, M. S., & Azam, A. (2012). Depth dependent study of radon, thoron and their progeny in tube-wells. *Journal of Radioanalytical and Nuclear Chemistry*, *294*(2), 289–293. https://doi.org/10.1007/s10967-011-1487-y

- Khutia, S., Dawn, A., Seal, K., Chaudhuri, H., Maji, C., & Mukherjee, S. (2023). Age-dependent potential health risk assessment due to radioactive radon-222 in the environs of highly populated Durgapur industrial zone and nearby Bakreswar hot spring, India. *Environmental Geochemistry and Health*, *45*(8), 5727–5759. https://doi.org/10.1007/s10653-023-01478-y

- Kumar, A., Sharma, S., Mehra, R., Kanwar, P., Mishra, R., & Kaur, I. (2018). Assessment of radon concentration and heavy metal contamination in groundwater of Udhampur district, Jammu & Kashmir, India. *Environmental Geochemistry and Health*, *40*(2), 815–831. https://doi.org/10.1007/s10653-017-0027-2

- Kumar, M., Kaushal, A., Sahoo, B. K., Sarin, A., Mehra, R., Jakhu, R., Bhalla, A., & Sharma, N. (2019). Measurement of uranium and radon concentration in drinking water samples and assessment of ingestion dose to local population in Jalandhar district of Punjab, India. *Indoor and Built Environment*, *28*(5), 611–618. https://doi.org/10.1177/1420326X17703773

- Marques, A. L., dos Santos, W., & Geraldo, L. P. (2004). Direct measurements of radon activity in water from various natural sources using nuclear track detectors. *Applied Radiation and Isotopes*, *60*(6), 801–804. https://doi.org/10.1016/j.apradiso.2004.01.015

- Mir, J. A., Bhat, I. M., Murtaza, K. O., Qader, W., & Dar, R. A. (2023). Geological Heritage of the Kashmir Valley, North-Western Himalaya, India. *Geoheritage*, *15*(1), 26. https://doi.org/10.1007/s12371-023-00791-3

- Nazir, S., Sahoo, B. K., Rani, S., Masood, S., Mishra, R., Ahmad, N., Rashid, I., Zahoor Ahmad, S., & Simnani, S. (2021). Radon mapping in groundwater and indoor environs of Budgam, Jammu and Kashmir. *Journal of Radioanalytical and Nuclear Chemistry*, *329*(2), 923–934. https://doi.org/10.1007/s10967-021-07856-z

- Neri, A., Stewart, S. L., & Angell, W. (2013). Radon Control Activities for Lung Cancer Prevention in National Comprehensive Cancer Control Program Plans, 2005–2011. *Preventing Chronic Disease*, *10*, 120337. https://doi.org/10.5888/pcd10.120337

- Nsiah-Akoto, I., Fletcher, J. J., Oppon, O. C., & Andam, A. B. (2011). Indoor radon levels and the associated effective dose rate determination at Dome in the Greater Accra Region of Ghana. *Research Journal of Environmental and Earth Sciences, 3(2),* 124-130.https://www.airitilibrary.com/Article/Detail/20410492-201103-201507240030-201507240030-124-130

- Nunes, L. J. R., Curado, A., & Lopes, S. I. (2023). The Relationship between Radon and Geology: Sources, Transport and Indoor Accumulation. *Applied Sciences*, *13*(13), 7460. https://doi.org/10.3390/app13137460

- Nunes, L. J. R., Curado, A., Graça, L. C. C. da, Soares, S., & Lopes, S. I. (2022). Impacts of Indoor Radon on Health: A Comprehensive Review on Causes, Assessment and Remediation Strategies. *International Journal of Environmental Research and Public Health*, *19*(7), 3929. https://doi.org/10.3390/ijerph19073929

- Panghal, A., Kumar, A., Kumar, S., Singh, J., Sharma, S., Singh, P., & Bajwa, B. S. (2017). Radiation dose-dependent risk on individuals due to ingestion of uranium and radon concentration in drinking water samples of four districts of Haryana, India. Radiation Effects and Defects in Solids, 172(5-6),441-455.https://doi.org/10.1080/10420150.2017.1336762

- Pant, D., Keesari, T., Rishi, M., Sharma, D. A., Thakur, N., Singh, G., Sangwan, P., Jaryal, A., Sinha, U. K., & Tripathi, R. M. (2020). Spatiotemporal distribution of dissolved radon in uranium impacted aquifers of southwest Punjab. *Journal of Radioanalytical and Nuclear Chemistry*, *323*(3), 1237–1249. https://doi.org/10.1007/s10967-019-06656-w

- Park, J. H., Lee, C. M., Lee, H. Y., & Kang, D. R. (2018). Estimation of Seasonal Correction Factors for Indoor Radon Concentrations in Korea. *International Journal of Environmental Research and Public Health*, *15*(10), 2251. https://doi.org/10.3390/ijerph15102251

- Raju, S. (2020). Geological Survey of India.Proceedings of the Indian National Science Academy, 86(1), 651–674.

- Rani, S., Kansal, S., Singla, A. K., & Mehra, R. (2021). Radiological risk assessment to the public due to the presence of radon in water of Barnala district, Punjab, India. *Environmental Geochemistry and Health*, *43*(12), 5011–5024.

https://doi.org/10.1007/s10653-021-01012-y

- Rani, S., Kansal, S., Singla, A. K., Nazir, S., & Mehra, R. (2023). Estimation of Annual Effective Dose Due to Radon Concentration in Water Samples of Moga District of Northern Punjab, India. Indian Journal of Pure and Applied Physics, 61(6),423-428. https://doi.org/10.56042/ijpap.v61i6.2412

- Rao, K. V., Reddy, B. L., Reddy, P. Y., Ramchander, R. B., & Reddy, K. R. (2001). Airborne radon and its progeny levels in the coal mines of Godavarikhani, Andhra Pradesh, India*. *Journal of Radiological Protection*, *21*(3), 259–268. https://doi.org/10.1088/0952-4746/21/3/304

- Ravikumar, P., & Somashekar, R. K. (2014). Determination of the radiation dose due to radon ingestion and inhalation. *International Journal of Environmental Science and Technology*, *11*(2), 493–508. https://doi.org/10.1007/s13762-013-0252-x

- Remlalsiama, Hmingchungnunga, Vanramlawma, Z.Pachuau, L.Z.Chhangte, B. Zoliana, B.K Sahoo, B.K Sapra (2022). Correlation Between Ground Level Gamma Radiation and Radon Gas Concentration in Soil At Different Baptism Depth of Oil Exploration Areas within Aizawl District of Mizoram, India.International Journal of Engineering Research & Technology pane – 2021, 10(07).

- Reviews, S. (2015): Indian Mineral Yearbook 2013, part -1: Yearbook 2013, 2013 (0712).

- Rößler, F. A., & Villert, J. (2017). On-site determination of the radon concentration in water: sampling & on-line methods.www.bertin-technologies.com

- Deshmukh, P. N., Patil, D. V, & Sawant, R. N. (2012). Physico-chemical parameters for testing of water - A review. *International Journal of Environmental Sciences*, *3*(3), 1194–1207. http://www.ipublishing.co.in/ijesarticles/twelve/articles/volthree/EIJES31120.pdf

- Sahoo, B. K., Sapra, B. K., Kanse, S. D., Gaware, J. J., & Mayya, Y. S. (2013). A new pin-hole discriminated 222Rn/220Rn passive measurement device with single entry face. *Radiation Measurements*, *58*, 52–60. https://doi.org/10.1016/j.radmeas.2013.08.003

- Sapra, B. K., Sahoo, B. K., Mishra, R., Joshi, M., Kanse, S. D., Rout, R. P., & Gole, A. C. (2010 b). Handbook on radon transport models and measurement methods. Mumbai, India:Radiological Protection and Advisory Division, Bhabha Atomic Research Centre.https://doi.org/10.1007/s10653-022-01304-x

- Sapra, B. K., Sahoo, B. K., Mishra, R., Joshi, M., Kanse, S. D., Rout, R. P., ... & Gole, A. C. (2010). Handbook on radon transport models and measurement methods. *Mumbai, India: Radiological Protection and Advisory Division, Bhabha Atomic Research Centre*.

- Sharma, S., Kumar, A., Mehra, R., & Kaur, R. (2019). Ingestion and inhalation doses due to intake of radon in drinking water samples of amritsar province, Punjab, India. *Radiation Protection Dosimetry*, *187*(2), 230–242. https://doi.org/10.1093/rpd/ncz157

- Sharma, S., Kumar, A., Mehra, R., & Mishra, R. (2017). Ingestion doses and hazard quotients due to intake of Uranium in drinking water from Udhampur District of Jammu and Kashmir State, India. *Radioprotection*, *52*(2), 109–118. https://doi.org/10.1051/radiopro/2017009

- Singh, J., Singh, H., Singh, S., & Bajwa, B. S. (2009). Estimation of uranium and radon concentration in some drinking water samples of Upper Siwaliks, India. *Environmental Monitoring and Assessment*, *154*(1–4), 15–22. https://doi.org/10.1007/s10661-008-0373-8

- Singh, K. P., Chandra, S., Panwar, P., Joshi, A., Prasad, G., Gusain, G. S., & Ramola, R. C. (2023). Measurement of radon concentration in soil gas and radon exhalation rate from soil samples along and across the Main Central Thrust of Garhwal Himalaya, India. *Environmental Geochemistry and Health*, *45*(11), 8771–8786. https://doi.org/10.1007/s10653-023-01758-7

- Singh, K. P., Chandra, S., Prasad, M., Joshi, A., Prasad, G., & Ramola, R. C. (2024). Estimation of radiation dose due to ingestion of radon in water samples of Garhwal Himalaya, India. *Journal of Radioanalytical and Nuclear Chemistry*, *333*(6), 2867–2879. https://doi.org/10.1007/s10967-023-09002-3

- Singh, P., Nautiyal, O. P., Joshi, M., Kumar, A., Ahamad, T., & Singh, K. (2021). Assessment of physicochemical and radon-attributable radiological parameters of drinking water samples of Pithoragarh district, Uttarakhand. *Journal of Radioanalytical and Nuclear Chemistry*, *330*(3), 1559–1570. https://doi.org/10.1007/s10967-021-08056-5

- Singh, S., Kumar, M., & Kumar Mahajan, R. (2005). The study of indoor radon in dwellings of Bathinda district, Punjab, India and its correlation with uranium and radon exhalation rate in soil. *Radiation Measurements*, *39*(5), 535–542. https://doi.org/10.1016/j.radmeas.2004.10.008

- Singla, A. K., Kansal, S., & Mehra, R. (2021). Quantification of radon contamination in drinking water of Rajasthan, India. *Journal of Radioanalytical and Nuclear Chemistry*, *327*(3), 1149–1157. https://doi.org/10.1007/s10967-021-07599-x

- Singla, A. K., Kanse, S., Kansal, S., Rani, S., & Mehra, R. (2023). A comprehensive study of radon in drinking waters of Hanumangarh district and the assessment of resulting dose to local population. *Environmental Geochemistry and Health*, *45*(2), 443–455. https://doi.org/10.1007/s10653-022-01304-x

- Srilatha, M. C., Rangaswamy, D. R., &Sannappa, J. (2014). Studies on concentration of Radon and Physicochemical parameters in ground water around Ramanagara and Tumkur districts, Karnataka, India. International Journal of Advanced Scientific and Technical Research. 2(4),641-660.

- Tauseef, M., Ray, E., Paul, D., Malik, J. N., & Ahmad, I. (2022). Mineralogical, geochemical, and magnetic susceptibility variations in the loess-paleosol sequence from Pattan, Kashmir Valley, India record an enhanced Indian summer monsoon around 35 ka. *Quaternary International*, *616*, 55–66. https://doi.org/10.1016/j.quaint.2021.12.014

- Phong Thu, H. N., Van Thang, N., & Hao, L. C. (2020). The effects of some soil characteristics on radon emanation and diffusion. *Journal of Environmental Radioactivity*, *216*, 106189. https://doi.org/10.1016/j.jenvrad.2020.106189

- Tufail, M., Matiullah, Ali, A., Orfi, S. D., Qureshi, A. A., Hussain, G., & Khan, H. A. (1988). Radon measurements in coal mines using polymeric nuclear track detectors. *International Journal of Radiation Applications and Instrumentation. Part D. Nuclear Tracks and Radiation Measurements*, *15*(1–4), 655–658. https://doi.org/10.1016/1359-0189(88)90222-1

- UNSCEAR (2000). Exposures from natural radiation sources. United Nations Scientific Committee on the Effects of Atomic Radiation, & Annex, B.Cosmic rays, 9(11).

- Villalba, L., Colmenero Sujo, L., Montero Cabrera, M. E., Cano Jiménez, A., Rentería Villalobos, M., Delgado Mendoza, C. J., Jurado Tenorio, L. A., Dávila Rangel, I., & Herrera Peraza, E. F. (2005). Radon concentrations in ground and drinking water in the state of Chihuahua, Mexico. *Journal of Environmental Radioactivity*, *80*(2), 139–151. https://doi.org/10.1016/j.jenvrad.2004.08.005

- Wen, T., Du, J., Ji, T., Wang, X., & Deng, B. (2014). Use of 222Rn to trace submarine

groundwater discharge in a tidal period along the coast of Xiangshan, Zhejiang, China. *Journal of Radioanalytical and Nuclear Chemistry*, *299*(1), 53–60. https://doi.org/10.1007/s10967-013-2786-2

- Xinwei, L. (2006). Analysis of radon concentration in drinking water in Baoji (China) and the associated health effects. *Radiation Protection Dosimetry*, *121*(4), 452–455. https://doi.org/10.1093/rpd/ncl048

- Yalım, H. A., Sandıkcıoğlu, A., Ünal, R., & Orhun, Ö. (2007). Measurements of radon concentrations in well waters near the Akşehir fault zone in Afyonkarahisar, Turkey. *Radiation Measurements*, *42*(3), 505–508. https://doi.org/10.1016/j.radmeas.2006.12.013

CHAPTER 6

URANIUM ANALYSIS IN GROUNDWATER OF KARGIL AND LADAKH, INDIA

6.1 Study Analysis

Naturally occurring uranium, in groundwater can be harmful to human health because of its chemical toxicity and radioactive effects. This study used an LED fluorimeter (LF-2a) to measure uranium in different groundwater samples collected across the geologically diverse Ladakh region in India's northwest Himalayas. In this arid region, reliance on imported food makes groundwater essential, raising concerns over uranium contamination and food safety. The average uranium concentration among the 73 samples analyzed was 2.5 µg/L, with only one sample exceeding the USEPA permissible limit of 30 µg/L, and all samples remained below the AERB guideline of 60 µg/L. Males had higher exposure than females, based on radiological dose assessments, particularly for older age groups, with children and infants coming in second and third. Hazard quotient (HQ) and lifetime average daily dose (LADD)-based chemical risk assessments, on the other hand, indicated non-carcinogenic safety and were significantly below the AERB recommendation of 4.4µg/kg/day. In comparison to wells and hand pump sources, physicochemical analysis revealed spring water, derived from snowmelt with low dissolved salts, as the most suitable source for drinking purposes. This study highlights the need for continuous monitoring of uranium levels in drinking water to protect public health.

6.2 Materials and Methods

6.2.1 Geological Setting

The geology of Ladakh reflects its dynamic tectonic evolution, shaped by the collision of the Indian and Eurasian plates (Chatterjee et al., 2013; Phartiyal and Nag, 2022). The region, located inside the Trans-Himalayan belt, includes a variety of lithological units, including ophiolites, granitic intrusions, and sedimentary sequences, which are predominantly connected with the Indus Suture Zone (Jain et al., 2020). This suture zone marks the northern boundary of the Indian plate and contains remnants of the Tethyan Ocean, which closed during the Himalayan orogeny

153

(Garzanti & van Haver, 1988). The Ladakh Batholith is a significant feature composed of granitoids generated during subduction processes and subsequent continental collision (Weinberg et al., 2000; Shellnut et al., 2014). These formations, coupled with Quaternary deposits in the Indus and Shyok river valleys, show ongoing tectonic activity and geomorphic change, providing important insights into the region's complicated geological history.

In this study 73 groundwater samples (used for drinking purpose) were collected from various residential sites of Leh-Ladakh,Kargil regions of Northwestern Himalayas, India (Figure **1**). Located between China, Tibet, and Pakistan, the Union Territory (UT) of Ladakh in northern India is of great geopolitical, climatic, cryospheric, and hydrological importance. The whole area of the Indian-administered region of Ladakh is 59,146 km², including the districts of Leh and Kargil,each each with respective areas of 45,110 km² and 14,036 km², with Leh being the second-largest district in India in terms of area. The district, which is further divided into 16 blocks, 112 villages, and 8 tehsils, is well-known for its advanced tourist attractions and infrastructure.A wide range of geological structures and lithological formations that are crucial for groundwater dynamics have contributed to the hydrogeology of Leh, Ladakh, and Kargil. Three foremost aquifer systems have been identified in the area: At first, about 75% of the area has been dominated by granitic aquifers, like those identified in the Ladakh and KPC batholiths and the Shyok Suture Zone.

Sedimentary aquifers, such as the Indus and Zanskar geological formations, where flow of groundwater is controlled by inter granular spaces and fractures, complement these aquifers, that are supported by fractured hard rocks. Additionally, alluvial aquifers are prevalent in glacial-fluvial plains and valleys and are composed of unconsolidated deposits that include sands, gravels, and moraines. These high-permeability aquifers frequently serve as important sources of water. Third, piedmont aquifers serve as vital source for groundwater recharge and storage as they exist ingently sloped locations at the foothills and comprises interlayered sediments of clay, sand, and gravel (Jeelani et al., 2021).
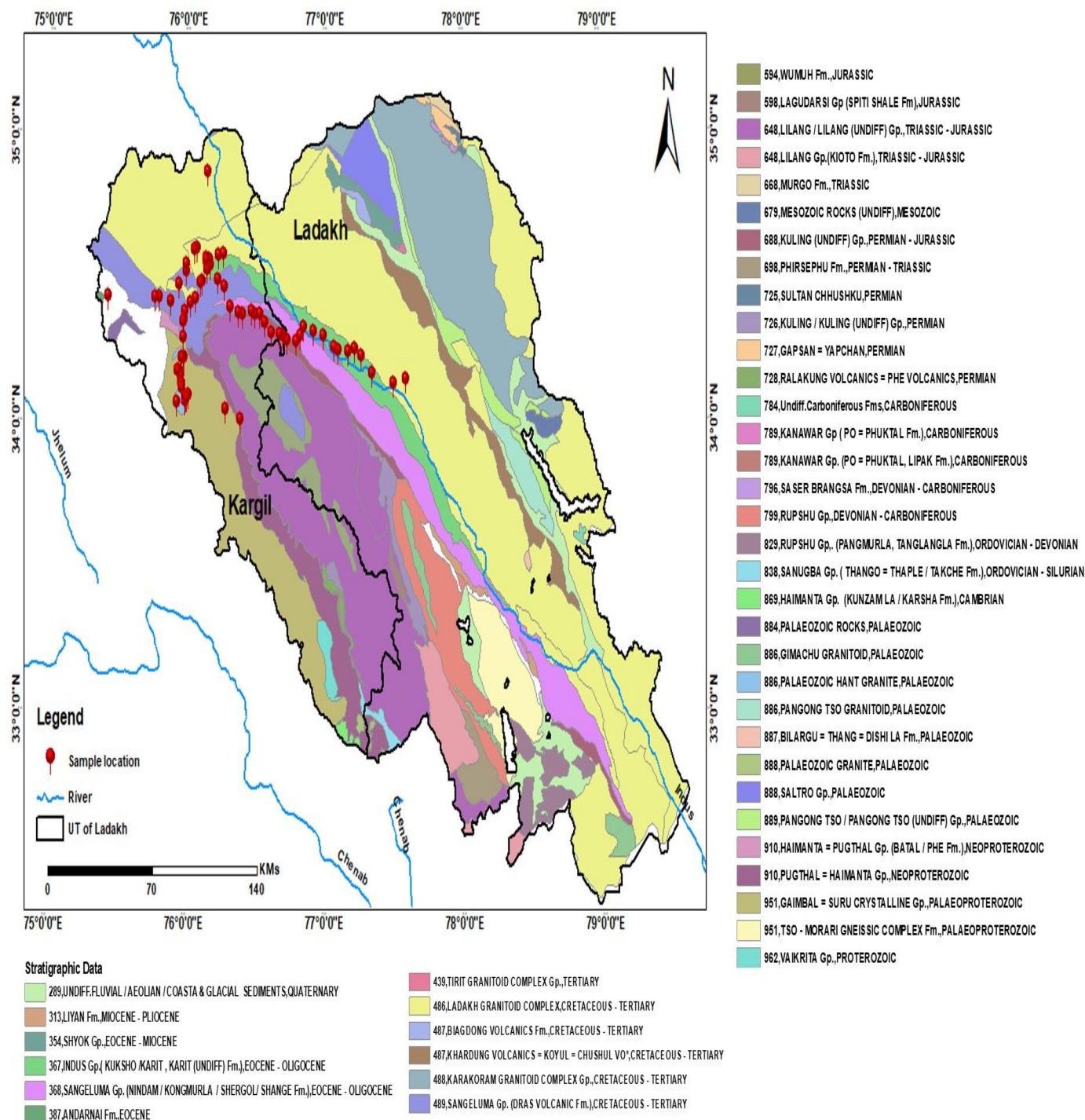
Figure 6.1: Sampling sites along with geology of Leh-Ladakh and Kargil regions of Northwestern Himalayas, India.

6.2.2 Sample Collection and Fluorimetry Analysis

High-altitude regions of the Indian Himalayas, specifically the Kargil and Leh-Ladakh regions, were the focus of the current study. The Latitude and Longitude (GPS) coordinates at each sampling location were taken using Garmin Inc GPS., as it being the sole source of taking coordinates in remote areas which lack network coverage. Before collecting samples usually stagnant water from the source was thrown away and then freshwater samples were being taken. Pre-sampling, measurement bottles were properly cleaned and rinsed with deionized water. Uranium concentration was analyzed by LED Fluorimeter LF-2a model by Quantalase (Sharma et al., 2017) which is discussed in detail in section 3.7 of chapter 3.

6.3 Results and Discussion

Analysis of Physico-Chemical Parameters

In order to establish a representative sampling process, groundwater samples were carefully taken from various sources, including hand pumps, wells, and springs, over a period of ten to fifteen minutes. While Physico-chemical factors like temperature, pH, electrical conductivity, and total dissolved solids (TDS) were measured on-site using a Benchtop conductivity/TDS master kit, pre-cleaned polypropylene bottles were used in order to prevent contamination (Pandith et al., 2024). To ensure accurate physicochemical characterization, approximately one liter of water was collected from each of the 73 sites in polythene containers after the stagnant water was removed. When important parameters like pH, temperature, conductivity, and TDS were analyzed in the considered samples, significant departures from recognized water quality standards were found. Low pH values suggest more corrosive water, and abrupt temperature changes can disrupt aquatic ecosystems. These results showed the vital role these parameters play in ecological assessments. This study emphasizes the need for regular evaluation to protect biological and environmental systems by pointing out parameter variability (Ahmad et al., 2024).

The results of the physico chemical parameters of the studied water samples were depicted in Table 6.**1** and compared with acceptable limits of drinking water (that is totally relying on the groundwater sources in the study area) given by the bureau of Indian standards (BIS,2012). The temperature was recorded in a range of 3-11°C with an average of 7.55°C. Since the distribution of groundwater temperature is mainly affected by geographical latitude, air temperature and local topographic elevations with the low temperatures in ground water in the current study are

attributed to the high elevation in the region. Since the region is usually a cold climatic area so the slight increase well water temperature during summer season may not make its variation significantly visible with different seasons (Lee, 2006).

The pH of water plays an important role in determining the quality of water, if it is nearly 6.5 it will definitely prohibit the body from processing or uptake vitamins and minerals so important in regarding the physiology of human health and high pH value generally is an indicator of the alkaline nature of water (Panwar et al., 2024). For all the groundwater, analyzed samples shows maximum and minimum values of 8.5 and 6.88 respectively with an average of 7.56 which is considered to be in feasible range for drinking water purposes (Bureau of Indian Standards (BIS, 2012). The observed variation in pH is may be due to underlying lime stone rocks (Sharma et al., 2017).   The electrical conductivity of all the samples was measured, which shows some increments above the recommended values of IBS shows with in the range of 140-1938 μS/cm with an average of 7.56. The elevated values EC shows the presence of good amounts of dissolved salts (inorganic substances) in an ionized form (Menaria et al., 2023). Similarly, the TDS values shows maximum and minimum values of 997 and 72 with an average of 392.8mg/L. The few higher values of TDS at some sampling sites may be attributed to the lithology and mineralogical characteristics of the aquifer (Srilata et al., 2014). Only 68 % samples show TDS higher than 300 mg/l and clearly, no sample in the current study exceed the USEPA, 2003 and BIS, 2012 standard limits.

Table 6.1 Analysis of Physicochemical quantities.

Parameters	TEMP (°c)	EC (µS/cm)	PH	TDS (mg/L)	U (µg/L)
Average	7.5	758.8	7.5	392.8	2.5
SD	2.0	365.5	0.3	198.1	4.6
Min	3	140	6.8	72	0.02
Max	11	1938	8.5	997	30.7

Table 6.2 Average physicochemical quantities and uranium concentration in different water sources.

Average Quantity	Hand pump	Natural Spring	Well Water
TDS (mg/L)	452.5	320.7	377
EC (µS/cm)	862.0	633.3	742
PH	7.5	7.5	7.6
TEMP (°c)	7.6	7.3	11
U (µg/L)	3.2	1.7	0.5

Uranium Concentration in Groundwater

The uranium concentration of all the analyzed samples shows varying concentrations of 0.02 to 30.7 with an average of 2.5µg/L. From the data analysis of current study, only a single sample is exhibited to show slightly above value than the limit of 30 µg/L as recommended by WHO and USEPA which may be attributed to the uranium mineralization in this region (Prasad et al.,

158

2024) and all the samples remain well below the recommended limit of 60 µg/L as suggested by AERB. Thus, via the above analysis of contamination of drinking water sources by uranium, the residents of the study area are less likely to get affected due to uranium toxicity. Only four of the samples show uranium concentrations above 10 µg/L. The uranium content in groundwater may be important in the geochemical exploration and understanding of geochemical processes in Himalayan areas (Kaushik et al., 2023). The observed uranium concentration in groundwater is mainly from natural sources as there are no nuclear installations in the study area. The topography and geological feature of the study area influence the concentration of uranium in groundwater. The random changes observed in the activity concentration of uranium in groundwater as discussed in table 6.**1** and table 6.**2** above are because of heterogeneous diverse lithology of the study area (Dhiman et al., 2024).
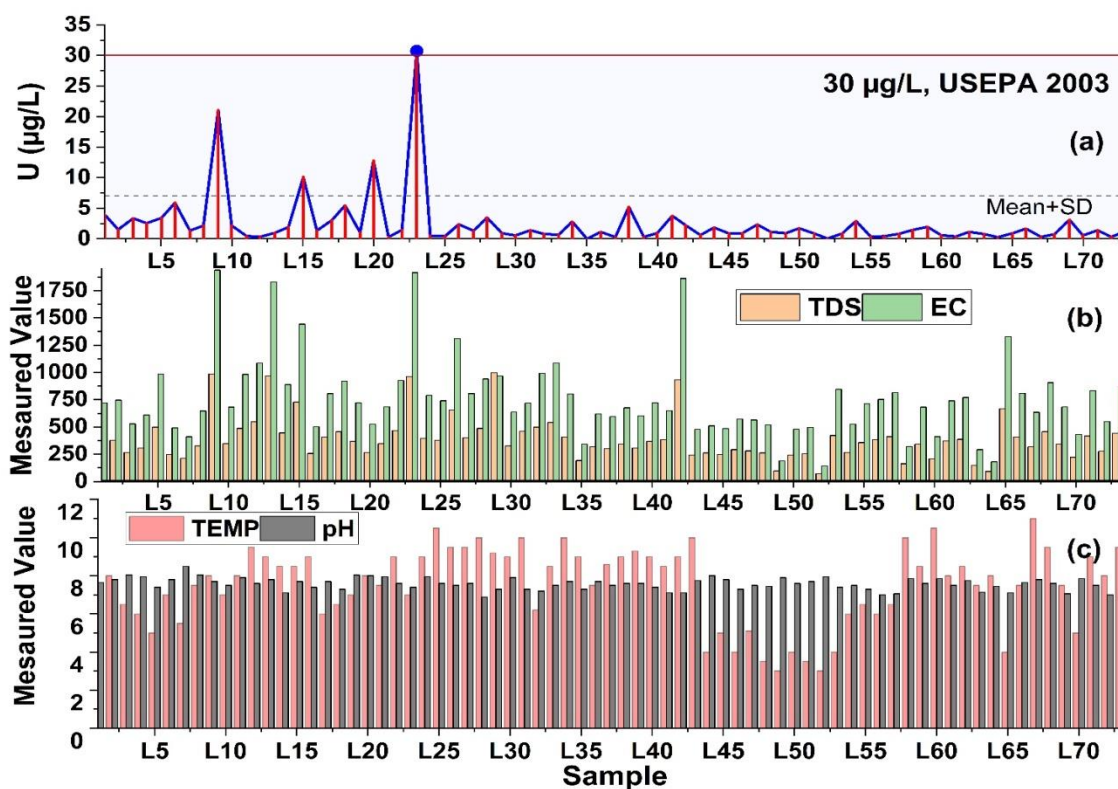
Figure 6.2: Variation of physicochemical quantities and uranium concentration (µg/L) in the study region.

The above figure clearly represents the variation of uranium, TDS, EC, pH and temperature at each sampling point of location in study area. It is seen that only one sample show uranium concentration (30.7µg/L) just above the global recommended value and all other values are well below it (USEPA, 2003).

(a) Uranium Concentration (µg/L)

(b) Total Dissolved Solids (mg/L)
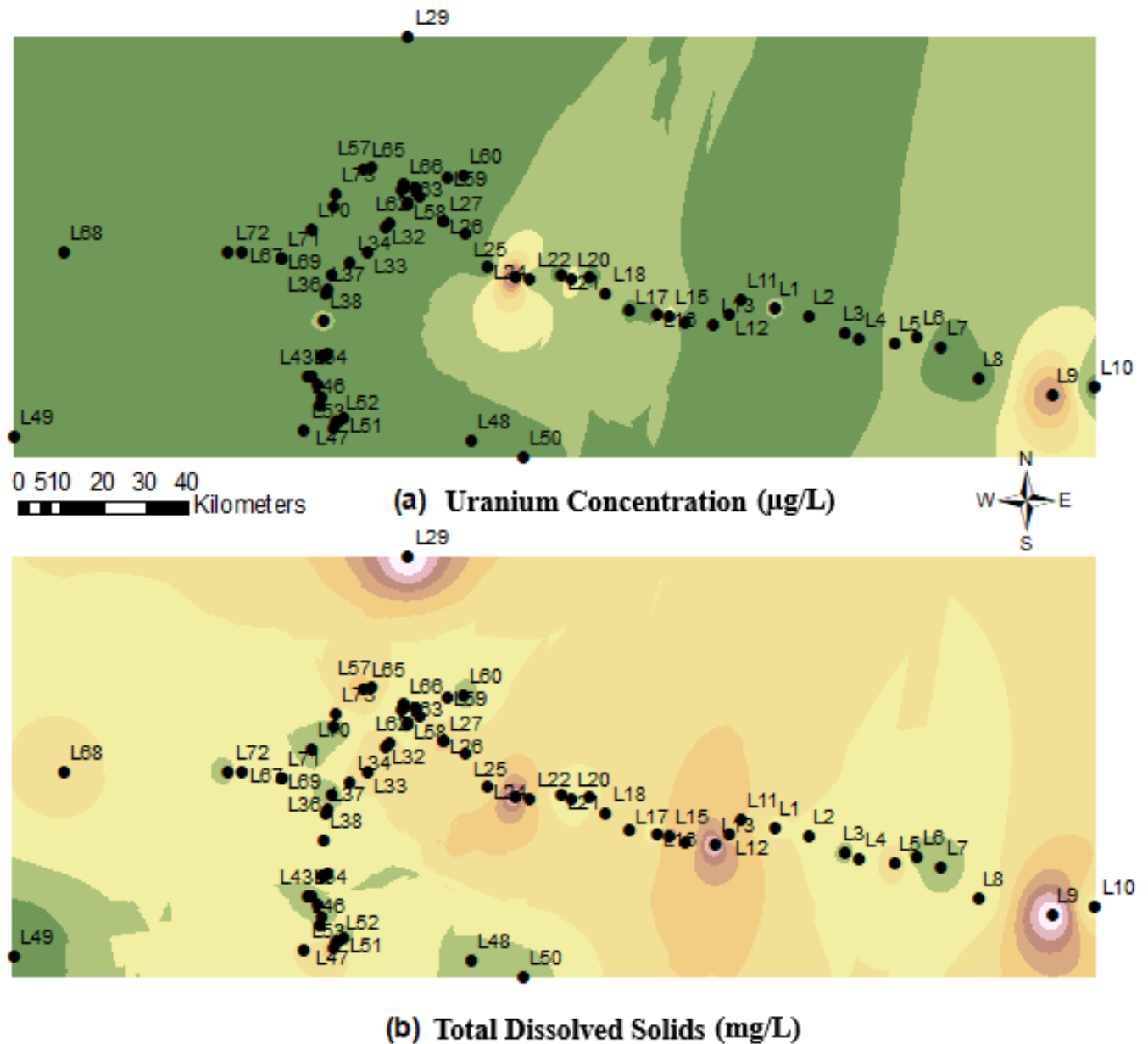
Figure 6.3: Spatial distribution contour map of uranium concentration (µg/L) and TDS (mg/L) in drinking water of study region.
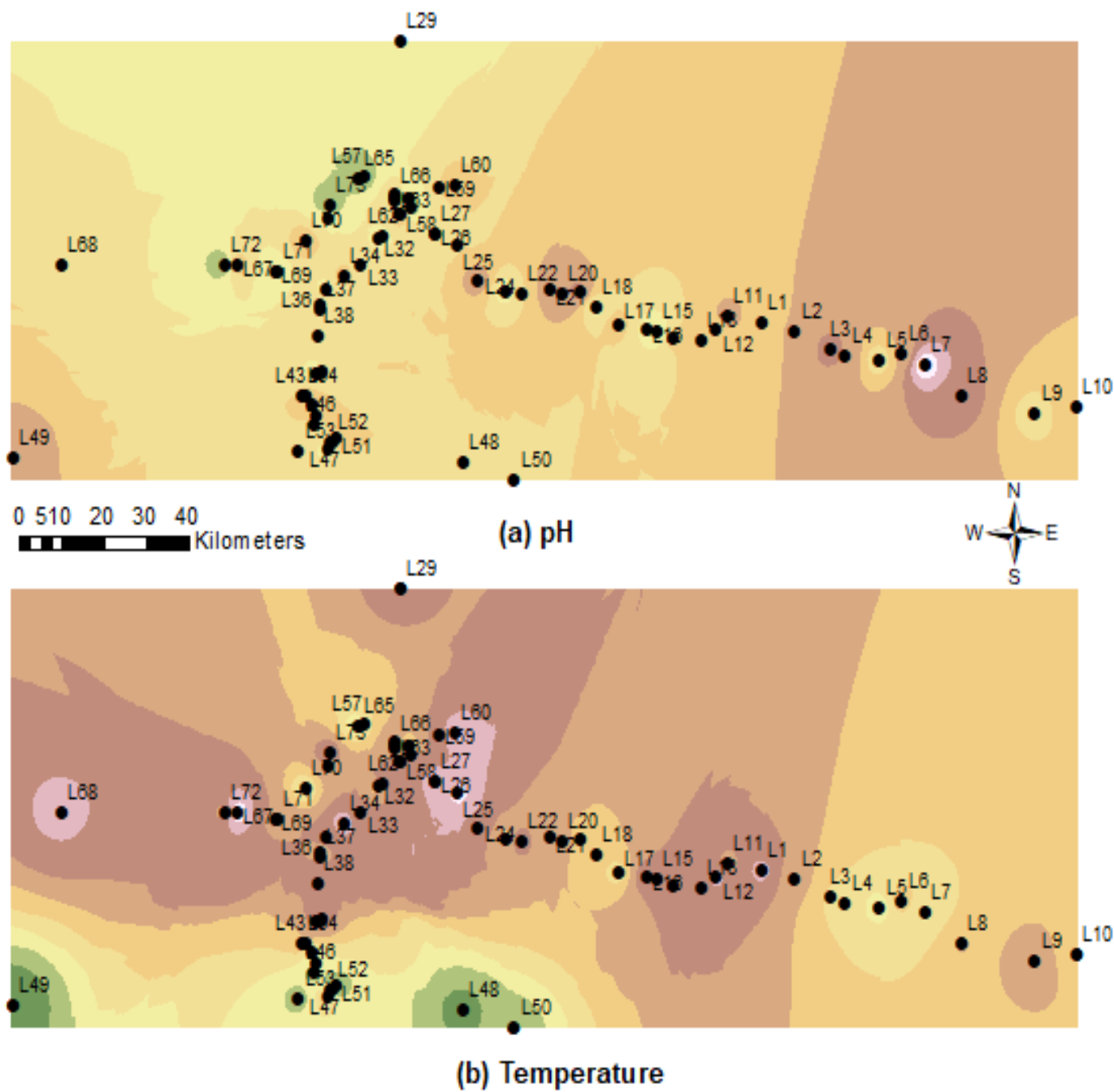
Figure 6.4: Spatial distribution contour map of pH and temperature in drinking water of study region.

The spatial distribution of uranium along with TDS, EC and pH is represented in Figures 6.3 (**a** and **b**) and 6.4 (**a** and **b**). The spatial distribution map was produced by using Arc GIS software ESRI with IDW (inverse distance weight) approximation method. The spatial maps are useful to visualize the obtained data (Ahamad et al., 2024). Clearly, locations L23 (Mulbek) and L9 (Phyang) shows higher uranium concentration and TDS in drinking water of the study region. The possible region of the uranium in this region may be due to the continuous leaching of bedrock present over the area (Sajwan et al., 2024). Further, Figures 6.4 (**a** and **b**) help in visualizing the variation of pH and temperature all over the study area in different water samples.

To ensure the validity of statistical interpretations, an outlier analysis was performed on the groundwater dataset using the Interquartile Range (IQR) method for uranium and TDS, respectively. The IQR analysis revealed that uranium concentrations exhibited seven outliers, with notably elevated values such as 5.9, 10.1, 12.8, 21.1, and 30.7 µg/L, which significantly exceeded the upper quartile threshold. In the same way, six outliers were identified in TDS, including values such as 727, 932, 962, 967, 987, and 997 mg/L, indicating localized zones of high salinity.The above outliers in uranium and TDS are interpreted as natural geogenic anomalies, likely arising from mineral dissolution and prolonged interaction of rock-water of aquifer systems in the study area.

Furthermore, the normality of measured parameters in groundwater such as uranium (µg/L), Total Dissolved Solids (TDS), and pH was statistically examined using the Shapiro-Wilk test, a reliable tool for assessing whether a dataset follows a Gaussian (normal) distribution. According to the test results, Uranium (W = 0.4511, p = 0.0000) and TDS (W = 0.8439, p = 0.0000) exhibit p-values significantly below the standard threshold of 0.05, indicating a strong departure from normality. Whereas, pH (W = 0.9782, p = 0.2366) demonstrated a p-value well above 0.05, suggesting that pH levels in the region are approximately normally distributed. The non-normal distribution of uranium and TDS concentrations in this high-altitude region can be attributed to the unique hydrogeological and geochemical landscape of the Ladakh Trans Himalaya.

Source-wise Distribution of Uranium Concentration in Groundwater

The uranium concentration on average from various groundwater sources varies as 3.2 µg/L for hand pumps, 1.7µg/Lfor natural springs and 0.5µg/L for well water. So, the uranium concentration on average in the studied samples from various underground water sources varies as UHP >UNS >UWell, where UHP is the sample taken from hand pump for uranium analysis, UNS and UWell are the sample taken from natural spring and well water respectively for uranium analysis. It is cleared from the above analysis that the handpump bearing samples on average shows the greater values of uranium concentration than spring and well water sources, the possible reason for this can be attributed to the factor of pumping water from greater depths (Mehta et al., 2024). As water from such sources is mainly used for irrigation purposes in agricultural use at few places of the study area, the high amount of uranium can cause contamination of crops with radionuclides which can be associated with some health risks by consuming these contaminated crops. So, in order to understand the effects of dissolved uranium in drinking water on human health, health surveys in these areas are recommended for radiation protection purposes. The findings of the present study therefore may help and encourage new researchers for further study in the area.
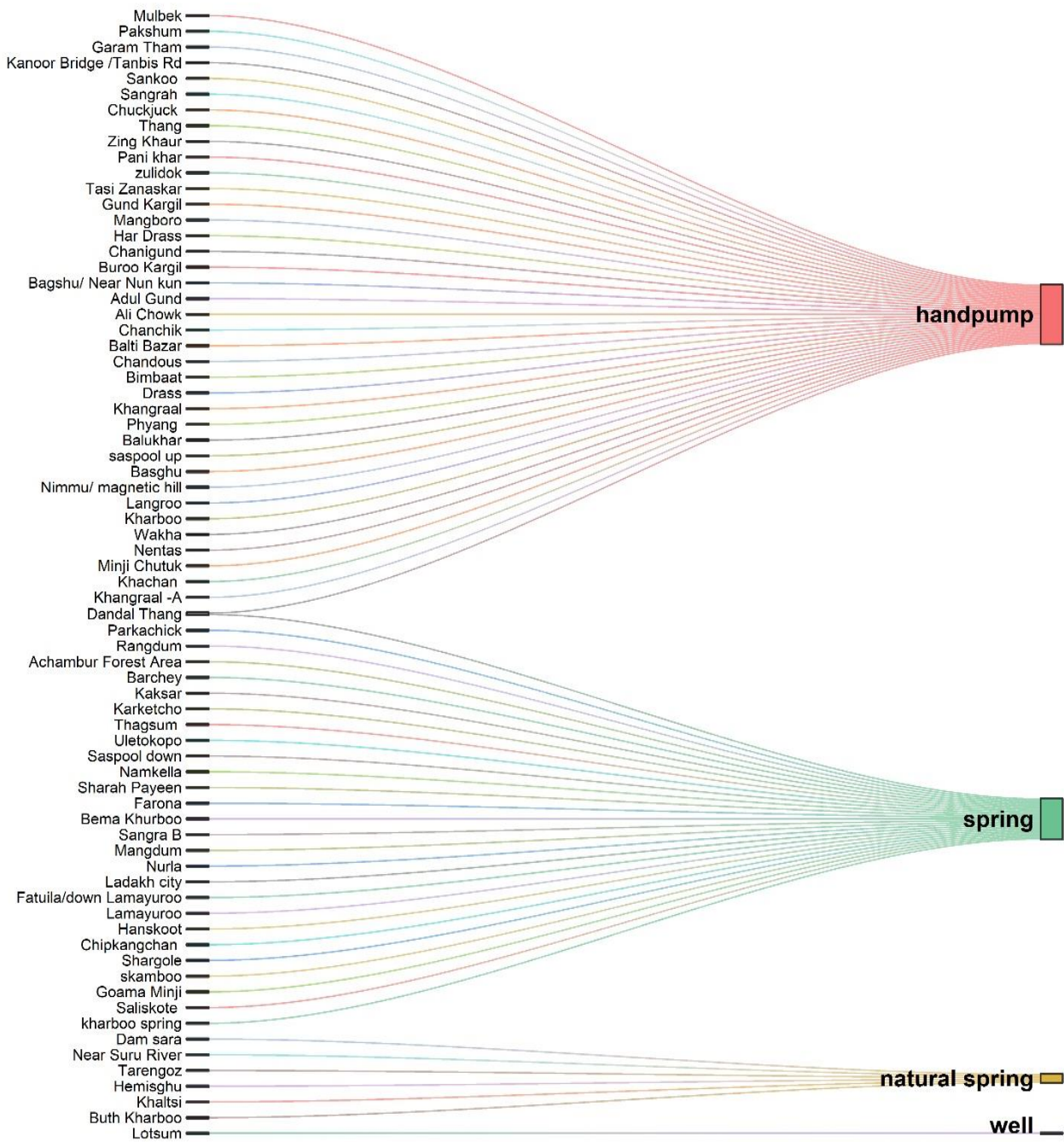
Figure 6.5: Source wise analysis in drinking water of study region.

Figure 6.5 depicts water samples obtained from various sites and classified by their source hand pumps, springs, and wells for water quality testing. The Sankey diagram depicts the link between sampling sites and their corresponding water sources. The majority of samples were collected from hand pumps (red), followed by springs (green), indicating a reliance on natural water flows in specific places. Wells (blue) contribute only a small portion of the overall number of samples collected. This image not only depicts the variety of water sources examined throughout the region, but it also emphasises the significance of each source in understanding regional water quality and identifying possible risks for human and environmental health particularly from hand pump derived uranium contaminated sources.

6.3.1 Radiological Ingestion Dose Due to Exposure of Uranium Concentration in Groundwater

The statistical description of radiological ingestion dose is summarized in Table **6.3**. The maximum radiological dose due to uranium in infants of age group 0-6 months is 8.84 μSv/y with an average 0.74 μSv/y and 10.10 μSv/y with an average of 0.84 μSv/y in infants of age group 7-12 months. The maximum radiological dose assessment was found to be 16.41 μSv/y and 21.46 μSv/y in children of age groups 1-3 year and 4-8 year respectively. Similarly in age groups of males the radiological dose due to uranium was found to be increasing with the age with 30.29 μSv/y in males of 9-13 year age ,41.65 μSv/y for 14-18 year age groups and 46.70 μSv/y in adultmales. Similar trend was dose assessment was observed in females increasing with age as 26.51 μSv/y,29.03 μSv/yand 34.08 μSv/y aged in increments as 9–13-year, 14-18 year and 18 above respectively. Adult male receives higher dose because of large water intake as compared to otherage groups. Moreover estimated ingestion doses received by the people of different age groups are considerably low and did not pose any significant risk on the individual's body. According to WHO, USEPAand AERB, the recommended maximum limit for excess cancer risk for uranium are 8.4 $\times 10^{-5}$,8.5$\times 10^{-5}$, and 16.8 $\times 10^{-5}$, respectively (Table **6.4**). The maximum value of ECR in all the analyzed samples lies well below the recommended limits, showing no potential threat owing to the uranium radiotoxicity via the drinking water route. Calculated ELCR value comes out to be in order with ELCR values estimated by other researchers in northern India viz. Udhampur, Jammu region of Kashmir (Sharma et al., 2017). Lifetime average daily dose found to be in the range from 0.0001-0.878 μg/kg/day with an

average LADD of 0.073 µg/kg/day which is quite low and falls below the reference dose (4.4 µg/kg/day) recommended by AERB (2004). In the present analysis, health quotient (HQ) is also estimated using reference dose given by USEPA, 2003 and 0.024 is the obtained average value of HQ which falls well below than 1. Therefore, no significant chemical toxicity was observed with exposure to uranium in analyzed groundwater samples via the ingestion pathway.

Table 6.3 Radiological age-dependent dose (**µSv/y**)due to exposure of uranium concentration in water sources.

	Infants		Children		Males			Females			Pregnancy	Lactation	Total AEID (µSv/y)
	0-6 months	7-12 months	1-3 y	4-8 y	9-13 y	14-18 y	Adults	9-13 y	14-18 y	Adults	14-50y	14-18 y	
Average	0.74	0.84	1.37	1.79	2.53	3.48	3.9	2.21	2.42	2.85	3.16	4.01	22.14
SD	1.34	1.53	2.49	3.25	4.59	6.31	7.08	4.02	4.4	5.16	5.74	7.27	40.17
Min	0	0	0	0	0	0	0	0	0	0	0	0	0.01
Max	8.84	10.1	16.41	21.46	30.29	41.65	46.7	26.51	29.03	34.08	37.87	47.97	265.07
Skewness	4.5	4.5	4.5	4.5	4.5	4.5	4.5	4.5	4.5	4.5	4.5	4.5	4.5
Median	0.33	0.38	0.62	0.81	1.14	1.57	1.76	1	1.1	1.29	1.43	1.81	10

The radiological dose for different tissues was assessed due to uranium ingestion in water among different age groups which is described in Table 6.5. The annual effective ingestion dose was observed to be high in adult males among all age groups because of more water intake. Figure 6.**6** represents box plot which depicts the descriptive statistics of for age dependent ingestion dose due to ingestion of uranium in water. Outliers in the figure represents wide variation in the obtained data.

Table 6.4 Radiological and Chemical risk due to exposure of uranium in water sources.

	Uranium concentration (μg/L)	Excess Cancer Risk	LADD	HQ (RfD, USEPA)
Average	2.57	0.000003551	0.073	0.024
SD	4.66	0.000006444	0.133	0.044
Min	0.00	0.000000001	0.000	0.000
Max	30.74	0.000042525	0.878	0.293
Skewness	4.50	2.066606604	4.499	4.499

Table 6.5 Radiological tissue-dependent dose for different age groups due to exposure to uranium in water sources.

	Annual Effective Ingestion Dose D(ing) (μSv/y) for different age groups									
	Infants	Children Age Group			Male		Adult Male	Female		Adult Female
	0-6 (0.2)	07-12 (0.8)	1–3 y (1.3)	4–8 y (1.7)	9–13 y (2.4)	14–18 y (3.3)	>18y (3.7)	9–13 y (2.1)	14–18 y (2.3)	>18y (2.7)
Average	0.09	0.1	0.16	0.21	0.29	0.4	0.45	0.26	0.28	0.33
SD	0.16	0.18	0.29	0.38	0.53	0.73	0.82	0.47	0.51	0.6
Min	0	0	0	0	0	0	0	0	0	0
Max	1.06	1.21	1.97	2.58	3.64	5	5.6	3.18	3.48	4.09
Skewness	4.53	4.53	4.53	4.53	4.53	4.53	4.53	4.53	4.53	4.53
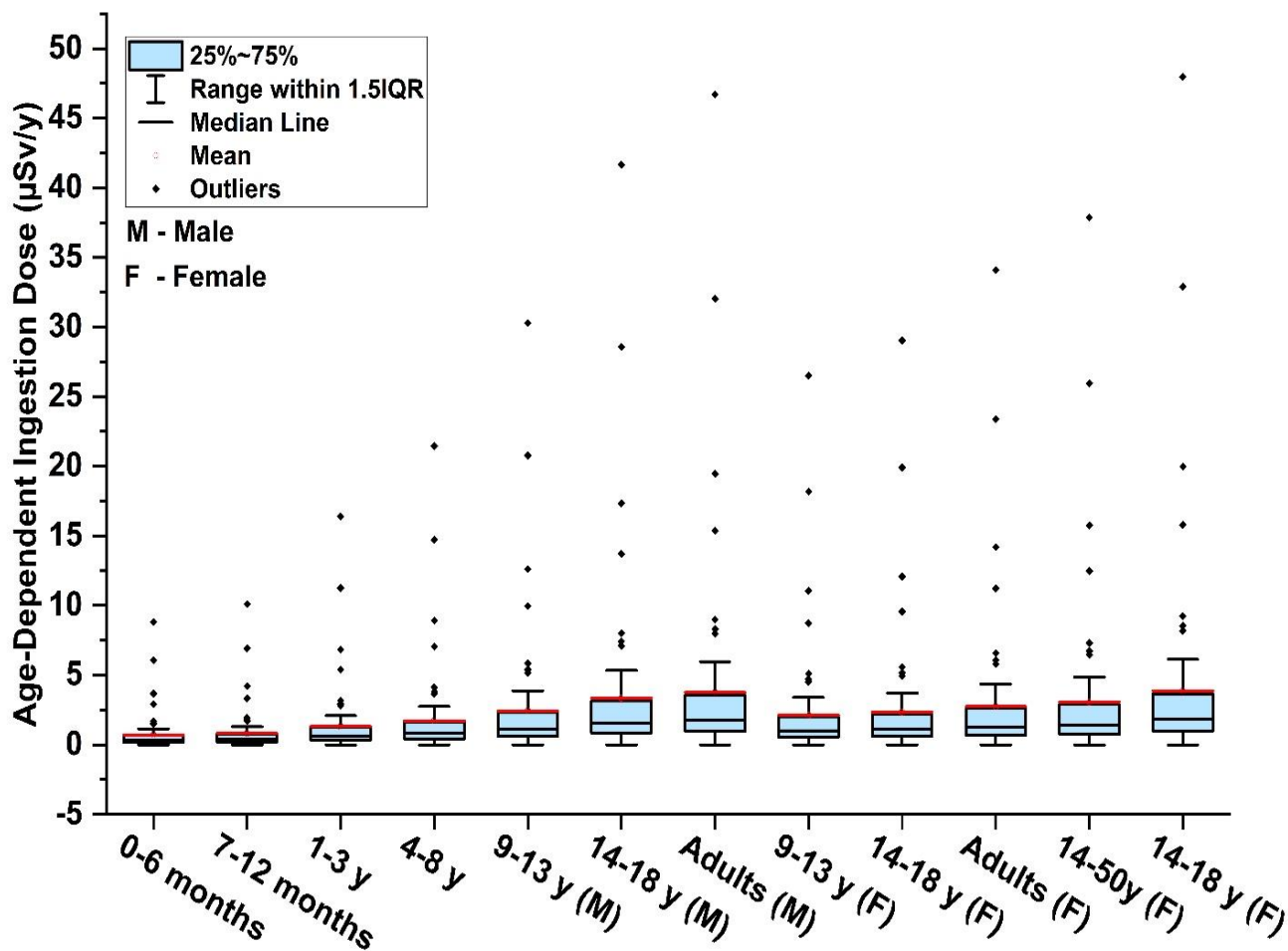
Figure 6.6: Box plot for age dependent ingestion dose due to ingestion of uranium in water.

6.4 Correlation Analysis

The statistical description of correlation study and distribution of different entities viz. pH, TDS, EC and uranium concentration in ground water is given in matrix plot (Figure 6.**7**), consists of histogram representing the frequency distribution of uranium concentration, TDS, pH, EC and temperature obtained from water analysis. The matrix plot reveals interrelationships among variables, highlighting hydro geochemical patterns consistent with global findings. Positive correlations of uranium with EC and TDS suggest rock–water interactions influence its mobility.

Histogram trends indicate most values are within safe limits, with slight anomalies pointing to localized geochemical effects. The diagonal element of the matrix plot shows the correlation between each pair. Uranium and TDS are positively correlated with each other with Pearson r value 0.47 showing the trend between them. In this context, current study supports the previous study carried out in different parts of the globe Table 6.**6**. Uranium is poorly correlated with pH and temperature of the water samples. With Pearson r value 0.52, electrical conductivity (EC) is also showing positive correlation with uranium concentration.
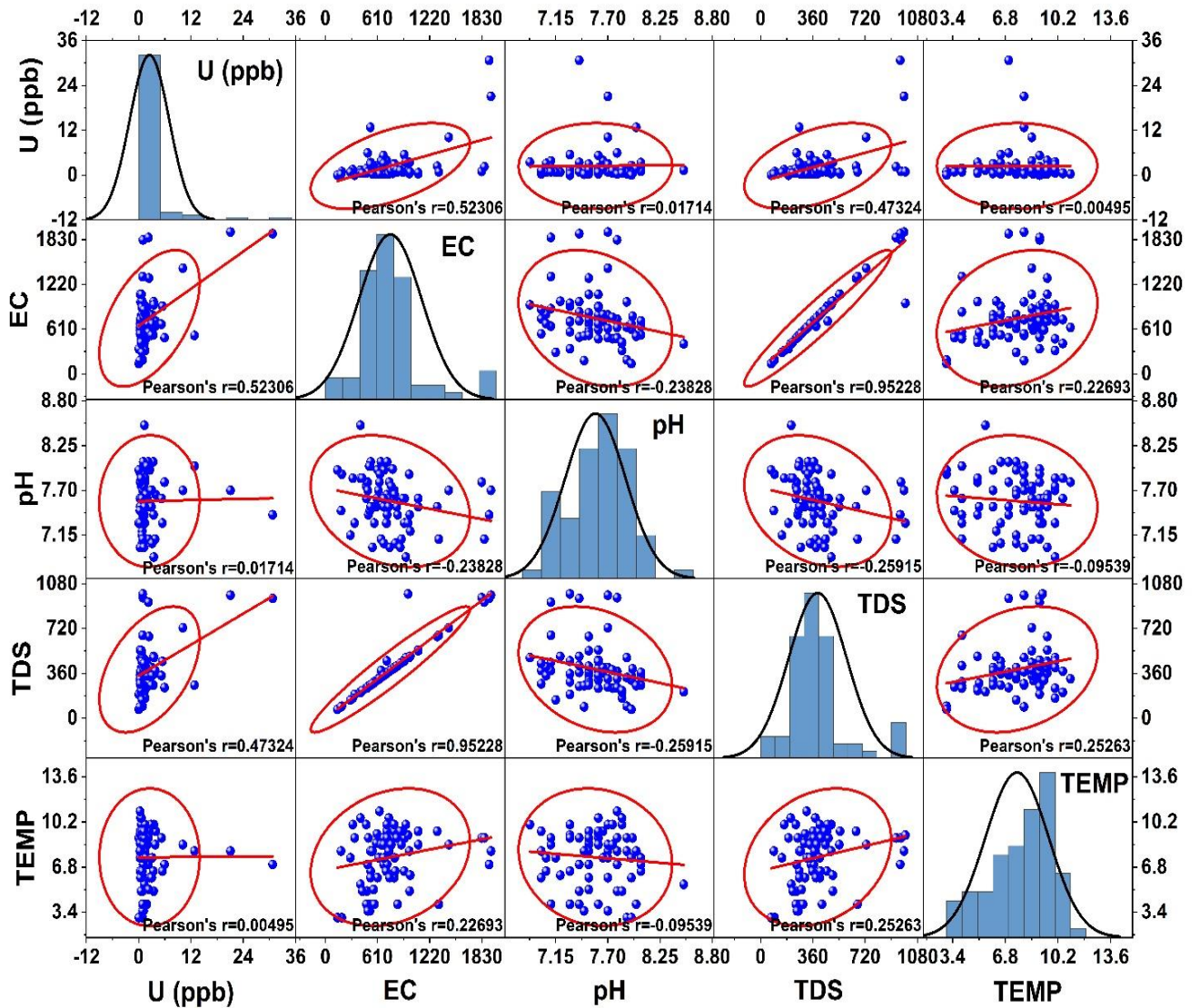
Figure 6.7: Matrix plot for correlation analysis of different parameters obtain in water sources.

6.4.1 Comparative Study

In the present study, the data of uranium concentration in water samples were compared with the studies carried in different parts around the globe. The comparative study is depicted in Table 6. **6**. Dehghani et al., 2024 measured uranium concentration in tap water with a range of 0.18-1.12 μg/L in Shiraz region of Iran. Iyakwari Shekwonyadu, 2024 analyzed uranium concentration in a very high range of 372 to 19964 μg/L in Nigeria. Similarly, Raji et al., 2022 estimated higher uranium concentration 781μg/L in South Africa. Haakonde et al., 2020 in Zambia also observed high uranium concentration in ground water. Various researchers observed similar low concentration in Iraq, Republic of Korea, Morocco, Pakistan and Yemen in different sources of water viz. groundwater and tap water. Overall no such significant anomaly was seen in uranium concentration in the drinking water samples collected from diverse location of the study area.

Table 6.6 Comparison of present work with previous worldwide studies.

Country	Water Type	Range of Uranium (µg/L)	References
Shiraz (Iran)	Tap water	0.18-1.12 µg/L	Dehghani et al., 2024
South Africa*	Rietspruit water	781.9 µg/L	Raji et al. 2022
Al Kufa Iraq*	Groundwater	1.20 µg/L	Abojassimet al., 2020
Republic Of Korea	Groundwater	3.7 µg/l	Hashemi et al., 2024
Zambia*	Drinking water	(135.30 µg/L) > dams (115.62 µg/L) > boreholes (111.31 µg/L) > shallow wells (110.03 µg/L)	Haakondeet al., 2020
Nigeria	Groundwater	372 to 19964 µg/L	IyakwariS. 2024
Morocco*	Groundwater	3.73 µg/L	Samyhet al. 2024
Yemen*	Tap water	64.48 µg/L	AS-Subaihi et al., 2024
Pakistan	Groundwater	30 µg/L to 54 µg/L	Ishaq et al. 2024
Shiwalik Jammu and Kashmir	Drinking Water	6 ± 3 µg/L	Kauret al 2017
Himachal Pradesh	Drinking Water	0.26 ± 0.1 to 29.5 µg/L	Singh et al., 2016
Rajasthan	Groundwater	31.6 µg/L	Rani et al., 2023
Uttarakhand	Drinking water	0.02-63.7 µg/L	Prasad, 2019
Leh-Ladakh	**Drinking Water**	**0.02-30.74** µg/L **with an average of 2.57** µg/L	**Present study**

Table 6.7 Description of Sample ID, Location name, Uranium concentration and Physico chemical parameters

Location ID	Village	Temperature (°C)	EC	pH	TDS	Source	Uranium (µg/L)
L1	Balukhar	9.50	719	7.65	362	H	3.93
L2	Nurla	8.00	746	7.8	377	S	1.53
L3	Hemisghu	6.50	530	8.05	267	S	3.37
L4	Uletokopo	6.00	609	7.95	307	S	2.56
L5	Saspool Down	5.00	986	7.4	497	S	3.43
L6	Saspool Up	7.00	492	7.8	247	H	5.92
L7	Basghu	5.50	410	8.5	212	H	1.34
L8	Nimmu/ Magnetic Hill	7.50	648	8.05	327	H	2.16
L9	Phyang	8.00	1938	7.5	987	H	21.08
L10	Ladakh City	7.00	682	7.7	347	S	2.18
L11	Khaltsi	8.00	982	7.9	487	S	0.46
L12	Langroo	9.50	1086	7.6	547	H	0.36
L13	Fatuila/Down Lamayuroo	9.00	1829	7.8	967	S	0.98
L14	Lamayuroo	8.50	890	7.7	447	S	1.91
L15	Hanskoot	8.50	1443	7.1	727	S	10.12
L16	Chipkangchan	9.00	502	7.4	257	S	1.36
L17	Buth Kharboo	6.00	806	7.7	407	S	3.05
L18	Kharboo	6.50	922	7.3	457	H	5.47

L19	Khangraal	7.00	722	8.05	367	H	1.03
L20	Khangraal -A	8.00	526	8	267	H	12.8
L21	Namkella	7.50	686	7.95	347	S	0.3
L22	Wakha	9.00	926	7.6	467	H	1.46
L23	Mulbek	7.00	1915	7.2	962	H	30.74
L24	Shargole	9.00	789	7.96	397	S	0.51
L25	Lotsum	10.50	742	7.6	377	w	0.46
L26	Skamboo	9.50	1309	7.5	657	S	2.39
L27	Pakshum	9.50	806	7.6	402	H	1.32
L28	Nentas	10.00	941	6.88	487	H	3.49
L29	Sharah Payeen	9.20	966	7.3	997	S	0.95
L30	Minji Chutuk	9.00	637	7.9	327	H	0.56
L31	Garam Tham	10.00	719	7.3	462	H	1.41
L32	Goama Minji	6.20	992	7.4	497	S	0.81
L33	Kanoor Bridge /Tanbis Rd	8.50	1086	7.5	542	H	0.66
L34	Saliskote	10.00	803	7.7	407	S	2.84
L35	Farona	9.00	342	7.3	192	S	0.02
L36	Khachan	7.50	621	7.7	317	H	1.12
L37	Bema Khurboo	8.60	595	7.5	302	S	0.3
L38	Sankoo	9.00	676	7.6	342	H	5.24
L39	Sangrah	9.30	602	7.6	307	H	0.32
L40	Sangra B	9.00	722	7.4	367	S	0.94

L41	Mangdum	8.50	651	7.1	382	S	3.77
L42	Chuckjuck	9.00	1862	7.1	932	H	2.24
L43	Dam Sara	10.00	478	7.75	242	S	0.61
L44	Thang	4.00	512	8	262	H	1.86
L45	Zing Khaur	5.00	485	7.8	247	H	0.89
L46	Pani Khar	4.00	572	7.3	292	H	0.94
L47	Parkachick	5.10	564	7.5	282	S	2.34
L48	Zulidok	3.50	520	7.45	262	H	1.16
L49	Rangdum	3.00	191	7.9	97	S	0.92
L50	Tasi Zanaskar	4.00	480	7.6	242	H	1.72
L51	Near Suru River	3.50	496	7.7	252	S	0.89
L52	Tarengoz	3.00	140	7.95	72	S	0.05
L53	Achambur Forest Area	4.00	846	7.4	422	S	0.9
L54	Gund Kargil	6.00	527	7.5	267	H	2.93
L55	Mangboro	6.50	712	7.3	357	H	0.35
L56	Har Drass	6.00	752	7	382	H	0.43
L57	Chanigund	6.50	816	7.05	412	H	0.84
L58	Buroo Kargil	10.00	320	7.85	162	H	1.45
L59	Bagshu/ Near Nun Kun	8.50	683	7.6	342	H	1.98
L60	Barchey	10.50	412	7.85	207	S	0.63
L61	Adul Gund	8.00	740	7.5	372	H	0.39
L62	Ali Chowk	8.50	770	7.75	387	H	1.16

L63	Chanchik	7.50	292	7.15	147	H	0.77
L64	Kaksar	8.00	182	7.45	92	S	0.26
L65	Karketcho	4.00	1327	7.1	667	S	0.91
L66	Balti Bazar	7.50	810	7.65	407	H	1.67
L67	Chandous	11.00	634	7.8	317	H	0.32
L68	Bimbaat	9.50	906	7.6	457	H	0.76
L69	Dandal Thang	7.50	684	7.05	342	S	3.12
L70	Thagsum	5.00	431	7.85	222	S	0.57
L71	Dandal Thang	9.00	834	7.5	417	H	1.39
L72	Drass	8.00	549	7	277	H	0.33
L73	Kharboo Spring	9.50	876	7	442	S	1.23

6.5 Conclusions

The current study evaluates 73 groundwater samples from various sources in the upper Himalayan region of Ladakh. The results show that the groundwater in this area is generally safe to drink, with uranium concentrations ranging from 0.02 to 30.7 µg/L with an average of 2.5 µg/L. All samples were well within the AERB threshold of 60 µg/Land only one sample exceeds USEPA recommended limit of 30 µg/L showing that there were no notable radiological or chemo-toxic effects. Ingestion doses, Hazard Quotients (HQ), and Lifetime Average Daily Doses (LADD) all fall well within safe limits for all age groups, which is further supported by health risk assessments. The concentrations of uranium varied according to the source, with higher concentrations found in water from hand pumps, which were attributed to deeper extraction depths and lithological influences.Although localized variations have been found because of geological and lithological factors, physicochemical analysis revealed that parameters like pH (6.88–8.5), temperature (3–11°C), and TDS (72–997 mg/L) generally adhered to drinking water

standards. Hand pump sources had the highest average uranium levels (3.17µg/L), while spatial mapping showed higher uranium concentrations at particular sites (L23 and L9) attributed to bedrock leaching. Even though the study finds no uranium-related risks in Ladakh's groundwater, regular monitoring is advised, particularly in regions that primarily rely on deep aquifers. These results provide valuable insights on the geochemical processes in the Himalayan region and suggest that future comprehensive investigations should be carried out in other parts of the Upper Himalayan Range. These investigations should include advanced geochemical analyses and long-term monitoring techniques to ensure the sustainable use of groundwater resources in this lithologically diverse area.

References

- Abojassim, A. A., Neama, H. H., 2020. Radiological and chemical risk assessment from uranium concentrations in groundwater samples collected from Al-Kufa area, Iraq. Water Supply. 20(8), 3194-3206. https://doi.org/10.2166/ws.2020.207

- AERB (Atomic Energy Regulatory Board) (2004). Drinking water specifications in India. Department of Atomic Energy, Govt. of India.

- Ahmad, T., Shakeel, P., Rayees, S., Pal, K., Jeeban, S., Gewali, P., 2024. Radon quantification in water and dose estimation via inhalation and ingestion across age groups in the Pattan region of North Kashmir, India. Environ. Geochem. Health. https://doi.org/10.1007/s10653-024-02302-x

- Ashish, A., Bangotra, P., Dillu, V., 2024. Human exposure to uranium through drinking water and its detrimental impact on the human body organs. Environ. Geochem. Health. 46(10), 1–18. https://doi.org/10.1007/s10653-024-02150-9

- AS-Subaihi, F.A., Bazohair, A.O., 2024. Evaluation of Ingestion doses and Hazard Quotients due to Intake of Uranium in tap Drinking Water from Aden Governorate, Yemen.

- BIS (Bureau of Indian Standard) (2012). Indian standards specifications for drinking water, IS: 10500, Second revision, Bureau of Indian Standards, India.

- Chatterjee, S., Goswami, A., Scotese, C. R., 2013. The longest voyage: Tectonic, magmatic, and paleoclimatic evolution of the Indian plate during its northward flight from Gondwana to Asia. Gondwana Res. 23(1), 238-267.

- Dehghani, M., Rezaie Rahimi, N., Zarei, M., Parseh, I., Soleimani, H., Keshtkar, M., Zarei, A.A. Khaksefidi, R., 2024. Chemical and radiological human health risk assessment from uranium and fluoride concentrations in tap water samples collected from Shiraz, Iran; Monte-Carlo simulation and sensitivity analysis. Int. J. Environ. Anal. Chem. 104(6), 1349-1364.

- Dhiman, R., Khyalia, B., Kumar, N., Kumar, S., Kataria, N., Kumar, R., 2024. Investigation of radiation dose - dependent risk on individuals due to drinking water ingestion in Yamunanagar District , India. J. Radioanal. Nucl. Chem. 333(6), 3279–3289. https://doi.org/10.1007/s10967-024-09387-9

- Hashemi, S., Shin, I., Kim, S.O., Lee, W.C., Lee, S.W., Jeong, D.H., Kim, M., Kim, H.K. Yang, J., 2024. Health risk assessment of uranium intake from private residential drinking groundwater facilities based on geological characteristics across the Republic of Korea. Sci. Tot. Environ. 913, 169252. https://doi.org/10.1016/j.scitotenv.2023.169252

- Haakonde, T., Yabe, J., Choongo, K., Chongwe, G., Islam, M. S., 2020. Preliminary assessment of uranium contamination in drinking water sources near a uranium mine in the Siavonga District, Zambia, and associated health risks. Mine Water Environ. 39(4), 735-745. https://doi.org/10.1007/s10230-020-00731-5

- Ishaq, S., Nasir, T., Ali, N., Baloch, M.K., Khan, E.U., Ali, M.M., Sherazi, M.R.H., Ahmad, F., Muhammad, J., Usmani, M.Y., 2024. Evaluation of natural radioactivity and radiological hazards in water sample of Tounsa Sharif, South Punjab, Pakistan. Phys. Scripta. 99(6), 065312

- Iyakwari, S., 2024. Radiotoxicity and groundwater quality for drinking in a multi-layered saline sedimentary terrain of Keana, Central Benue trough, Nigeria. African Sci. Rep. 169-169. https://doi.org/10.46481/asr.2024.3.2.169

- Jain, A. K., Banerjee, D. M., Kale, V. S., Jain, A. K., Banerjee, D. M., Kale, V. S., 2020. Trans-Himalayan and Karakoram Ranges. Tectonics Ind. Subcont. 449-485

- Kaushik, H., Soheb, M., Biswal, K., Om, A. L. R., Arbind, K., Patel, K., 2023. Understanding the hydrochemical functioning of glacierized catchments of the Upper Indus Basin in Ladakh , Indian Himalayas. Environ. Sci. Pol. Res. 20631–20649. https://doi.org/10.1007/s11356-022-23477-9

- Kumar, M. P., Nagalakshmi, K., Jayaraju, N., Prasad, T. L., Lakshmanna, B., 2020. Deciphering water quality using WQI and GIS in Tummalapalle Uranium Mining area, Cuddapah Basin, India. Water Sci. 34(1), 65-74

- Lee, J., 2006. Characterization of groundwater temperature obtained from the Korean national groundwater monitoring stations : Implications for heat pumps. 514–526. https://doi.org/10.1016/j.jhydrol.2006.03.007

- Mitchell, E., Frisbie, S., Sarkar, B., 2011. Exposure to multiple metals from groundwater -A global crisis: Geology, climate change, health effects, testing, and mitigation. Metallomics. 3(9), 874–908. https://doi.org/10.1039/c1mt00052g

- Monica, S., 2018. Assessment of age-dependent uranium intake due to drinking water in

Neendakara, Kollam district Kerala. Int. J. Sci. Res. Phys. Appl. Sci. 6, 31-44.. https://doi.org/10.26438/ijsrpas/v6i3.3134

- Mehta, V., Kaur, J., Shikha, D., Kanse, S., 2024. Age - dependent ingestion doses to the public of Rupnagar and Una regions of India due to intake of uranium. J. Radioanal. Nucl. Chem. 333(6), 2937–2951. https://doi.org/10.1007/s10967-023-09185-9

- Naik, P. R., Rajashekara, V. A., Mudbidre, R., 2024. Quantification of natural uranium and its risk evaluation in groundwater of Chikkaballapur district in Karnataka, India. Environ. Mon. Assess. 196(9), 779.https://doi.org/10.1007/s10661-024-12913-7

- Negi, R.S., Prasad, M., Aswal, R.S., Negi, J.S., Shrivastava, U., Panwar, P., Kaintura, S.S., Uniyal, S.C., Ramola, R.C., 2024. LED fluorimetric analysis of uranium in potable groundwater and associated health concerns. J. Radioanal. Nucl. Chem. 1-10.https://doi.org/10.1007/s10967-024-09770-6

- Pandith, T.A., Gewali, J.P., Simnani, S., Nazir, S., Singh, K.P., Chakan, M.R., 2024. Exploring tectonic sites with radon from groundwater sources and dose evaluation in various age groups in Baramulla, J&K, India. Ground. Sustain. Dev. 26, 101232. https://doi.org/10.1016/j.gsd.2024.101232

- Phartiyal, B., Nag, D., 2022. Sedimentation, tectonics and climate in Ladakh, NW trans-Himalaya-with a special reference to late quaternary period. Geosys. Geoenviron. 1(4), 100031.

- Porcelli, D.2003. The Behavior of U- and Th-series Nuclides in Groundwater. *Reviews in Mineralogy and Geochemistry*, *52*(1), 317–361. https://doi.org/10.2113/0520317

- Prasad, M., Utpal, R. S. A., Abhishek, S., Pooja, J., Pargin, P., 2024. Levels and effects of uranium in groundwater sources of Shivalik hills , outer Himalaya , India. J. Radioanal. Nucl. Chem. 333(5), 2495–2504. https://doi.org/10.1007/s10967-023-08906-4

- Rani, A., Parashar, K., Meena, R., Sharma, S. K., Tiwari, K. K., Ajaykumar, V., Mondal, N. C., 2023. Hydrochemical characteristics and potential health risks of nitrate, fluoride, and uranium in Kota district, Rajasthan, India. Environ. Sci. Pol. Res. 30(34), 82485-82505. https://doi.org/10.1007/s11356-023-28071-1

- Raji, I. B., Hoffmann, E., Erasmus, E., Ngie, A., Winde, F., 2022. Assessing health risk associated with uranium in Rietspruit water, far West Rand goldfield, South Africa. Int. J. Environ. Sci. Tech. 20(9), 10229-10242. https://doi.org/10.1007/s13762-022-04673-z

- Sajwan, R. S., Joshi, V., Ahamad, T., Kumar, N., Parmar, P., Jindal, M. K., 2024. Assessment of radon transportation and uranium content in the tectonically active zone of Himalaya, India. Sci. Tot. Environ. 926, 171823. https://doi.org/10.1016/j.scitotenv.2024.171823

- Samyh, B., Nachab, A., Jabbade, M., Nourreddine, A. M., 2024. Dose assessment from exposure to uranium and radon in groundwater in Safi province, Morocco. Int. J. Environ. Health. Res.1-12.

- Saikia, R., Chetia, D., Bhattacharyya, K. G., 2021. Estimation of uranium in groundwater and assessment of age-dependent radiation dose in Nalbari district of Assam, India. SN App. Sci. *3*, 1-12.

- Shellnutt, J. G., Lee, T. Y., Brookfield, M. E., Chung, S. L., 2014. Correlation between magmatism of the Ladakh Batholith and plate convergence rates during the India–Eurasia collision. Gondwana Res. *26*(3-4), 1051-1059.21.https://doi.org/10.1007/s10967-018-6281-7

- Sharma, S., Kumar, A., Mehra, R., Mishra, R., 2017. Ingestion doses and hazard quotients due to intake of Uranium in drinking water from Udhampur District of Jammu and Kashmir State, India. Radioprot. *52*(2), 109-118. https://doi.org/10.1051/radiopro/2017009

- Srilatha, M.C., Rangaswamy, D.R., Sannappa, J., 2014. Studies on concentration of Radon and Physicochemi- cal parameters in ground water around Ramanagara and Tumkur districts, Karnataka, India. Int. J. Adv. Sci. Tech. Res. 2(4), 641–660.

- USEPA (United State Environmental Protection Agency) (2003). Current drinking water standards, Ground water and drinking water protection Agency, 1–12

- UNSCEAR (United Nations Scientific Committee on the Effect of Atomic radiation) (2000). United Nations general assembly. Vol. 1, Annex B, United Nations 84–140.

- Weinberg, R. F., Dunlap, W. J., 2000. Growth and deformation of the Ladakh Batholith, Northwest Himalayas: implications for timing of continental collision and origin of calc-alkaline batholiths. The J. Geol. 108(3), 303-320.

- World Health Organization(WHO) 2017. Guidelines for drinking-water quality, 4th edn. World Health Organization, Geneva, Switzerland (ISBN: 978-92-4-154995-0)

- WHO (2004). Guidelines for drinking-water quality, vol 1, 3rd edn. World Health Organization, Geneva.

CHAPTER 7

SEASONAL VARIATION IN INDOOR RADON / THORON PROGENY LEVELS AND ASSOCIATED DOSE IN BARAMULLA, J &K

7.1 Radon-222: A Major Indoor Radiation Hazard

Radon-222 (222Rn) is the most abundant naturally occurring isotope of radon, comprising 99.27% of its total presence and significantly contributing to radiation exposure. As a Naturally Occurring Radioactive Material (NORM), it originates from the radioactive decay of (226Ra) within the uranium decay series. Its decay products including (218Po), (214Pb), (214Bi), readily attach to airborne particles, intensifying radiation exposure particularly in high-dust environments. This process increases the risk of surface contamination and inhalation indoors (Vogiannis & Nikolopoulos, 2015).

With a short half life of 3.82 days, (Rn) is a dominant contributor to indoor radiation exposure and is easily measurable. In contrast, thoron (220Rn), with a much shorter half-life of 55.6 seconds, plays a lesser role in indoor dosimetry. Tokonami was the first to emphasize thoron's significance in radiation dose estimation, asserting that radon, thoron, and their decay products require independent measurement. Subsequent studies have reinforced thoron's contribution to total radiation exposure (Tokonami, 2010).

The primary entry point of radon into buildings is the soil beneath them. Radon infiltrates through convective flow and diffusion, regulated by temperature and humidity. Fine-grained soils, such as clay, tend to retain radon more than sand or silt. Factors such as soil and bedrock permeability and porosity dictate radon movement. The "chimney effect," caused by indoor heating during colder months, draws radon-rich soil gases into buildings, while wind speed and direction further influence infiltration (Selinus et al., 2013).

Structural elements, including crawl spaces, basements, slab-on-grade foundations, significantly impact radon accumulation. Entry points include cracks, pipe inlets and drainage systems, with

ventilation systems playing a crucial role in either increasing or mitigating infiltration (Nazaroff., 1988).

There are four primary sources of indoor radon:

1. **Soil Gas**: The most significant source, entering buildings through slab openings, diffusion, or foundation cracks.
2. **Building Materials**: Concrete, brick, and stone contribute radon based on their radium content and emanation rates.
3. **Groundwater**: Radon dissolves in water sourced from radium-rich aquifers and is released into indoor air when used.
4. **Outdoor Air and Natural Gas**: These typically contribute minimal radon exposure, with natural gas concentrations diminishing before reaching homes.

Radon levels correlate directly with soil uranium content, regardless of foundation type. Homes with basements or partial cellars accumulate more radon than those built on crawl spaces or slab foundations (Bruno, 1983).Long-term residential exposure to 222-Rn are strongly associated with increasing cause of lung cancer. (Darby et al., 2006) conducted an in-depth study revealing that lung cancer risk rises by over 15% with every 100 Bq/m³ increase in indoor radon levels. Smokers are particularly vulnerable, facing up to 25times greater risk than non-smokers due to the linear dose-response relationship (Kang et al., 2019). Other health concerns include nervous system tumors, hematological cancers, and COPD (Ruano-Ravina et al., 2018). Studies in uranium-rich areas also suggest associations with reduced fertility, higher urinary tract infections, and chronic bronchitis (Bersimbaev and Bulgakova, 2015). Radon exposure has been linked to increased mortality from cardiac and respiratory diseases, especially when combined with fine particulate matter (Blomberg et al., 2019). Additionally, ingestion of radon-contaminated water is linked with an increased risk of gastric cancer (Thabayneh, 2015).

Radon concentrations are usually low in outdoors, ranging from a few to 100-1000Bq/m³. However, indoor levels can vary significantly, from tens to several thousand Bq/m³. A 2009 WHO report documented indoor radon averages of 140Bq/m³ in Mexico and the Czech Republic, 49Bq/m³ in Poland and 46Bq/m³ in the USA. Lower values were observed in Canada (28Bq/m³), the UK (20Bq/m³), Japan (16Bq/m³), and Australia (11Bq/m³), with the global indoor

radon average estimated at 39Bq/m³ (Kozak et al., 2011). Radon enters into the environment and Infiltrates buildings through multiple pathways. Approximately 80% of indoor radon originates from subsurface soil, 12% from building materials, and 9.3% from atmospheric air, with natural gas and water contributing less than 1% (Al-Zoughool & Krewski, 2009).

Radon, geologically sourced a decay of uranium present in rocks and soils, enters into the atmosphere and built environments is significantly influenced by environmental processes such as the thawing of permafrost, a phenomenon enhanced by global climate change. This thawing can mobilize previously trapped radon, enhancing its release into surrounding areas, including residential spaces. From an architectural perspective, the trend toward energy-efficient construction has led to the development of tightly sealed buildings designed to minimize energy loss. While beneficial for thermal efficiency, such designs often limit natural ventilation, inadvertently creating conditions conducive to radon accumulation indoors. Meteorological factors further compound the issue while, climate change-induced variations in temperature and precipitation patterns may exacerbate these seasonal trends. Human behaviors play a critical role in this dynamic. The increased use of heating and air conditioning systems, along with a general tendency to keep living spaces sealed, reduces indoor-outdoor air exchange, creates an environment where indoor radon concentrations can rise to potentially hazardous levels (Rathebe et al., 2025).

A case study from Thailand shop houses demonstrated that radon concentrations were found in increasing exhalation amount in buildings constructed with fly ash and phosphogypsum added cement (Srisuwan, 2025).

Construction activities that disturb deeper soil layers expose regions with higher radon concentrations due to increased 226Ra. Variations in pressure between inside and outer environments drive radon intrusion, enhanced by ventilation systems, sewage exhausts, and temperature variations. Warmer indoor air generates an upward draft, further drawing radon from the ground. Additionally, naturally occurring radium-containing building materials, such as fly ash, slag, and phosphor gypsum, release radon, contributing to indoor concentrations (Kreft, 2017). Alpha-particle radiation from radon decay products, primarily 214Po and 218Po, accounts for over 90% of radiation exposure. While most inhaled radon gas is exhaled, its decay products attach to airborne particles, penetrate the respiratory system, and emit high-energy alpha

particles, causing DNA damage and increasing cancer risk (Mittal et al., 2016).

7.2 Methods and Formulae Used

In the present study, LR-115 films coupled with dosimeter were employed for analysis of Rn, Th activity concentrations. To evaluate the Equilibrium Equivalent Concentrations of radon and thoron, Direct Radon Progeny Sensors and Direct Thoron Progeny Sensors) were used for alpha particle flux measurements. After the dosimeters were retrieved, they underwent chemical etching using a (NaOH) solution at 60°C for approximately 90 minutes. A comprehensive description of this methodology is detailed in Section 3.5 of Chapter 3.

The concentrations of thoron (CTh) and radon (CRn) were evaluated by the following equations (Prasad et al., 2015).

$$C_{Th} = (T_{R+T} - T_R) / (d \times k_T) \qquad (7.1)$$

$$C_{Rn} = (T_R) / (d \times k_R) \qquad (7.2)$$

In this study, radon (CRn) and thoron (CTh) concentrations, expressed in Bq/m^3, were determined using track density data obtained from the two distinct chambers of the twin-cup dosimeter. The first chamber, designed exclusively for radon detection, provided the track density denoted as T_R, while the second chamber, which registers both radon and thoron contributions, yielded the combined track density labeled as T_{R+T}. The calculation employed specific calibration factors: $k_R = 0.0172 \pm 0.002$ tracks cm^{-2} per $Bqm^{-3}d$ for radon and $k_T = 0.010 \pm 0.001$ tracks cm^{-2} per $Bqm^{-3}d$ for thoron, with *d* representing the total exposure duration in days during which the detectors were deployed.

The calibration factor is a conversion constant that translates observed track densities into the activity concentration of the radioactive gas. A small calibration factor associated with thoron in the dosimetric compartment assures negligible interference of thoron on radon measurements (Ahamad et al., 2024).

Determination of Equilibrium Equivalent Concentrations

The decay of these gases results in the formation of radioactive progenies. These decay products, referred to as Equilibrium Equivalent Concentrations (EECs), are highly reactive and may exist as ions or neutral atoms before aggregating into condensed phase molecules or binding to airborne particulates. When inhaled, these progeny deposit in the respiratory tract and emit alpha particles, making them essential for estimating the effective dose from parent radio nuclides.

The Equilibrium Concentrations were obtained by deducting the track density attributed to thoron progeny (recorded using DTPS) from the total progeny track count. These Concentrations were calculated using established equations as outlined by (Ramola et al., 2016).

$$\text{EETC} = T_{DTPS} / d \times K_{Th} \qquad (7.3)$$

$$\text{EERC} = (T_{DRPS} / d \times K_{Rn}) - \text{EETC} \qquad (7.4)$$

The track densities registered by these detectors are denoted as T_{DTPS} and T_{DRPS} respectively. The calibration constants, representing the sensitivity of the detectors, are K_{Th} for thoron and K_{Rn} for radon as reported by (Mishra and Mayya , 2008) and further supported by (Mishra et al.,(2010).

Estimation of Annual Inhalation and Corresponding Effective Dose

The Annual Inhalation Dose (AID) along with the Annual Effective Doses due to radon (AEDR) and thoron (AEDT) progeny were evaluated using established methodologies and dose conversion factors as suggested in the (UNSCEAR , 2000) guidelines.

$$\text{AID } (\mu Sv/y) = [(0.17 + 9F_{Rn})\, C_{Rn} + (0.11 + 40F_{Tn})C_{Th}] \times O_C \times 8760\ (h/y) \times 10^{-6} \quad (7.5)$$

$$\text{AEDR } (\mu Sv/y) = \text{EERC } (Bqm^{-3}) \times 9\ (n\ Sv) \times O_C \times 8760\ (h/y) \times 10^{-6} \qquad (7.6)$$

$$\text{AEDT } (\mu Sv/y) = \text{EETC } (Bqm^{-3}) \times 40\ (n\ Sv) \times O_C \times 8760\ (h/y) \times 10^{-6} \qquad (7.7)$$

In this context, AID refers to the cumulative inhalation dose, while AEDR and AEDT correspond to the annual effective doses resulting from radon and thoron exposure, respectively. The equilibrium factors for radon and thoron are represented by F_{Rn} and F_{Th} with O_C stands for the indoor occupancy factor, and the value 8760 hours represents the total duration of annual exposure (Prasad et al., 2016).

7.3 Data Interpretation

Table 7.1 Representation of annual effective doses from radon, thoron, and their progeny with ambient gamma radiation levels

S. No.	House Type	Rn220	Rn222	EETC	EERC	Ft	Fr	AEDT	AEDR	AID	Gamma field (nsv/h)
1	Mamoosa	78.89	87.42	2.54	13.58	0.03	0.16	0.71	0.86	1.73	201
2	Babgund	69.44	23.37	0.97	19.23	0.01	0.84	0.27	1.21	1.57	158
3	shirpora	65.56	50.16	3.29	20.65	0.05	0.44	0.92	1.30	2.33	137
4	zangam	67.22	92.48	3.47	17.16	0.05	0.20	0.97	1.08	2.22	142
5	Hanjiwera Bala	71.39	47.39	2.62	25.56	0.04	0.58	0.73	1.61	2.46	156
6	Buran	48.61	49.35	2.76	24.41	0.06	0.55	0.77	1.54	2.41	168
7	Pattan	74.17	99.18	4.28	32.07	0.06	0.32	1.20	2.02	3.40	112
8	Shouch	56.67	94.28	3.55	29.97	0.06	0.33	1.00	1.89	3.04	132
9	Dangerpora	88.06	62.42	2.51	29.63	0.03	0.49	0.70	1.87	2.71	167
10	Nehalpora	25.00	30.72	2.18	16.79	0.09	0.65	0.61	1.06	1.73	172
11	Cheksari	113.33	99.18	2.74	19.14	0.02	0.20	0.77	1.21	2.18	129
12	Chek palhallan	102.50	46.57	2.38	25.68	0.02	0.59	0.67	1.62	2.42	158
13	palhallan	44.72	31.86	2.21	9.85	0.05	0.33	0.62	0.62	1.31	163
14	Umer colony Noorbag	56.11	38.73	3.60	17.04	0.07	0.51	1.01	1.07	2.17	141
15	Ussan	73.61	58.99	4.26	15.09	0.07	0.26	1.19	0.95	2.27	128
16	Palpora	72.22	65.69	2.79	17.35	0.04	0.28	0.78	1.09	2.01	123
17	Wanigam bala	26.39	69.44	2.08	23.86	0.08	0.36	0.58	1.50	2.19	163
18	Tilgam	40.28	75.16	3.30	13.30	0.08	0.18	0.93	0.84	1.88	124
19	Khaipora	95.83	97.55	3.47	29.17	0.04	0.30	0.97	1.84	3.00	167
20	Hari watnoo	14.72	60.29	2.83	14.57	0.21	0.27	0.79	0.92	1.80	179
21	Wagoora	30.56	129.90	4.42	20.83	0.16	0.16	1.24	1.31	2.73	138
22	Hamray	98.89	95.42	3.34	15.90	0.03	0.17	0.94	1.00	2.13	149
23	Khambyar	72.22	113.40	4.56	23.73	0.07	0.21	1.28	1.50	2.97	155
24	Andergam	40.28	107.19	4.50	20.62	0.13	0.20	1.26	1.30	2.72	146
25	Lolipora	70.56	76.47	3.39	36.17	0.05	0.61	0.95	2.28	3.38	127
26	Magraypora	121.11	84.97	6.57	20.03	0.20	0.24	1.84	1.26	3.30	121
27	Margipora	30.56	18.63	1.59	15.74	0.06	1.29	0.45	0.99	1.49	117
28	Sheerbugh	46.39	10.29	1.65	21.36	0.04	4.11	0.46	1.35	1.86	139
29	Sultanpora	93.61	140.85	5.35	21.82	0.06	0.16	1.50	1.38	3.12	137
30	Goushbugh	98.89	108.99	4.51	32.19	0.06	0.30	1.26	2.03	3.50	131
31	Wanigam payeen	98.06	171.57	7.15	22.84	0.25	0.15	2.01	1.44	3.73	109
32	Ghat gopalun	65.00	78.43	3.61	49.51	0.06	0.63	1.01	3.12	4.28	116
33	Boniyar uri	18.61	33.82	1.49	9.14	0.09	0.28	0.42	0.58	1.05	174
34	Sheri bla	57.78	79.41	2.67	17.16	0.05	0.23	0.75	1.08	1.97	165
35	Janbazpora bla	57.22	77.78	2.54	40.28	0.04	0.53	0.71	2.54	3.39	152
36	Tapper	106.94	139.38	4.19	20.15	0.04	0.15	1.17	1.27	2.69	139
37	Sopore	69.17	141.83	4.31	30.31	0.07	0.20	1.21	1.91	3.34	153
38	Watergam kreeri	80.83	149.51	3.84	42.25	0.05	0.28	1.08	2.66	3.98	149
39	kohlina	76.94	56.70	2.13	21.82	0.03	0.37	0.60	1.38	2.10	206
40	Nambalnar	72.50	71.08	2.80	34.97	0.04	0.48	0.79	2.21	3.13	192
41	Show sopore	156.67	124.02	5.23	34.04	0.12	0.27	1.47	2.15	3.88	153
42	Singhpora	50.56	86.93	2.94	56.54	0.06	0.65	0.82	3.57	4.53	136
43	Rafiabad	104.17	148.37	4.35	43.15	0.04	0.29	1.22	2.72	4.20	187
44	Saidpora uri	55.28	46.73	2.20	15.15	0.04	0.29	0.62	0.96	1.67	162
45	Delina bla	76.39	140.52	3.64	29.94	0.05	0.21	1.02	1.89	3.14	128

46	Aglar	91.11	98.86	3.70	24.88	0.07	0.29	1.04	1.57	2.79	152
47	Chandil wanigam	12.78	13.89	0.61	11.45	0.19	0.85	0.17	0.72	0.92	213
48	Hygam	26.94	39.38	1.33	21.11	0.05	0.56	0.37	1.33	1.77	137
49	Panzalla rafiabad	80.56	97.55	5.27	36.17	0.14	0.41	1.48	2.28	3.94	197
50	Tengpora	22.22	24.51	1.09	29.41	0.05	1.41	0.31	1.86	2.21	171

Table 7.2 (a) Descriptive statistical evaluation of radon, thoron, and their progeny concentrations during winter and summer seasons

			Winter						Summer			
	Rn220	**Rn222**	**EETC**	**EERC**	**Ft**	**Fr**	**Rn220**	**Rn222**	**EETC**	**EERC**	**Ft**	**Fr**
Average	76.20	96.95	3.12	27.52	0.06	0.34	71.55	75.31	3.37	22.88	0.07	0.50
Std. Dev.	55.34	44.91	1.47	14.37	0.05	0.21	39.73	43.32	1.46	9.22	0.08	0.70
Min	10.83	19.61	0.22	10.65	0.01	0.10	1.67	4.41	0.85	7.13	0.02	0.12
Max	317.50	228.43	7.40	69.17	0.30	1.00	250.00	194.12	7.12	46.94	0.51	4.87
Kurtosis	6.19	0.17	0.88	1.07	8.00	1.66	6.98	-0.35	0.02	0.50	22.08	30.57
Skewness	1.95	0.57	0.56	1.27	2.51	1.32	1.77	0.42	0.52	0.79	4.35	4.98

Table 7.2 (b) Statistical analysis of (AED), (Rn), (Tn), and their progeny concentrations for the annual and rainy seasons

|		Rainy						Annual Concentration					Annual Dose (μSv/y)	
	Rn222	EETC	EERC	Ft	Fr	Rn220	Rn222	EETC	EERC	Ft	Fr	AEDT	AEDR	**AID**
Average	66.93	3.28	23.57	0.09	0.59	67.35	79.73	3.26	24.65	0.07	0.48	0.91	1.56	2.61
Std. Dev.	35.79	1.40	10.60	0.10	0.93	30.01	39.73	1.34	10.06	0.05	0.58	0.38	0.63	0.86
Min	3.43	0.77	2.22	0.01	0.06	12.78	10.29	0.61	9.14	0.01	0.15	0.17	0.58	0.92
Max	138.73	6.94	53.52	0.64	6.61	156.67	171.57	7.15	56.54	0.25	4.11	2.01	3.57	4.53
Kurtosis	-0.78	0.27	1.30	18.05	35.37	0.29	-0.63	0.62	1.08	3.44	30.78	0.62	1.08	-0.59
Skewness	0.20	0.51	0.89	3.75	5.44	0.28	0.26	0.52	1.00	1.90	4.97	0.52	1.00	0.26

Table 7.3: Statistical analysis of annual radon, thoron and progeny variations across different types of dwellings

Annual Concentration (Mud-19 Samples)						
Parameters	**Rn220**	**Rn222**	**EETC**	**EERC**	**Ft**	**Fr**
Average	74.30	92.52	3.71	28.79	0.08	0.59
Std. Dev.	32.32	43.70	1.57	12.02	0.06	0.87
Min	18.61	10.29	1.49	9.14	0.03	0.15
Max	156.67	171.57	7.15	56.54	0.25	4.11
Kurtosis	0.80	-0.59	-0.23	-0.05	3.87	15.03
Skewness	0.66	-0.12	0.54	0.68	2.05	3.75
Annual Concentration (Cement-23 Samples)						
Parameters	**Rn220**	**Rn222**	**EETC**	**EERC**	**Ft**	**Fr**
Average	64.63	70.39	3.05	20.63	0.06	0.36
Std. Dev.	25.65	28.23	0.85	5.97	0.04	0.18
Min	14.72	23.37	0.97	9.85	0.01	0.16
Max	113.33	129.90	4.56	32.07	0.21	0.84
Kurtosis	-0.54	-0.83	0.24	-0.86	5.80	0.20
Skewness	-0.14	0.21	-0.14	0.29	2.21	0.91
Annual Concentration (Wood-08 Samples)						
Parameters	**Rn220**	**Rn222**	**EETC**	**EERC**	**Ft**	**Fr**
Average	58.68	76.23	2.78	26.41	0.08	0.54
Std. Dev.	32.34	48.85	1.59	9.86	0.05	0.38
Min	12.78	13.89	0.61	11.45	0.04	0.21
Max	104.17	148.37	5.27	43.15	0.19	1.41
Kurtosis	-1.80	-1.70	-1.59	-0.60	1.35	2.66
Skewness	-0.15	0.28	0.11	0.13	1.57	1.71

7.3.1 Annual Indoor Radon and Thoron Concentrations

Figure 7.1 illustrates annual indoor concentrations of radon and thoron across 50 dwellings, highlighting significant spatial variability. Radon peaks in dwellings 11, 24, 32, 39, and 41, likely influenced by poor ventilation, subsoil characteristics, and construction materials, while the lowest levels are noted in dwellings 26 and 50. Thoron concentrations show greater fluctuation, with sharp increases in dwellings 11, 24, and 41. The absence of a direct correlation

between radon and thoron reflects their distinct physical behaviors radon's longer half-life enables uniform indoor dispersion, whereas thoron's short half-life limits its distribution, resulting in localized concentration patterns.
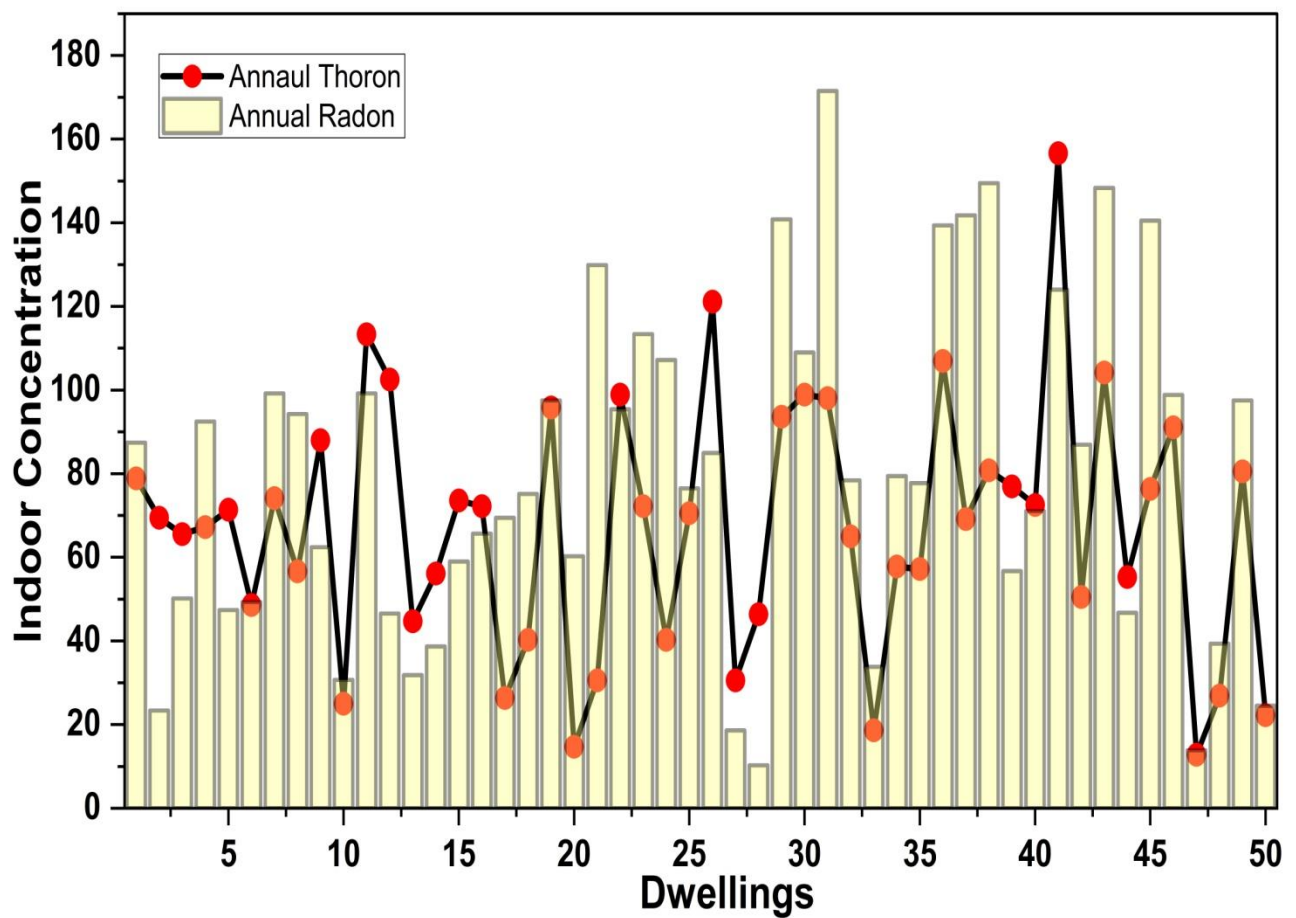
Figure 7.1: Spatial distribution of indoor radon and thoron concentrations

7.3.2 Equilibrum Factor F_r and F_t Analysis

The thoron equilibrium factor (Ft) exhibits considerable variability across the surveyed dwellings, particularly in dwellings 20 and 35. This fluctuation may be attributed to differences in surface emissions, ventilation efficiency, and indoor air mixing. In contrast, the radon equilibrium factor (Fr) appears more consistent and generally remains lower than Ft. Notably, dwellings 28 and 30 display unusually high Fr values that are likely unrealistic under normal indoor conditions, suggesting the presence of outliers or possible measurement anomalies. Continuous monitoring of both equilibrium factors is crucial for precise dose assessment, as the variability of Ft often exceeding expected levels emphasizes the need for dwelling-specific evaluation.
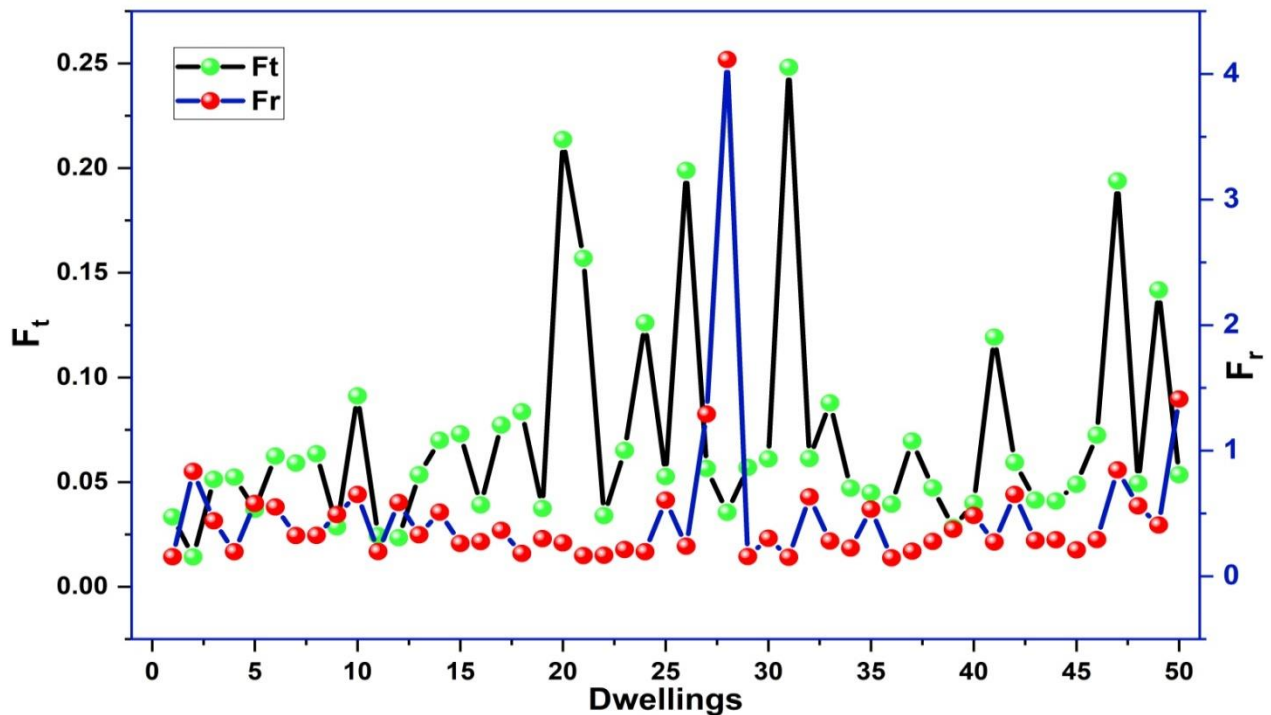
Figure 7.2: variation of radon, thoron equilibrium factors across dwellings

7.3.3 EETC and EERC Variations

EETC and EERC exhibit notable fluctuations across the surveyed dwellings, without following a consistent or parallel pattern. For instance, dwelling 31 records the highest EETC, around 7 Bq/m³ (highlighted by a green square), while dwelling 42 shows the highest EERC, approximately 60 Bq/m³ (marked with a blue triangle). This lack of correlation indicates that radon and thoron may originate from distinct sources or behave differently indoors, influenced by varying environmental or structural conditions. These concentrations are critical inputs in dose assessment models, where elevated values correspond to a greater risk of radiation exposure for the occupants.
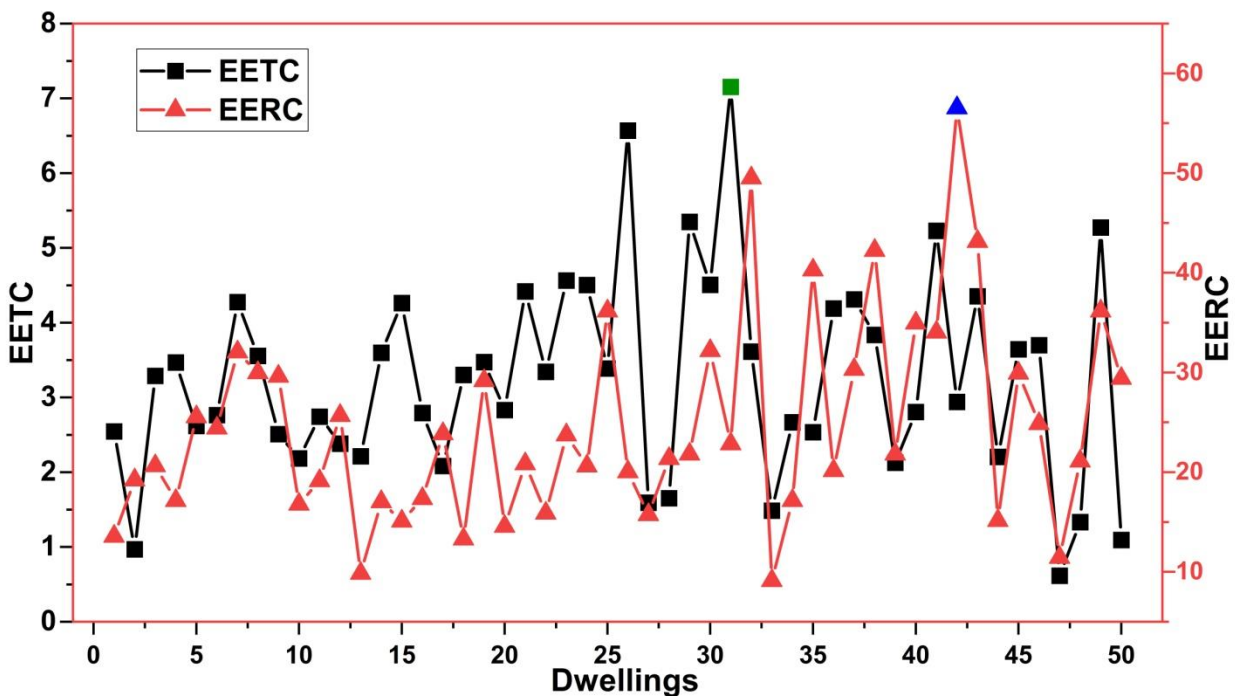
Figure 7.3: Distribution of equilibrium equivalent thoron (EETC) and radon (EERC) concentrations across dwellings

7.3.4 Q-Q Plots and Seasonal Variations

Summer

Radon (Rn-222) concentrations generally follow a normal distribution with a slight positive skew due to a few high-value outliers. Thoron (Rn-220) shows near-normal distribution but with some tail deviations and a peaked (leptokurtic) pattern, likely influenced by material differences. The radon progeny (EERC) displays a strong normal distribution, indicating stable equilibrium conditions. Thoron progeny (EETC) shows mild skewness and upper-tail deviations, possibly from localized thoron emissions. Overall, data mostly conform to normality, with small deviations linked to environmental and structural factors.
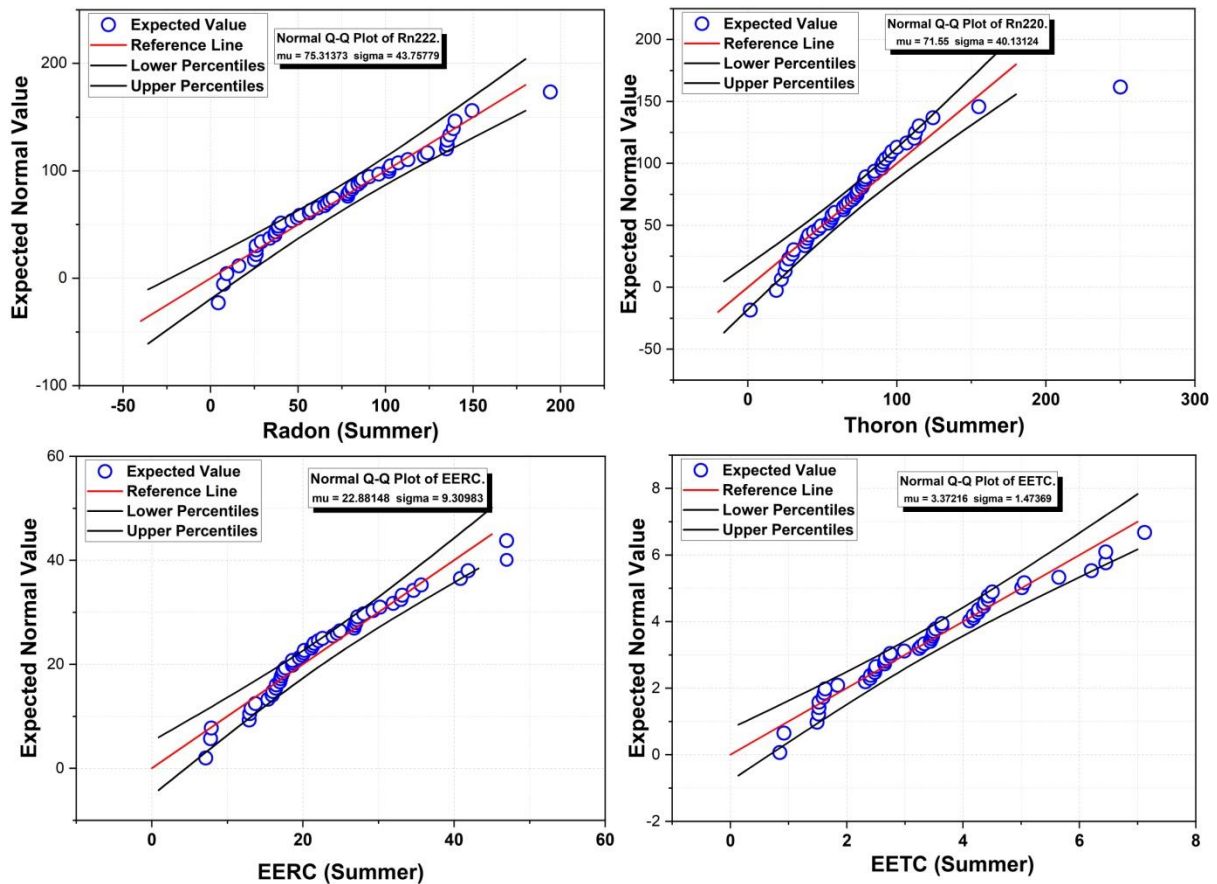

Figure 7.4: Q-Q plot Radon, Thoron and effective equiliubrum concentration in summer

Rainy

Radon levels continue to approximate a normal distribution with minor tail deviations, reflecting occasional high radon spikes likely caused by increased soil moisture and humidity enhancing radon entry. EERC remains consistently normal with slight upper-tail irregularities, showing stable radon decay processes. All datasets largely maintain normality, with EERC and EETC fitting best, while radon and thoron show some skewness but remain statistically valid for analysis.
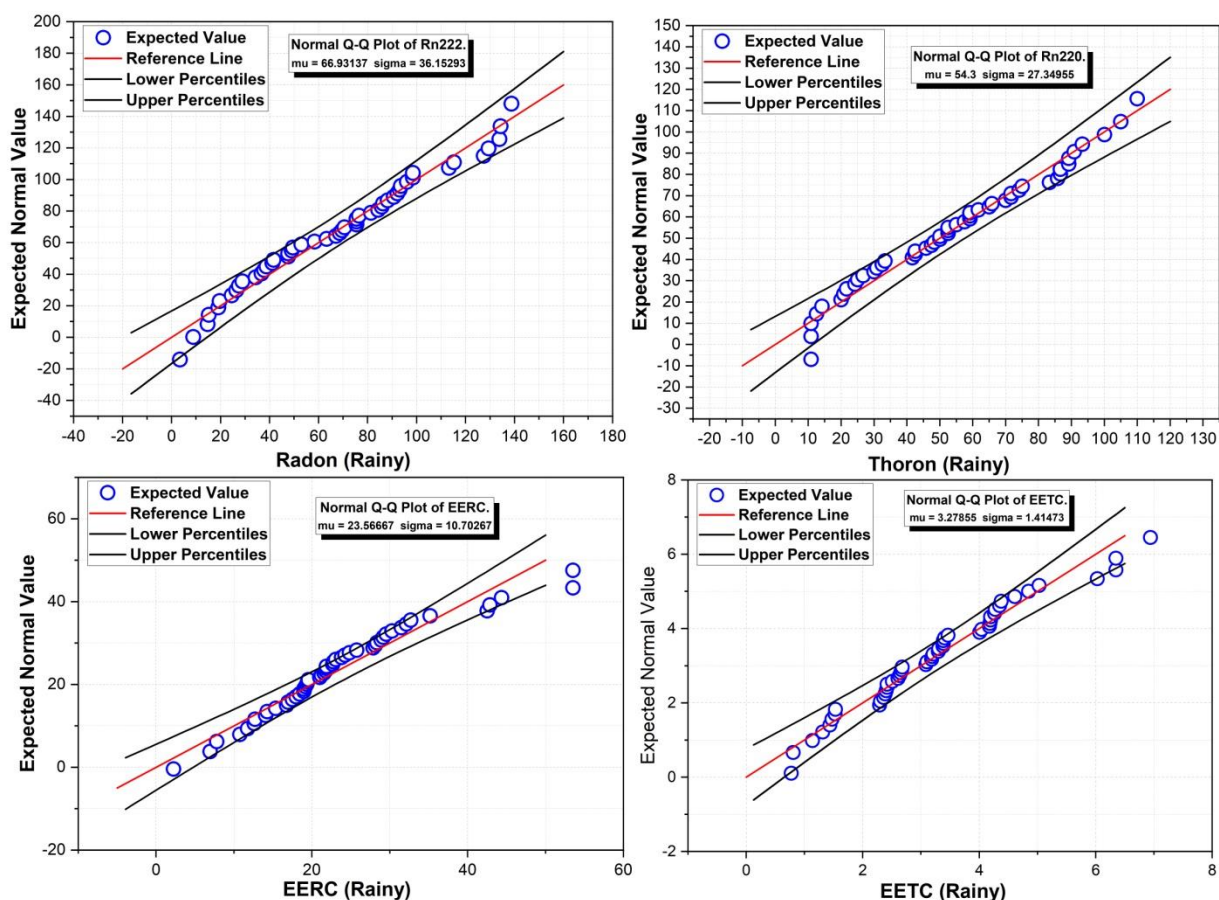
Figure 7.5: Q-Q Plot variation of radon, thoron concentrations in Rainy season

Winter

Radon and EETC data closely follow normal distribution, suitable for statistical evaluation. Thoron data diverges more due to prominent high-value outliers, potentially from localized

sources or limited ventilation. EETC stays stable and normally distributed, indicating consistent thoron progeny behavior indoors. The highest average concentrations across all variables occur in winter, reflecting greater indoor accumulation driven by reduced ventilation and increased occupancy typical of this season.
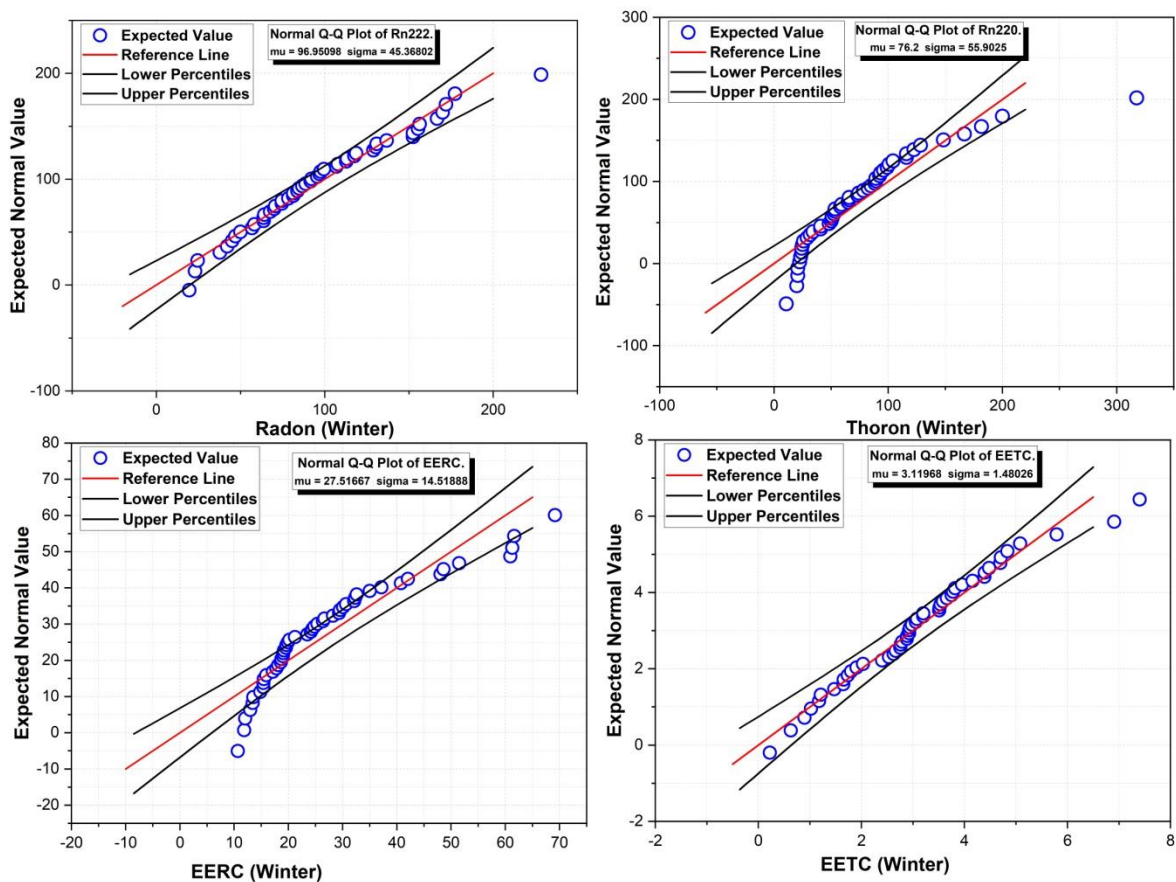
Figure 7.6: Q-Q plot variation of radon ,thoron concentrations in winter

7.3.5 AEDT, AEDR, AID

The figure 7.5 contains two sub plots providing histograms with fitted distribution curves representing (Annual Effective Dose due to thoron), (Annual Effective Dose due to Radon) and (Annual Inhalation Dose). Most dwellings receive a higher dose from radon than thoron, implies in most of the houses radon contributes more significantly to the effective dose than thoron.

The AID integrates the contribution from both radon and thoron progeny inhalation, with symmetrical bell shaped curve suggesting a central tendency in the population, which indicates most individuals receive moderate inhalation dose, with few outliers on both extremes.
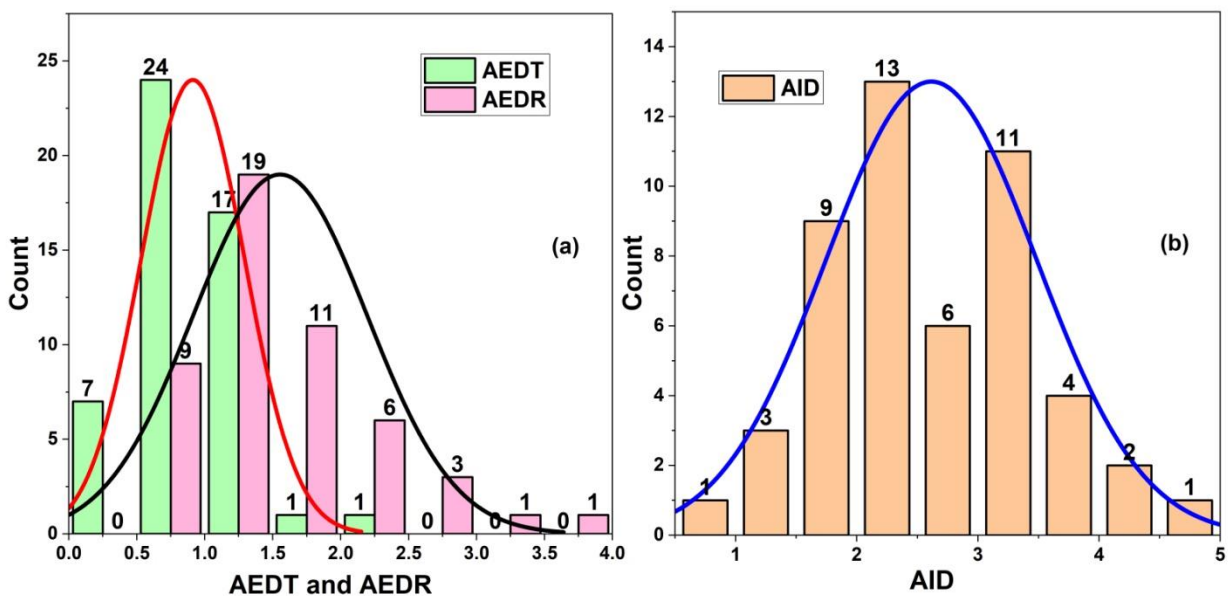
Figure 7.7: Histogram showing the distribution of (AEDR), (AEDT), and the total (AID)

7.4 Conclusion

In this study, passive techniques were employed to measure the annual indoor concentrations of ^{222}Rn and ^{220}Rn, which averaged 79.73 ± 39.73Bq/m³ and 67.35 ± 30.01Bq/m³, respectively both falling within the WHO's reference limit of 100Bq/m³. Equilibrium effective thoron and radon concentrations were found to be 3.26 ± 1.34Bq/m³ and 24.65 ± 10.06Bq/m³. Resulting annual inhalation doses from these radio nuclides were also found to be well within the safety limits as suggested by UNSCEAR and the ICRP. Statistical analysis revealed that the distributions of ^{222}Rn and its Effective Equilibrium Radon Concentration (EERC) were non-normal. Seasonal evaluations of equilibrium factors showed that ^{222}Rn had values of 0.59 (rainy), 0.50 (winter), and 0.34 (summer), closely aligning with the global reference of 0.40. In contrast, ^{220}Rn displayed higher-than-recommended equilibrium factors of 0.09 (rainy) and 0.07 (winter), and 0.06 (summer), exceeding the internationally accepted value of 0.02.

References

- Ahamad, T., Nautiyal, O. P., Joshi, M., Singh, P., Sajwan, R. S., Rana, A. S., & Bourai, A. A. (2024). Measurement of indoor radioactivity and dose derived from 222Rn, 220Rn and EECs by using SSNTD based technique. *Radiation Protection Dosimetry*, *200*(11–12), 1011–1017. https://doi.org/10.1093/rpd/ncad321

- Al-Zoughool, M., & Krewski, D. (2009). Health effects of radon: A review of the literature. *International Journal of Radiation Biology*, *85*(1), 57–69. https://doi.org/10.1080/09553000802635054

- Bersimbaev, R.I., Bulgakova, O., 2015. The health effects of radon and uranium on the population of Kazakhstan. Gene Environ. 37, 18. https://doi.org/10.1186/s41021- 015-0019-3

- Blomberg, A.J., Coull, B.A., Jhun, I., Vieira, C.L., Zanobetti, A., Garshick, E., Schwartz, J., Koutrakis, P., 2019. Effect modification of ambient particle mortality by radon: a time series analysis in 108 US cities. J. Air Waste Manag. Assoc. 69, 266–276.

- Bruno, R. C. (1983). Sources of indoor radon in houses: A review. *Journal of the Air Pollution Control Association*, *33*(2), 105–109. https://doi.org/10.1080/00022470.1983.10465550

- Darby, S., Hill, D., Deo, H., Auvinen, A., Barros-Dios, J.M., Baysson, H., Bochicchio, F., Falk, R., Farchi, S., Figueiras, A., 2006. Residential radon and lung cancer—detailed results of a collaborative analysis of individual data on 7148 persons with lung cancer and 14 208 persons without lung cancer from 13 epidemiologic studies in Europe. Scand. J. Work. Environ. Health 1–84.

- Kang, J.-K., Seo, S., Jin, Y.W., 2019. Health effects of radon exposure. Yonsei Med. J. 60, 597–603. https://doi.org/10.3349/ymj.2019.60.7.597.

- Kreft, O. (2017). Autoclaved aerated concrete with sulphate content: an environmentally friendly, durable and recyclable building material. *Mauerwerk*, *21*(5), 287–296. https://doi.org/10.1002/dama.201700012

- Kozak, K., Mazur, J., KozŁowska, B., Karpińska, M., Przylibski, T. A., Mamont-Cieśla, K., Grzązdziel, D., Stawarz, O., Wysocka, M., Dorda, J., Żebrowski, A., Olszewski, J., Hovhannisyan, H., Dohojda, M., KapaŁa, J., Chmielewska, I., KŁos, B., Jankowski, J.,

Mnich, S., & Kołodziej, R. (2011). Correction factors for determination of annual average radon concentration in dwellings of Poland resulting from seasonal variability of indoor radon. *Applied Radiation and Isotopes*, *69*(10), 1459–1465. https://doi.org/10.1016/j.apradiso.2011.05.018

- Mittal, S., Rani, A., & Mehra, R. (2016). Estimation of radon concentration in soil and groundwater samples of Northern Rajasthan, India. *Journal of Radiation Research and Applied Sciences*, *9*(2), 125–130. https://doi.org/10.1016/j.jrras.2015.10.006

- Mishra, R., & Mayya, Y. S. (2008). Study of a deposition-based direct thoron progeny sensor (DTPS) technique for estimating equilibrium equivalent thoron concentration (EETC) in indoor environment. *Radiation Measurements*, *43*(8), 1408–1416. https://doi.org/10.1016/j.radmeas.2008.03.002

- Mishra, R., Prajith, R., Sapra, B. K., & Mayya, Y. S. (2010). Response of direct thoron progeny sensors (DTPS) to various aerosol concentrations and ventilation rates. *Nuclear Instruments and Methods in Physics Research Section B: Beam Interactions with Materials and Atoms*, *268*(6), 671–675. https://doi.org/10.1016/j.nimb.2009.12.012

- Nazaroff, W. (1988). Soil as a Source of Indoor Radon: Generation, Migration, and Entry. *Radon and Its Decay Products in Indoor Air*, 92-94

- Prasad, M., Rawat, M., Dangwal, A., Yadav, M., Gusain, G. S., Mishra, R., & Ramola, R. C. (2015). Measurements of radon and thoron progeny concentrations in dwellings of Tehri Garhwal, India, using LR-115 deposition-based DTPS/DRPS technique. *Radiation Protection Dosimetry*, *167*(1–3), 102–106. https://doi.org/10.1093/rpd/ncv224

- Prasad, M., Rawat, M., Dangwal, A., Kandari, T., Gusain, G. S., Mishra, R., & Ramola, R. C. (2016). Variability of radon and thoron equilibrium factors in indoor environment of Garhwal Himalaya. *Journal of Environmental Radioactivity*, *151*, 238–243. https://doi.org/10.1016/j.jenvrad.2015.10.017

- Ramola, R. C., Prasad, M., Kandari, T., Pant, P., Bossew, P., Mishra, R., & Tokonami, S. (2016). Dose estimation derived from the exposure to radon, thoron and their progeny in the indoor environment. *Scientific Reports*, *6*, 1–16. https://doi.org/10.1038/srep31061

- Rathebe, P.C., Mphaga, K.V., Masekameni, D.M., 2025. Climate change and environmental radioactivity: a review of studies on climate conditions in variation on indoor radon concentrations. Environ. Monit. Assess. 197, 446.

https://doi.org/10.1007/s10661-025-13889-8

- Ruano-Ravina, A., Dacosta-Urbieta, A., Barros-Dios, J.M., Kelsey, K.T., 2018. Radon exposure and tumors of the central nervous system. Gac. Sanit. 32, 567–575. https://doi.org/10.1016/j.gaceta.2017.01.002.

- Selinus, O., Alloway, B., Centeno, J. A., Finkelman, R. B., Fuge, R., Lindh, U., & Smedley, P. (2013). Essentials of medical geology: Revised edition. In *Essentials of Medical Geology: Revised Edition* (Issue iii). https://doi.org/10.1007/978-94-007-4375-5

- Srisuwan, T. (2025). Accumulation of Radon Gas in Shophouses: Case Study of Using Concrete with Fly Ash and Phosphogypsum Additives as Building Materials. *International Journal of Building, Urban, Interior and Landscape Technology*, *23*(1), 256808. https://doi.org/10.56261/built.v23.256808

- Thabayneh, K.M., 2015. Measurement of (222)Rn concentration levels in drinking water and the associated health effects in the Southern part of West Bank - Palestine. Appl. Radiat. Isot. 103, 48–53. https://doi.org/10.1016/j.apradiso.2015.05.007.

- Tokonami, S. (2010). Why is 220Rn (thoron) measurement important? *Radiation Protection Dosimetry*, *141*(4), 335–339. https://doi.org/10.1093/rpd/ncq246

- United Nations Scientific Committee on the Effects of Atomic Radiation (2000). *Sources and effects of ionizing radiation: Annex B—Exposures from natural radiation sources* (Vol. I, pp. 104).

CHAPTER 8

ASSESSMENT OF EXHALATION RATE AND NATURAL RADIOACTIVITY IN (BUDGAM), CENTRAL KASHMIR

8.1 Natural Radioactivity in Various Geological Substrates

The distribution of radioactive elements like uranium (U) and thorium (Th) is influenced by geological, chemical, and physical factors, which in turn determine the prevalence of radioactivity in the environment. Over millions of years, these persistent radio nuclides were absorbed by various minerals and rock formations and embedded in the Earth's crust. Their decay affects terrestrial, aquatic, and atmospheric environments by adding to natural background radiation levels. The properties of different geological substrates, such as igneous, metamorphic, and sedimentary rocks, as well as phosphorites and water bodies, determine how these radio nuclides are distributed (Fudali, 1965).

Environmental factors and geological processes are closely related to the distribution of natural radioactivity. Background radiation levels are constantly affected by U, Th and their daughter products, which are embedded in various types of rocks, sediments, and aquifer bodies. While sedimentary rocks like sandstones and shales act as accumulation sites because of their capacity to chemically trap uranium and thorium, igneous and metamorphic rocks are the main sources of these elements. Because they weather and discharge radio nuclides into groundwater, marine phosphorites also aid in uranium enrichment. The distribution of radio nuclides all over ecosystems is further influenced by water systems, which serve as organic carriers of radioactive elements. Evaluating environmental radiation exposure and possible health risks related to naturally occurring radioactivity requires an understanding of these processes (Johnson, 1973).

A major reservoir of natural radioactivity is found in igneous and metamorphic rocks. These rocks, which were formed under high pressure and high temperature, often contain uranium and thorium, which are incompatible with most mineral structures and have a tendency

to accumulate in particular kinds of rocks. Igneous rocks that are silica-rich, especially granites, have high levels of uranium and thorium, which may occasionally exceed 30 mg/kg of uranium. Radio nuclides are gradually released from these crystalline rocks into the environment due to weathering and erosion. The constant release of ionizing radiation from the natural radioactive decay of uranium, thorium, and potassium raises background radiation levels, particularly in areas that have elevated granite sources (Bondietti & Francis, 1979; Fadol et al., 2024).

Another significant source of natural radioactivity is sedimentary rocks, where uranium can change chemically, affecting its concentration and mobility. The potential of coal seams and organic-rich shales to hold onto uranium is especially notable. By acting as chemical traps, these formations stop uranium from dispersing and produce high concentrations in specific areas. Likewise, uranium enrichment takes place in sandstone deposits, particularly at redox boundaries where uranium precipitates and builds up to form economically important uranium ore bodies (Carroll & Lerche, 2003).Since carbonate rocks such as dolomites and lime stones also contain uranium in their mineral structures, they are useful for uranium-series dating, which defines the chronology of geological events. Additionally, by releasing radon gas (^{222}Rn) into the atmosphere, residual soils like terra rossa soils created by extra weathering processes also contribute to natural radioactivity. These soils' high radon emissions demonstrate how weathering contributes to the natural radionuclide redistribution process (Burnett et al., 1988).

Phosphorites, which are rocks that are rich in phosphate, are another essential geological source of uranium. While phosphorites are generally found in marine environments, they have relatively low thorium content (often less than 5 mg/kg) and uranium concentrations of up to 100 mg/kg. Most of the uranium in these deposits is attached to apatite minerals, which weather and release radio nuclides gradually. Regions like Florida, where elevated levels of radium-226 (^{226}Ra) in groundwater created health concerns, reveal the environmental importance of phosphorites. Radium, a byproduct of uranium decay, can enter drinking water sources and is soluble under certain geochemical conditions, raising the risk of radiation exposure. In the geochemical cycling of radioactive elements, this points out the function of phosphate deposits (Kolodny & Kaplan, 1970).

Radioactive elements are carried and redistributed in large part by water bodies, such as rivers, lakes, and oceans. Depending on the local geology and chemistry, these environments have varying levels of uranium and its daughter products. The concentrations of uranium in rivers are usually between 0.000083 and 0.0048Bq/L, whereas the concentrations in ocean water are around 0.041Bq/L. Some radio nuclides, like radium (Ra), which desorbs from river sediments when it enters saline environments, are affected by the mixing of fresh and saltwater, which raises the overall radioactivity of marine waters. Lead (Pb), polonium (Po), thorium (Th), and other radio nuclides easily attach to suspended particles in water before settling in marine sediments, where they raise long-term environmental radiation levels. Localized areas of high radon concentration can result from the diffusion of radon gas (Rn), which is highly soluble in water, from sediments into groundwater. When used for drinking purpose, groundwater radon levels in some areas can surpass 35,000 Bq/L, which presents a serious inhalation risk (Dinh Chau et al., 2011).

8.2 Radon Exhalation and Mobility

The exhalation rate, or flux density, of radioactive gases, particularly radon and thoron, determines their escape into the atmosphere. Moisture content in soil significantly impacts radon exhalation, influencing its diffusion dynamics. At low to moderate moisture levels, radon efficiently diffuses through air-filled pores, increasing its concentration as air and water equilibrate. However, at high moisture levels, water-filled pores limit radon movement, reducing diffusion and presence in soil air. This shift in diffusion mechanisms underscores the critical role of moisture in radon mobility and exhalation efficiency (Meslin et al., 2011).Factors such as grain size, permeability, moisture content, and recoil efficiency also affect radon exhalation rates. Larger grains limit radon release due to their narrow recoil range (~0.07 μm), while smaller grains enhance emanation due to their higher surface-area-to-volume ratio. Moderate moisture levels facilitate radon diffusion through air-filled pores, whereas higher moisture levels saturate voids, trapping radon and reducing exhalation. Permeability further dictates radon transport; highly permeable soils permit movement, whereas compacted or water-saturated sediments inhibit it. These interdependencies highlight the necessity of precise soil property characterization in radon risk assessments (Shweikani et al., 1995).

Soil moisture content governs pore space availability and diffusion pathways, significantly affecting radon and thoron exhalation rates. Exhalation rates increase at low moisture levels (below 6–8%) due to enhanced transport through air-filled pores. However, above 8% moisture content, water saturation begins to block diffusion pathways, reducing exhalation rates to nearly one-fifth of their initial levels. Comparative analysis reveals that thoron diffusion closely follows predicted values, whereas radon exhalation is lower than theoretical estimates (~25%), emphasizing the need for continuous soil condition monitoring (Hosoda et al., 2007).Radon permeability and exhalation in building materials depend more on structural properties such as porosity and surface configuration than on radionuclide content alone. Highly porous materials with lower radionuclide content release more radon due to increased permeability, whereas materials with a closed surface, such as slag and fly ash-mixed stones, exhibit lower exhalation despite potentially higher radionuclide levels. Effective barriers against radon infiltration include thick plastic coatings (>2 mm), whereas thinner coatings like paint and wallpaper permit radon diffusion. Experimental mitigation techniques such as polymer bitumen, polyurethane coatings, and plastic foils have demonstrated long-term radon reduction, emphasizing the importance of material selection, processing, and consolidation. Environmental variables such as temperature, material aging, and pressure difference further influence permeability over time (Keller et al., 2001).

8.3 Geological and Structural Factors in Radon Mobility

In various soil and rock types, uranium mobility is influenced by its distribution, mineral composition, grain size, and permeability, all of which affect radon emanation. The release of radon from uranium-rich sources is more dependent on host material characteristics than on absolute uranium concentration. For instance, sandy soils, despite their higher uranium levels, exhibit lower radon exhalation due to coarse grains and reduced radium availability, whereas fine-grained clay-rich soils enhance radon diffusion and recoil efficiency. Similarly, compacted structures like alum shale restrict radon escape despite their uranium richness. Depth variations also play a role, with radon concentrations exceeding 100 kBq/m³ at 1 meter, particularly in clay-dominated environments, underscoring the importance of geological composition in radon mobility assessments (Baixeras et al., 2001).

8.4 Methodology

Study Area
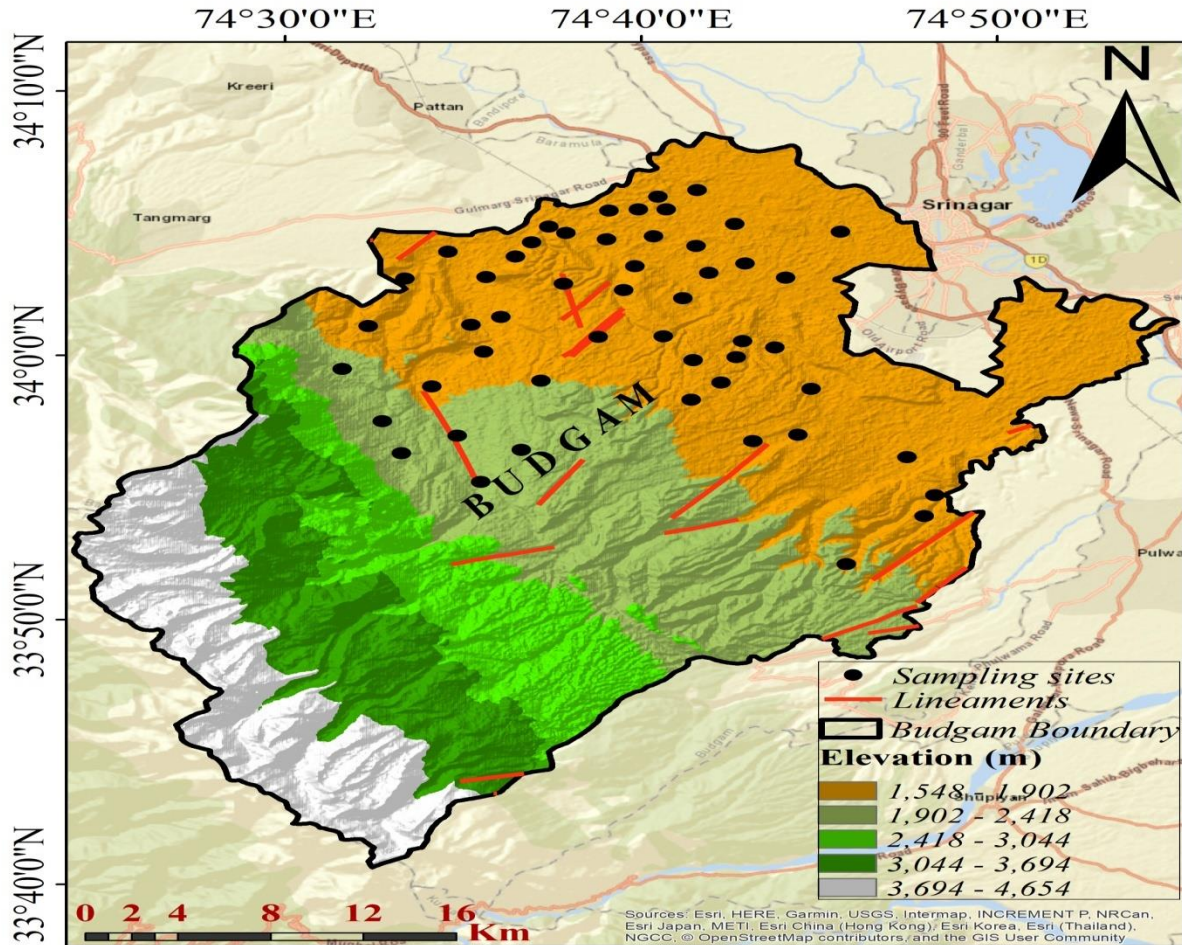
Figure 8.1: Sampling map of Budgam

This study uses two advanced experimental methodologies to quantify the activity concentrations of natural radio nuclides (Ra, Th, K) and the soil gas emissions from ^{222}Rn and ^{220}Rn. Natural radioactivity levels were assessed gamma spectrometry, while radon and thoron exhalation rates were measured with the Smart Radon RnDuo monitor operated in both diffusion and flow modes. Linear regression analyses were conducted using ORIGIN software to support data

interpretation. A comprehensive account of these procedures is detailed in Sections 3.3 and 3.9 of Chapter 3.

In contrast to passive approaches, these active, in-situ monitoring techniques provide improved accuracy and reliability in radiological assessments. The experimental phase of the study was conducted in collaboration with the National Institute of Technology (NIT) Jalandhar and the University of Kashmir, where access to advanced instrumentation and laboratory facilities facilitated the successful execution of the research objectives.

8.5 Exhalation Rate (J_m, J_s) Analysis

Radon and thoron exhalation rates were evaluated through standard computational models. The radon concentration inside the enclosed chamber at a specific time t is represented by the following expression

$$C(t) = \left(\frac{MJm}{\rho}\right)t + Co \qquad (8.1)$$

Where, J_m denotes the mass exhalation rate of radon from the soil sample, measured in $mBqkg^{-1}h^{-1}$, ρ corresponds to the effective volume of the detection chamber, expressed in cubic meters (m³), while C_0 indicates the initial radon concentration, generally considered negligible at the beginning of the monitoring process. For thoron flux (J_s) is determined using the relation

$$Js = C(t)\rho\lambda/A \qquad (8.2)$$

Where C(t) is the thoron concentration at time t, λ is the decay constant of thoron and A is the surface area (in m²) of the enclosed detection chamber with soil. This model allows for the estimation of thoron emission based on chamber geometry and decay kinetics (Semwal et al., 2017; Kumar et al., 2024).

8.6 Gamma Spectrometric Assessment of Ra, Th, and K Activity and Related Radiological Parameters

NaI-Tl based detector was used to quantitatively determine the 226Ra, 232Th, and 40K activity in all the soil samples. These measured values were subsequently used to derive several radiological hazard parameters through standardized computational formulas.

Radium Equivalent Activity and Absorbed Dose Rate

To express the combined radiological effects of these radioactive elements in a single index, the radium equivalent activity is calculated using the following formula

$$Ra_{eq} = A\,Ra + 1.43A_{Th} + 0.077\,A_K \qquad\qquad 8.3$$

Where ARa, A_{Th} and A_K is the activity concentrations in (Bq/kg) of radium, thorium, and potassium, respectively. This equation is designed to maintain the absorbed dose rate within permissible limits as per international guidelines.

The outdoor absorbed dose rate in air at some height above surface level, due to gamma radiation from natural radio nuclides, was computed using

$$^{air}_{abs}D = 0.463^* A_{Ra} + 0.604^* A_T + 0.0417^* A_K \qquad\qquad 8.4$$

Where $^{air}_{abs}D$ (nGyh^{-1}) is the absorbed dose. This model reflects the conversion coefficients provided by UNSCEAR for estimating the dose from individual radio nuclides.

Hazard Indices (External and Internal)

To evaluate the potential radiological risks posed by materials containing natural radio nuclides, the external and internal hazard indices were determined. These indices are crucial for assessing the suitability of materials for construction purposes and potential inhalation risks from radioactive elements and should ideally remain below unity (1 mSv/y) to be considered radiologically safe for human occupancy (C V & Joseph., 2022).

$$H_{ex} = \frac{A_{Ra}}{370} + \frac{A_{Th}}{259} + \frac{A_K}{4180}$$ 8.5

$$H_{in} = \frac{A_{Ra}}{185} + \frac{A_{Th}}{259} + \frac{A_K}{4180}$$ 8.6

Here, both hazard indices ideally remain below unity (1 mSv/y) to be considered radiologically safe for human occupancy.

Gamma Index

The gamma activity concentration index I_r provides a screening tool for identifying materials with elevated levels of gamma-emitting radio nuclides and serves as a preliminary measure for indoor gamma dose assessments.

$$I_r = \frac{AC\ (Ra)}{370} + \frac{AC\ (Th)}{259} + \frac{AC\ (K)}{4180}$$ 8.7

Annual Effective Dose Equivalent (AEDE)

To assess the potential radiation-related effects on human health gamma exposure, both indoor and outdoor annual effective dose equivalents were calculated. The conversion factor of 0.7 Sv·Gy^{-1}, along with occupancy factors of 20% for outdoor and 80% for indoor exposure, were used as per (Bangotra et al., 2016), the AEDE values were derived using the following equations.

$$AEDE_{OUTDOOR} = D(nGyh^{-1}) * 8760\ (h) * 0.2 * 0.7\ SvGy^{-1} * 10^{-3}$$ 8.8

$$AEDE_{INDOOR} = D(nGyh^{-1}) * 8760\ (h) * 0.8 * 0.7\ SvGy^{-1} * 10^{-3}$$ 8.9

These estimations provide a comprehensive understanding of the potential radiological risks experienced by individuals due to prolonged radiation exposure.

8.7 Results and Discussion

Table 8.1 Statistical analysis of natural radioactivity (Ra,Th, K), effective dose and hazard indices with exhalation rates

Parameters	Ra	±Error	Th	±Error	K	±Error	Ra Equ Activity concentration(Bq/kg)	D	AEDE outdoor (mSv)	AEDE indoor (mSv)	H ex	H In	Gamma Index IΥ	Js (Bq/m²s⁻¹)	±SE	Jm (mBqKg⁻¹h⁻¹)	±SE	Gamma (nsv/h)
Min	15.94	0.61	15.28	1.01	255.07	23.12	59.72	28.35	0.03	0.14	0.16	0.21	0.45	1.99	0.18	5.19	0.43	114.00
Max	32.71	6.45	42.22	3.32	450.32	56.65	122.38	56.51	0.07	0.28	0.33	0.42	0.89	6.47	0.40	62.03	3.43	183.00
Avg	22.37	2.71	28.68	1.70	334.20	37.27	89.14	41.63	0.05	0.20	0.24	0.30	0.66	3.86	0.32	27.76	1.25	143.76
SD	4.20	1.52	5.31	0.46	44.61	9.35	12.31	5.63	0.01	0.03	0.03	0.04	0.09	1.13	0.04	15.36	0.48	15.89
GM	21.99	2.34	28.18	1.65	331.33	36.11	88.30	41.25	0.05	0.20	0.24	0.30	0.65	3.71	0.31	23.19	1.17	142.89
Skewness	0.64	1.06	0.24	1.06	0.60	0.32	0.41	0.40	0.40	0.40	0.41	0.56	0.38	0.65	-0.32	0.55	1.62	0.16
Kurtosis	0.07	0.07	0.04	1.93	-0.15	-1.09	0.23	0.12	0.12	0.12	0.24	0.36	0.11	-0.25	0.84	-0.45	6.93	-0.40

8.7.1 Statistical Analysis

The observed spatial heterogeneity in exhalation rates and radionuclide concentrations likely reflects the influence of localized geological formations, including differences in mineral content, soil composition, and lithological substrates, statistical analysis including correlation and normality analyses was performed.
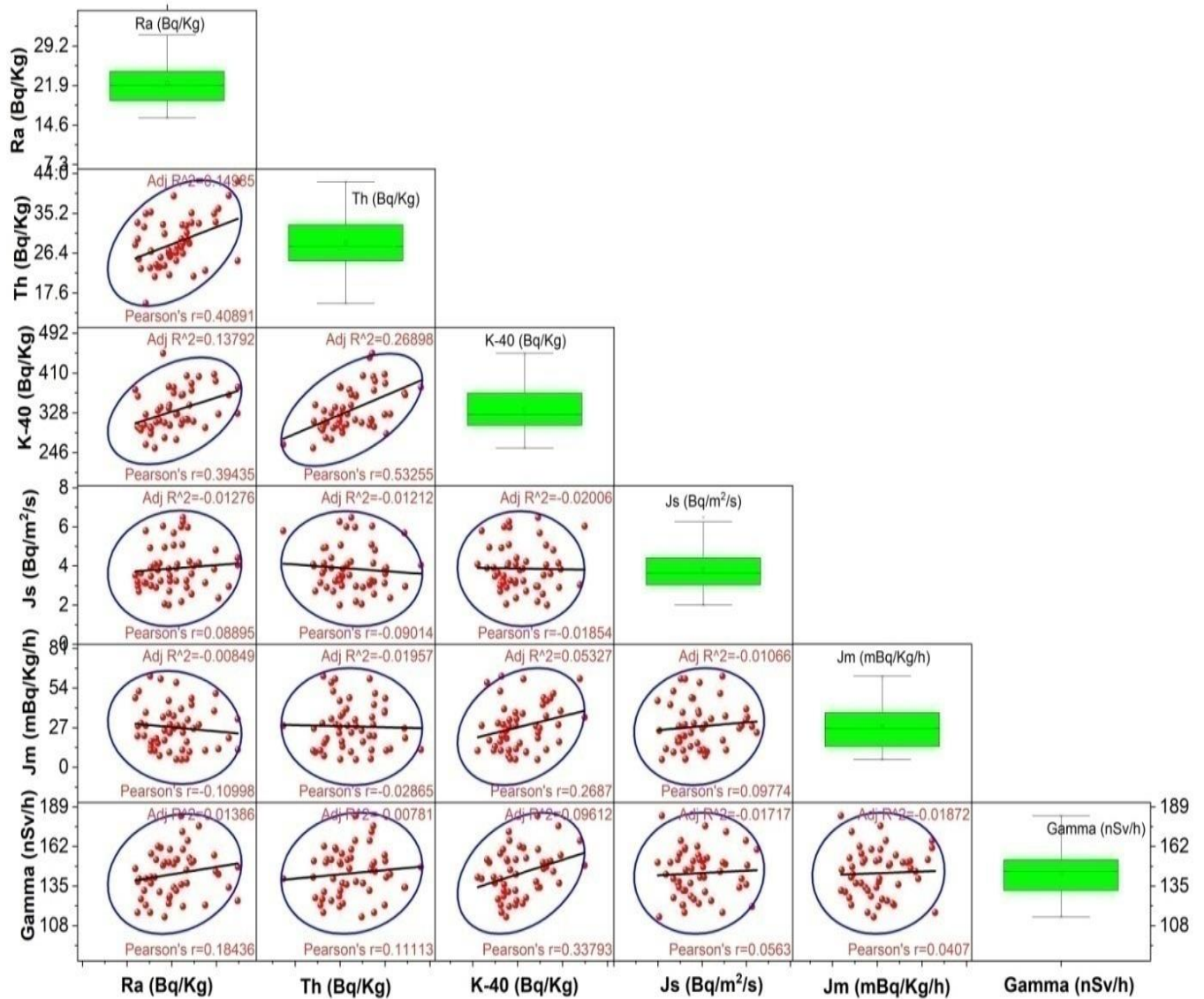
Figure 8.2: Scatter plot matrix depicting the relationships among natural radionuclide concentrations J_m, J_s and ambient gamma dose rate (nSv/h)

The correlation scatter plot matrix (Figure 8.2) presented in this study offers valuable insight into the interrelationship among natural radionuclide concentrations (Ra, Th, and K), radon exhalation parameters (surface exhalation rate, J_s, and mass exhalation rate, J_m), and ambient gamma dose rate. Among the notable trends, radium shows a moderate positive correlation with thorium ($r = 0.41$) and potassium-40 ($r = 0.39$), reflecting the likely co-existence of these radionuclides in similar lithological units, especially those rich in granitic minerals. The association between thorium and K-40 appears particularly strong ($r = 0.53$), suggesting that they may originate from potassium-bearing accessory minerals such as monazite and feldspar. These elements, known for their incompatible behavior during magmatic differentiation, often accumulate together in crustal rocks.

However, when evaluating the linkage between radionuclide concentrations and radon exhalation rates, both J_s and J_m exhibit weak and inconsistent correlations. For instance, Ra demonstrates a very low correlation with both J_s ($r = 0.08$) and J_m ($r = 0.11$), despite being the parent of radon-222. This indicates that radon release to the atmosphere is not governed solely by radium content but is also influenced by soil porosity, grain size distribution, and the moisture content that affects radon emanation and diffusion. Similarly, thorium, the parent of thoron (^{220}Rn), shows minimal correlation with both exhalation parameters, which is likely due to the very short half-life of thoron, limiting its transport from subsurface to surface. Potassium-40, a non-radon-generating radionuclide, naturally displays negligible relationships with J_s and J_m, confirming its independence from radon release dynamics.

The ambient gamma dose rate exhibits a relatively stronger correlation with K-40 ($r = 0.34$), compared to radium or thorium, highlighting the prominent role of K-40 as a gamma-emitting radionuclide in the natural background radiation environment. Nevertheless, its relationship with exhalation rates remains weak, as expected, given that gamma radiation arises from fixed radionuclide content, whereas radon exhalation is a dynamic, diffusive process. Interestingly, J_s and J_m, which are often assumed to behave in tandem, show an unexpectedly low correlation ($r = 0.05$), possibly due to local heterogeneities in soil composition or measurement uncertainties. This finding emphasizes the need to consider both surface and bulk radon transport mechanisms separately when assessing environmental radon flux.

Overall, the scatter plot matrix underscores the complexity of radon mobility in the environment. While parent radionuclide content provides a foundational source term, actual exhalation to the atmosphere is modulated by a host of environmental and soil-specific factors. The weak statistical relationships between gamma dose and radon exhalation further reinforce the notion that dose measurements alone may not reliably indicate radon behavior in soil-air systems. Thus, the plot provides a detailed statistical overview of the relationships between natural radio nuclides (Ra-226, Th-232, K-40) and key radiological parameters such as gamma dose rate, radon mass exhalation and thoron surface exhalation.

Further, to evaluate the distribution pattern of the radionuclide concentration data, a normality test was performed using three standard statistical methods: the Shapiro-Wilk test, the D'Agostino and Pearson omnibus test, and the Anderson-Darling test. These tests are essential to determine whether parametric statistical tools are appropriate for subsequent analysis or if non-parametric alternatives should be considered.

For radium (Ra), the Shapiro-Wilk test yielded a p-value of 0.045, which is just below the commonly used 0.05 significance threshold, suggesting a slight deviation from normality. The D'Agostino-Pearson test, however, produced a p-value of 0.143, indicating no significant evidence to reject the null hypothesis of normal distribution. Meanwhile, the Anderson-Darling statistic (0.545) was slightly above the 15% critical value but still within acceptable bounds relative to higher significance levels. Taken together, these results suggest that the distribution of Ra concentrations is approximately normal, though marginally skewed in the tails.

In the case of thorium (Th), all three tests confirmed that the data are normally distributed. The Shapiro-Wilk test showed a high p-value of 0.588, and the D'Agostino-Pearson test further supported this with a p-value of 0.711. Additionally, the Anderson-Darling test statistic (0.413) was well below even the 15% critical value, strongly indicating a good fit to the normal distribution. This consistency across tests confirms that thorium concentrations follow a Gaussian distribution across the sampling sites.

For potassium-40 (K), the results are mixed. The Shapiro-Wilk test reported a p-value of 0.043, suggesting non-normality at the 5% level. However, both the D'Agostino-Pearson test (p = 0.179) and the Anderson-Darling test (statistic = 0.943, below the 1% critical value of 1.022)

imply that the data do not significantly deviate from normal distribution. These discrepancies might be due to mild kurtosis or minor outliers influencing the Shapiro-Wilk test. Therefore, while the K-40 data may not be perfectly normal, the evidence does not strongly argue against applying parametric methods, especially if robust techniques are employed.

Clearly, thorium data meet the assumptions of normality, while radium and potassium show mild deviations that are unlikely to undermine statistical interpretations if treated with care. These insights help in justifying the appropriate selection of statistical tools in the broader analysis of radiological risks.

8.8 Conclusion

In this study, active radon monitor was used to quantify the exhalation rates of radon and thoron from soil samples collected at 50 different sites within the central Kashmir area of Jammu & Kashmir. The radon mass exhalation rate (J_m) ranged from 5.19 ± 0.43 to 62.03 ± 3.43 mBqkg^{-1}h^{-1}, with a mean value of 22.76 ± 1.25 mBqkg^{-1}h^{-1}. This average is notably below the UNSCEAR safety regulation of 57 mBqkg^{-1}h^{-1}, indicating no significant radiological hazard from radon exhalation in the assessed soils. The thoron surface exhalation rate (J_s) was observed to lie between 1.99 ± 0.18 and 6.47 ± 0.40 Bqm^{-2}s^{-1}, yielding an average of 3.86 ± 0.32 Bqm^{-2}s^{-1}. While this slightly exceeds the UNSCEAR reference limit of 3.06 Bqm^{-2}s^{-1}, the elevation remains marginal and is likely influenced by geochemical variability in the local soil matrix and mineralogical structure. Radiological indices in Table 8.1 revealed a mean radium equivalent activity (Ra$_{eq}$) of 122.38 Bqkg^{-1}, which is well under the recommended limit of 370 Bqkg^{-1}, affirming the minimal gamma radiation risk from terrestrial radio nuclides (UNSCEAR, 2000). The mean activity concentrations for ^{232}Th and ^{40}K were found to be 28.68 ± 5.31 Bqkg^{-1} and 334.10 ± 44.61 Bqkg^{-1}, respectively, both aligning with UNSCEAR's permissible ranges of 11–48 Bqkg^{-1} for thorium and up to 400 Bqkg^{-1} for potassium (UNSCEAR., 1993; 2008).

Assessment of the Annual Effective Dose Equivalent (AEDE) supports the radiological safety of the region. The indoor AEDE was measured at 0.20 ± 0.03 mSvy^{-1}, and outdoor AEDE at 0.05 ± 0.01 mSvy^{-1}, both remaining below the global average reference level of 0.41 mSvy^{-1} (which comprises 0.34 mSvy^{-1} for indoor and 0.07 mSvy^{-1} for outdoor exposures). Furthermore,

both external hazard index (H_{ex}) and internal hazard index (H_{int}) were significantly less than unity, signifying an insignificant long-term health risk. Finally, the results indicate that the central Kashmir region exhibits natural radioactivity levels that fall within internationally accepted safety standards and support the suitability of the soils for residential and agricultural use, with minimal radiological health concerns.

References

- Baixeras, C., Erlandsson, B., Font, L., & Jönsson, G. (2001). Radon emanation from soil samples. *Radiation Measurements*, *34*(1–6), 441–443. https://doi.org/10.1016/S1350-4487(01)00203-7

- Bangotra, P., Mehra, R., Kaur, K., & Jakhu, R. (2016). *Study of natural radioactivity (226 Ra , 232 Th AND 40 K) in soil samples for the assessment of average effective*. 1–5.

- Bondietti, E. A., & Francis, C. W. (1979). Chemistry of Tc-99 and Np-237 in Contact with Unweathered Igneous Rocks. In *Scientific Basis for Nuclear Waste Management* (pp. 417–418). Springer US. https://doi.org/10.1007/978-1-4615-9107-8_51

- Burnett, W. C., Chin, P., Deetae, S., & Panik, P. (1988). *Release of Radium and other decay-series isotopes from florida phosphate rock*. 178.

- Carroll, J., & Lerche, I. (Eds.). (2003). *Sedimentary processes: Quantification using radio nuclides.* Elsevier.

- C V, V., & Joseph, A. (2022). Evaluation of Natural Radioactivity Levels and Exhalation rate of 222Rn and 220Rn in the Soil Samples from the Kuthiran Hills, Kerala, India. *Journal of Nuclear Physics, Material Sciences, Radiation and Applications*, *9*(2), 229–239. https://doi.org/10.15415/jnp.2022.92034.

- Dinh Chau, N., Dulinski, M., Jodlowski, P., Nowak, J., Rozanski, K., Sleziak, M., & Wachniew, P. (2011). Natural radioactivity in groundwater – a review. *Isotopes in Environmental and Health Studies*, *47*(4), 415–437. https://doi.org/10.1080/10256016.2011.628123 Doll, R. (1995). Hazards of ionising radiation: 100 years of observations on man. *British Journal of Cancer*, *72*(6), 1339–1349. https://doi.org/10.1038/bjc.1995.513

- Fadol, N., Abdelrazig, A., Idriss, H., Alashban, Y., & Shubayr, N. (2024). Natural Radioactivity of Granitic Rocks and Their Health Risk around Ingesana Mountains, Sudan. *Health Physics*, *126*(1), 18–24. https://doi.org/10.1097/HP.0000000000001760

- Fudali, R. (1965). *Downloaded from gsabulletin.gsapubs.org on August 5, 2015*. *57*(October), 1191–1196.

- Hosoda, M., Shimo, M., Sugino, M., Furukawa, M., & Fukushi, M. (2007). Effect of soil moisture content on radon and thoron exhalation. *Journal of Nuclear Science and Technology*, *44*(4), 664–672. https://doi.org/10.1080/18811248.2007.9711855

- Johnson, S. S. (1973). Natural radiation. *Environment*, *15*(10), 31–35. https://doi.org/10.1080/00139157.1973.9928413

- Keller, G., Hoffmann, B., & Feigenspan, T. (2001). Radon permeability and radon exhalation of building materials. *Science of the Total Environment*, *272*(1–3), 85–89. https://doi.org/10.1016/S0048-9697(01)00669-6

- Kolodny, Y., & Kaplan, I. . (1970). Uranium isotopes in sea-floor phosphorites. *Geochimica et Cosmochimica Acta*, *34*(1), 3–24. https://doi.org/10.1016/0016-7037(70)90148-1

- Kumar, A., Singh, P., Singh, D., Singh, K., Kandari, T., Saklani, C. P., & Deep, A. (2024). Assessment of exhalation rates of radon and thoron in soil from the Jaunsar-Bawar region of the Indian Himalayas. *Journal of Radioanalytical and Nuclear Chemistry*, *333*(6), 3147–3158. https://doi.org/10.1007/s10967-024-09407-8

- Meslin, P. Y., Sabroux, J. C., Bassot, S., & Chassefière, E. (2011). Experimental study of radon production and transport in an analogue for the Martian regolith. *Geochimica et Cosmochimica Acta*, *75*(9), 2256–2270. https://doi.org/10.1016/j.gca.2011.01.028

- Semwal, P., Singh, K., Gusain, G. S., Kumar, A., & Ramola, R. C. (2017). *Correlation of Radon and Thoron Exhalation Rate with Gamma Level from Soil Sample in the Tehri Garhwal, Uttrakhand, India ,September 2021*.

- Shweikani, R., Giaddui, T. G., & Durrani, S. A. (1995). The effect of soil parameters on the radon concentration values in the environment. *Radiation Measurements*, *25*(1–4), 581–584. https://doi.org/10.1016/1350-4487(95)00188-K

- UNSCEAR (1993) Sources and effects of ionizing radiation, United Nations scientific committee on the effects of atomic radiation report: report to the general assembly, with scientific annexes. United Nations.

- UNSCEAR (2010) Sources and Effects of Ionizing Radiation, United Nations.

CHAPTER 9

FUTURE SCOPE OF THE WORK

This study provides a comprehensive assessment of natural radioactivity in groundwater across Jammu and Kashmir, focusing on radon and uranium distribution in regions like Baramulla, Pattan, Ladakh, and Budgam. The findings reveal significant variations in radon levels, particularly in tectonically active zones, while uranium concentrations in Ladakh remain mostly within permissible limits, with isolated exceedances. The observed radon anomalies suggest a strong correlation with geological faults, indicating the potential for further geophysical research to validate these links and explore radon as a geochemical tracer for seismic activity. Long-term monitoring is essential to capture seasonal variations and better understand environmental influences on radionuclide distribution. Additionally, health risk assessments highlight that infants and children are particularly vulnerable to radon exposure, necessitating more precise dose modeling and longitudinal health studies to evaluate long-term effects. Given that water samples from multiple regions exceed USEPA's radon limits, research should focus on cost-effective mitigation strategies, such as aeration and adsorption techniques, to ensure safe water consumption.Expanding the study to other regions with similar geological settings in the Northwestern Himalayas could provide broader insights into natural radioactivity patterns. Additionally, assessing groundwater contamination by other radio nuclides such as thorium and radium is crucial for a more comprehensive environmental risk evaluation.

The present study lays a robust foundation for extensive future investigations aimed at comprehensively understanding and mitigating the radiological health risks associated with naturally occurring and radioactive nuclides. Given the persistent and often invisible threat these radio nuclides pose to human health particularly through prolonged exposure via environmental pathways such as groundwater, soil, and air there exist a significant need for continued monitoring and evaluation using advanced scientific techniques. Future work can significantly benefit from the integration of advanced dosimetric models and computational risk assessment tools to quantify internal and external radiation doses with higher precision. These models, when applied to region-specific environmental and demographic parameters, can enhance our ability to predict long-term health outcomes and establish exposure thresholds critical for public safety.

Moreover, the scope of this research can be meaningfully expanded through interdisciplinary collaborations with national and international scientific bodies, environmental monitoring agencies, health professionals, and policy-making institutions. Such partnerships would facilitate the exchange of data, harmonization of radiological safety standards, and development of coordinated mitigation strategies. Through joint efforts, it becomes increasingly feasible to devise and implement evidence-based remediation measures, enhance public awareness campaigns, and inform community health initiatives. The findings of this work not only contribute to the existing body of knowledge but also provide a scalable framework for continuous surveillance, early warning systems, and policy formulation in the context of radiological risk management. This trajectory of the present research holds immense promise in safeguarding human populations from the adverse effects of radioactive contamination, especially in geologically vulnerable or high-risk regions.

Author's Bio – data

Tanveer Ahmad Pandith

Research Scholar

Department of Physics, School of Chemical Engineering & Physical Sciences, LPU

E mail: pandithtanveer37@gmail.com

Phone: +918492961967

Academic Qualification

> **Ph. D (Thesis Submitted) in March, 2025 to Lovely Professional University, Punjab, India**

Title of Thesis:

"The Study of Health Hazards Due to Radon In The Environs of The Central Kashmir Valley, J&K, India"

> **M.Sc.** (Physics), University of Kashmir, Srinagar, J&K, India (2019).

> **B.Sc.** (Non-Medical), Govt. Degree College Baramulla, J&K, India (2016).

Computer Proficiency

MS Office (Word, Excel, PPT.), Origin

Research Publications in Journals

1. **Tanveer Ahmad Pandith,** Jeeban Prasad Gewali,Shakeel Simnani, Krishna Pal Singh, Salik Nazir and Mohd Rafiq Chakan (2024), "Exploring Tectonic Sites With Radon from Ground water Sources and Dose Evaluation in Various Age Groups in Baramulla, J&K, India," *Groundwater for Sustainable Development* (GSD), Elsevier 26(2024)101232, Impact Factor 5.9

2. **Tanveer Ahmad Pandith,** Jeeban Prasad Gewali, Shakeel Simnani, Rayees Ahmad and Krishna Pal Singh (2024), " Radon Quantification in Water and Dose Estimation Via Inhalation and Ingestion across Age Groups in the Pattan Region of North Kashmir ,India," *Environ Geochem Health* (EGAH),Springer Nature, 46:522 (2024)

3. **Under Review** *"Evaluating Radiological and Chemo-toxic Risks from Uranium in Groundwater in the Ladakh Region of Northwestern Himalayas, India", Journal of Food Composition and Analysis,* **Manuscript No. JFCA-D-25-00424**.

Paper Presented In Conferences

1. **Tanveer Ahmad Pandith,** Jeeban Prasad Gewali, "Lung Cancer Toxicity Attributed to Indoor Radon Concentration in Three Cities of Punjab, India, in International Conference On Current Trends in Toxicology & 43rd Annual Meeting of Society of Toxicology, India, 2024 (STOX 2024) Human Health and Environmental Safety, held on 16-18th October 2024 Organized by School of Bioengineering and Biosciences in Collaboration with Society of Toxicology(STOX), India, at Lovely Professional University, Punjab.

2.**Tanveer Ahmad Pandith,** Jeeban Prasad Gewali, Ankit Bhagat, Quantification of Radon Exhalation Rate from Ludhiana and Moga Regions of Punjab," in 2nd International Conference on "Recent Advances in Functional Materials" (RAFM-2024), Organized by

Atma Ram Sanatan Dharma College (Department of Physics) Under the Aegis of IQAC ARSD College, (University of Delhi).

Courses /Workshops & Review Certificates

- ➢ Participated in the Course on Environmental Radioactivity Monitoring and its Impact for Health Risk Assessment, A Course Conducted by NIT Jalandhar, India.
- ➢ Worked as a Reviewer in Evaluating the Manuscript entitled "Sediment Quality Assessment on Bartlett Pond in Laredo, Southern Texas, USA, Paper in *Open Journal of Soil Science.*
- ➢ A Letter of Thanks from the Editorial Board of *Open Journal of Geology* in Reviewing the Manuscript entitled "Architecture and Petrographic, Minerologic and Geochemical Signatures of Large Plutonic Masses Dioudioukounkou, Tinkoto, Koulountou, Tiguida Hosted by Maco, Sesam and Diabba Formations: Impacts on Genesis and Deposits of Orogenic Gold(Kedougou- Kenieba Inlier, South-East Senegal /West Africa).